

THE CHARACTERISATION OF HUMAN CORONAVIRUS NL63 PROTEINS



BIANCA GORDON

A thesis submitted in partial fulfilment of the requirements for the degree of Doctor of Philosophy (PhD) in the Department of Medical Biosciences, University of the Western Cape.

Name of supervisor: Prof. B. C. Fielding

Date submitted for examination: 18 January 2021

Key words

Human coronavirus (HCoV)

Coronavirus (CoV)

HCoV-NL63

Structural proteins

Nucleocapsid (N)

Membrane (M)

Antibody, antibodies

Expression

Interaction



UNIVERSITY *of the*
WESTERN CAPE

Abstract

The characterisation of Human Coronavirus NL63 proteins

B. Gordon

PhD Thesis, Department of Medical Biosciences, University of the Western Cape

Human Coronavirus NL63 (HCoV-NL63) is one of seven coronaviruses (CoVs) that cause respiratory disease in the global population. The Membrane (M) and Nucleocapsid (N) proteins are part of the core CoV-structural proteins, crucial in viral replication and virion assembly. Here the expression of HCoV-NL63 M and N was characterized across multiple *in vitro* systems including bacterial, insect and mammalian. To detect untagged proteins in viral structural studies, anti-peptide antibodies were generated in a mouse model. Polyclonal antisera and hybridoma-secreted antibodies exhibited specific binding to their respective full length protein antigens. Anti-peptide monoclonal antibodies were successfully generated against the HCoV-NL63 M and N proteins. During CoV infection, the interaction of CoV M and N is necessary for the production of infectious virions. For the first time, co-expressed, full length HCoV-NL63 M and N were assayed for protein-protein interaction in a mammalian cell system, allowing for native protein folding and modification. M protein formed higher order homomultimers in the presence and absence of co-expressed N. Complexed M and N were co-purified from mammalian cells and confirmed as interaction partners, even under denaturing conditions. HCoV-NL63 M and N proteins formed stable interactions when co-expressed *in vitro*. The strong M-N association in the absence of other viral components highlights the importance of this interaction during virus replication in the host cell. The subcellular localization of HCoV-NL63 N was evaluated from early to late expression, and N exhibited no nucleocytoplasmic shuttling during protein synthesis and maturation. The identified pat4/pat7 nuclear localisation motifs within N may have been inactive; alternatively the localization of N expressed alone was modulated by multiple directive signals provided within the protein. A recombinant Baculovirus was used to express HCoV-NL63 M, towards examining CoV structural protein dynamics in an alternate eukaryotic insect system. Preliminary results indicated that M was expressed at 48-72 hours post-infection. CoV M and N each play multifunctional roles in the viral life cycle, and are implicated in the host-immune response. Investigating the relationships between these and other CoV structural components brings us closer to understanding CoV replication. Important viral protein-protein interactions could present new targets for exploitation in the hunt for an effective anti-coronaviral agent. HCoV-NL63 has been a human pathogen for over 500 years, and continues to adapt genetically, retaining viral fitness in the environment. Able to cause both upper and lower respiratory tract infections, HCoV-NL63 remains a clinically relevant and interesting HCoV

species, that may hold the secrets to viral persistence and seasonal infection patterns of endemic HCoVs.

18 January 2021




UNIVERSITY *of the*
WESTERN CAPE

DECLARATION

I declare that *The characterisation of Human Coronavirus NL63 proteins* is my own work, that it has not been submitted for any degree or examination in any other university, and that all the sources I have used or quoted have been indicated and acknowledged by complete references.

Bianca Gordon

18 January 2021

Signed: 



UNIVERSITY *of the*
WESTERN CAPE

Acknowledgements

I would like to express my sincere gratitude to Professor Burtram C. Fielding, for his guidance as my PhD supervisor and for the opportunity to do my project in his laboratory. I would also like to express my gratitude to the Faculty of Science for the opportunity to undertake my studies at the Department of Medical Biosciences, University of the Western Cape. My gratitude extends to the National Research Foundation (NRF) for the funding provided for this research study. I would like to offer my special thanks to Professor Edmund J. Pool, for his assistance with the antibody work. I would like to express my sincere thanks to my mother, for her unwavering support throughout my PhD project. This would not have been possible without her. I would also like to thank my friends Palesa Makoti and Jihaan Adonis, for their supportive words and for making my post-graduate experience some of the best years of my life.



Table of Contents

Abstract	ii
Declaration	iv
Acknowledgements	v
List of figures	x
List of tables	xii
List of abbreviations	xiii
Chapter 1: Introduction	1
Chapter 2: Literature review	5
2.1. General coronavirus (CoV) characteristics	5
2.1.1. The emergence of pathogenic human CoVs (HCoVs).....	5
2.1.2. HCoV transmission.....	7
2.1.3. Clinical significance of CoVs.....	8
2.2. Human coronavirus NL63 (HCoV-NL63)	9
2.2.1. The HCoV-NL63 genome.....	9
2.2.3. The CoV Nucleocapsid (N) protein.....	21
2.3. Research justification	25
2.4. Study objective	28
2.5. Specific research objectives	28
2.5.1. Objective 1.....	28
2.5.2. Objective 2.....	28
2.5.3. Objective 3.....	28
2.5.4. Objective 4.....	28
Chapter 3: Methodology	29
3.1. The production of antibodies against the HCoV-NL63 M and N proteins	29
3.1.1. Antigenic peptide synthesis.....	29
3.1.2. Animal handling/husbandry and immunisations.....	29

3.1.3. Screening polyclonal antibodies (PAbs) against M and N proteins	31
3.1.4. Hybridoma generation and selection.....	34
3.1.5. Screening and cloning of hybridoma cell lines.....	36
3.2. Assessing the <i>in vitro</i> interaction between the M and N structural proteins of HCoV-NL63	39
3.2.1. Cloning of the HCoV-NL63 M gene in a mammalian system	39
3.2.2. Co-expression of the M and N proteins in Cos7 cells	41
3.3. An <i>in vitro</i> localisation study on the HCoV-NL63 N protein	43
3.3.1. Cloning of the HCoV-NL63 N gene in a mammalian system.....	43
3.3.2. Expression of the N protein in Cos7 cells	48
3.3.3. Localisation study of the N protein in Cos7 cells.....	49
3.4. Expression of the HCoV-NL63 M protein using a recombinant baculovirus in an insect cell system	50
3.4.1. Cloning of the HCoV-NL63 M gene in a baculovirus system.....	50
3.4.2. Generation of a recombinant bacmid-M DNA.....	52
3.4.3. Expression of the HCoV-NL63 M protein	55
Chapter 4: Results and Discussions	60
4.1. The production of anti-peptide antibodies specific to the M and N proteins of HCoV-NL63	60
4.1.1. Antigenic peptide selection.....	61
4.1.2. Antigenic peptide suitability screening.....	64
4.1.3. Enhancing peptide immunogenicity	64
4.1.4. HCoV-NL63 N-specific peptides are strong inducers of mouse polyclonal antibody response.....	66
4.1.5. Polyclonal antibodies (PAbs) recognise their immunising peptide antigens by indirect ELISA.....	69
4.1.6. Polyclonal antibodies are specific and sensitive to their full-length protein antigens	75

4.1.7. Antibody production by hybridomas	80
4.1.8. Hybridoma antibodies are specific to their denatured protein antigens.....	83
4.1.9. Generating clonal hybridoma cell lines.....	86
4.1.10. Monoclonal antibodies are specific to native HCoV-NL3 M and N	96
4.1.11. Hybridoma-secreted mAbs in crude cell supernatants exhibit specific binding to M and N protein antigens.....	99
4.1.12. The development of CoV-specific antibodies	100
4.1.13. CoV antibody generation for non-therapeutic use.....	103
4.2. Assessing <i>in vitro</i> interaction between the M and N structural proteins of HCoV-NL63	106
4.2.1. Preparation of the M and N genes and pXJ40 vectors for cloning	106
4.2.2. Generating the pXJ40-HCoV-NL63 M and pXJ40-HCoV-NL63 N expression constructs	108
4.2.3. The <i>in vitro</i> expression of HCoV-NL63 M and N proteins in a mammalian system ...	110
4.2.4. Lower MW N protein is not present during co-expression	117
4.2.5. HCoV-NL63 M and N proteins exhibit interaction in a mammalian <i>in vitro</i> system...	119
4.3. An <i>in vitro</i> localisation study on the HCoV-NL63 N protein	128
4.3.1. Subcellular localisation of the HCoV-NL63 N protein	128
4.3.2. Subcellular localisation of N protein in Cos7 cells by immunofluorescence (IF).....	131
4.4. The expression of HCoV-NL63 M protein in a baculovirus system	135
4.4.1. Cloning the HCoV-NL63 M gene into the pFastbac1 shuttle vector	135
4.4.2. Generation of the recombinant bacmid-HCoV-NL63 M expression construct	138
4.4.3. The generation of a high titre recombinant baculovirus stock expressing HCoV-NL63 M	141
4.4.4. Plaque assay of P2 stock – Calculating viral titre	144
4.4.5. The expression of recombinant HCoV-NL63 M protein in an insect cell line.....	145
Chapter 5: General conclusions	150
Summary and future perspectives	154
References	156

Appendix 1. Plasmid vectors used in the study	215
Appendix 2. Media, buffers, and stains	220
Appendix 3. List of reagents	225
Appendix 4. Primer sequences.....	230



UNIVERSITY *of the*
WESTERN CAPE

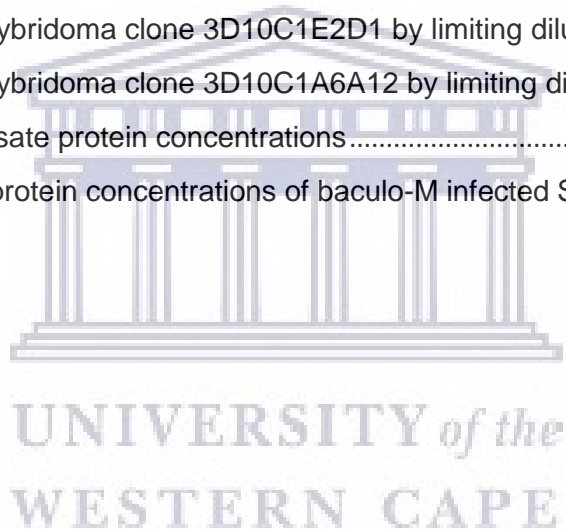
List of figures

Figure 2.1. Schematic of the coronavirus virion, with the minimal set of structural proteins	15
Figure 2.2. The predicted domain order and topology of the CoV Membrane (M) protein	20
Figure 2.3. The domain organisation of the Cov Nucleocapsid (N) protein	21
Figure 3.1. Experimental immunisation timetable	31
Figure 4.1. The identification of antigenic epitopes within HCoV-NL63 Membrane (M) and Nucleocapsid (N) proteins.....	60
Figure 4.2. Screening synthetic peptides for antigen suitability	63
Figure 4.3. The polyclonal antibody response to immunising peptide antigens over time.	66
Figure 4.4. Anti-M polyclonal titration curve, binding against immunising peptide antigen	69
Figure 4.5. Mouse serum anti-N exhibits high peptide antigen specificity.....	73
Figure 4.6. Western blot screening of anti-M polyclonal antibodies against full-length HCoV-NL63 Membrane (M) protein	75
Figure 4.7. Anti-N polyclonal antibody screening against HCoV-NL63 Nucleocapsid (N) protein antigens	77
Figure 4.8. The original positive screening wells identified post-fusion	80
Figure 4.9. The binding affinity of anti-M and anti-N hybridoma-secreted antibodies isolated from the initial positive cell lines.....	81
Figure 4.10. Anti-M hybridoma-secreted antibodies bind full-length HCoV-NL63 M expressed as a GST-fusion protein.....	83
Figure 4.11. Hybridoma line 5F2 secretes HCoV-NL63 M-specific mAbs.....	84
Figure 4.12. Western blots to screen primary antibodies (hybridoma supernatants) against HCoV-NL63 full-length N protein expressed in mammalian and bacterial systems	85
Figure 4.13. Indirect ELISA of anti-M 5E11G7A5A3 mAb affinity for bound MC peptide antigen and bound purified HCoV-NL63 M protein	87
Figure 4.14. Indirect ELISA of anti-M 5E11G7G8H8 mAb affinity for bound MC peptide antigen and bound purified HCoV-NL63 M protein	88
Figure 4.15. Indirect ELISA of anti-M 5E11D10H7D12 mAb affinity for bound MC peptide antigen and bound purified HCoV-NL63 M protein	89
Figure 4.16. Indirect ELISA of anti-M 5E11D10B7A4 mAb affinity for bound MC peptide antigen and bound purified HCoV-NL63 M protein	90
Figure 4.17. Indirect ELISA of anti-M mAb produced by clone 3D10E2A6C2 for bound NN peptide antigen and bound purified HCoV-NL63 N protein.....	93

Figure 4.18. Indirect ELISA of anti-N mAb produced by clone 3D10C1E2D1 for bound NN peptide antigen and bound purified HCoV-NL63 N protein.....	94
Figure 4.19. Indirect ELISA of anti-N mAb produced by clone 3D10C1A6A12 for bound NN peptide antigen and bound purified HCoV-NL63 N protein.....	95
Figure 4.20. Binding assay of anti-M and anti-N mAbs against folded full-length protein antigens	96
Figure 4.21. mAbs binding specificity to HCoV-NL63 M and N.....	98
Figure 4.22. The preparation of HCoV-NL63 M and N genes for subcloning in the pXJ40-HA/FLAG mammalian expression vectors.....	106
Figure 4.23. Cloning the HCoV-NL63 M and N genes in a mammalian expression vector.....	108
Figure 4.24. The determination of whole cell protein lysate concentrations of Cos7 cells transfected with pxj40 M and N constructs.....	110
Figure 4.25. Optimising the expression of HCoV-NL63 M and N proteins in a mammalian cell system	111
Figure 4.26. The co-expression of HCoV-NL63 M and N proteins in a Cos7 cell line.....	117
Figure 4.27. Western blot analysis of Cos7 HCoV-NL63 M and N expression lysates and co-immunoprecipitation (co-IP) protein interaction partners	118
Figure 4.28. The interaction of HCoV-NL63 M and N in a non-stringent/ non-denaturing lysis buffer system	121
Figure 4.29. Extended protein denaturation time reveals M and N as interaction partners in a Cos7 cell system.....	124
Figure 4.30. The single-letter code amino acid sequence for HCoV-NL63 N protein.....	128
Figure 4.31. Multiple sequence alignment of the sequenced N gene with reference HCoV-NL63 N gene	129
Figure 4.32. Immunofluorescence of Cos7 cells transfected with pXJ40-HA-HCoV-NL63 N constructs	131
Figure 4.33. Cloning the HCoV-NL63 M gene in the pFastbac1 shuttle vector.....	135
Figure 4.34. PCR amplification of the transposed bacmid.....	137
Figure 4.35. P0 and P1 generation of baculovirus stock in transfected Sf9 cells	140
Figure 4.36. Plaque assay to determine virus titre of P2 baculoviral M stock	143
Figure 4.37. The determination of whole cell protein lysate concentrations of Sf9 cells infected with a recombinant baculovirus expressing HCoV-NL63 M protein.....	145
Figure 4.38. SDS-PAGE of Sf9 whole cell expression lysates.....	146

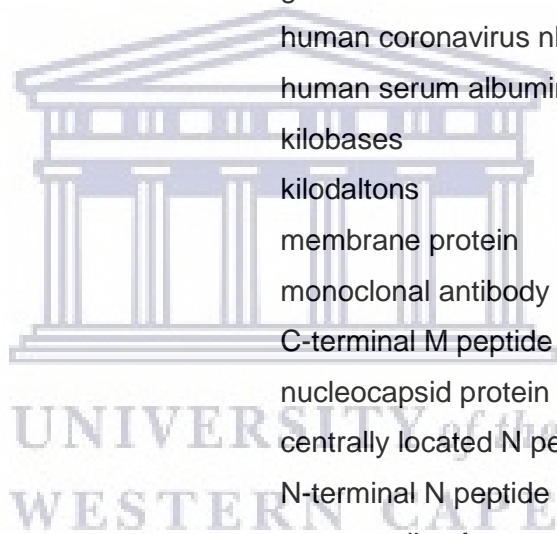
List of tables

Table 2.1. The identified functions of CoV non-structural proteins (nsps).....	11
Table 2.2. Summarised known functions of the CoV Membrane (M) protein	18
Table 2.3. The summarised known functions of the CoV Nucleocapsid (N) protein.....	23
Table 3.1. 96-well plate layout for screening polyclonal serum.....	33
Table 4.1. The isolation of M-hybridoma clone 5E11G7A5A3 by limiting dilution cloning	86
Table 4.2. The isolation of M-hybridoma clone 5E11G7G8H8 by limiting dilution cloning	88
Table 4.3. The isolation of M-hybridoma clone 5E11D10H7D12 by limiting dilution cloning	89
Table 4.4. The isolation of M-hybridoma clone 5E11D10B7A4 by limiting dilution cloning	90
Table 4.5. The isolation of M-hybridoma clone 5F2F12F10E3 by limiting dilution cloning	91
Table 4.6. The isolation of N-hybridoma clone 3D10E2A6C2 by limiting dilution cloning	93
Table 4.7. The isolation of N hybridoma clone 3D10C1E2D1 by limiting dilution cloning	94
Table 4.8. The isolation of N hybridoma clone 3D10C1A6A12 by limiting dilution cloning	95
Table 4.9. Cos7 transfected lysate protein concentrations	110
Table 4.10. Whole cell lysate protein concentrations of baculo-M infected Sf9 cells	145



List of abbreviations

Ab	antibody
Ag	antigen
BSA	bovine serum albumin
Cos7	fibroblast-like monkey kidney cells
CoV	coronavirus
DNA	deoxyribonucleic acid
<i>E.coli</i>	<i>Escherichia coli</i>
ELISA	enzyme-linked immunosorbent assay
FBS	fetal bovine serum
GST	glutathione-s-transferase
HCoV-NL63	human coronavirus nl63
HSA	human serum albumin
KB	kilobases
kDa	kilodaltons
M	membrane protein
mAb	monoclonal antibody
M-C	C-terminal M peptide
N	nucleocapsid protein
N-C	centrally located N peptide
N-N	N-terminal N peptide
ORF	open reading frame
PAb	polyclonal antibody
RBD	receptor-binding domain
RNA	ribonucleic acid
SDS-PAGE	sodium dodecyl sulfate polyacrylamide gel electrophoreses
Sf9	<i>Spodoptera frugiperda</i> insect cells
Sp2	murine myeloma cells



Chapter 1: Introduction

Coronaviruses (CoVs) are a large family of enveloped ribonucleic acid (RNA) viruses with crown-like protein projections on the virion surface (Fehr & Perlman, 2015; Ke et al., 2020; Poutanen, 2018; Siddell, 1995). Most CoVs are mammalian viruses and are able to infect an extensive range of species, including humans. The human pathogen group comprises seven respiratory viruses identified to date. Three of these are highly pathogenic, and the remaining four are ever-present and circulating, presenting as seasonal respiratory infections (Masse et al., 2020; Nickbakhsh et al., 2020; Zeng et al., 2018). The latest highly pathogenic human coronavirus (HCoV) is responsible for the current human Covid-19 pandemic, the biggest viral outbreak in over a century (Abduljalil & Abduljalil, 2020; Sharma et al., 2020). To date, there have been approximately 89 million clinically confirmed cases of severe acute respiratory syndrome coronavirus 2 (SARS-CoV-2) infection globally, and there have been over 1.9 million reported Covid-19-related deaths ("COVID-19 alert Coronavirus disease," 2020; Dong et al., 2020). A high number of cases are suspected of presenting as subclinical or even asymptomatic infections (Li, R. et al., 2020; Long et al., 2020; Nikolai et al., 2020; Ooi & Low, 2020), and as such, the actual infection numbers may be much higher than those indicated by current testing methods.

All HCoVs are respiratory pathogens, and they all encode the same set of replicative enzymes and core structural proteins Spike (S), Envelope (E), Membrane (M), and Nucleocapsid (N) (Payne, 2017; Weiss & Navas-Martin, 2005). These core CoV proteins form the virion (Chen et al., 2020; Machamer, 2007; Xu et al., 2020). Each HCoV also encodes a species-specific set of accessory proteins, ranging from one accessory protein in NL63 to eight in SARS-CoV (Abdul-Rasool & Fielding, 2010; Marra et al., 2003; Rota et al., 2003). The recently identified SARS-CoV-2 encodes six accessory open reading frames (ORFs) (Yoshimoto, 2020). Even within genogroups, HCoVs exhibit variation in host cell receptor specificity. HCoV-NL63 and the closest related alpha-CoV HCoV-229E bind different molecules, with NL63 binding human ACE2 and 229E utilising Aminopeptidase N (Yeager et al., 1992). The beta-CoV derived SARS-CoV and SARS-CoV-2 share the ACE2 host receptor specificity of NL63. *BetaCoV* MERS-CoV binds host DPP4, while endemic human *betaCoVs* OC43 and HKU1 utilise 9-O-acetylated sialic acid for host cell binding. SARS-CoV-2 is the third HCoV that utilises the ACE2 receptor to gain access to the host cell. However, even within this ACE2 binding group, HCoV-NL63 and SARS-CoV bind ACE2 with different conformations (Mathewson et al., 2008). Furthermore, SARS-CoV-2 binds ACE2 with a higher affinity than the first SARS-CoV (Nguyen et al., 2020; Shang et al., 2020). Similar to the differential binding of CoV species to ACE2, *betaCoVs* OC43 and HKU1 bind the same receptor with a considerably different binding affinity (Hulswit et al., 2019). The high level of species-specific variation within the CoV-encoded proteins indicates the adaptability and evolutionary recombinational

potential of CoVs. HCoV-NL63 is a lower pathogenic endemic HCoV identified in 2004. This respiratory virus is predicted to have a global distribution pattern and exhibits seasonal prevalence (Friedman et al., 2018; Gaunt et al., 2010; Huang et al., 2017; Leung et al., 2009; Rucinski et al., 2020).

We understand viruses by demonstrating their specific proteins' role and interactions (Berrow et al., 2006; Brucz et al., 2007; Portolano et al., 2014; Spencer et al., 2007; Trowitzsch et al., 2010). Through *in vitro* assessment of recombinant viral protein expression we have bettered our understanding of the virus-host relationship, viral pathogenesis and molecular mechanisms (Arevalo et al., 2016; Assenberg et al., 2013; Geisse & Henke, 2005; Liu et al., 2008; Uma et al., 2016; Zhang et al., 2001). The establishment of routine protein expression protocols in pro- and eukaryotic systems is essential for assessing the role of single and interacting virus subunits. Each core CoV viral structural protein serves multiple functions, including roles in virus replication, virus assembly, and host immune modulation to ACE2-S interaction (Fang et al., 2007; McBride et al., 2014; Milewska et al., 2014). Other CoVs, including SARS-CoV, have also demonstrated HSPG-binding (Huan et al., 2015; Lang et al., 2011; Watanabe et al., 2007). M and N are both essential components for virion formation – without either, a full infectious viral particle cannot be successfully produced. CoV N is highly antigenic and contains potentially virus-neutralising epitopes (Li, T. et al., 2020; Lin et al., 2003; Qiu et al., 2005; Tilocca et al., 2020). M is the director protein of virion morphogenesis, through previously observed intra- and inter-protein interactions (Klumperman et al., 1994; Nguyen & Hogue, 1997; Opstelten et al., 1995; Vennema et al., 1996). Homotypic M-M interactions are responsible for the basic envelope lattice structure, while the S and E proteins can be found interspersed throughout the membrane envelope (Arndt et al., 2010; de Haan, C. A. et al., 1998; de Haan et al., 1999; de Haan et al., 2000; Locker et al., 1995; Verma et al., 2007). Some evidence in M-tomography and M-mutant studies suggest that M-M monomer interactions occur between the transmembrane domains (TMDs) of M, whereas larger, multi-M homodimer formation is driven/determined by the large endodomain (Kuo & Masters, 2010; Neuman et al., 2011). CoV M has also recently been shown to play a role in initial virus-host contact, interacting with heparan-sulfate proteoglycans (HSPGs) on the surface of mammalian cells (Huan et al., 2015; Lang et al., 2011; Milewska et al., 2014; Naskalska et al., 2019; Watanabe et al., 2007).

Endemic HCoVs have a global distribution, and epidemiological studies indicate a significant seroprevalence level to these viruses in the human population (Gao, Xin et al., 2015; Khan et al., 2020; Nickbakhsh et al., 2020). Due to their persistent presence in the population and lower pathogenicity, HCoVs are more easily monitored and present ideal candidates for HCoV study. Endemic HCoVs are being brought into the spotlight since the global spread of the pandemic has highlighted the complex nature of CoV-host immune response interplay. Recently, scientists have started to explore a possible relationship between the endemic HCoV immune responses and the response to the novel SARS-CoV-

2 (Huang, A. T. et al., 2020; Ma et al., 2020; Sagar et al., 2020). Will this new pathogen, which has now gained access to a global population of hosts, learn from the circulating HCoVs and assume a seasonal-infection pattern? (Biswas et al., 2020). This important question is answered by molecular biology, immunology, and epidemiology. Research into CoV structural proteins has greatly impacted our understanding of virus-host binding dynamics, as well as our current global antiviral approach to the biggest pandemic virus in over a century – the structural CoV S protein is the main target in neutralising antibody development (Rogers et al., 2020; Sun et al., 2020; Wang, C. et al., 2020). In order to gain more insight into the endemic HCoVs, it is necessary to be able to differentiate between HCoV species, which is made possible through the detection of specific structural and non-structural proteins (nsps). Expressed core CoV structural proteins have been used in diagnostic applications and to identify infected samples from patients or *in vitro* in cultured cells (Burbelo, Riedo, Morishima, Rawlings, Smith, Das, Strich, Chertow, Davey, et al., 2020; El-Duah et al., 2019). The ability to differentiate between species of HCoVs would enable more accurate data collection on the seasonal prevalence and serostatus of the population against each specific HCoV. In this research study, the author attempted to develop and optimise *in vitro* expression systems for the expression/characterisation of the structural proteins of the endemic HCoV-NL63. For a variety of analyses, full-length and truncated forms of the M, E, and N core CoV proteins had to be expressed across different species including bacterial, insect, and mammalian cells. In this attempt to enrich the body of information available on this distinct HCoV and its protein subunit functionality, the expression, localisation patterns, and protein-protein interactions of native-like HCoV-NL63 proteins were examined.

Antibodies (Abs) are proteins, produced by B-lymphocytes, which are specific to a particular molecule, usually a foreign body called an antigen (Ag). Physiologically, Abs function as part of the immune system to bind to their specific Ag, allowing the Ag to be recognised and destroyed by immune cells (Forthal, 2014). Antibodies contain highly specific binding sites, making them crucial tools in protein structure and function studies (immunology and molecular biology). There is no commercially available antibody specific for HCoV-NL63 M protein. Currently, the author is aware of a single available mAb specific for HCoV-NL63 N protein. The intention is to develop optimised *in vitro* systems to use routinely for protein expression (across species systems). A hybridoma cell line producing specific antibodies would therefore be an invaluable molecular biology tool, for this and future research studies. N or M specific antibodies have previously been used to identify or differentiate CoV species during infection (Sastre et al., 2011), as the N protein is highly immunogenic and both M and N are highly expressed, crucial structural components of the virus. Considering the increase in recent research efforts in to the endemic HCoVs, an NL63 specific antibody may have implications in epidemiological HCoV research or diagnostic assaying of infected samples for the presence of HCoV-NL63 (El-Duah et al., 2019; Naskalska et al., 2018).

CoV replication occurs in the cytoplasm. Viral assembly/budding occurs in the host cell cytosol (Fehr & Perlman, 2015). Some CoV N proteins locate to the nucleus or subnuclear structures within the host cell during infection/expression, at times disrupting the host cell cycle (Chen et al., 2002; Ding et al., 2014; Hiscox et al., 2001; McBride et al., 2014). When expressed *in vitro*, the HCoV-NL63 N protein localises to the host cell cytoplasm at 24 hours post-transfection (Zuwała et al., 2015). During protein synthesis and maturation, the protein can be transported between different cell sub-compartments, for example, between the host cell nucleus and cytoplasm. The mammalian cell includes the necessary cell machinery for complete post-translational processing and modification of recombinant viral protein (Gray, 2001). The N protein contains a classic pat4/pat7 nuclear localisation signal (NLS). In this analysis, the author cloned and expressed full-length N in a mammalian *in vitro* system. The subcellular localisation pattern of N was monitored for nucleo-cytoplasmic trafficking from early to late-stage transient expression.

The major CoV structural components M and N have been shown to interact during infection with other CoVs and HCoVs (He, Runtao et al., 2004; Kuo, Lili et al., 2016; Luo et al., 2006). There is *in vitro* evidence that HCoV-NL63 M and N may associate when expressed together (visual localisation evidence) in an insect system (Naskalska et al., 2018). HCoV-NL63 M and N have not previously been co-expressed in a mammalian cell line, which would allow for native-like protein folding and modification. In this study the author determined if full-length M and N exhibit viral protein-protein interactions when expressed in a more suitable mammalian cell system (CoVs are mammalian viruses).

To increase the robustness of the protein analyses, expressed HCoV-NL63 structural proteins were examined in two different eukaryotic systems – insect and mammalian. Insect expression was done by generating recombinant baculoviruses encoding the structural proteins. Here, the author attempted to produce a baculovirus encoding full-length M gene and assay infected cells to express HCoV-NL63 M protein. Optimal M-expression timeline and multiplicity of infection (MOI) were determined *in vitro*.

Chapter 2: Literature review

2.1. General coronavirus (CoV) characteristics

CoVs belong to a family of viruses called Coronaviridae, within the order Nidovirales. Four genera are present within CoVs, namely 1) *Alphacoronaviruses*, 2) *Betacoronaviruses*, 3) *Gammacoronaviruses*, and 4) *Deltacoronaviruses* (Adams & Carstens, 2012). All mammalian CoVs belong to the first two groups – *Alphacoronaviruses* and *Betacoronaviruses*, while the avian CoVs belong to the third group – *Gammacoronaviruses* (Balboni et al., 2012). CoVs are enveloped and have a large, linear, non-segmented, positive-sense, single-stranded RNA (ssRNA) genome approximately 27 to 32 kilobases (kb) in size. These viruses have a distinct genome organisation, wherein the 5' two-thirds of the genome includes large replicase ORFs ORF1a and ORF1b. These encode for the non-structural polyproteins, which contain all the enzymes needed for viral RNA replication. The remaining 3' one-third of the genome, lying downstream from ORF1a/b, possesses the genes encoding for the virus' structural proteins, namely the S, M, N, and E proteins. These proteins are translated from the CoVs' sub-genomic mRNAs. Sub-genomic mRNAs are made up of a conserved 5' leader sequence (identical to genomic 5' leader sequence region) and a variable 3' one-third. Different sub-genomic mRNAs allow for the translation of different 3' CoV ORFs (van Boheemen et al., 2012). The structural proteins play a role in virus budding and may also be incorporated into the viral particle. There are also minor structural and nsps encoded by ORFs situated between the 1b and S genes, M and N genes, or downstream of the N gene (van der Hoek et al., 2004). They are considered accessory genes, and their sequence and number differ between species of CoV (species-specific). For example, HCoV-NL63 expresses only one accessory protein (ORF3), whereas SARS-CoV is known to express eight accessory proteins (Schaecher & Pekosz, 2009). Research indicates that accessory proteins have variable effects on virulence, viral replication, and the specific host immune response (Abdul-Rasool & Fielding, 2010; Liu et al., 2014; McBride & Fielding, 2012; Narayanan, Huang, & Makino, 2008).

2.1.1. The emergence of pathogenic human CoVs (HCoVs)

HCoVs were first isolated in the 1960s when HCoV-229E and HCoV-OC43 were isolated from patients with cold-like symptoms (Tyrrell & Bynoe, 1965). SARS-CoV was the first highly pathogenic HCoV identified, and the subsequent respiratory disease pandemic from 2002 to 2003, led to a major increase in research efforts towards understanding HCoVs (Drosten et al., 2003; Ksiazek et al., 2003; Peiris et al., 2003; Poutanen et al., 2003). Advances in sequencing methods quickly enabled the identification of two novel HCoVs following the SARS-CoV outbreak. HCoV-NL63 and HCoV-HKU1 were identified in 2004 and 2005, respectively (van der Hoek et al., 2004; Woo et al., 2005). These two

HCoVs cause mild respiratory disease in otherwise healthy hosts but can cause serious lung immunopathology in immunocompromised patients. In 2012, Middle East respiratory syndrome CoV (MERS-CoV) was identified as a highly pathogenic emerging HCoV (Zaki et al., 2012). The most recently identified pathogenic HCoV is SARS-CoV-2. Identified genetically in January 2020, this novel virus causes Covid-19, a potentially fatal respiratory disease with pneumonia symptoms similar to SARS and MERS (Huang, C. et al., 2020; Li, Q. et al., 2020). The Covid-19 emerging disease outbreak was declared a global pandemic on 11 March 2020. SARS-CoV emerged in the human population near the end of 2002, in Guangdong province, southern China (Zhao, 2007). Although quick and strict measures abolished the outbreak in less than a year, the virus had successfully spread to 37 countries and caused 8 422 human infections. SARS-CoV caused significant outbreaks throughout Southeast Asia, and infections were reported across Europe, the USA, and Canada, with a few cases as far as Australia, New Zealand, and South Africa (Organization, 2003). The pandemic potential of a zoonotic CoV was first seen with SARS-CoV. In 2012, a decade later after the SARS outbreak, MERS-CoV emerged in the Arabian Peninsula, and a CoV is discovered as the causative agent behind another pathogenic human outbreak (Zaki et al., 2012). According to the World Health Organisation (WHO), between April 2012 and January 2020, MERS-CoV has caused 2 519 laboratory-confirmed infections, and resulted in at least 866 associated deaths (Organisation, 2019). The mortality/fatality rate of MERS-CoV infection is approximately 35 per cent (Organization, 2019). Infections have been documented in the Kingdom of Saudi Arabia (KSA), Jordan, Qatar, United Arab Emirates (UAE), and Oman. Outside of the Arabian Peninsula, infections have been reported in Europe, Asia, and the USA (Coleman & Frieman, 2014). The current SARS-CoV-2 pandemic includes to date over 89 million clinically confirmed cases globally and more than 1.9 million recorded Covid-19 deaths ("COVID-19 alert Coronavirus disease," 2020). SARS-CoV-2 is the most dangerous HCoV in recorded history. The pandemic is ongoing and has had huge global implications for human society. The four other identified species of HCoV, namely -OC43, -229E, -NL63, and -HKU1 have not claimed much notoriety in the past, and these are considered low-pathogenic. These lower pathogenic HCoVs cause milder respiratory symptoms, and while they are known to persist within the human population, infections rarely result in hospitalisation. MERS-CoV, SARS-CoV, and SARS-CoV-2 infections cause serious disease with often fatal outcomes. Specific antiviral therapies or vaccination strategies are lacking most of these emerging pathogenic viruses, and treatment usually involves primarily non-specific supportive care (Venkatesan et al., 2010). The CoV outbreaks caused by SARS-CoV, MERS-CoV, and the current SARS-CoV-2 have put CoVs forward as important human pathogens. Prior to the SARS-CoV-2 pandemic, MERS-CoV and SARS-CoV were already listed as prioritised diseases under the 2018 review of the WHO Research and Development (R&D) Blueprint. This report identifies severe emerging diseases that have human epidemic potential and for which there are currently no effective prophylactic or curative treatments. As such, it recognised

the existing urgent need for accelerated research and development into highly pathogenic HCoVs (Mehand et al., 2018). The epidemics, which accompanied the emergence of SARS- and MERS-CoV, exhibited these viruses' ability to generate smaller-scale, localised human outbreaks that indicate the epidemic potential of pathogenic HCoVs. The current global pandemic has confirmed the impact a novel CoV can have on the human population as a global health crisis. Currently there are 64 Covid-19 vaccines in human clinical testing stages, with 20 having reached the final stage of human trials (phase 3 human trials). More than 85 are still in pre-clinical testing stages. While vaccine trials are ongoing, to date, various nations around the world have approved the emergency use of a specific SARS-CoV-2 vaccine, based on the available safety and efficacy data obtained in human trials (Anderson et al., 2020; Corum et al., 2020; Folegatti et al., 2020; Knoll & Wonodi, 2021; Polack et al., 2020; Rubin & Longo, 2020; Widge et al., 2020). These vaccines are targeted at the viral pandemic-causing agent SARS-CoV-2, and are intended to decrease the current burden of infection globally. Considering the broad range of mammalian host species susceptible to CoV infection (potential animal reservoirs), the persistent nature of circulating CoVs in the environment, as well as the adaptation/recombination propensity of this family of viruses, the emergence or re-emergence of highly pathogenic HCoVs in the future is likely to be unavoidable. It is crucial that the threat to human health is mitigated with future outbreaks. To this end, the development of a pan anti-Coronaviral agent is necessary.

2.1.2. HCoV transmission

During the initial stages of the global SARS-CoV pandemic, the virus was dubbed a 'super-spreader' for the ease with which it was transmitted from human-to-human (Wong et al., 2015). MERS-CoV has proven to be less transmissible locally. Current research indicates that each SARS-CoV-2 infection generally results in two to five secondary infections (D'Arienzo & Coniglio, 2020; Steven et al., 2020). During an outbreak, the pattern of viral transmission forms a network of infections, branching out from a primary or index case/patient. The direct or indirect contact required to transmit a virus from one individual to another makes it a largely traceable route of transmission. Respiratory viruses such as SARS-CoV, MERS-CoV, and SARS-CoV-2 are spread via infected bodily fluids, including but not limited to mucus secretions, saliva, and faeces (Richard et al., 2017; Van Doremalen et al., 2013). Symptoms associated with respiratory illness, such as excess mucus production and secretion, coupled with expulsive symptoms like sneezing and/or coughing, generally make respiratory viruses easily transmissible.

2.1.3. Clinical significance of CoVs

The first identified CoV was the infectious bronchitis virus (IBV), which was isolated in chick embryos in 1947 (Cunningham & Stuart, 1947). Following that, mammalian CoVs, including mouse hepatitis virus (MHV) and transmissible gastroenteritis virus (TGEV), were discovered in the 1940s (Cheever et al., 1949; Doyle & Hutchings, 1946). The first HCoVs were discovered in the 1960s (Hamre & Procknow, 1966; Tyrrell & Bynoe, 1966). The most important of the HCoVs that have been identified to date include SARS-CoV, isolated in 2002 (Vlasova et al., 2007), MERS-CoV, and SARS-CoV-2, which is currently causing a vast global disease burden of respiratory infections (Lai et al., 2020). CoVs have been found to cause disease in a wide variety of mammals, including swine, dogs, horses, cattle, mice, rats, and humans. Some also cause disease in birds. Animal CoVs cause serious infections, like severe enteric and respiratory disease; however, an infection can also result in respiratory, hepatic, or neurological symptoms. The severity of the disease varies among hosts (van Boheemen et al., 2012). HCoVs include a range of viral species, some which cause relatively mild respiratory illnesses and others which result in life-threatening pneumonia. Acute respiratory diseases constitute a significant health issue worldwide as these types of illnesses affect people across all age groups, thereby placing a large economic burden on the healthcare systems of countries (Cabeça & Bellei, 2012). Seven HCoVs are known to cause respiratory infections. HCoV-229E and HCoV-OC43 are known to cause the common cold. These two species cause five to thirty per cent of common-cold type respiratory illnesses (Holmes, 2001). The SARS-CoV causes life-threatening pneumonia (Pyrce et al., 2004; van der Hoek et al., 2004). It was first isolated in 2000 but is thought to have been circulating within the human population for some time prior to that, as the nasopharyngeal sample from which it was first isolated had been frozen for months before testing. In 2003 and 2004, it caused 8 000 human infections and led to over 700 deaths (Balboni et al., 2012). SARS could be considered a zoonotic infection. After it was identified as the causative agent in humans, SARS-CoV-like viruses were isolated from wild animals in the same area, including bats. The increased research led to the identification of HCoV-NL63 in 2004 and then HCoV-HKU1 in the following year (van der Hoek et al., 2004). Along with respiratory symptoms, abdominal pain, vomiting, and diarrhoea can present as the initial HCoV infection symptoms, particularly in HCoV-OC43 and HCoV-NL63 infection. These specific symptoms are most likely a result of viral invasion of the intestinal mucosa, as stool samples of infected individuals tested positive for the presence of HCoV-like viral particles (Principi et al., 2010). Since its discovery in 2012, MERS-CoV has shown a mortality rate of approximately 34 per cent and is not easily spread from human to human. Most infected individuals develop severe acute respiratory illness. The most recently identified HCoV is SARS-CoV-2, another highly pathogenic HCoV with suspected zoonotic origins that is able to cause severe pneumonia (Zhu, N. et al., 2020).

2.2. Human coronavirus NL63 (HCoV-NL63)

The first identification of HCoV-NL63 was from the nasopharyngeal aspirate of a seven-month-old infant in Amsterdam in 2004. The patient presented with respiratory symptoms, including coryza, high temperature, and conjunctivitis. A chest X-ray revealed features of bronchiolitis; however, the patient's sample was tested and found to be negative for all known respiratory viruses. A group of Dutch researchers noticed that the virus exhibited a cytopathic effect (CPE) on the cultured cells upon inoculation into monkey kidney cells. As the genome was not known, a method using complementary deoxyribonucleic acid (cDNA)-amplified fragment length polymorphism was used to clone and amplify the viral genome. This method of genomic sequencing is known as VIDISCA (van der Hoek et al., 2004). Upon identification and comparison to known viral genomes, this novel strain was placed in the *Alphacoronavirus* group.

2.2.1. The HCoV-NL63 genome

The genome of HCoV-NL63 is 27 553 base pairs in size and is capped and polyadenylated (Pyrce et al., 2007). The genome order is as follows: 5'-ORF1a-ORF1b-S-ORF3-E-M-N-polyT tail-3' (Abdul-Rasool & Fielding, 2010). Six mRNAs are produced in the membrane-associated replication centres, including the full genomic RNA (gRNA), as well as a nested set of five sub-genomic mRNAs (sg mRNAs). From these, seven ORFs are made (Brockway et al., 2003; Pyrc et al., 2004). The sg mRNAs are translated to produce the virus' structural and accessory proteins. The genes encoding for the viral structural proteins S, E, M, and N, are found at the 3' end of the genome. The S glycoprotein is 180 – 190 kilodalton (kDa) in size, M is approximately 26 kDa, E is approximately 9 kDa, and N is 50 – 60 kDa in size (Pyrce et al., 2005). These sg mRNAs are produced for all the ORFs, including S, ORF3, E, M, and N. They are generated by a discontinuous replication strategy during the minus-strand synthesis of HCoV-NL63's viral replication cycle. This results in the sg mRNAs being synthesised in a minus-strand fashion, and these are later made into plus-strand mRNAs. The plus-strand mRNAs have a leader sequence at their 5' ends, approximately 70 nucleotides in length. This nucleotide sequence is identical to that at the 5' end of the gRNA (Abdul-Rasool & Fielding, 2010). The core sequence of HCoV-NL63's leader transcription regulatory sequence (TRS) is AACUAAA, and it is situated within the genomic order before every ORF with the exception of E. The E TRS has a core sequence of AACUAUA. HCoV-NL63 is most genetically similar to another member of the *Alphacoronavirus* group, HCoV-229E. The two share sequence similarity of around 65 per cent. The ORF3 accessory gene in HCoV-NL63 takes the place (in the gene sequence) of two genes – 4A and 4B in the HCoV-229E genome. Also, in cell culture, HCoV-229E is fastidious and has a narrower host cell range than HCoV-NL63, which grows readily in monkey kidney cells (Vero E6). HCoV-NL63 has one of the lowest GC contents within the CoV family

at approximately 34 per cent. The average GC content for a CoV is 32 – 42 per cent. The HCoV-NL63 genome includes two untranslated regions – the first is at the 5' end and consists of 286 nucleotides, and the second is at the 3' end and is 287 nucleotides in length (van der Hoek et al., 2004).

2.2.1.1. ORF 1a/1b

The CoV family possess the largest genomes among known RNA viruses. These linear, positive-sense, ssRNA genomes are 5' capped and polyadenylated, and while CoV genome organisation is distinct among viral families, it is for the most part conserved among CoVs (Gorbalenya et al., 2006; Milewska et al., 2016). The 5' two-thirds of the CoV genome includes two large replicase ORFs – 1ORF1a and ORF1b. These encode for replicase polyproteins pp1a and pp1b. Pp1a (> 4000AA) is produced by ORF1a, while pp1b (> 7000AA) is produced by ORF1a and ORF1b, following a ribosomal frameshift at the junction of ORF1a/b. This activity is regulated by a ribosomal frameshifting (RFS) element, in this case, a hairpin-pseudoknot structure, which provides a ribosomal entry site (RES) for bicistronic translation of ORF1a and ORF1b (Brierley et al., 1989; Namy et al., 2006; Snijder et al., 2003). The resulting polyproteins are cleaved by ORF1a-encoded proteases. Nsp3 encodes either one or two papain-like proteases (PL_{pro}) – PL1_{pro} and PL2_{pro}. The activity of one or both of these proteases in N-terminal processing of the polyproteins varies between CoV species (Gorbalenya, 2001; Snijder et al., 2003; Ziebuhr et al., 2000). Nsp5 encodes a 3C-like cysteine protease (3CL_{pro}), also referred to as the main protease (M^{pro}). M^{pro} is responsible for all viral cleavage downstream of nsp4 and is active in all CoVs (Mielech et al., 2014). Proteolytic cleavage yields 15 or 16 mature, nsps. These subunits of the replicase proteins associate in a complex, which drives viral RNA replication and viral assembly, and plays a role in generating a nested set of sg mRNAs (Snijder et al., 2016). Viral RNA-dependent RNA polymerase (RdRp), helicase, endonuclease, exoribonuclease, as well as methyltransferase activity are all carried out by nsps. Correct proteolytic processing by virally-encoded proteases is therefore essential for viral replication (Bailey-Elkin et al., 2014; Ivanov, Thiel, et al., 2004; Marra et al., 2003; Raj et al., 2014; Snijder et al., 2003; Thiel et al., 2003; Tomar et al., 2015; Zumla et al., 2015). In table 2.1 below, the functions of the CoV nsps are summarized.

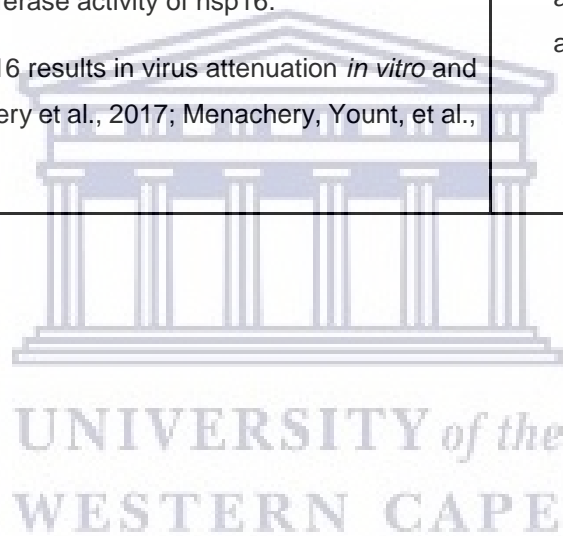
TABLE 2.1. THE IDENTIFIED FUNCTIONS OF CoV NON-STRUCTURAL PROTEINS (NSPS)

NSP (1 – 16)	FUNCTION IN COV TRANSCRIPTION/REPLICATION	REFERENCES
nsp1	<ul style="list-style-type: none"> • Inhibits host protein synthesis at transcriptional and translational level. MERS-CoV nsp1 inhibits host translation, does not stably bind 40S, targets translationally competent mRNAs transcribed in the nucleus and transported to the cytoplasm. • Promotes host mRNA degradation (through Xm-1 mediated 5 – 3' exonucleolytic mRNA decay pathway in two ways: 1) binding the 40S ribosomal subunit (part of translation machinery) in the cytoplasm and preventing translation, and 2) inducing endonucleolytic, template-dependent RNA cleavage within the 5'UTR of host mRNAs. • Inhibits endogenous gene expression, including genes involved in antiviral/innate immunity. SARS-CoV nsp1 inhibits IFN-inducible genes by mediating virus- and IFN-dependent signalling through innate antiviral pathways. • Inhibits cell progression from G0/G1 phase and inhibits cellular replication in transfected cells (MHV nsp1/p28). 	<ul style="list-style-type: none"> • (Lokugamage et al., 2015; Wang et al., 2010) • (Gaglia et al., 2012; Huang et al., 2011; Kamitani et al., 2009) • (Kamitani et al., 2006; Narayanan, Huang, Lokugamage, et al., 2008; Wathelet et al., 2007) • (Chen et al., 2004)
nsp2	<ul style="list-style-type: none"> • Interacts with prohibitin 1 (PHB1) and PHB2 – cellular proteins involved in mitochondrial function and host transcription. Nsp2 may also play a role in disrupting intracellular host signalling during SARS-CoV infections. 	<ul style="list-style-type: none"> • (Cornillez-Ty et al., 2009)
nsp3	<ul style="list-style-type: none"> • Papain-like protease (PLpro), responsible for cleavage at nsp1/2, nsp2/3, and nsp3/4. Depending on CoV species, either one or two PLpro enzymes are active during cleavage (SARS and MERS have only one). • Exhibits deubiquitinase activity. 	<ul style="list-style-type: none"> • (Mielech et al., 2014) (Thiel et al., 2003) • (Ratia et al., 2006)

nsp4	<ul style="list-style-type: none"> Interaction of nsp4 with nsp3 is necessary for membrane rearrangement and the formation of viral replicative organelles. 	<ul style="list-style-type: none"> (Oudshoorn et al., 2017; Sakai et al., 2017)
nsp5	<ul style="list-style-type: none"> Chymotrypsin-like fold protease (3CLpro or M^{Pro}). Main protease, responsible for cleavage at seven sites from nsp4-nsp11 in pp1a, and eleven sites from nsp4 – nsp16 in pp1ab. 	<ul style="list-style-type: none"> (Snijder et al., 2016)
nsp6	<ul style="list-style-type: none"> Co-localisation of nsp6 with co-expressed nsp4 suggests the interaction of nsp4 with nsp6 (Hagemeijer et al., 2011). Nsp6 is essential for double-membrane vesicle (DMV) formation during CoV replication. 	<ul style="list-style-type: none"> (Angelini et al., 2013)
nsp7	<ul style="list-style-type: none"> Complexes with nsp8 and acts as a cofactor to replicative enzymes. 	<ul style="list-style-type: none"> (Subissi et al., 2014)
nsp8	<ul style="list-style-type: none"> Nsp7/nsp8 complex interacts with and may enhance the processing capability of nsp12 (RdRp). Evidence for nsp8-RNA interaction, which may play a role in minus-strand viral RNA synthesis. Possible primase activity of nsp8 (producing primers for nsp12) in <i>de novo</i> RNA synthesis (low fidelity, ssRNA template). Nsp7/8/12 complex may also interact with Nsp14 (proofreading enzyme) (Imbert et al., 2006). 	<ul style="list-style-type: none"> (Subissi et al., 2014) (te Velthuis et al., 2012; Züst et al., 2008) (Imbert et al., 2006)
nsp9	<ul style="list-style-type: none"> Evidence for nsp9-RNA interaction, may play a role in CoV transcription and replication (RNA synthesis). May have relevance in viral pathogenesis. May play a role in CoV replication, with a function in regulating polyprotein processing (mutation of nsp9 leads to defective cleavage at positions nsp4-nsp11). Nsp9 may play a role in assembling a functional transcriptase complex (mutations in nsp9 lead to defective minus-strand RNA synthesis). 	<ul style="list-style-type: none"> (Züst et al., 2008) (Frieman et al., 2012) (Donaldson et al., 2007) (Sawicki et al., 2005)
nsp10	<ul style="list-style-type: none"> Multifunctional cofactor to CoV replicative enzymes. Nsp10 can bind RNA (weakly) and may form part of an RNA-binding complex. 	<ul style="list-style-type: none"> (Matthes et al., 2006)

	<ul style="list-style-type: none"> • Interacts with nsp14 and nsp16; plays a role in regulation of methyltransferase (nsp14 and 16) activities. 	<ul style="list-style-type: none"> • (Bouvet et al., 2010; Bouvet et al., 2012)
nsp11	<ul style="list-style-type: none"> • *Nsp12 sequence includes ORF1a/b ribosomal frameshift; therefore, polyprotein ORF1b includes nsp12. N-terminus cleavage site of nsp12 is also the nsp10/nsp11 junction/cleavage site, thus nsp11 is the N-terminus of nsp12. 	<ul style="list-style-type: none"> • (Gorbalenya et al., 2006)
nsp12	<ul style="list-style-type: none"> • Includes an N-terminus RdRp-associated nucleotidyltransferase (NiRAN) domain, as well as a C-terminus canonical RNA-dependent RNA polymerase (RdRp) domain, responsible for binding and elongation of RNA templates. 	<ul style="list-style-type: none"> • (Gorbalenya et al., 1989; Lehmann et al., 2015; Ng et al., 2008; te Velthuis, 2014)
nsp13	<ul style="list-style-type: none"> • Exhibits helicase activity; NTP-dependent protein, which functions in RNA replication, sg mRNA transcription and mRNA capping, as well as posttranscriptional viral RNA quality control. • Interacts with RdRp and promotes RdRp action by unwinding double-stranded viral RNA intermediates and removing secondary RNA structures within single-stranded templates. Along with RdRp, serves to ensure viral genome replication. 	<ul style="list-style-type: none"> • (Ivanov, Thiel, et al., 2004; Ivanov & Ziebuhr, 2004) • (Imbert et al., 2008) (Kadaré & Haenni, 1997)
nsp14	<ul style="list-style-type: none"> • Bifunctional enzyme – nsp14 N-terminal domain has 3'-5' exonuclease (ExoN) proofreading activity, promotes fidelity during CoV RNA synthesis. • Nsp14 C-terminal domain exhibits AdoMet-dependent guanosine N7-MTase activity (guanine-7 methyltransferase), methylates 5' cap structures of viral RNAs. <p>Complexes with nsp10, nsp10 stabilises and enhances nsp14 activity.</p>	<ul style="list-style-type: none"> • (Becares et al., 2016; Bouvet et al., 2014; Eckerle et al., 2010; Minskaia et al., 2006; Smith et al., 2014) • (Bouvet et al., 2012; Chen et al., 2009; Jin et al., 2013; Ma et al., 2015)
nsp15	<ul style="list-style-type: none"> • Poly (U)-specific endoribonuclease (NendoU) activity, a conserved trait within vertebrate CoVs suggesting a role in viral replicative cycle. Relevant biological EndoU substrates not yet elucidated. • Mutation of nsp15 leads to decreased viral titre and viral RNA accumulation. 	<ul style="list-style-type: none"> • (Snijder et al., 2003; Snijder et al., 2016) • (Posthuma et al., 2006) (Bhardwaj et al., 2004; Ricagno

	Inferred RNase A-like catalytic activity (similar mechanisms).	et al., 2006) (Ivanov, Hertzig, et al., 2004; Nedialkova et al., 2009)
nsp16	<ul style="list-style-type: none"> • Functions as an S-adenosylmethionine-dependent ribo-2'-O-methyltransferase (2'-O-MTase); function of 2'-O-MTase activity is highly conserved in Coronaviridae. • 2'-O-MTase activity is implicated in 5' methyl capping of viral RNA transcripts, as well plays a role in evading detection of viral RNA by host innate immune receptors. • Interacts with nsp10; nsp10 promotes methyltransferase activity of nsp16. <p>Mutation in nsp16 results in virus attenuation <i>in vitro</i> and <i>in vivo</i> (Menachery et al., 2017; Menachery, Yount, et al., 2014).</p>	<ul style="list-style-type: none"> • (Snijder et al., 2003) • (Gao, X. et al., 2015; Menachery, Debbink, et al., 2014) (Habjan et al., 2013; Züst et al., 2011) • (Bouvet et al., 2010; Decroly et al., 2011; Imbert et al., 2008; Lugari et al., 2010; Menachery et al., 2017; Menachery, Yount, et al., 2014)



2.2.2. The CoV Membrane (M) protein

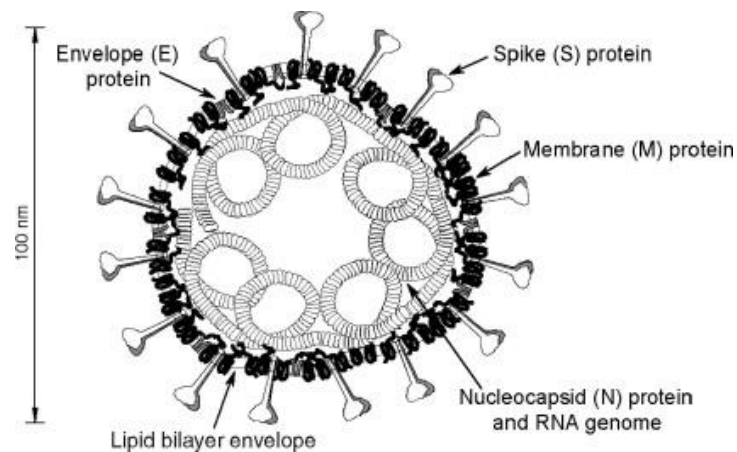


FIGURE 2.1. SCHEMATIC OF THE CORONAVIRUS VIRION, WITH THE MINIMAL SET OF STRUCTURAL PROTEINS (MASTERS, 2006).

2.2.2.1. The role of M in virion assembly and budding

The budding of enveloped viruses requires the acquisition of a lipid envelope. The envelope encloses the virus Nucleocapsid and protects the viral RNA genome outside of the cell. In figure 1 above, the basic coronavirion structure is depicted, indicating the 4 major structural proteins S, E, M and N. Through budding from intracellular membranes, it allows for the viral particle to leave the cell easily, without damage. The envelope also allows delivery of the virus easily into the host cell by fusion of the lipid membranes. The viral envelope contains proteins that mediate its binding to and fusion with the target cell (Vennema et al., 1996). Intracellular budding sites differ between enveloped viruses. Coronaviruses assembly occurs intracellularly at the intermediate compartment between the endoplasmic reticulum (ER) and Golgi apparatus. Nucleocapsids synthesised in the cytoplasm are transported to the intermediate compartment where they likely interact with the cytoplasmic domains of the M proteins. The immature virus is then moved along the exocytic pathway while undergoing virion maturation events such as proteolytic processing (Vennema et al., 1996). The virions acquire their envelope when they bud from intracellular membranes. Multiple CoV structural proteins are found in this envelope, namely the M, S, and E proteins. The M protein plays an important role in the assembly of the virion and is responsible for mediating the incorporation of the S protein into the viral envelope (de Haan et al., 1999), as well as being the primary determinant of the site of intracellular virus budding (Corse & Machamer, 2000). CoV M is the most abundant glycoprotein in the viral particle and within the infected cells. At 25 – 30 kDa in size, M is a triple-membrane spanning protein with three domain types – a short amino (N)-terminal ectodomain (protrudes from virion outer surface), the TMDs, and a long Carboxy (C)-terminal endodomain (intravirion) (Nal et al., 2005;)(Narayanan et al., 2000; Neuman et al., 2011; Rottier, 1995; Ujike & Taguchi, 2015). Although there is great diversity in the sequence of M

across CoVs, the predicted protein structure remains similar (Arndt et al., 2010). During the co- or post-translational processing of CoV M protein, the glycosylation of M is necessary to maintain the correct protein-protein interactions. N-linked glycosylation is known to occur with *alpha-* and *deltacoronaviruses*, whereas O-linked glycosylation occurs in the *betacoronaviruses* (de Haan, Cornelis AM et al., 1998; Oostra et al., 2006). The treatment of cells with Tunicamycin, which inhibits N-linked glycosylation, effectively prevents the incorporation of the S protein into the CoV lipid envelope. Under these conditions, the envelope contains only M. However, the processes of virion assembly and virus budding are unaffected by the glycosylation status of M, suggesting that only the M protein is needed in the envelope for successful budding (Klumperman et al., 1994; Locker et al., 1992). Glycosylation may play a less conspicuous role in CoV M protein bioactivity, perhaps maintaining the structural conformation and/or antigenic properties of specific viral proteins (L. Kuo, Koetzner, & Masters, 2016)(Braakman & Van Anken, 2000; de Haan et al., 2003). During viral replication, the CoV M protein is co-translationally inserted into the ER membrane (Neuman et al., 2011). The M protein of IBV is found to localise in the ER-Golgi intermediate compartment (ERGIC) and Golgi membrane network when expressed alone; this is slightly beyond the budding site of IBV (Machamer et al., 1990). CoV M protein has also been found to localise mainly in the Golgi apparatus of the cell (Müller et al., 2010). The M protein functions to incorporate the viral N into the virion. M likely interacts with E and N at the site of viral budding, and these molecular interactions help to ensure that the N becomes enclosed in a lipid envelope as it buds out of the cell. It has been demonstrated that M protein and viral RNA interact *in vitro* and that the M protein and N interact with each other in MHV infected cells (Sturman et al., 1980). MHV is the prototypic CoV and has been used extensively in research investigating the roles of CoV structural proteins in viral replication. MHV belongs to the CoV family. This virus undergoes budding at a site close to the Golgi complex and rough ER of the cell. Using immunofluorescence (IF) and immunoperoxidase electron microscopy, the M protein of MHV has been found to localise in these regions around the time of budding. This indicates that the M protein accumulation determines when and where virus budding occurs (Klumperman et al., 1994; Locker et al., 1992).

2.2.2.2. M interactions

CoV M proteins are responsible for the overall structure and shape of the virion envelope. Envelope formation is accomplished through M self-interactions and interactions with other viral structural proteins (Neuman et al., 2011). During virion assembly, the M protein interacts with the S, E, and N viral proteins (Arndt et al., 2010; Boscarino et al., 2008; Kuo & Masters, 2002; Nguyen & Hogue, 1997; Rottier, 1995). The S and E proteins are incorporated into the M-lattice by lateral interactions with M at the ERGIC membranes (Bosch et al., 2005; Corse & Machamer, 2003; de Haan et al., 1999; Escors, Ortego, Laude, et al., 2001). The N protein and viral RNA interact with M via the M-protein C-terminal domain (CTD) (Hurst et al., 2005; Kuo & Masters, 2002; McBride et al., 2007; Narayanan & Makino, 2001). Interactions

between the M and N proteins occurred independently of M-E and M-S interactions (Narayanan et al., 2003; Narayanan et al., 2000; Schelle et al., 2006). It is suggested that the M protein dimerises in the cell during infection. Depending on its form, its functions regulate membrane curvature and spike protein density (Neuman & Buchmeier, 2016; Neuman et al., 2011). Mutational analysis and co-expression of CoV M and S indicate that the TMDs of M are crucial for the association of the M and S proteins. Furthermore, mutations within the N-terminal domain (NTD) or extreme CTD of M do not seem to interfere with M-S complex formation. Interestingly, such mutations at the M-termini are known to abrogate the formation of VLPs (de Haan, C. A. et al., 1998). Different structural domains within M are then necessary for viral protein-protein interaction and VLP formation, respectively (de Haan et al., 1999). The S and N proteins, as well as the viral RNA, all play a role in determining exact virion or VLP structure and composition through their interactions with the M/Matrix protein (Neuman et al., 2011).

2.2.2.3. CoV M and the immune response

The CoV M protein plays a major role in inducing a humoral immune response in the host. The serum containing anti-M antibodies shows sufficient neutralising activity against SARS-CoV in infected patients. The CoV M protein contains neutralising epitopes, making this protein a potential target for antiviral research and development (He, Y., Zhou, Y., et al., 2005; Hu et al., 2003). There is also evidence to suggest that a combination of antibodies to various CoV epitopes (M and S proteins) would have an enhanced neutralising capacity against SARS-CoV (Pang et al., 2004). CoV M also contains immunogenic T cell epitopes and is able to elicit cellular immune responses (CD8 T cells) (Li et al., 2008; Liu et al., 2010). SARS-CoV M protein modulates the host immune response through direct interaction with IKK β *in vitro*, thereby downregulating the expression and activity of inflammatory signalling molecules such as Cox-2 and transcription factors like NF- κ B (Fang et al., 2007).

2.2.2.4. Other roles for M in the virus life cycle

HCoV-NL63 uses host cell heparan sulfate proteoglycans (HSPGs) as initial attachment factors (El-Duah et al., 2019; Naskalska et al., 2019). Recently (2019), a major new function of HCoV-NL63 M during the virus life cycle has been elucidated. Observation of successful viral attachment to the cell, by VLPs expressing M but lacking/devoid of S protein, indicates that the M protein is responsible for mediating the initial attachment of HCoV-NL63 to the host cell. Therefore, it is suspected that the viral M and S proteins play synergistic, crucial roles in the infection of host respiratory cells (El-Duah et al., 2019; Naskalska et al., 2019). Table 2.2. below summarises the known functions of the CoV M protein.

TABLE 2.2. SUMMARISED KNOWN FUNCTIONS OF THE CoV MEMBRANE (M) PROTEIN

	Functions of Membrane (M) protein	References
Viral assembly	<ul style="list-style-type: none"> • Major determinant of CoV site of budding • M is the only CoV protein required for pseudovirion budding • Mediates S and E protein incorporation into the viral envelope • Mediates the encapsidation of CoV nucleoprotein complex (N protein + viral gRNA) into the virion • M drives the correct virion assembly and directs the overall CoV particle shape 	<ul style="list-style-type: none"> • (Corse & Machamer, 2000; Klumperman et al., 1994; Locker et al., 1992; Müller et al., 2010) • (Klumperman et al., 1994; Locker et al., 1992) • (C. A. de Haan, Smeets, Vernooij, Vennema, & Rottier, 1999)(Bosch et al., 2005; Corse & Machamer, 2003; Escors, Ortego, Laude, et al., 2001; McBride et al., 2007). • (Hurst et al., 2005; Kuo & Masters, 2002; Narayanan & Makino, 2001) • (de Haan et al., 2000; Klumperman et al., 1994; Kuo & Masters, 2010; Neuman et al., 2011; Stertz et al., 2007).
Viral pathogenesis	<ul style="list-style-type: none"> • M mediates the initial attachment of HCoV-NL63 to host cell 	<ul style="list-style-type: none"> • (El-Duah et al., 2019; Naskalska et al., 2019).
Host immunity	<ul style="list-style-type: none"> • SARS-CoV M contains neutralising B cell epitopes • M protein contains T cell epitopes and can elicit CD8 + T cells • SARS-CoV M protein modulates the host immune response; downregulates the inflammatory signalling molecule Cox-2 and transcription factor NF-κB 	<ul style="list-style-type: none"> • (He, Y., Zhou, Y., et al., 2005; Hu et al., 2003). • (Li et al., 2008; Liu et al., 2010). • (Fang et al., 2007).

2.2.2.5. M protein topology

The M protein is one of the four core conserved structural CoV proteins. This core includes the S, E, M, and N proteins (Masters, 2006). CoV membrane proteins share a low degree of amino acid (AA) sequence similarity, but they all share the same basic structure (Arndt et al., 2010). M proteins form part of the lipid bilayer in cells and have a specific topology. They are either simple, meaning they span the membrane once, or complex, spanning the membrane multiple times. Protein topology is determined by signals present in their AA sequence (Locker et al., 1992). The M protein is a three-time membrane-spanning glycoprotein flanked by a large endodomain (C-terminus, inside the virion) and a small ectodomain (outside the virion) (Rottier et al., 1984; Rottier et al., 1986). The endodomain consists of an amphiphilic region proximal to the membrane, followed by a short hydrophilic domain (Rottier et al., 1986). There is a conserved amphiphilic domain directly following the TMDs within the M protein. This conserved sequence (SWWSFNPETNNL) associates closely with the membrane at the N-terminal end of the amphiphilic domain (Kapke et al., 1988; Rottier et al., 1984). This short sequence of AA is conserved across most of the Coronaviridae family and has proven important in the functionality of the M protein interactions in viral assembly (Arndt et al., 2010). The M protein is the most abundantly expressed CoV E protein and is crucial in maintaining virion integrity. The M/matrix protein interacts with and directs most of the other major structural proteins into the CoV structure during assembly in the host cell (Bos et al., 1996; Boscarino et al., 2008; Corse & Machamer, 2000; Fischer et al., 1998; Hurst et al., 2005; Raamsman et al., 2000; Siu et al., 2008).

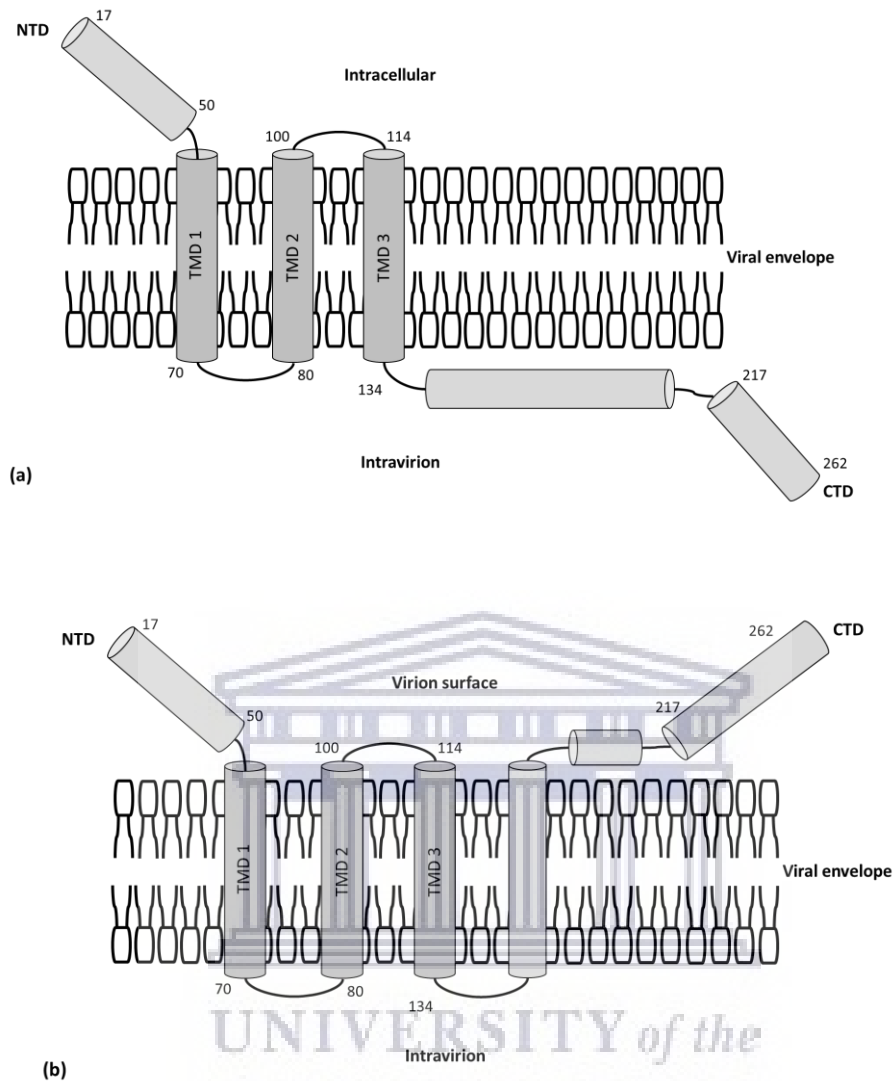


FIGURE 2.2. THE PREDICTED DOMAIN ORDER AND TOPOLOGY OF THE CoV MEMBRANE (M) PROTEIN. (A) THE NTD ECTODOMAIN IS SHOWN, ALONG WITH THREE TMDs AND A LONG, CYTOPLASMIC CTD ENDODOMAIN. THE CoV M PROTEIN GENERALLY FOLLOWS THIS DOMAIN ORDER. (B) THE ALTERNATE INFERRED/PREDICTED TOPOLOGY OF CoV M INCLUDES A PART OF THE CTD AS A FOURTH TMD, WITH A SHORT CTD NOW PRESENT IN THE INTRACELLULAR REGION (SEE FIGURE 2.2 B). THIS ALTERNATE M TOPOLOGY HAS BEEN IDENTIFIED IN TRANSMISSIBLE GASTROENTERITIS VIRUS (TGEV) VIRIONS (BY MAB BINDING) AND HAS BEEN PREDICTED BASED ON THE AA SEQUENCE OF HCoV-NL63 M PROTEIN. DIFFERENTIAL STRUCTURAL FORMS OF M MAY BE EXPRESSED DURING CoV INFECTION. THE ESTIMATED AA POSITIONS OF EACH DOMAIN ARE INDICATED. ADAPTED FROM (RISCO ET AL., 1995)(C. A. DE HAAN, SMEETS, VERNOOIJ, VENNEMA, & ROTTIER, 1999)(ESCORS, CAMAFEITA, ET AL., 2001; NASKALSKA ET AL., 2019).

2.2.3. The CoV Nucleocapsid (N) protein

2.2.3.1. General features of CoV N

The N protein found in CoVs ranges from 377 – 455 AAs in length (Kumar, 2020). The N protein is alkaline and has a seven to eleven per cent serine content, which is considered relatively high; these serine-containing sites may serve as protein phosphorylation target sites (Hiscox et al., 2001). It has been shown that the CoV N protein is a phosphoprotein that plays a role in viral replication and interaction with the host cell surface. The N protein is CoV species-specific, with HCoV-NL63's N protein showing only 42 per cent AA sequence similarity to the N protein of its closest relative, HCoV 229E. Between the *Alpha-*, *Beta-*, and *Gammacoronavirus* groups, it has been found that the percentage of sequence conservation in the N protein is not very high. For example, the IBV in group three and the porcine infectious gastroenteritis virus of group one show only a 29 per cent N sequence similarity with the bovine CoV in group two. Furthermore, even within the respective groupings, sequences differ quite highly, as in the murine hepatitis virus and bovine CoV that share only a 70 per cent identity with regards to their N protein (Lapps et al., 1987). Three conserved structural domains have been identified within the CoV protein N, namely the RNA-binding NTD, dimerisation and RNA-binding CTD, and middlemost linker domain, which has a high serine-arginine (SR) content. The NTD and CTD are flanked on the outer ends by intrinsically disordered regions (IDRs) (Calvo et al., 2005; Hsin et al., 2018; Parker & Masters, 1990; Spencer & Lee, 2006).

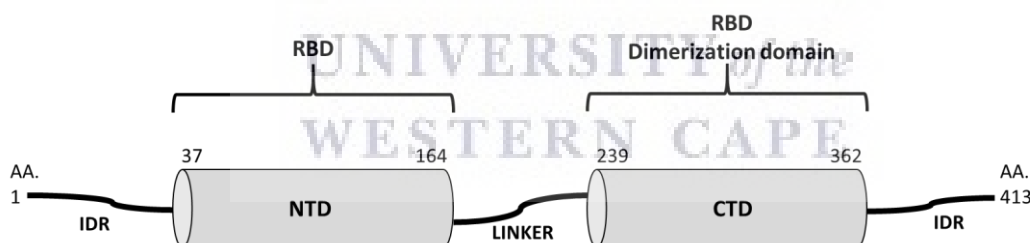


FIGURE 2.3. THE DOMAIN ORGANISATION OF THE COV NUCLEOCAPSID (N) PROTEIN. THE ESTIMATED AA POSITIONS OF EACH DOMAIN ARE INDICATED BY NUMBER. IDRS ARE SHOWN FLANKING BOTH THE NTD AND CTD FUNCTIONAL DOMAINS. THESE ARE SR-RICH REGIONS. A FLEXIBLE SR-RICH LINKER REGION LIES BETWEEN THE FUNCTIONAL DOMAINS. RIBOSOME BINDING (RBD) FUNCTION AND DIMERISATION DOMAINS ARE INDICATED (AS PREDICTED). ADAPTED FROM: (PAPAGEORGIU ET AL., 2016); (HSIN ET AL., 2018).

2.2.3.2. The multifunctional CoV N protein

N protein is the main component of the ribonucleoprotein complex, which is at the centre of each CoV infectious particle (Bárcena et al., 2009; Fehr & Perlman, 2015; Hagemeyer & de Haan, 2015). There are leader sequences (TRSs) both at the 5' and 3' ends of the CoV gRNA that are thought to be involved in CoV RNA synthesis; the observed association of the N protein with these regions initially suggested that N has a role at the level of sgRNA transcription and translation (Chang & Brian, 1996; Compton et al., 1987). Conversely, in the related arterivirus, equine arteritis virus (EAV), transcription and viral replication occur in the absence of N expression, suggesting that the N protein may not be essential for these processes (Molenkamp et al., 2000). Determining the complete CoV virion architecture requires a network of interactions, including N-N self-interactions, N-CoV RNA interactions, and N-M protein interactions (Knoops et al., 2008; McBride et al., 2014). The CoV N protein is the only structural protein associated with the cytoplasmic viral replication-transcription centres (RTCs) created by the nsps (Hurst et al., 2013; Hurst et al., 2010; Verheije et al., 2010). To incorporate the CoV gRNA into the virus particle, N must bind the gRNA generated at the RTCs (Kuo, L. et al., 2016; Ma et al., 2010). This N-gRNA binding is also essential for CoV transcription 'template-switching' and discontinuous replication processes (Mateos-Gómez et al., 2011; Zúñiga et al., 2010). During CoV infection, the N protein shows the highest expression between the viral proteins. This is due, most likely because during transcription, the N protein mRNA template is the most highly-produced sgRNA fragment (Hiscox et al., 1995). The N protein takes part in viral evasion of the innate host immune system, through avoiding detection by pattern recognition receptors (PRRs) like retinoic acid-inducible gene 1 (RIG-1) helicase and RIG-1-like melanoma differentiation-associated protein 5 (Mda5) (Lu et al., 2011). This is perhaps why N evokes the strongest host immune response compared to the other structural proteins (Dijkman et al., 2008). CoV N may play a role in redirecting host resources away from host protein synthesis and allowing the virus to effectively utilise host machinery to make new viral proteins instead (Zuwała et al., 2015). The N protein has been shown to affect a range of host cell processes, including actin rearrangement, cell-cycle progression, intracellular host cell signaling and apoptosis (Harrison et al., 2007; Surjit et al., 2006; Surjit et al., 2004; Zhao et al., 2006; Zhou et al., 2008). Table 2.3. below summarises the known functions of the CoV N protein.

TABLE 2.3. THE SUMMARISED KNOWN FUNCTIONS OF THE CoV NUCLEOCAPSID (N) PROTEIN

	Functions of Nucleocapsid (N) protein	References
Viral replication and assembly	<ul style="list-style-type: none"> • N associates with replicase-transcriptase complexes (RTCs). • NTD and CTD bind viral gRNA and are necessary for the incorporation of viral genome into virions. • Major component of CoV nucleoprotein core – associates with viral genome in 'beads-on-a-string' conformation. • Plays a role in virion assembly and genome encapsidation through self-interactions and interactions with viral RNA and M protein. 	<ul style="list-style-type: none"> • (Kelley R. Hurst, Koetzner, & Masters, 2013)(Hurst et al., 2010; Verheije et al., 2010) • (Chen et al., 2007; Kuo, L. et al., 2016; Zhao & Perlman, 2010) • (Fehr & Perlman, 2015; Hagemeijer & de Haan, 2015) • (Hagemeijer & de Haan, 2015; Knoops et al., 2008; McBride et al., 2014)
Viral pathogenesis	<ul style="list-style-type: none"> • SARS-CoV N induces apoptosis when expressed <i>in vitro</i>. • Interferes with host cell-cycle progression. • N protein induces host cell actin filament rearrangement. 	<ul style="list-style-type: none"> • (Surjit et al., 2004; Zhao et al., 2006) • (Harrison et al., 2007; Surjit et al., 2006; Zhou et al., 2008) • (Surjit et al., 2004)
Host immunity	<ul style="list-style-type: none"> • N protein aids in viral evasion of the host innate immune system. 	<ul style="list-style-type: none"> • (Lu et al., 2011)

2.2.3.3. N protein localisation

The arteriviruses and CoVs both belong to families of positive-sense single-stranded RNA ((+)ssRNA) viruses, within the order *Nidovirales* (Meulenberg et al., 1993). Although these two families exhibit a difference in genetic complexity, their viral replication mechanisms and genome organisation are similar (De Vries et al., 1997). Arterivirus N proteins are capable of nuclear localisation, including the N protein of porcine reproductive and respiratory syndrome virus (PRRSV), EAV, and lactate dehydrogenase-elevating virus (LDV) (Tijms, van der Meer, & Snijder, 2002)(Yoo, Wootton, Li, Song, & Rowland, 2003)(Mohammadi et al., 2009; Pei et al., 2008; Rowland et al., 1999). It was initially thought that the CoV N protein localises only to the cytoplasm of the host cell (Laude & Masters, 1995); however, it has been shown that the CoV N protein can localise in the cell cytoplasm and nucleolus. Confocal microscopy, investigating the intracellular localisation sites of the IBV CoV N protein, found that the N

protein is capable of co-localising to both the nucleolus, as well as the cytoplasm of the host cell. Within the cell cycle, in phase G1, there are multiple nucleoli, whereas later in the cycle (S and G2), only one nucleolus is present. During mitosis, there are no nucleoli in the cell. This explains why, in cells undergoing mitotic division, the N protein was only identified in the cytoplasm (Hiscox et al., 2001). Coronavirus IBV and MHV N proteins localise to the nucleolus, a nuclear substructure, at some point during viral replication (Wurm et al., 2001)(Chen et al., 2002; Hiscox et al., 2001; Reed et al., 2006). The active shuttling of N protein was suggested by a 2001 study, in which it was shown that an IBV N-GFP (green fluorescent protein) fusion protein exhibits cytoplasmic and nuclear distribution. As this fusion protein is 74 kDa in size, it cannot be passively transported through the nuclear pore complex from cytoplasm to nucleus (Hiscox et al., 2001; Wang & Brattain, 2007). This nuclear-cytoplasmic protein trafficking is accomplished with active signals, including NLSs, nucleolar localisation signals (NoLSs), and nuclear export signals (NESs) (Wulan et al., 2015). Nucleolar localisation of N protein may play a role in viral pathogenesis (Lee et al., 2006; Pei et al., 2008). CoV N's nucleocytoplasmic transport is known to arrest the cell cycle (G2/M phase), resulting in a decreased rate of cell replication. The ability of N protein to bind at the 5' end of CoV gRNA may suggest that in doing so, the N protein recruits ribosomes for viral RNA translation (Nelson et al., 2000). In CoV-infected cells, the translation of host cell genetic material is decreased, whereas the translation of viral RNA is increased (Siddell et al., 1981; Tahara et al., 1994). The cell cycle delay created by N-translocation could potentially interfere with host ribosome recruitment and may play a role in redirecting the host resources towards viral protein synthesis and replication (Chen et al., 2002; Ding et al., 2014; McBride et al., 2014). PRRSV has also been shown to localise within the host cell cytoplasm and nucleolus. This type of co-localisation of the N protein has been reported in various members of *Coronaviridae*, including TGEV in group 1, MHV from group 2 and IBV in group 3. This observation was similar in species-specific, as well as non-species-specific host cells. Together, this data suggests that the localisation of protein N to the nucleolus is a conserved trait in the *Nidovirales*. It may also point to this pattern of N subcellular localisation being important for successful infection and viral replication (Wurm et al., 2001). Domain 2 of CoV protein N is capable of RNA-binding, and once the N protein has reached the nucleolus, it likely associates with ribosomal RNA (rRNA). The N protein of EAV, also of the order *Nidovirales*, shows partial nuclear localisation. Upon inactivation of the chromosomal maintenance 1 (CRM1) pathway, which is utilised by proteins for nuclear export, N was found to localise solely to the nucleus. Cells infected with EAV, in which the CRM1 pathway was inactivated, showed N protein only in the nucleus throughout infection. This suggests immediate post-translational transport to the nucleus. The formation of the N and budding of arteriviruses is thought to occur in the cytoplasm, indicating that the N protein must be transported back to the cytoplasm to play its role in these processes. This nucleo-cytoplasmic shuttling of EAV-N may lead to the phosphorylation of the N protein (Tijms, van der Meer, & Snijder,

2002). SARS-N, in contrast to other CoVs, exhibits only cytoplasmic subcellular localisation. While the N sequence contains multiple identified NLSs, a NoLS, as well as a single NES within the protein CTD, full-length SARS-N does not localise to any nuclear or subnuclear structure during infection/transfection (Wulan et al., 2015; You et al., 2007; You et al., 2005). The localisation of HCoV-NL63 N has been characterised in a number of different cell lines, including 293T, LLC-MK2 and fully differentiated cultured human airway epithelium (HAE) cells. During infection of these cell lines with HCoV-NL63, or single transfection with N alone, the N protein does not display *in vitro* nuclear localisation in any of these cell lines. The N protein CTD is the active site of oligomerisation, while the NTD binds nucleic acids (Zuwala et al., 2015).

2.3. Research justification

HCoVs have been identified in the global population since the 1960s (Hamre & Procknow, 1966). This group of seven human pathogens now includes three highly pathogenic species: SARS-CoV, MERS-CoV, and the novel Covid-19 pandemic causing viral agent SARS-CoV-2 (Zhu, Z. et al., 2020). The four lower-pathogenic HCoV species are endemic human pathogens, including HCoV-229E, -OC43, -NL63, and -HKU1 (Corman et al., 2018; Galanti & Shaman, 2020). While lower pathogenic HCoVs are known to persist within the environment, highly pathogenic SARS-CoV, MERS-CoV, and SARS-CoV-2 are all known to cause life-threatening respiratory disease (Casella et al., 2020; Yin & Wunderink, 2018; Zheng, 2020). The first HCoV epidemic occurred in 2002 – 2003 with SARS-CoV. Less than 20 years on the current pandemic caused by SARS-CoV-2, it has become a global health crisis, with far-reaching and profound implications in the health-, social-, and economic sectors (Chakraborty & Maity, 2020; Hiscott et al., 2020; Javed et al., 2020; Nicola et al., 2020). The WHO has acknowledged the considerable need for increased research and development in HCoVs since 2018 (Mehand et al., 2018). The global SARS-CoV-2 Covid-19 pandemic has provided a massive impetus to increase clinical and non-clinical research efforts into HCoVs. As such, the body of knowledge on HCoVs is currently growing rapidly. The hunt for a SARS-CoV-2 vaccine has been the major drive behind the majority of recent CoV research. The isolation of neutralising antibodies (NAbs) from convalescent patient plasma, along with advances in hybridoma technology and humanised antibody production have enabled the production of NAbs with a high capacity for protection against SARS-CoV-2 infection (Rogers et al., 2020).

The endemic human respiratory virus HCoV-NL63 may not be considered highly pathogenic, but like SARS-CoV-2, this HCoV causes life-threatening symptoms mainly in immunocompromised individuals. HCoV-NL63 infection-associated deaths have been reported (Cabeça & Bellei, 2012)(Mayer et al., 2016)(Konca et al., 2017; Oosterhof et al., 2010). Cases of severe acute infections and fatalities in healthy adults have been reported for all four endemic HCoV species (Veiga et al.). There is currently

contradicting evidence available on a potential link between the individual's immune response to the endemic HCoVs and SARS-CoV-2 (Hicks et al., 2020)(Ma et al., 2020; Sagar et al., 2020). These highlight the clinical relevance of endemic HCoVs, especially within the current global SARS-CoV-2 and development of an effective antiviral strategy. Prior to the Covid-19 pandemic, endemic HCoVs provided the most robust and routinely available data on the human immune response to CoVs (Edridge et al., 2020). The antibody response to SARS-CoV-2 does not last longer than six months PI, and published data indicates that convalescent plasma must be collected early, following diagnosis with SARS-CoV-2 (Compeer & Uhl, 2020; Crawford et al., 2020). As such, once the Covid-19 pandemic has been overcome, the persistent circulating endemic HCoVs may once again be the only apparent 'inexhaustible' source of information regarding CoV immunity in the global population. Gaining insight into HCoV pathogenesis is essential as we move forward. A prophylactic vaccine, which may provide what we need to overcome this pandemic virus, is not likely to protect against infection by emerging HCoVs. Looking at the past 20 years (SARS-CoV – 2002/03; MERS-CoV – 2012 and ongoing; SARS-CoV-2 – 2019 and ongoing), novel pathogenic HCoVs are likely to continue arising from previously known and unknown zoonotic sources. The success of the measures taken to curb SARS-CoV-2 infection rates throughout this pandemic (restriction of movement, screening and testing, self-isolation of symptomatic individuals) has made it clear that early detection is crucial in preventing larger outbreaks (Luo et al., 2020).

There have been reports of severe illness caused by HCoV-NL63 in adults and children. Seroconversion to this virus occurs in childhood, and as such, HCoV-NL63 may be common childhood pathogen similar to the respiratory syncytial virus (RSV) or Rhinovirus (Dijkman et al., 2008; Dijkman et al., 2012; Sarna et al., 2018; Zhou et al., 2013). HCoV-NL63 has zoonotic origins, and there is evidence for ongoing HCoV-NL63 mutation within the human environment. This virus is able to persist and retain viral fitness, adapting over time to humans but still retaining the ability to bind bat cells (Huynh et al., 2012; Wang, C. et al., 2020). The ability to prevail as a seasonal virus and persist in human infection hints at a lower level of virulence; however, HCoV-NL63 is also able to cause severe pneumonia and bronchiolitis in children and adults. A 2018 study reported a cluster of 23 HCoV-NL63 infections in hospitalised children with severe respiratory illness, including pneumonia and bronchitis. This is the first report of an HCoV-NL63-associated viral outbreak, indicating the potential of this endemic HCoV to dynamically adapt for infection within the human population (Wang, Y. et al., 2020). Suspected to have evolved to infect humans over 500 years ago (Huynh et al., 2012; Pyrc et al., 2006), HCoV-NL63 remains a clinically relevant virus with potentially vast amounts of immunological data on the human anti-CoV response available in the global population. CoV antibodies last six months, but seasonal viruses and the re-exposure they provide allow for developing a highly specific immune response to an endemic human virus such as HCoV-NL63 (Galanti & Shaman, 2020). Furthermore, insights into the

evolution of this virus and its functional genetic/proteomic units may provide us with a better understanding of how this group of viruses has adapted to co-exist within the human population (Corman et al., 2018; Wei et al., 2020; Ye et al., 2020).

Understanding the virus-host relationship involves being able to analyse whole viruses, as well as virus protein subunits. *In vitro* infection and transfection systems are important tools in elucidating viral dynamics in the host cell. Molecular and cell biology provide platforms for scientists to evaluate viral pathogenesis and molecular mechanisms of infection. The core structural components of the CoV virion include the S, E, M, and N proteins. These proteins play crucial roles in CoV replication and propagation, and understanding how these major CoV components express and interact within the host cell is important. To this end, scientists deconstruct viral replication dynamics to understand the various roles of viral subunits. Acquired knowledge on CoV M and N contributes to broadening our knowledge of the HCoV subunits and their function in the viral-host dynamic. It is necessary to build a more robust understanding of the role of CoVs in the global human health context to develop a well-informed plan to mitigate future CoV threats to human health. HCoV research requires increased investigation in epidemiology, immunology, and molecular biology. As much information as possible is needed to build our understanding of this family/group of viruses, so we may understand how to design vaccines or antiviral strategies that are able to combat this dynamic group of human pathogens effectively.

In this study, the author developed antibodies for the identification and characterisation of HCoV-NL63 major structural proteins M and N. Furthermore, protocols were developed for the optimal expression of these two proteins in a higher eukaryotic cell system, to shed some light on the *in vitro* behaviour of the HCoV-NL63 structural subunits.

UNIVERSITY of the
WESTERN CAPE

2.4. Study objective

The author aimed to clone and express two of the major structural proteins of the endemic HCoV NL63 – the M and N proteins. To this end, antibodies were produced for full-length M and N protein characterisation across various expression systems, including bacterial, insect, and mammalian. The author intended to investigate the M-N protein interaction *in vitro* in a mammalian system, as well as assess the subcellular protein localisation pattern of N. Furthermore, M was cloned and expressed in an alternate eukaryotic expression system, in contribution to the overall aims of the umbrella project of which this body of work is a part. The author has aimed to optimise a system for expressing the major NL63 structural proteins in different cell species, enabling further assessment of expression and interaction characteristics of these important, multifunctional viral proteins.

2.5. Specific research objectives

2.5.1. Objective 1

Design peptide antigens and generate mAbs specific to the HCoV-NL63 M and N proteins in a mouse model. Polyclonal and mAbs will be screened for binding against viral peptide and protein antigens.

2.5.2. Objective 2

Optimise the expression of full-length HCoV-NL63 M and N protein in a mammalian cell system. Co-express the M and N proteins in order to investigate possible *in vitro* protein-protein interactions between the two core HCoV-NL63 structural components.

2.5.3. Objective 3

Monitor the subcellular localisation pattern of HCoV-NL63 N in intervals from early to late expression to determine if N exhibits any nucleo-cytoplasmic trafficking during protein synthesis in the cell.

2.5.4. Objective 4

Produce a recombinant baculovirus encoding HCoV-NL63 M. Optimise the expression of M and determine the expression timeline for full-length M protein in infected insect cells.

Chapter 3: Methodology

3.1. The production of antibodies against the HCoV-NL63 M and N proteins

3.1.1. Antigenic peptide synthesis

Peptide antigens (Ags) were used to immunise experimental animals. These short AA sequences were derived from antigenic epitopes recognised within the proteins of interest, the HCoV-NL63 N and M proteins, respectively. An Antigenic Peptide Prediction Tool (Expasy-Uniprot) was used to analyse our protein sequences and identify epitopes exhibiting antigenicity. On their own, peptide antigens are not efficiently immunogenic. They require conjugation to a larger molecule such as a carrier protein. Within this research study, short peptide sequences were synthesised (BioSynthesis – USA) using multiple antigenic peptide (MAP)-8 technology. Upon receipt, lyophilised peptides were reconstituted in sterile distilled water (possible due to adequate/good peptide solubility) at a 5mg/mL concentration. Three different peptide antigens were synthesised, specific to the N-terminus of the HCoV-NL63 N (N-N) protein, the C-terminus of N (N-C) and the C-terminus of the HCoV-NL63 M protein (M-C), respectively.

3.1.2. Animal handling/husbandry and immunisations

Male Balb/C mice were obtained for use in this experiment, following ethical clearance obtained from the UWC (Ethics Clearance No 06/06/11). Mice were maintained in a climate-controlled room, with a natural light/dark cycle (night/day), and supplied with commercial rodent food *ad libitum*. The initial immunisations were formulated as follow:

N peptide immunisation

- 50µl N-N peptide antigen (@ 5mg/mL)
- + 50µl N-C peptide antigen (@ 5mg/mL)
- + 150µl 1x phosphate-buffered saline (PBS)
- + 250µl Complete Freund's Adjuvant (CFA) (F5881, Sigma)

- = 500µl (antigen concentration of 50µg/100µl)

M peptide immunisation

- 50µl M-C peptide antigen (@ 5mg/mL)
- + 200µl 1xPBS
- + 250µl Complete Freund's Adjuvant (CFA) (F5881, Sigma)

- = 500µl (antigen concentration of 50µg/100µl)

The N-N and N-C peptide antigens were combined in the N-immunisation formulations, while the M-immunisations contained only the M-C peptide. Two mice were immunised per antigen group (M and N). The final immunisation volume was 100µl and was administered via intraperitoneal injection. Follow-up immunisations were formulated as follows:

N peptide immunisation

- 50µl N-N peptide antigen (@ 5mg/mL)
- + 50µl N-C peptide antigen (@ 5mg/mL)
- + 150µl 1xPBS
- + 250µl Incomplete Freund's Adjuvant (IFA) (F5506, Sigma)

- = 500µl (antigen concentration of 50µg/100µl)

M peptide immunisation

- 50µl M-C peptide antigen (@ 5mg/mL)
- + 200µl 1xPBS
- + 250µl Incomplete Freund's Adjuvant (IFA) (F5506, Sigma)

- = 500µl (antigen concentration of 50µg/100µl)

Blood samples (approx. 30µl) were collected from each mouse by tail-bleed prior to the initial immunisations (pre-immune), 14 days after the initial immunisation (post-immune 1), as well as before each subsequent immunisation (post-immune 2, 3, and 4). Blood was diluted 1/10 in 1xPBS and centrifuged at 2 000 revolutions per minute (rpm) for 10 mins at room temperature. Supernatants were collected and aliquoted (20µl) and stored at -20°C. The timeline for experimental animal immunisations is shown in figure 3.1 below.

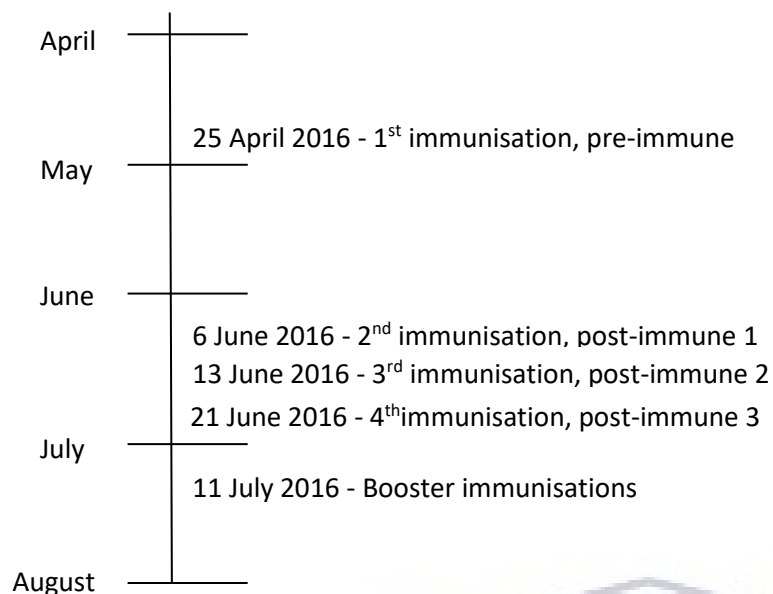


FIGURE 3.1. EXPERIMENTAL IMMUNISATION TIMETABLE

3.1.3. Screening polyclonal antibodies (PAb)s against M and N proteins

3.1.3.1. Expression of M and N proteins

Bacterial plasmid expression constructs encoding full-length M and N proteins tagged with glutathione S-transferase (GST) were previously cloned in the Molecular Biology and Virology Research Laboratory at the University of the Western Cape. To obtain full-length proteins for use in screening polyclonal (serum) and monoclonal (hybridoma supernatant) antibodies, these pFN2a Flexi Vector constructs were used to express these tagged proteins in a KRX *Escherichia coli* (*E. Coli*) strain (L3002, Promega), using an early autoinduction protocol (Schagat et al., 2008). Briefly, cryofrozen glycerol stocks of KRX containing either pF2Na-MGST or pF2Na-NGST were thawed, and a sterile loop used to perform a four-way streak for single colonies on Luria-Bertani (LB) agar plates. Plates were incubated at 37°C for 16 – 20 hours. LB broth 10mL starter cultures were inoculated with the appropriate single bacterial colony and tubes were incubated overnight at 37°C, shaking at approximately 220 rpm. Starter cultures were diluted 1:100 (4mL into 400mL) into larger LB broths. A total of 20% D-Glucose (G8270, Merck) and 20% L-Rhamnose (83650, Merck) were added to the larger broths to a final working concentration of 0.05% and 0.2%, respectively. Flasks were incubated for 8 hours at 37°C, shaking at 220 rpm. Following incubation, cells were pelleted by centrifugation at 4°C for 15 minutes at 4 000 rpm. Pellets were either processed immediately (see Section 3.1.2.2) or stored at -80°C for future use.

3.1.3.2. Cell lysis

E. Coli expression pellets were weighed and resuspended in a 4mL *E. Coli* lysis buffer – 2mL lysis buffer per gram of pellet weight (see Appendix 2 for *E. Coli* lysis buffer recipe). Cells were incubated on ice for 20 – 30 minutes and then sonicated (four cycles – ten second spin, one minute rest on ice). Samples were centrifuged at 12 000 rpm for 25 minutes at 4°C to separate the soluble (supernatant) and insoluble (pellet) fractions. The supernatant was aspirated, re-sonicated (four cycles), and once again, the supernatant was separated out. These clarified whole cell lysates were aliquoted and stored at -20°C for future analysis. The insoluble fractions and unlysed cell pellets from the first round of centrifugation were also stored at -20°C.

3.1.3.3. GST-purification protocol

Soluble whole cell lysates containing NGST or MGST were purified with the MagneGST™ protein purification system (V8600, Promega) according to manufacturer instructions. Briefly, 100µL paramagnetic beads were added to a 1.5mL microcentrifuge tube and then bound on a magnetic stand. Beads were washed three times with wash buffer, and 200µL of the appropriate lysates were added to the beads to be bound by the beads. Beads were then bound on the magnetic stand again, and any unbound lysate was removed. Beads were washed three times to remove any unbound proteins, and GST-tagged proteins were then eluted from the beads in 100µL Glutathione elution buffer. Purified proteins were stored at -20°C.

3.1.3.4. On-column cleavage

In order to obtain untagged Membrane and Nucleocapsid proteins, tobacco etch virus (TEV) cleavage was performed using a modified GST-purification protocol. Following the same protocol as stated in Section 3.1.3.3 above, after binding the cell lysate to the beads and washing away unbound proteins, beads were removed from the magnetic stand and 'on-column cleavage' was done by incubating the protein-bound beads with ProTEV protease enzyme (V6101, Promega), according to manufacturer instructions in a final reaction volume of 300µL/tube with reagent volumes adjusted accordingly. Briefly, 6µL ProTEV plus (10U, V610A, Promega) was diluted in 1X ProTEV buffer (20X, V602A, Promega), containing 1mM dithiothreitol (DTT) (P117B, Promega), in a final volume of 300µL. Reactions were incubated at 4°C for 4 – 6 hours on a nutating mixer. Following cleavage, beads were once again placed on the magnetic stand and supernatants (containing TEV reaction mixture and GST tag proteins) were removed. Beads were washed three times, and untagged proteins were then eluted from the beads in 100µL Glutathione elution buffer. Purified proteins were stored at -20°C.

3.1.3.5. Screening tail blood – Enzyme-linked immunosorbent assay (ELISA)

Assays were carried out in 96-well Nunc-Immuno MaxiSorp plates (44-2404-21, ThermoFisher Scientific). In order to establish a polyclonal antibody titer within mouse serum, one plate was coated

for screening serum samples (pre-immune, post-immune 1, and post-immune 2) against each peptide. Plates were coated with 50µL peptide antigen per well consisting of N-N (at 1µg/mL), N-C (at 1µg/mL) and M-C (at 1µg/mL), respectively. Dilution from stock concentration of Ags (5mg/mL) was done in Wash buffer (WB – 0, .1% Tween 20; 1xPBS). Plates were coated overnight at 4°C (additional plates coated for future use were decanted and stored at -20°C). Plates were decanted and washed five times in WB and blocked with 2% human serum albumin (HSA) at 200µL/well for 1 hour at room temperature (RT) on a shaker. Plates were washed five times and dried. Doubling dilutions of serum (in 0.1% HSA diluent) was done from row 1 (1/100 dilution) down to row 7 (1/6400). The entire row 8 contained diluent only (see Table 3.1 below).

TABLE 3.1. 96-WELL PLATE LAYOUT FOR SCREENING POLYCLONAL SERUM

		1	2	3	4	5	6	7	8	9	10
		Pre-immune		Post-immune 1		Post-immune 2		Post-immune 3		Post-immune 4	
A	1/100										
B	1/200										
C	1/400										
D	1/800										
E	1/1600										
F	1/3200										
G	1/6400										
H	diluent										

Plates were incubated at RT for 1 hour on a shaker and then washed five times. Secondary rabbit anti-mouse antibody (cat#, supplier – Pools PAb), conjugated to HRP (Horse Radish Peroxidase) enzyme, was added at 1:5000 dilution at 50µL/well. Plates were incubated on a shaker for no longer than 1 hour and then washed a total of seven times. Pre-warmed substrate (37°C), tetramethylbenzidine (TMB) (5120-0053 (50-76-11), Sera care KPL) was added to each well (50µL/well) and plates were incubated in the dark for 2 – 15 minutes until adequate reaction colour formation. Following incubation, 50µL per well of Stop solution (0.5M H₂SO₄) was added, and optical densities were measured immediately with a spectrophotometer at 450nm.

3.1.3.6. Screening tail blood – Western blot

Proteins were separated by size by running cell lysates on a 12.5% denaturing polyacrylamide gel (SDS-PAGE) compared to a protein marker. Total proteins were then transferred to a polyvinylidene fluoride (PVDF) membrane (wet transfer system, 90V for 95 minutes). Unbound sites on the membrane (background) were blocked with 2% HSA at room temperature for 2 hours, with slight agitation on a tube roller. The primary antibody used was polyclonal antiserum (anti-N – mouse 1 post-immune 4; anti-M – mouse 2 post-immune 3) diluted (1/800* for N-antisera; 1/500* For M-antisera) in 0.2% HSA diluent. Primary antibody incubation was done at 4°C overnight with mixing (tube roller). Following incubation,

membranes were washed with 1xPBST wash buffer for 15 minutes at room temperature on a rocker. Washing was repeated with fresh buffer three times. Secondary antibody incubation with HRP-conjugated goat anti-mouse antibody was carried out at room temperature for a maximum of 1 hour with agitation/mixing. Blots were washed four times in fresh wash buffer and then 1 – 2mL of pre-warmed (37°C) TMB membrane substrate (5420-0025 (50-77-00), Sera care KPL) was added to each membrane followed by incubation in the dark for 1 – 10 minutes to allow reaction development (purple/blue colour precipitate). Following the appropriate incubation time with TMB, membranes were rinsed with distilled water to decrease background staining further.

*Working PAb concentrations were estimated from previous ELISA (enzyme-linked immunosorbent assay) results

3.1.4. Hybridoma generation and selection

3.1.4.1. Culturing of Sp2/0-Ag14 myelomas

Sp2 murine myeloma cells were seeded from frozen stocks and maintained in Sp2 full growth media (EX-CELL) in T25 and then T75 cell culture treated flasks in a 37°C incubator with 5% CO₂.

3.1.4.2. Booster immunisations

Three days prior to sacrificing the immunised mice, booster immunisations were administered. These boosters contained only diluted antigen at 50µg/100µL in 1xPBS; no adjuvant was included. Each mouse was immunised intra-peritoneally with 100µL of the antigen solution.

3.1.4.3. Animal sacrifice and spleen harvesting

Approximately 72 hours after the booster immunisations, mice were sacrificed individually by cervical dislocation. Each mouse was then sterilised by submersion in 70% ethanol and laid down on its back. A vertical incision was made along the midline through the abdomen. Skin and fascia were pulled away, and the spleen was carefully removed from the abdominal cavity. Each spleen was transferred to a 60mm petri dish, and approximately 10mL of serum-free media was added to the dish. A depressive force was applied multiple times to the spleen with the rubber stopper end of the inner part of a 5mL syringe. This action served to break up the splenic tissue and to separate cells into a solution. The cells were then resuspended by pipetting gently up and down (serological pipette), and the 10mL volume was transferred to a 15mL conical tube and centrifuged at 2 000 rpm for 10 minutes.

3.1.4.4. B cell in vitro immunisation

Splenocytes were incubated in a peptide-media solution prior to fusion with myeloma cells, to promote clonal expansion/mitosis of the B cells. The *in vitro* boost solution consisted of full hybridoma growth media without fetal bovine serum (FBS), as well as the appropriate peptide antigen at a final working

concentration of 5µg/mL. Peptide-media solutions were filter-sterilised prior to use. Following the centrifugation of splenic cells mentioned above (booster immunisations, animal sacrifice, and spleen harvesting), supernatants were decanted, and the cell pellets were resuspended in the appropriate peptide antigen solution. Cell solutions were transferred to a T25 cell culture treated flask and incubated at 37°C with 5% CO₂ for four to five days.

3.1.4.5. B cell fusion

On the day of cell fusion, 2 x T75 flasks confluent with Sp2 murine myelomas were harvested. Cells were loosened from the treated flask surface by pipetting media with slight force over the monolayer. Cells were resuspended and added collectively to a 50mL conical tube and filled up to 50mL with full Sp2 media. The *in vitro*-boosted murine B cells in a T25 flask were washed with 10mL of serum-free media and then also loosened and added to a separate 50mL conical tube. Both the myelomas and B cells were centrifuged at 2 000 rpm for 10 minutes. After decanting supernatants, cells in each tube were resuspended in 1mL EX-CELL media without FBS, and 10µl of each cell type was used to do a cell count on the haemocytometer. Approximately equal numbers of myelomas and B cells (cell count yielded 2.5×10^7 myelomas and 2.9×10^7 B cells) (10mL + 10mL) were added together in a 50mL conical tube and 1xPBS was added up to 35mL. Cells were centrifuged at 2 000 rpm for 10 minutes at room temperature. PBS was completely removed, and cell pellets were very slowly resuspended in 1mL of pre-warmed (37°C), undiluted polyethylene glycol (PEG) (02393, Supelco-Merck). Resuspension was done by slow PEG addition while rotating the tube to avoid shocking the cells. The 1mL of PEG was added over at least 90 seconds after which cells were incubated in the PEG for one minute at 37°C (held in hand). Following PEG addition, 4mL of serum-free growth media (RPMI-1640) was very slowly added to the cells, dropwise, at a rate of approximately 1mL per minute, in order to avoid cellular osmotic shock. With the addition of PEG, as well as fresh media, aggregates/clumps of cells began to form. Care was taken not to disturb or break up these fusing cells while carrying out resuspension. Once the cells had been resuspended in 4mL of media, additional serum-free media was added up to 20mL, and the cells were centrifuged at 2 000 rpm for 10 minutes. Supernatants were decanted, and cell pellets resuspended first in 1mL full hybridoma media with 1X hypoxanthine-aminopterin-thymidine (HAT) supplement (21060017, ThermoFisher Scientific) after which HAT-supplemented media was added up to 50mL and cells were gently mixed by inverting the tube once only. From this cell suspension, 5 x 96-well plates were seeded at 100µl per well (five plates each for M and N). Plates were incubated at 37°C with 5% CO₂. After 72 hours, 100µl fresh HAT media was added to each well.

3.1.4.6. Repeating N-peptide antigen administration: Single-round immunisation

Hybridoma cells generated against N were compromised at a crucial developmental/growth stage (unexpected CO₂ cuts to the building incubators). While colonies of cells did form, all the cells died between four to five days post-fusion. A single male mouse, of the same age as those previously used, was immunised with the following formulation:

	100µl N-N peptide antigen (@ 1mg/mL)
+	100µl N-C peptide antigen (@ 1mg/mL)
+	200µl Complete Freund's Adjuvant (CFA)
<hr/>	
=	400µl (total antigen concentration of 50µg/100µl; 25µg of each antigen per 100µl)

The final immunisation volume was 200µl, and the immunisation was administered intra-peritoneally.

The N-immunised mouse received only a single immunisation and was sacrificed 72 hours post-immunisation. At this point, the animal's spleen was harvested (see Section 3.1.3.3) and processed identically to the samples from the M-immunised mice (see Sections 3.1.3.4 and 3.1.3.5).

3.1.5. Screening and cloning of hybridoma cell lines

3.1.5.1. Original hybridoma screen – peptide ELISA, protein ELISA

The supernatants/media of growing hybridomas were screened for the first time seven days post-fusion. Antibodies in these media were tested using an indirect ELISA against M-C, N-N, and N-C peptides, as well as full-length M and N proteins (see Section 3.1.3.1. for expression details). Briefly, Nunc MaxiSorp 96-well plates were coated with either 0.1µg/mL full-length protein or 1µg/mL peptide antigen. Wells were coated with 50µl per well, and plates incubated overnight at 4°C (fridge). Following incubation, plates were decanted and washed five times in 1xPBST (1xPBS + 0, 1% Tween-20) with agitation (360° shaker/rotator). Blocking of unbound sites was done with the addition of a high protein block solution (2% HSA in 1xPBS) at 50µl/well. Blocking was done for 2 hours at room temperature with agitation. Hybridoma supernatants containing antibodies were added (neat/undiluted) to the appropriate wells at 50µl per well. Primary antibody incubation was done for at least 1 hour at room temperature with agitation. Plates were washed five times after primary antibody incubation and secondary rabbit anti-mouse antibody, conjugated to HRP enzyme (diluted 1:5000 in dilute protein block 0.2% HSA), was added to each well at 50µl per well. Plates were incubated for no longer than 1 hour at room temperature with agitation and then washed seven times in 1xPBST. Following this last wash, 50µl of pre-warmed (37°C) TMB Microwell Substrate was added to each well. Plates were incubated in the dark at room temperature for 2 – 15minutes to allow for colour development. Checking periodically, once the desired blue colour formation occurred, Stop solution (0.5M H₂SO₄/sulfuric acid) was added to each well at 50µl

per well. Adding Stop solution turned the blue reaction colour to a yellow end product (acid terminates enzyme-substrate reaction). Plates were read within 10 minutes after adding Stop solution, with a spectrophotometer measuring absorbance at 450nm.

3.1.5.2. ELISA screening of hybridoma supernatants

In order to assess the binding of each surviving hybridoma cell line, a binding kinetics assay was performed via indirect ELISA. Nunc 96-well MaxiSorp plates were coated with either the appropriate peptide antigen at 1µg/mL or the appropriate protein (GST-tagged) at 0.1µg/mL. The same indirect ELISA protocol was followed as previously stated (see Section 3.1.5.1) except for primary antibody addition (hybridoma media). Collected media containing antibodies was added to the wells vertically down the plate at different dilutions (neat; 1/10 (lowest dilution – top well); 1/100; 1/500; 1/1000; 1/2000). Hybridoma media was diluted in 0.2% HSA diluent. The final well in each column received diluent only (no antibodies).

3.1.5.3. Western blot screening of hybridoma supernatants

Proteins were separated by size by running lysates on a 12.5% denaturing polyacrylamide gel (SDS-PAGE), in comparison with a protein marker. Total proteins were then transferred to a PVDF membrane (wet transfer system, 90V for 95 minutes). Unbound sites on the membrane (background) were blocked with 2% bovine serum albumin (BSA) at room temperature for 2 hours, with slight agitation (tube roller). Membranes were incubated with primary antibodies in hybridoma (5F2) supernatant (either neat or diluted 1/50) at 4°C overnight, with slight agitation. Following incubation, membranes were washed with 1xPBST wash buffer for 15 minutes at room temperature on a rocker. Washing was repeated with fresh buffer three times. Secondary antibody incubation with HRP-conjugated goat rabbit-mouse antibody (61-6520, Invitrogen), diluted 1/5000, was carried out at room temperature for a maximum of 1 hour with agitation/mixing. Blots were washed four times in fresh wash buffer, then 1 – 2mL of pre-warmed (37°C) TMB membrane substrate was added to each membrane followed by incubation in the dark for 1 – 10 minutes to allow reaction development (purple/blue colour precipitate). Following the appropriate incubation time with TMB, membranes were rinsed with distilled water to decrease background staining further.

3.1.5.4. Limiting dilution cloning of hybridoma cell lines - First cloning and screening first-round clones

In order to isolate pure hybridoma colonies, hybridoma cell lines, which screened positive against their appropriate peptide antigens, were seeded at one cell per well. Briefly, hybridoma cells were loosened (treated cell culture plate/flask) and centrifuged at 2 000 rpm for 3 minutes. Cell pellets were resuspended in 1mL fresh hybridoma growth media, and 10µL of cell suspension was used to perform a cell count on a haemocytometer. Cells were then seeded in a 96-well plate at a density of one cell/well

in 50 – 100µL media over 48 wells. Plates were incubated at 37°C with 5% CO₂ and checked every 24 – 48 hours in order to monitor cell colony growth. Fresh media was added to wells as appropriate when necessary, and hybridoma media was screened again when colonies of cells were large enough. Screening hybridomas was done following the same procedure as previously used. The clones with the highest positive results were selected for a further round of cloning.

3.1.5.5. Second cloning and screening second round clones

Previously screened positive hybridoma cell lines were seeded again at one cell per well. Briefly, hybridoma cells were loosened (treated cell culture plate/flask) and centrifuged at 2 000 rpm for 3 minutes. Cell pellets were resuspended in 1mL fresh hybridoma growth media, and 10µL of cell suspension was used to perform a cell count on a haemocytometer. Cells were then seeded in a 96-well plate at a density of one cell/well in 50 – 100µL media over 48 wells. Plates were incubated at 37°C with 5% CO₂ and checked every 24 – 48 hours in order to monitor cell colony growth. Fresh media was added to wells as appropriate when necessary, and hybridoma media was screened again when colonies of cells were large enough. Screening hybridomas was done following the same procedure as previously used (indirect ELISA – see Section 3.1.5.1). The clones with the highest positive results were selected for a further round of cloning.

3.1.5.5. Binding kinetics assay

In order to assess the binding affinities of antibodies from each selected hybridoma cell line, a binding kinetics assay was performed via indirect ELISA. Nunc 96-well MaxiSorp plates were coated with either the appropriate peptide antigen at 1µg/mL or the appropriate protein (GST-tagged) at 0.1µg/mL. The same ELISA protocol was followed as previously stated (see Section 3.1.5.1) except for primary antibody addition (hybridoma media). Collected hybridoma media was added to the wells vertically down the plate at different dilutions ranging from 1/10 (lowest dilution – top well) to 1/640. Media was diluted in 0.2% HSA diluent. The final well in each column received diluent only.

3.2. Assessing the *in vitro* interaction between the M and N structural proteins of HCoV-NL63

3.2.1. Cloning of the HCoV-NL63 M gene in a mammalian system

3.2.1.1. Preparation of vector for cloning – Restriction enzyme digest

The mammalian expression vector (plasmid) pXJ40-3'HA was used to clone the HCoV-NL63 M gene. This vector was previously used for the cloning and expression of the N gene (Chapter 3). As such, the same restriction enzymes, BamH1 and Xho1, were used to prepare the vector for ligation of the M gene. 5µg of plasmid DNA was digested with 2µl of BamH1 and 2µl Xho1. 10µl of buffer H and 0.5µl acetylated BSA were added to each reaction, as well as nuclease-free water up to a final volume of 50µl. The reaction was run in a thermocycler at 37°C for 90 minutes. Enzyme inactivation was then carried out at 65°C for 20 minutes. The sample product was mixed with loading dye (6:1) and electrophoresed through a 1% agarose gel containing ethidium bromide (EtBr). The gel was run at 70V for 80 minutes and then viewed under ultraviolet (UV) light to confirm the linearised pX40 vector at the correct size (bp). Bands of interest were cut out and DNA purified using the peqGOLD Cycle-Pure Kit, according to manufacturer instructions (previously described). DNA was eluted from the column in a final volume of 30µL.

3.2.1.2. Preparation of the gene for cloning – Restriction enzyme digest of M

In order to create compatible sticky ends for M for directional cloning into the pXJ40-HA, the M gene was digested with the same enzymes as the pXJ40-HA vector. The M gene was digested out of pFastbac1, a baculovirus vector previously used to clone M ([section 3.4.2.](#)) with BamH1 and Xho1. 5µg of pFastbac1-M was digested with 2µL of each enzyme, BamH1 and Xho1. 10µl of buffer H and 0.5µl acetylated BSA were added to the reaction, as well as nuclease-free water up to a final volume of 50µl. The reaction was run in a thermocycler at 37°C for 90 minutes. Enzyme inactivation was then carried out at 65°C for 20 minutes. The sample product was mixed with loading dye (6:1) and electrophoresed through a 1% agarose gel containing EtBr. The gel was run at 70V for 80 minutes and then viewed under UV light to confirm the gene at the correct size (bp). The DNA fragment of interest was cut out of the gel and purified using the peqGOLD Cycle-Pure Kit, according to manufacturer instructions (previously described). DNA was eluted from the column in a final volume of 30µL.

3.2.1.3. Generating the pXJ40-HA-M construct – Ligation

Two ligation reactions were set up to ligate the M gene into the pXJ40-HA vector. One reaction tube contained 1µL pXJ40-HA vector DNA, 16µL M gene DNA, 2µL 10X ligase buffer, and 1µL T4 DNA ligase. The other ligation reaction included 2µL pXJ40-HA vector DNA, 15µL C, 2µL 10X ligase buffer, and 1µL T4 DNA ligase. The final reaction volume was 20µL. Tubes were incubated at 4°C overnight. Ligation reactions were used to transform JM109 *E.Coli* competent cells. Briefly, competent cells were

removed from -80°C and thawed on ice. Once thawed, 50µL was added to each pre-cooled reaction tube. 10µL of each ligation was added to 50µL cells, gently flicked to mix, and placed on ice for 30 minutes. Tubes were then 'heat-shocked' in a 42°C water bath for 45 seconds, then placed back on ice for 2 minutes. 950µL of room temperature LB broth was added to each reaction, and tubes were incubated at 37°C, shaking for 90 minutes. Following incubation, cells were pelleted at 3 000 rpm for 10 minutes, 800µL of media was removed, and pellets were resuspended in the remaining 200µL. Entire reaction volumes (200µL) were plated on LB agar plates containing 50mg/mL Ampicillin (antibiotic selection), 0.1M IPTG, and 30mg/mL X-Gal (for blue/white colony screening). Plates were incubated at 37°C for 14 – 18 hours. Following incubation, white colonies were picked and inoculated into LB broth containing Ampicillin and incubated at 37°C, shaking for 14 – 18 hours. Cells were pelleted at 4 000 rpm for 10 minutes, and DNA was purified using the NucleoBond PC 100 DNA purification kit (Machery-Nagel), according to manufacturer instructions. Recombinant DNA samples were quantified using the NanoDrop 2000.

3.2.1.4. Generating the pXJ40-HA-M construct – Confirmation of pXJ40-M clones

Restriction endonuclease digest reactions were performed to confirm successful recombinant pXJ40-3'HA-M constructs. The M gene was digested out of pXJ40-3'HA with BamH1 and Xho1. Reactions were performed in 500µl polymerase chain reaction (PCR) tubes, and each reaction tube contained approximately 600ng pXJ40-3'HA-M DNA, 1µl of each enzyme BamH1 and Xho1, 10µl of buffer H and 0.5µl acetylated BSA. Nuclease-free water was added to each tube up to a final reaction volume of 50µl. The reaction was run in a thermocycler at 37°C for 90 minutes. Enzyme inactivation was then carried out at 65°C for 20 minutes. The sample product was mixed with loading dye (6:1) and electrophoresed through a 1% agarose gel containing EtBr. The gel ran at 70V for 80 minutes and was viewed under UV light to confirm the recombinant DNA at the correct size (bp). *E.Coli* cells (JM109) containing the confirmed DNA constructs were grown up in large culture volumes. Glycerol stocks were used to inoculate 10mL LB broths containing Ampicillin and starter cultures were incubated at 37°C, shaking at approximately 225 rpm for 8 hours. Starter cultures were diluted into larger 400mL LB broth and incubated at 37°C, shaking at ~225 rpm for 14 – 18 hours. Following incubation, cultures were spun down at 4°C at 4 000 rpm for 15 minutes. Plasmid DNA was purified out of the cells using the NucleoBond Xtra Midi kit (Machery-Nagel), according to manufacturer instructions. Purified DNA samples were quantified with the NanoDrop 2000.

3.2.2. Co-expression of the M and N proteins in Cos7 cells

3.2.2.1. Transfection and co-transfection

Cos7 (African Green monkey kidney epithelial) cells were seeded from frozen stocks, grown, and maintained in complete Dulbecco's Modified Eagle Media (DMEM) supplemented with 10% FBS. Cells were maintained in a 37°C incubator with 5% CO₂. Cells were transfected with pXJ40-3'HA constructs containing the M gene. Cells were seeded/plated in 6-well tissue culture plates at a density of 500 000 cells in 2mL of complete media (250 000 cells/mL). Cells were monitored and grown to 80 – 90% confluency at the time of transfection. For each transfection reaction, i.e., per well, 6µL Lipofectamine 2000 reagent was diluted in 150µL reduced-serum Opti-MEM media. 1µg, 2µg, and 4µg of pX40-3'HA-M DNA was diluted in 150µL Opti-MEM media. For co-transfection experiments with M and N, a previously generated pXJ40-FLAG-N DNA construct ([section 3.3.1.10](#)) was used in conjunction with pXJ40-3'HA-M DNA. For each experimental well, either 1µg of pXJ4-3'HA-M DNA and 1µg pX40-FLAG-N DNA, or 2µg of pXJ4-3'HA-M DNA and 2µg pXJ40-FLAG-N DNA were diluted together in 150µL Opti-MEM media. In order to equalise total DNA in each well, empty pXJ40-3'HA vector DNA was added up to 4µg total DNA/well. Diluted DNA was added to the diluted Lipofectamine 2000 and incubated for 5 minutes at room temperature to form DNA-lipid complexes. 250µL of the appropriate DNA-lipid complex was added, dropwise, to the cells in each well. Plates were incubated in a 37°C incubator with 5% CO₂. After 24 and 48 hours of incubation, cells were harvested and lysed. Briefly, after removing media, the cells in each well were washed three times with 1mL of cold (4°C) 1xPBS. 200µL of cold radioimmunoprecipitation assay (RIPA) lysis buffer was then added to each well, and cells were detached using a cell scraper. After homogenising the cell suspension by pipetting, cells were transferred to 1.5mL tubes and centrifuged at 14 000 rpm for 20 minutes in a 4°C microcentrifuge. Following centrifugation, clarified supernatant (cell lysate) was removed and stored at -20°C for further analysis.

3.2.2.2. BCA protein quantitation assay

The protein concentrations of the Cos7 experimental lysates were determined by BCA protein assay. The relative concentrations of the lysates were calculated with the use of a standard curve equation. The standard curve was generated for each experiment by plotting the absorbance of a range of dilutions of protein diluted in the specific cell lysis buffer. BSA was made up to a range of dilutions (2mg/mL; 1.5mg/mL; 1mg/mL; 0.75mg/mL; 0.5mg/mL; 0.25mg/mL; 0.125mg/mL; 0.025mg/mL) in 1.5mL microcentrifuge tubes. The microplate procedure was performed in a 96-well flat-bottomed Greiner plate (cat #, supplier). Each standard curve dilution was added in duplicate to the appropriate wells (highest to lowest across row A and B). 25µL of cell lysate was added, in duplicate, to the appropriate wells. Working reagent was added to all wells at 200µL/well, and plates were mixed

thoroughly by vortexing for 30 seconds. Plates were covered in foil and incubated at 37°C for 30 minutes to 1 hour. Following incubation, plates were cooled down to room temperature and then read on a spectrophotometer at 562nm.

3.2.2.3. SDS-PAGE and Western blotting

Proteins were separated by size by running lysates on a 12.5% denaturing polyacrylamide gel (SDS-PAGE), in comparison with a protein marker. Total proteins were then transferred to a PVDF membrane (wet transfer system, 90V for 95 minutes). Unbound sites on the membrane (background) were blocked with 2% BSA at room temperature for 2 hours, with slight agitation (tube roller). Membranes were treated with the appropriate primary antibody or antibodies. The mouse monoclonal anti-FLAG (anti-OctA, F-tag-01, sc-51590, Santa Cruz Biotechnology) primary antibody was used at 1/1000 (250mg/mL), and the rabbit polyclonal anti-HA (Y-11, sc-805, rabbit polyclonal, Santa Cruz Biotechnology) was used at either 1/200 or 1/1000. Primary antibody incubation was done at 4°C overnight, with slight agitation. Following incubation, membranes were washed with 1xPBST wash buffer for 15 minutes at room temperature on a rocker. Washing was repeated with fresh buffer three times. Membranes were then incubated with the appropriate secondary antibody/antibodies. Both the goat anti-mouse (goat anti-mouse IgG-HRP: sc-2005, Santa Cruz Biotechnology) and the goat anti-rabbit (goat anti-rabbit IgG-HRP: sc-2004, Santa Cruz Biotechnology) antibodies were used at 1/1000 and incubation was done for 60 minutes at room temperature on a rocker. Following secondary antibody incubation, membranes were washed as previously described, and washing was repeated four times. Then, 1 – 2mL of pre-warmed (37°C) TMB membrane substrate was added to each membrane followed by incubation in the dark for 1 – 10 mins to allow reaction development (purple colour precipitate). Following the appropriate incubation time with TMB, membranes were rinsed with distilled water and then viewed.

3.2.2.4. Co-immunoprecipitation of M and N

In order to investigate protein-protein interactions between M and N, co-expression lysates were co-immunoprecipitated with both the anti-FLAG/anti-N and anti-HA antibodies. Briefly, 500µL of total cell lysate was incubated with the appropriate amount (2-5µg) of primary antibody, in the presence of pre-washed A/G-linked magnetic beads, and incubated at 4°C overnight on a nutating (top-over-bottom rotation) mixer. Following incubation, magnetic beads were bound on a magnetic stand. 1XTBST Wash buffer was added to the beads and the washing step was repeated twice in 500µL and 1mL wash buffer. Elution of the affinity-purified proteins from the beads was performed in 100µL low pH elution buffer (0.1M glycine, pH 2.0). Samples were immediately neutralized by the addition of 10µL high-ionic strength alkaline buffer (1M Tris, pH 7.5-9) per 100µL eluted protein sample. Co-immunoprecipitated samples were analysed by western blotting.

3.3. An *in vitro* localisation study on the HCoV-NL63 N protein

Another task of this body of work is to optimise the expression of HCoV-NL63 major structural proteins within a system that can produce proteins that have a native-like structure. When evaluating structural protein-protein interactions, it becomes essential for the proteins involved to be fully processed and mature within the expression system to get an accurate functional and structural representation, or at least one which mimics native protein as closely as possible. Mammalian cells are capable of expressing fully functional quaternary structures of proteins.

3.3.1. Cloning of the HCoV-NL63 N gene in a mammalian system

3.3.1.1. Preparation of vectors for cloning – Selecting restriction enzymes

The plasmid vector pXJ40 encodes a multiple cloning site (MCS), including recognition sites for various restriction endonucleases. In order to establish which enzymes to select, glycerol stocks of empty vectors pXJ40-FLAG and pXJ40-3'HA, in host cell JM109 *E. Coli* (L2005, Promega), were grown up and plasmid DNA was isolated using the PureYield Plasmid Miniprep System (A1223, Promega), according to manufacturer instructions. Briefly, single bacterial colonies on LB agar plates containing Ampicillin at 50µg/mL were inoculated into 20mL LB medium containing Ampicillin and incubated at 37°C overnight. The culture was pelleted 1.5mL at a time at 14 000 rpm and in two-minute intervals. Supernatants were discarded and pellets resuspended in 250µL resuspension buffer (Solution I), 250µL sodium dodecyl sulfate (SDS) and sodium hydroxide (Solution II), and 350µL neutralising solution (Solution III) to a final volume of 850µL. Microcentrifuge tubes were centrifuged at 14 000 rpm for 10 minutes. Spin columns were inserted into sterile microcentrifuge tubes, and 750µL of supernatant was added to the top of the column. After centrifugation, tube contents were discarded, and the membrane was washed once with 500µL plasmid buffer, spun down, and then washed twice with 750µL DNA wash buffer (+EtOH). Following washing and discarding flow through, tubes were dry centrifuged to get rid of excess EtOH. DNA was eluted from the membrane using 50µL elution buffer and centrifuging at 14 000 rpm for one minute. DNA samples were stored at -20°C for further use.

Purified vector DNA was quantified using the Qubit system, and 0.5µg DNA was used in each reaction. Vectors were cut using Not1, Xho1, Hind3, and BamH1 (Promega products R6431, R6161, R6041, and R6021). These enzymes were tested based on the vector map, as well as those enzymes available in the laboratory. A single enzyme digest was performed in all cases, using the pXJ40-FLAG and pXJ40-3'HA vectors. Generally, 0.5µg DNA was digested with 1µl of the specific restriction enzyme in a reaction tube containing 2µl 10x Flexi Digest Buffer, 0.5µl acetylated BSA, and nuclease-free water to make up a final reaction volume of 20µl. The digest was run in a thermocycler at 37°C for 90 minutes, followed by enzyme inactivation at 65°C for 15 minutes. Products were mixed with 6x blue/orange

loading dye (1:1) and loaded onto a 1% agarose gel containing ethidium bromide (EtBr) (H5041, Promega). The gel was run at 70V for 80 minutes, after which the gel was visualised under UV light for confirmation.

3.3.1.2. Preparation of vectors for cloning – Plasmid DNA purification

Both pXJ40-FLAG and pXJ40-3'HA were again grown up from glycerol stocks, streaked onto LB agar plates containing Ampicillin, after which single colonies were inoculated into 20mL LB broth (+Amp) and incubated at 37°C for 8 hours in order for cells to reach the log growth phase. Cultures were then diluted 1:100 into 250mL LB broth (+ Ampicillin) and grown at 37°C overnight, after which cells were pelleted at 4 000 rpm for 10 minutes at a time at 4°C. Plasmid DNA was isolated from the bacterial pellets using the NucleoBond DNA purification kit. Briefly, pellets were resuspended in 8mL buffer S1 (+RNase), and 8mL buffer S2 contents were mixed by inverting 6 – 8 times and incubated at room temperature (RT = 22°C – 25°C) for 3 minutes. 8mL of pre-cooled (4°C) buffer S3 was added to each sample tube and inverted 6 – 8 times to mix. At this point, a white flocculent formed, and samples were incubated on ice for 5 minutes. While incubating, columns were equilibrated using 2.5mL buffer N2 per column and allowed to empty by gravity. Samples were filtered by gravity through filter papers provided in the kit and cleared lysate was loaded onto columns and allowed to filter through by gravity. The DNA bound to the column was washed with 10mL buffer N3, and flow-through was discarded. Elution was done using 5mL buffer N5. Following elution, DNA was precipitated out of solution by adding 3.5mL isopropanol, mixing and pelleting at 14 000 rpm for 30 minutes at 4°C. 2mL 70% EtOH was added to the pellet, briefly vortexed, and centrifuged at 14 000 rpm for 10 minutes at RT. After centrifugation, EtOH was carefully aspirated, taking care not to disturb the clear DNA pellet, and tubes were left open to allow any excess ethanol to be removed. DNA was reconstituted in sterile distilled water, slowly over ~10minutes. Following purification, DNA concentrations were determined using the NanoDrop 2000.

3.3.1.3. Preparation of vectors for cloning – Restriction enzyme digest

Restriction enzymes BamH1 and Xho1 were chosen to perform a double-digest on pXJ40 vectors, as both these were confirmed previously to each cut only once within the vector sequence. Also, according to the vector map, the BamH1 and Xho1 recognition/cut sites lie > 12bp from each other, allowing for efficient cutting by each of the enzymes. A double-digest creates incompatible sticky ends, thereby ensuring that the plasmid vector does not self-ligate and re-circularise. It also allows for directional cloning of an insert into the vector. 5µg of plasmid DNA was digested with 2µl of BamH1 and 2µl Xho1. 10µl of buffer D was used, as both restriction endonucleases are functional (> 50% enzyme activity) in this buffer. 0.5µl acetylated BSA was added to each reaction, as well as nuclease-free water up to a final volume of 50µl. The reaction was run in a thermocycler at 37°C for 90 minutes.

3.3.1.4. Preparation of vectors for cloning – Alkaline phosphatase treatment

After digestion, 4µl calf-intestinal alkaline phosphatase (CIAP) (M1821, Promega) was added to each reaction tube and incubated at 37°C for 90 minutes. When the vector is cut and linearised, 5'-phosphate groups are generated. Dephosphorylation of these ends by alkaline phosphatase treatment prevents self-ligation/recircularisation. CIAP was inactivated at 65°C for 15 minutes, after which samples were mixed with 6x blue/orange loading dye (2:1) and loaded onto a 1% agarose gel containing EtBr. The gel was run at 70V for 80 minutes and then viewed under UV light to confirm linearised pXJ40 vectors at the correct sizes. Bands of interest were cut out and DNA purified using Wizard® SV Gel and PCR Clean-Up System (A9281, Promega), according to manufacturer instructions. Briefly, gel slices are weighed, and an equal amount of CP buffer was added to each tube. Tubes were then vortexed and kept at 60°C until the gel slice was completely dissolved. Samples were loaded onto a spin column and centrifuged at 14 000 rpm for one minute, after which columns were washed with wash buffer (+EtOH), dry centrifuged to remove excess EtOH, and DNA was eluted from the column in 30 – 50µL Elution buffer.

3.3.1.5. Preparation of vectors for cloning – DNA concentrations

Following gel purification, plasmid DNA was quantified using the Qubit system and Qubit BR dsDNA quantification kit, according to manufacturer protocol. Briefly, a working solution (WS) of reagent and buffer was made up in the correct ratio according to the number of samples ($n = 2$). Two standards were prepared (provided in the kit). Purified DNA to be quantified was then added to equal volumes of working solution in a ratio of 10µl DNA: 190µl WS, with a 200µL final volume. Samples were read using the Qubit fluorometer.

3.3.1.6. Preparation of the N gene for cloning – Checking gene insert

The gene of interest, full-length HCoV-NL63 N, had previously been cloned into a pF2Na Flexi Vector (pFN2A (GST) Flexi® Vector C8461, Promega). In order to confirm the presence of and assess integrity, pFlexi containing N in *E.Coli* KRX strain cells were grown up from glycerol stocks, single colonies from LB agar plates (+Amp) were inoculated into 20mL LB broth (+Amp) and incubated at 37°C overnight. Cells were pelleted and plasmid DNA isolated using the PureYield Plasmid Miniprep System (Promega), according to manufacturer protocol (as previously stated). DNA was quantified, and approximately 1µg of DNA was digested with 1µl Flexi enzyme blend, as pFN2a contains unique cut sites for SmaI and PmeI. 10µl Flexi Digest Buffer and 0.2µl BSA were added, and nuclease-free water was added up to a final volume of 30µl. The digest was run for 2 hours at 37°C, and enzymes then inactivated at 65°C for 15 minutes. Samples were run on a 1% agarose gel at 70V for 80 minutes and viewed under UV light to confirm N in pFN2a.

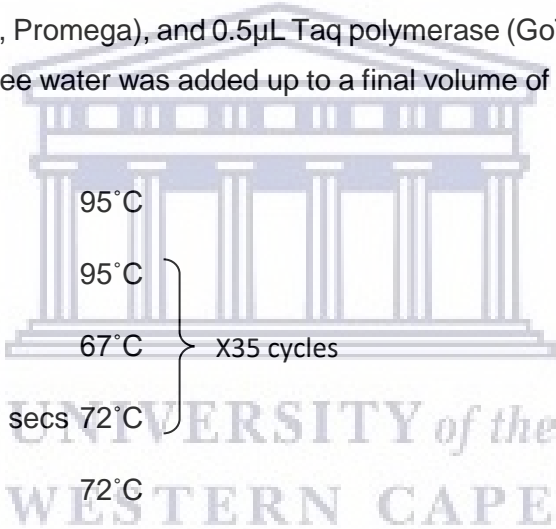
3.3.1.7. Preparation of the N gene for cloning – N primer design

In order to amplify the full-length N gene in the Flexi Vector, gene-specific (GS) primers were designed to flank and amplify the entire N gene (1.2KB). To allow for directional cloning into pXJ40 vectors, compatible sticky ends would need to be generated on either side of the N gene. To accomplish this, the PCR primers were designed to incorporate a restriction enzyme recognition site. As the vectors were cut using the enzymes BamH1 and Xho1, these primers were designed to incorporate a BamH1 cut site (GGA TCC) within the forward primer sequences, and an Xho1 cut site (CTC GAG) within the reverse primer sequences (see [Appendix 4](#) for all primer sequences).

3.3.1.8. Preparation of the N gene for cloning – PCR of N in pFlexi

DNA samples obtained from DNA purification were diluted 1/10 to a working concentration of 45.4ng/μL. From this, 5μL (~200ng) was used in each PCR, along with 2μL of both forward and reverse primers (either FLAG-N or 3'HA-N) and 8.5μL mastermix. Mastermix contained 2μL MgCl₂, 1μL dNTPs, 10μL Gotaq Flexi buffer, 1ml (M891A, Promega), and 0.5μL Taq polymerase (GoTaq® Flexi DNA Polymerase M8291, Promega). Nuclease-free water was added up to a final volume of 50μL. Thermocycler settings were as follow:

Pre-denaturation	3 mins	95°C	
Denaturation	1 min	95°C	} X35 cycles
Annealing	1 min	67°C	
Elongation	1 min 20 secs	72°C	
Final elongation	15 mins	72°C	



Following the reaction, a 15μL sample aliquot of both N-FLAG and N-3'HA was mixed with 5μL 6x loading dye and loaded onto a 1% agarose gel. Gel electrophoresis was done at 80V for 60 minutes, after which the gel was viewed under UV light, and DNA bands of interest (N) were excised and purified using the Wizard® SV Gel and PCR Clean-Up System (A9281, Promega).

3.3.1.9. Preparation of the N gene for cloning – Restriction endonuclease digest of N

In order to create compatible sticky ends on N for directional cloning into pXJ40 vectors, both N-FLAG and N-3'HA were digested with restriction enzymes BamH1 and Xho1. 1μg of N was digested with 1μL of each enzyme in 5μL 10x buffer D. Furthermore, 0.2μL acetylated BSA was added to each reaction, as well as nuclease-free water up to a final volume of 40μL. Digest was carried out at 37°C for 2 hours, followed by enzyme inactivation at 65°C for 15 minutes. Samples were run on a 0.7% agarose gel at 80V for 60 minutes, after which the gel was viewed under UV light, and N gene was excised and purified using the Wizard® SV Gel and PCR Clean-Up System (A9281, Promega).

3.3.1.10. Generating pXJ40-N constructs

DNA was quantified following restriction enzyme digest in order to calculate the amount of insert DNA to add in the ligation reaction. Insert and vector DNA was added in a molar ratio of 3:1. Using 100ng of vector DNA, the following equation was used to calculate the amount of insert DNA required:

$$\frac{\text{ng vector DNA} \times \text{size of insert (KB)}}{\text{size of vector (KB)}} \times \text{molar ratio of } \frac{\text{insert}}{\text{vector}} = \text{ng of insert DNA}$$

$$\frac{100\text{ng} \times 1,2\text{KB}}{5\text{KB}} \times \frac{3}{1} = 72\text{ng insert DNA}$$

Therefore, 3.6µL of pXJ40-FLAG vector DNA (from the previous quantification) + 4.9µL N-FLAG insert DNA and 3.9µL of pXJ40 3'HA vector DNA (from the previous quantification) + 5.8µL N-3'HA insert DNA were used. Ligation reactions included 1µL each of both 10x ligase buffer and T4 DNA ligase. Nuclease-free water was added to a final reaction volume of 20µL, and tubes were incubated at 4°C overnight. Ligation reactions containing recombinant DNA (N-pXJ40) were used to transform JM109 *E.Coli* competent cells. Briefly, competent cells were removed from -80°C and thawed on ice. Once thawed, 50µL was added to each pre-cooled reaction tube. 10µL of each ligation was added to 50µL cells, gently flicked to mix, and placed on ice for 30 minutes. Tubes were then 'heat-shocked' in a 42°C water bath for 45 seconds, then placed back on ice for 2 minutes. 950µL of room temperature LB broth was added to each reaction and tubes were incubated at 37°C, shaking for 90 minutes. Following incubation, cells were pelleted at 2 000 rpm for 10 minutes, 800µL of media was removed, and pellets resuspended in the remaining 200µL. Entire reaction volumes (200µL) were plated on LB agar plates containing 50mg/mL Ampicillin, 0.1M IPTG, and 30mg/mL X-Gal (for blue/white colony screening). Plates were incubated at 37°C for 14 – 18 hours. Following incubation, white colonies were selected and inoculated into LB broth containing Ampicillin and incubated at 37°C, shaking for 14 – 18 hours. Cells were pelleted at 4 000 rpm for 10 minutes, and N-pXJ40 DNA was purified using the NucleoBond PC 100 DNA purification kit (Machery-Nagel), according to manufacturer instructions (Machery-Nagel, 2020). DNA samples (recombinant vectors as well as 'empty' vectors) were quantified using the NanoDrop 2000.

3.3.2. Expression of the N protein in Cos7 cells

3.3.2.1. Transfection of Cos7 cells

Cos7 (African Green monkey kidney epithelial) cells were seeded from frozen stocks, grown and maintained in complete DMEM supplemented with 10% FBS. Cells were maintained in a 37°C incubator with 5% CO₂. Furthermore, pXJ40-FLAG and 3'HA constructs containing the N gene were transfected into Cos7 cells. Cells were seeded/plated in 6-well tissue culture plates at a density of 500 000 cells in 2mL of complete media (250 000 cells/mL). Cells were grown to 80 – 90% confluency at the time of transfection. For each transfection reaction, i.e., per well, 12µL Lipofectamine™ 2000 reagent (11668019, ThermoFisher Scientific) was diluted in 150µL reduced-serum OptiMEM media (31985062, ThermoFisher Scientific). 1µg, 2µg, and 4µg of pXJ40-N DNA were also diluted in 150µL OptiMEM media. In order to equalise total DNA in each well, empty pX40-FLAG and -3'HA vector DNA was added up to 4µg total DNA. The diluted DNA was then added to the diluted Lipofectamine 2000 and incubated for 5 minutes at room temperature to form DNA-lipid complexes. 250µL of the appropriate DNA-lipid complex was added, dropwise, to the cells in each well. Plates were incubated in a 37°C incubator with 5% CO₂. After 24-hour incubation, cells were harvested and lysed. Briefly, after removing media, the cells in each well were washed three times with 1mL of ice-cold 1xPBS. 200µL of ice-cold RIPA lysis buffer was then added to each well, and cells were detached using a cell scraper. After homogenising the cell suspension by pipetting, cells were transferred to 1.5mL tubes and centrifuged at 14 000 rpm for 15 minutes in a 4°C microcentrifuge. Following centrifugation, clarified supernatant (cell lysate) was removed and stored at -20°C for analysis.

3.3.2.2. SDS-PAGE and Western blotting

Proteins were separated by size by running lysates on a 12.5% denaturing polyacrylamide gel (SDS-PAGE) compared to a protein marker. Proteins were then transferred to a PVDF membrane (wet transfer system, 90V for 95 minutes). Unbound sites on the membrane (background) were blocked with 2% BSA at room temperature for 2 hours, with slight agitation (tube roller). Membranes were treated with anti-N primary antibody (anti-NL63 N mouse monoclonal, *Inmunología y Genética Aplicada SA* ((INGENASA), Madrid) at 1/1000 at 4°C overnight, with slight agitation. Following primary antibody incubation, membranes were washed with 1xPBST wash buffer for 15 minutes at room temperature, with slight agitation. Washing was repeated with fresh buffer three times. Membranes were then incubated with goat anti-mouse secondary antibody (1/1000) for 1 hour only at room temperature. Following incubation, membranes were washed as previously described, and washing was repeated four times. After that, 1 – 2mL of pre-warmed (37°C) TMB membrane substrate (5420-0029 (50-77-18), KPL South Africa) was added to each membrane, followed by incubation in the dark for 1 – 10 minutes to allow reaction development (colour precipitate). Following the appropriate incubation time with TMB,

membranes were rinsed with distilled water to halt further colour development and decrease background staining.

3.3.3. Localisation study of the N protein in Cos7 cells

3.3.3.1. Subcellular localisation of N protein in Cos7 cells by immunofluorescence (IF)

Cos7 cells were seeded for transfection in 60mm petri dishes at 600 000 cells/plate in 6mL of complete DMEM growth media. Prior to seeding cells, a glass coverslip (pre-treated with poly-L-lysine) was placed in the middle of each well. Treatment with poly-L-lysine ensures adherence/attachment of Cos7 cells to glass coverslips. Cells were grown to 80 – 90% confluency at the time of transfection. For each transfection reaction, 12µL Lipofectamine 2000 reagent was diluted in 150µL reduced-serum OptiMEM media. Furthermore, pXJ40-N DNA (4µg) was also diluted in 150µL OptiMEM media. The diluted DNA was then added to the diluted Lipofectamine 2000 and incubated for 5 minutes at room temperature to form DNA-lipid complexes. 250µL of the appropriate DNA-lipid complex was added, dropwise, to the cells in each well. Plates were incubated in a 37°C incubator with 5% CO₂. Cells were harvested after 6, 12, 18, 24, and 30 hours of incubation. For IF, coverslips were removed from wells and washed for five mins in 1xPBS with agitation (rocker). Cells were fixed and permeabilised in pre-chilled (-20°C) Acetone (100014, Supelco-Merck) by incubating for 10 minutes at -20°C. Cells were washed three times for 5 minutes each time and then blocked with 2% HSA for 2 hours at room temperature. Primary anti-N antibody (1/1000) was then added to blocking buffer and coverslips were incubated for 2 hours at room temperature, with slight agitation. Following primary antibody incubation, coverslips were washed three times and incubated with secondary rhodamine-conjugated anti-mouse antibody (31660, Invitrogen) at 1/1000 for 1 hour at room temperature, protected from light (covered in foil/darkroom), with slight agitation. Cells were washed 3 times and incubated with DAPI (62248, ThermoFisher Scientific) (diluted to working range of 15 – 20µg/mL in 1XPBS) for 5 minutes. For the final wash, coverslips were washed three times for 5 minutes with 1xPBST wash buffer. Coverslips were then placed (cells down) on to glass slides on top of a small drop of mounting media. Slides were stored at 4°C, protected from light. A Zeiss Axiovert 200M wide-field microscope system (Zeiss, Göttingen, Germany) for fluorescence light applications was used to view the IF slides. The microscope made use of a Zeiss Mercury Arc lamp (HBO-100). Appropriate filters were used, namely red excitation filter (540 nm), red emission filter (480 nm), blue excitation filter (359 nm), and blue emission filter (461 nm). Samples images were analysed with Axiovision software (version 4.9.1) at 10x and 40x magnifications.

3.4. Expression of the HCoV-NL63 M protein using a recombinant baculovirus in an insect cell system

3.4.1. Cloning of the HCoV-NL63 M gene in a baculovirus system

3.4.1.1. Preparation of the M gene primer design

In order to create compatible 'sticky ends' for cloning into subsequent expression vectors, oligonucleotide primers were designed to incorporate restriction enzyme cut sites flanking the M gene. The forward and reverse primers were designed to incorporate BamH1 (GGA TCC) and Xho1 (CTC GAG) restriction cut sites, at the respective M gene termini.

3.4.1.2. Preparation of the M gene – Checking gene insert

E. Coli glycerol stocks of pGEM-M (cloned with different, incompatible restriction sites EcoR1 and Not1) were inoculated on to LB agar plates containing Ampicillin (CAS 69-52-3|171254, Calbiochem) at 50µg/mL. 10mL LB broth cultures were inoculated with single colonies and grown for 14 – 18hrs at 37°C in a shaking incubator. Cells were pelleted by centrifugation, and plasmid DNA was purified using the Wizard Plus SV Miniprep System (A1330, Promega), according to manufacturer instructions (Brisco et al., 1996). Purified DNA was quantified using the NanoDrop 2000 (Thermo Scientific™), and ~400µg of each DNA sample was digested with EcoR1 restriction enzyme (*EcoR1*, R6011, Promega). Using EcoR1 allows for a single-enzyme digest to release any PCR fragment cloned into the pGEM (A362A, Promega) MCS. Reaction tubes included DNA template, 2µL EcoR1 enzyme, 3µL 10x Buffer D (R004A, Promega), and 0.5µL BSA (R3961, Promega). Nuclease-free water was added up to a final volume of 30µL. Digestion was performed at 37°C for 1 hour, followed by enzyme inactivation at 65°C for 15 minutes. Samples were loaded and run on a 1% agarose (50004, SeaKem® LE Agarose) TBE gel, at 80V for 70 minutes, after which the gel was viewed under UV light.

3.4.1.3. Preparation of the M gene – PCR of M in pGEM

Primers incorporating BamH1 and Xho1 cut sites were used to amplify the M gene from the pGEM vector. 2µL (~100ng) DNA was used in each PCR along with 1µL of each primer (forward and reverse) and 9.5µL mastermix. The mastermix was made using 1µL MgCl₂ (A3511, Promega), 1µL dNTPs (U1511, Promega), 5µL 5x Gotaq Flexi PCR buffer (M891A, Promega), and 0.5µL Gotaq DNA polymerase (M829A, Promega) per reaction. Nuclease-free water (P1195, Promega) was added up to a final volume of 25µL. Thermocycler settings were as follow:

Pre-denaturation	3 mins	95°C	
Denaturation	1 min	95°C	} X35 cycles
Annealing	1 min	67°C	
Elongation	1 min 20 secs	72°C	
Final elongation	15 min	72°C	

Following the reaction, samples were loaded and run on a 1% TBE agarose (50004, SeaKem® LE agarose) gel. Electrophoresis was performed at 80V for 70 minutes, after which the gel was viewed under UV light, and amplified bands of interest (M gene at ~681bp) were excised and purified using the Wizard® SV Gel and PCR Clean-Up System (A9281, Promega), according to manufacturer protocol.

3.4.1.4. Ligation into pGEM shuttle vector

Purified M gene (with flanking BamH1 and Xho1 restriction cut sites) was ligated into the pGEM shuttle vector. 8µL of sample DNA was used along with 1µL pGEM vector (A362A, Promega), 2µL 10x ligase buffer (C126A, Promega), and 1µL DNA ligase (M180A, Promega). Nuclease-free water was added up to a final reaction volume of 20µL. Ligations were done overnight at 4°C.

3.4.1.5. Transformation into competent *E.Coli* cells

Ligation reactions (M-pGEM) were transformed into JM109 competent *E.Coli* cells (L2005, Promega). Briefly, competent cells were removed from -80°C and thawed on ice. Once thawed, 50µL was added to each pre-cooled reaction tube. 10µL of each ligation was added to 50µL competent cells, gently flicked to mix, and placed on ice for 30 minutes. Tubes were then placed in a 42°C water bath for 45 seconds, then placed back on ice for 2 minutes. 950µL of room temperature LB broth (see Appendix 2 for recipe) was added to each reaction and tubes were incubated at 37°C, shaking for 90 minutes. Following incubation, cells were pelleted at 2 000 rpm for 10 minutes, 800µL of media was removed, and cell pellets were resuspended in the remaining 200µL. Entire reaction volumes (200µL) were plated on LB agar (see Appendix 2 for recipe) plates containing 50µg/mL Ampicillin (CAS 69-52-3|171254, Calbiochem), 0.1M IPTG (V395D, Promega), and 30mg/mL X-Gal (V3941, Promega) for blue/white colony screening. Plates were incubated at 37°C for 14 – 18 hours.

3.4.1.6. Confirmation of successful clones

White colonies were inoculated into LB broth containing Ampicillin and incubated at 37°C, shaking for 14 – 18 hours. Cells were pelleted at 14 000 rpm for 2 minutes, and M-pGEM DNA was purified using the Wizard Plus SV Miniprep System (A1330, Promega), according to manufacturer instructions. Following quantification of the DNA (NanoDrop 2000), an enzyme digest was performed using BamH1 and Xho1 restriction enzymes (R6021 and R6161, Promega). This digest served to confirm both the

presence of the M gene in the pGEM shuttle vector and the functionality of the incorporated cut sites. 10µL of DNA was digested using 1µL of each enzyme, 2.5µL of 10x Buffer D (R004A, Promega), and 0.5µL BSA (R3961, Promega). Nuclease-free water was added up to a final volume of 25µL. Digests were performed in a thermocycler at 37°C for 1 hour, followed by 65°C for 15 minutes to inactivate the enzymes. Reactions were loaded and run on a 1% TBE agarose gel. Electrophoresis was done at 80V for 70 minutes, and the gel was viewed under a UV light. The released M fragment was then excised and purified using the Wizard® SV Gel and PCR Clean-Up System (A9281, Promega), according to the manufacturer protocol.

3.4.2. Generation of a recombinant bacmid-M DNA

3.4.2.1. Cloning into pFastbac1 vector– Restriction enzyme digest

To ligate the M gene fragment into the pFastbac1 vector, compatible 'sticky ends' in the vector and the gene were generated by digestion with BamH1 and Xho1 restriction enzymes. 1µg (200µL) pFastbac1 (pFB1) vector (10360014, Gibco) and 1µg (10µL) M gene were digested using 1µL of each enzyme, 3µL 10x Buffer D, and 0.5µL BSA, with nuclease-free water added up to a final reaction volume of 30µL. Digests were carried out at 37°C for 1 hour, after which an additional 1µL of each enzyme was added and digestion continued for a further 1 hour. Enzyme deactivation was done at 65°C for 15 minutes. Samples were loaded and run on a 1% TBE agarose gel. Electrophoresis was performed at 80V for 70 minutes, and the gel was viewed under a UV transilluminator light (UVP, Inc. Bio-Imaging Systems, USA). Digested pFastbac1 vector and digested M gene fragments were excised and purified using the Wizard® SV Gel and PCR Clean-Up System (A9281, Promega), according to the manufacturer protocol.

3.4.2.2. Cloning into pFastbac1 vector– Ligation of M into pFastbac1 (pFB1)

15µL of insert (M) DNA was used for ligation along with 1µL pFB1 DNA. Each reaction included 2µL 10x DNA ligase buffer (C126A, Promega), 1µL DNA ligase (M180A, Promega), and nuclease-free water up to a final reaction volume of 20µL. Ligations were carried out overnight at 4°C.

3.4.2.3. Cloning into pFastbac1 vector – Transformation into DH5α competent cells

Ligation reactions (M-pFB) were transformed into DH5α *E.Coli* (18258012, Invitrogen) cells. Briefly, competent cells were removed from -80°C and thawed on ice. Once thawed, 50µL was added to each pre-cooled reaction tube. 10µL of each ligation was added to 50µL cells, gently flicked to mix, and placed on ice for 30 minutes. Tubes were then placed in a 42°C water bath for 45 seconds, then placed back on ice for 2 minutes. 950µL of room temperature LB broth was added to each reaction and tubes were incubated at 37°C, shaking for 90 minutes. Following incubation, cells were pelleted at 2 000 rpm for 10 minutes, 800µL of media was removed and pellets resuspended in the remaining 200µL. Entire

reaction volumes (200µL) were plated on LB agar plates containing 50mg/mL Ampicillin, 0.1M IPTG, and 30mg/mL X-Gal (for blue/white colony screening). Plates were incubated at 37°C for 14 – 18 hours.

3.4.2.4. Confirmation of successful clones

White colonies were inoculated into LB broth containing Ampicillin and incubated at 37°C, shaking for 14 – 18 hours. Cells were pelleted at 14 000 rpm for 2 minutes, and M-pFB DNA was purified using the Wizard Plus SV Miniprep System (A1330, Promega), according to manufacturer instructions. Following quantification of the DNA (NanoDrop 2000), an enzyme digest was performed using BamH1 and Xho1 restriction enzymes. 8µL of M-pFB DNA was digested using 1µL of each enzyme, 4µL of 10x digest buffer H (R008A, Promega), and 0.5µL BSA. Nuclease-free water was added up to a final volume of 40µL. Digests were performed in a thermocycler at 37°C for 2 hours, followed by 65°C for 15 minutes to inactivate the enzymes. Reactions were loaded and run on a 1.2% TBE agarose gel. Electrophoresis was done at 80V for 70 minutes, and the gel was viewed under a UV light.

3.4.2.5. Transposition of pFB1 in the bacmid (baculovirus expression construct)

Purified M-pFastbac DNA was transformed into DH10BAC *E.Coli* (10361012, Gibco) cells. pFastbac-GUS was also transformed and served as a positive control for expression in the baculovirus system. Briefly, competent cells were removed from -80°C and thawed on ice. Once thawed, 100µL was added to each pre-cooled reaction tube. 1µL (1ng) M-pFB DNA and 5µL (1ng) pFB-GUS DNA were added, respectively. Tubes were gently flicked to mix and placed on ice for 30 minutes. Tubes were then placed in a 42°C water bath for 45 seconds, then placed back on ice for 2 minutes. 900µL of room temperature super optimal broth with catabolite repression (SOC) media was added to each reaction and tubes were incubated at 37°C, shaking for 4 hours. Following incubation, cells were pelleted at 2 000 rpm for 5 minutes, 600µL of media was removed, and pellets resuspended in the remaining 400µL. 100µL of undiluted, 1/10 and 1/100 diluted (in SOC media – see Appendix 2 for recipe) reactions were plated on LB agar plates containing 0,1M IPTG, 30mg/mL X-Gal, 50µg/mL Kanamycin (10106801001, Merck), 10µg/mL Tetracycline (A39246, Gibco), and 7µg/mL Gentamicin (15750060, Gibco). Plates were incubated at 37°C for 48 hours.

3.4.2.6. Confirmation of transposition

White colonies were inoculated into 10mL SOC media each, and incubated, shaking at 37°C for 14 – 18 hours. Cells were pelleted at 14 000 rpm for 2 minutes, and recombinant bacmid DNA was purified using the Wizard® SV Gel and PCR Clean-Up System (A9281, Promega). Following DNA quantification, 100ng DNA was used in each PCR reaction. 1µL of each primer (M13 forward and reverse) was added along with 10µL 5x Gotaq buffer, 0.5µL Taq polymerase, 1µL dNTPs (10mM), and 3µL MgCl₂ (25mM). Nuclease-free water was added up to a final volume of 50µL. Thermocycler conditions were as follow:

Pre-denaturation	3 mins	93°C	
Denaturation	45 secs	94°C	} X30 cycles
Annealing	45 secs	55°C	
Elongation	5 mins	72°C	
Final elongation	15 mins	72°C	

Samples were loaded and run on a 1% TBE agarose gel. Electrophoresis was done at 80V for 70 minutes. DH10BAC *E.Coli* cells that contained the confirmed recombinant bacmid-M expression vector were grown up to large culture volumes (400mL), and bacmid-M DNA was purified out using the NucleoBond Xtra Midi DNA purification kit (740410.100, Machery-Nagel), according to the manufacturer instructions. DNA was quantified using the NanoDrop 2000 and working stocks of DNA at 500ng/μL were made up in nuclease-free water.

3.4.2.7. Final confirmation – Confirmation of correct M gene orientation in bacmid

In order to confirm the correct orientation of the M gene in the recombinant bacmid, a PCR was performed with different combinations of primers/primer pairs using bacmid-M DNA as the PCR template. Following DNA quantification (NanoDrop 2000), ~100ng DNA was used in each PCR reaction. 1μL of each primer of specific primer pairs (four different primer pairs: GS For and M13 Rev; M13 For and GS Rev; GS For and Rev; M13 For and Rev) was added, along with 10μL 5x Gotaq buffer, 0,5μL Taq polymerase, 1μL dNTPs (10mM), and 3μL MgCl₂ (25mM). Nuclease-free water was added up to a final volume of 50μL. Thermocycler conditions were as follow:

Pre-denaturation	3 mins	93°C	
Denaturation	45 secs	94°C	} X30 cycles
Annealing	45 secs	60/65°C	
Elongation	5 mins	72°C	
Final elongation	15 mins	72°C	

PCR reactions containing GS forward and reverse primers and M13 forward and reverse primers were run using an annealing temperature of 60°C. Reactions containing mixed primer pairs (GS forward and M13 reverse; M13 forward and GS reverse) were run using an annealing temperature of 65°C.

3.4.3. Expression of the HCoV-NL63 M protein

3.4.3.1. Sf9 (*Spodoptera frugiperda*) insect cell culture

Cryofrozen stocks of Sf9 cells were seeded into a T25 treated cell culture flask. Cells were maintained in complete media: 1x supplemented Grace's media (11605045, Gibco), additionally supplemented with 10% FBS. No antibiotics were included in the growth media. Cells were grown at 27°C in non-humidifying conditions and split at a ratio of 1:5 into another T25. Cells were expanded into T75 treated cell culture flasks and were maintained in these for several passages before use in experiments. Cells were used for experiments between passage numbers 3 – 7.

3.4.3.2. Transfection of Sf9 cells with recombinant bacmid

The recombinant bacmid construct encoding the M gene was transfected into Sf9 cells. Log phase cells (viability > 95%) were seeded in 6-well tissue culture plates at a density of 800 000 cells in 2mL complete Grace's media and incubated at room temperature for 1 hour to allow the cells to attach to the plate. For each transfection reaction, 6µL of Cellfectin II Reagent was diluted in 100µL unsupplemented Grace's media (11595030, Gibco) (no FBS) and 1µg or 2µg of bacmid-M DNA (working DNA stock) was diluted in 100µL unsupplemented Grace's media. The diluted DNA was then added to the diluted Cellfectin II, gently mixed, and then incubated for 15 – 30 minutes at room temperature to allow for the formation of DNA-lipid complexes. The total volume (~210µL) of the appropriate DNA-lipid complex was added, dropwise, to the cells in each well. Each reaction was performed in duplicate (duplicate wells). Plates were incubated at 27°C in humidified conditions. After 4 hours, media containing transfection mixture was removed and replaced with 2mL of fresh, complete supplemented Grace's media. Plates were incubated again at 27°C in humidified conditions, and cell media (containing baculovirus particles) was harvested once changes in the cells were observed (signs of infection), resulting in harvests at 72, 96, and 120 hours post-transfection. Media was centrifuged at 2 000 rpm for 3 – 4 mins to pellet any detached cells and cellular debris. Clarified media (viral P0 stock) was stored at 4°C, protected from light.

3.4.3.3. Infection and amplification

The low titre P0 viral stocks were amplified by infecting fresh Sf9 cells at a low estimated MOI. Sf9 cells were seeded in 6-well plates at a density of 2×10^6 cells/well, in 2mL of complete Grace's media and allowed to attach for 1 hour at room temperature. The titre of the P0 stocks had not been determined and was estimated to be approximately 1×10^6 plaque forming units per mL (pfu/mL). Cells were infected at a low MOI of 0.1. The volume of P0 to use per well was calculated as follows:

$$\text{Inoculum required (mL)} = \frac{\text{MOI} \left(\frac{\text{pfu}}{\text{cell}} \right) \times \text{number of cells}}{\text{titre of viral stock} \left(\frac{\text{pfu}}{\text{mL}} \right)}$$

$$= \frac{0.1 \times (2 \times 10^6)}{1 \times 10^6}$$

Inoculum (P0) required = 0.2mL (200µL)/well

Infected cells were incubated at 27°C in humidified conditions. After 72 and 96 hours PI, cell media containing the amplified P1 viral stock was collected and centrifuged at 2 000 rpm for 3 – 4 minutes to pellet dead cells and large debris. Clarified viral stocks were stored at 4°C, protected from light.

3.4.3.4. Determining titre of viral stocks – Plaque assay for virus purification

To obtain pure virus isolates, fresh Sf9 cells were infected with the 96-hour P1 viral stock at a range of dilutions, and infected cells were immobilised in agarose plaquing medium (see Appendix 2 for plaquing media recipe). On the day of infection, log phase Sf9 cells were harvested, counted, and used to prepare a 30mL cell suspension of 5×10^5 cells/mL in complete Grace's media. Cells were plated in 6-well plates, and 2mL of cell suspension was added to each well of 2 x 6-well plates. Cells were incubated at room temperature, covered in foil for 1 hour to allow for attachment. Serial dilutions were made of the P1 viral stock. Briefly, 300µL of stock or previously diluted stock was sequentially diluted in 2.7mL supplemented Grace's media without FBS or antibiotics (10^{-1}) and inverted a few times to mix. 300µL of this dilution was then removed and resuspended in 2.7mL fresh supplemented Grace's media without FBS or antibiotics (10^{-2}). Viral stock was serially diluted from 10^{-1} to 10^{-15} , and dilutions of 10^{-4} to 10^{-14} were used in the plaque assay. Following visual confirmation of attachment and approximately 50% confluency through the microscope, media was removed from the wells and replaced with 1mL of the appropriate virus dilution. Virus dilutions were added in a specific order, starting from the highest dilution wells (10^{-14}) to the lowest dilution (10^{-4}). Dilutions were done in duplicate wells. For the negative control wells, 1mL of Grace's media without virus was added to each well. Cells were allowed to incubate with the virus for 1 hour at room temperature. Following the incubation, virus dilutions were removed from the wells and replaced with 2mL of warm (42°C) plaquing media, two wells at a time. This removal and replacement were performed starting at the negative control wells, then the highest dilution wells followed by the lowest dilution wells (see 'Preparation of plaquing media' in Appendix 2). Plaquing media agarose overlays were allowed to harden for 1 hour at room temperature, after which plates were moved to a humidified 27°C incubator to incubate for 7 – 10 days. On day seven PI, once plaque formation had been confirmed by microscopy, the agarose overlays were stained with MTT (M5655, Sigma) at a working concentration of 5mg/mL for macroscopic visualisation. Briefly, 200µL MTT solution was added

to each well of each 6-well plate. Plates were incubated with the MTT for 3 – 4 hours at 27°C. MTT stained living cells purple/black, while plaques were visualised as cleared spots in the stained cells/agarose. On the day of infection, log phase Sf9 cells were harvested, counted, and used to prepare a 50mL cell suspension of 5×10^5 cells/mL in complete Grace's media. Cells were plated in 6-well plates, and 2mL of cell suspension was added to each well of 3 x 6-well plates (1×10^6 cells/well). Cells were incubated at room temperature, covered in foil for 1 hour prior to infection to allow the cells to settle in the plates. Using Pasteur pipettes, three individual and well-isolated clear plaques were picked from the plaque assay plates along with a small agarose plug. Each plaque-purified virus agarose plug was added to a 1.5mL microcentrifuge tube containing 500µl of complete Sf9 growth media, and vortexed thoroughly to mix. Cells were infected with 100µl of the agarose plug virus solution per well. The last well of each 6-well plate served as a 'no virus' negative control. Plates were incubated in a 27°C humidified incubator. After 72 hours, the medium from each well was collected and centrifuged at 4 000 rpm for 5 minutes at room temperature. Clarified supernatants were aspirated and transferred to fresh 15mL tubes. These plaque-purified viral stocks were stored at 4°C, protected from light.

3.4.3.5. Amplification of purified viral stock

The low-titre, purified baculovirus stocks were amplified to improve the viral titres. This was achieved by infecting fresh Sf9 cells with the purified P1 stock at a low estimated MOI. The same amplification procedure was followed as was previously used (see Section 3.4.3.3).

3.4.3.6. Plaque assay for virus titre

In order to establish the titre of the new plaque-purified P2 viral stocks, the plaque assay was performed again, using the P2 '96 hours P1' virus stock. The same procedure was followed as above (see Section 3.4.3.4), except for picking plaques. No individual plaques were isolated – plaques were visualised and counted to determine the viral titre of the purified P2 stock. The titre was calculated as follows:

$$\text{Titre } \left(\frac{\text{pfu}}{\text{mL}} \right) = \text{number of plaques} \times \text{dilution factor} \times \frac{1}{\text{mL inoculum /well}}$$

3.4.3.7. Expression of recombinant HCoV-NL63 M protein in an insect cell line

Mid-log phase Sf9 cells were seeded in a 24-well plate at 6×10^5 cells per well, and plates were incubated at room temperature for approximately 45 minutes to allow cells to settle. After 45 minutes, the media in each well was removed and replaced with fresh, full Sf9 growth media. The titred P2 virus stock was serially diluted five times (300µl into 2.7mL in supplemented Grace's media with no FBS) to a working concentration/titre of approximately 1×10^8 pfu/mL. Cells were infected with this P2 stock in duplicate wells at various MOIs, including 1, 5, 10, and 20. Plates were set up to allow for cell lysates

to be harvested at four different time points of 24, 48, 72 and 96 hours PI. The volume of purified P2 stock required for infection/expression was calculated as follows:

$$\text{MOI 1: inoculum required} = \frac{1 \times 600\,000}{1 \times 10^8} = 6\mu\text{L/well}$$

$$\text{MOI 5: inoculum required} = \frac{5 \times 600\,000}{1 \times 10^8} = 30\mu\text{L/well}$$

$$\text{MOI 10: inoculum required} = \frac{10 \times 600\,000}{1 \times 10^8} = 60\mu\text{L/well}$$

$$\text{MOI 20: inoculum required} = \frac{20 \times 600\,000}{1 \times 10^8} = 120\mu\text{L/well}$$

Infected cells were incubated at 27°C in a humidified incubator until the appropriate cell harvest time. When harvesting, the media in each appropriate well was removed, and cells were rinsed with 1xPBS. After removing the 1xPBS, 200µL lysis buffer (62.5mM Tris-HCl pH6.8; 2% SDS) was added to each well and cells were incubated in the buffer for 5 minutes. Cells were then pipetted loose and mixed to a homogenous suspension by pipetting up and down. Whole cell Sf9 lysates were stored at -20°C for further analysis.

3.4.3.8. SDS-PAGE of Sf9 lysates

Proteins were separated by size by running lysates on a 12.5% denaturing polyacrylamide gel (SDS-PAGE), in comparison with a protein marker. Gels were removed from between the glass plates and incubated in Coomassie Brilliant Blue stain solution for 1 hour with slight agitation (rocker). Following staining, gels were incubated in Coomassie destain solution (30% Methanol, 10% Acetic acid, 60% distilled water) until protein bands could be visualised and the gel background was adequately destained.

3.4.3.9. BCA protein quantitation assay

The protein concentrations of the Sf9 experimental lysates were determined by using the Pierce™ BCA Protein Assay Kit (23225, Merck). The relative concentrations of the lysates were calculated with the use of a standard curve equation. The standard curve is generated for each experiment by plotting the absorbance of a range of dilutions of protein, diluted in the specific cell lysis buffer. BSA was made up to a range of dilutions (2mg/mL; 1.5mg/mL; 1mg/mL; 0.75mg/mL; 0.5mg/mL; 0.25mg/mL; 0.125mg/mL; 0.025mg/mL) in 1.5mL microcentrifuge tubes. The microplate procedure was performed in a 96-well flat-bottomed Greiner plate (M456, Merck). Each standard curve dilution was added in duplicate to the appropriate wells (highest to lowest across rows A and B). 25µL of cell lysate was added, in duplicate, to the appropriate wells. Working reagent was added to all wells at 200µL/well, and plates were mixed thoroughly by vortexing for 30 seconds. Plates were covered in foil and incubated at 37°C for 30 minutes

to 1 hour. Following incubation, plates were cooled down to room temperature and then read on a spectrophotometer at 562nm.



UNIVERSITY *of the*
WESTERN CAPE

Chapter 4: Results and Discussions

4.1. The production of anti-peptide antibodies specific to the M and N proteins of HCoV-NL63

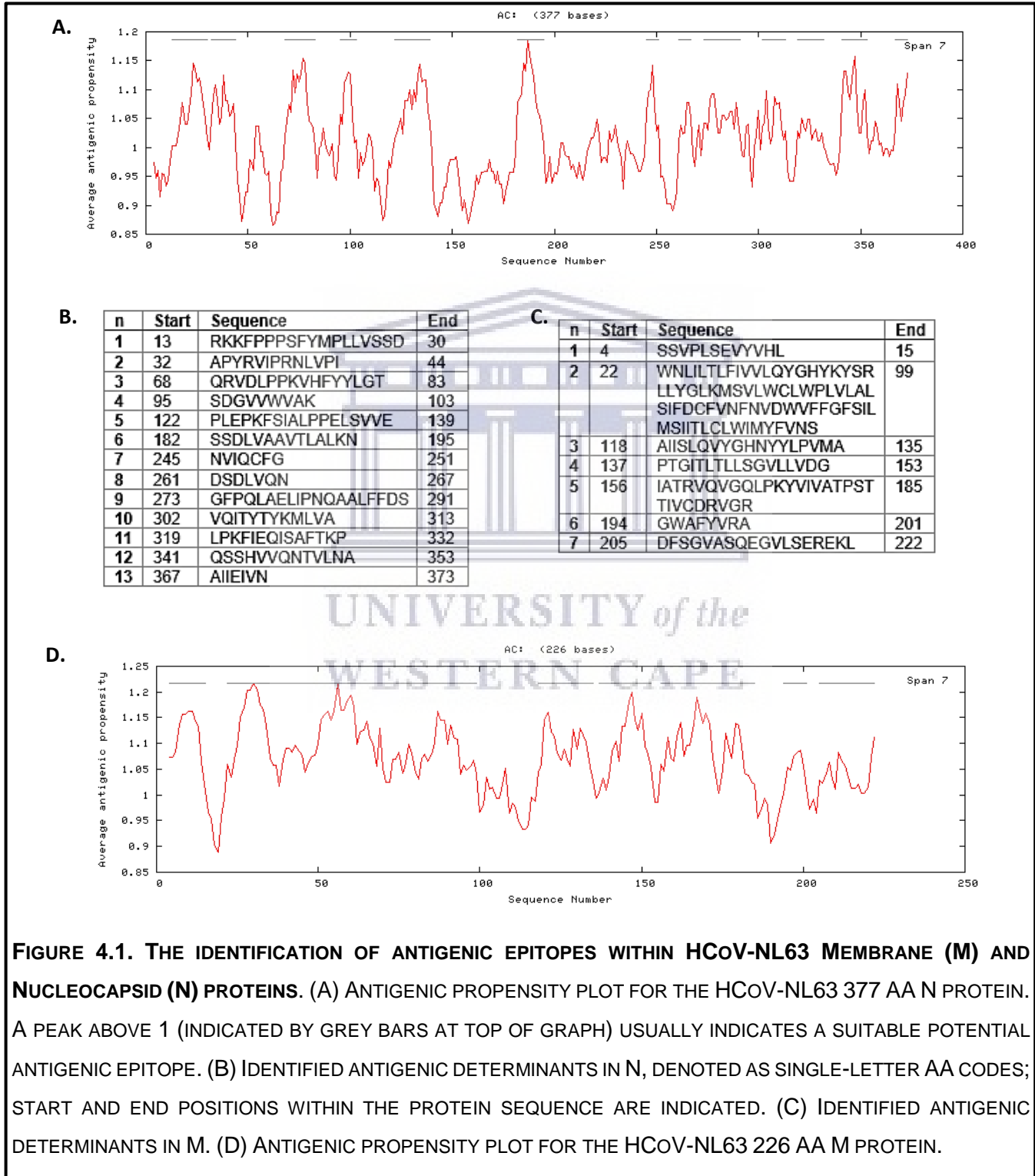


FIGURE 4.1. THE IDENTIFICATION OF ANTIGENIC EPITOPES WITHIN HCoV-NL63 MEMBRANE (M) AND NUCLEOCAPSID (N) PROTEINS. (A) ANTIGENIC PROPENSITY PLOT FOR THE HCoV-NL63 377 AA N PROTEIN. A PEAK ABOVE 1 (INDICATED BY GREY BARS AT TOP OF GRAPH) USUALLY INDICATES A SUITABLE POTENTIAL ANTIGENIC EPITOPE. (B) IDENTIFIED ANTIGENIC DETERMINANTS IN N, DENOTED AS SINGLE-LETTER AA CODES; START AND END POSITIONS WITHIN THE PROTEIN SEQUENCE ARE INDICATED. (C) IDENTIFIED ANTIGENIC DETERMINANTS IN M. (D) ANTIGENIC PROPENSITY PLOT FOR THE HCoV-NL63 226 AA M PROTEIN.

4.1.1. Antigenic peptide selection

In this research study, the author aimed to characterise the structural proteins or the structural dynamics between the major structural proteins of the HCoV-NL63. The characterisation of these proteins involved setting up optimised systems to express these proteins in a structurally and functionally mature state. While attempting to evaluate protein function/action, these polypeptides need to be expressed untagged. To this end, the author have aimed to develop antibodies for the detection of HCoV-NL63 proteins in further and future laboratory experiments falling under the “The characterisation of HCoV-NL63 proteins” umbrella project/research study.

When planning antibody production, the type of immunogen to use is an important consideration. Often, the recombinant protein of interest will be expressed as a fusion protein in bacterial cells such as *E.Coli* (Rancour et al., 2010). The protein is purified out of the whole cell lysate by affinity binding methods. Some proteins are challenging to express, and additionally, fusion proteins may take on an unusual conformation (Angeletti, 1999; Lee et al., 2010; Sastre et al., 2011). That purified protein serves as antigen for animal immunisation and the resulting antibody response (Antipova et al., 2020; Sørensen, 2010). At times, the viral protein antigen is expressed in eukaryotic cell lines, including mammalian, insect, and even plant cells (Castilho et al., 2011; Fulton et al., 2015; Goo et al., 2020; Qu et al., 2020). This is done if a fully-folded native-like protein is required for immunization, for instance, if the purpose of the antibody is to differentiate between two molecules that are differently processed (Gannon et al., 1990; Nishikori et al., 2012; van der Mijl et al., 2015).

We used antigenic peptide sequences as antigens for animal immunisation. Antigenic peptides have been critical in molecular biology and immunology for its uses in resolving antibody epitope binding specificity and elucidating B cell- and T cell-specific sequences within proteins (Murphy & Weaver, 2016; Owen et al., 2013). The ability to express and characterise single domains from within a complex polypeptide molecule has made peptides instrumental in the field of proteomics. While in recent years other small molecules have been developed for similar applications (Afrasiabi et al., 2020; Zhou & Rossi, 2017), today peptides and peptide antigens are still widely used in molecular biology research, diagnostics, and therapeutics (Trier et al., 2019). Synthetic peptides have proven to be an effective protein subunit fragment for antibody generation for whole protein recognition (Lee et al., 2016; Trier et al., 2019).

There exist several methods/models to predict possible antigenic determinants within a protein sequence. Each of these methods/models measures antigenic propensity by taking into consideration various physiochemical properties of the constituent AAs in a given epitope, such as hydrophobicity/hydrophilicity, charge, and accessibility (Chou & Fasman, 1977; Chou & Fasman, 1979; Doytchinova & Flower, 2007; Emini et al., 1985; Pellequer† & Westhof, 1993; Saha & Raghava, 2004).

While it is not always possible to predict with certainty if an epitope will prove antigenic *in vivo* (with conjugation), several of these methods can predict protein antigens with an accuracy above 50%. The Kolaskar and Tongaonkar method, an antigenic peptide prediction tool, was used to identify peptide epitopes within the M and N proteins (Figure 4.1) (Kolaskar & Tongaonkar, 1990; Rodrigues et al., 2019). This algorithm considers the physiochemical properties of the AAs and the documented experimental data, showcasing the antigenicity of the various residues based on their frequency of occurrence in known, experimentally determined epitopes. As the efficacy of an antigen is determined by the antibody-response elicited *in vivo*, this method may provide the best chance of identifying a suitable antigen from within our respective proteins. Within the database utilised by this method, the minimum number of residues required in a qualifying epitope is eight AAs. This antigenic peptide prediction method is straightforward to use and is reported to be approximately 75% accurate (Kolaskar & Tongaonkar, 1990).

Seven possible antigenic epitopes were identified from within the M protein sequence using the Kolaskar and Tongaonkar method ("Immunomedicine Group - Predicting Antigenic Peptides," 2020). Three of the peptides were C-terminal sequences and represent the hydrophilic, cytosolic region of the CoV M protein, including the immunogenic tail region (Voß et al., 2009). HCoV-NL63 M is predicted to have the alternate M-topology, including four transmembrane domains, and a short surface-exposed CTD (El-Duah et al., 2019; Naskalska et al., 2019). As such, the only sequence which would be exposed on the outer surface of the virion and be available for antibody binding is the most C-terminal peptide. Therefore, a single peptide epitope was selected for synthesis as an HCoV-NL63 M antigen (Figure 4.2).

The N protein sequence is considerably more soluble than the M protein. Due to its high level of antigenicity and high expression level during infection, CoV N protein has been commonly used as an immunising agent for antibody production against other CoVs and HCoV-NL63 N (Sastre et al., 2011; Timani et al., 2004). As the N protein is not a membrane-spanning protein, there is a larger proportional area of the protein available for possible antigenic determinants than an integral membrane protein. Using the same online bioinformatics tool as above, the average antigenic propensity calculated for the HCoV-NL63 N protein sequence was 1.0113 (Figure 4.1). Thirteen possible antigenic epitopes were identified within the N protein sequence ("Immunomedicine Group - Predicting Antigenic Peptides," 2020). To increase the diversity of our available N antibody repertoire and binding range, we chose to select two N-specific peptides for synthesis as HCoV-NL63 N antigens (Figure 4.2).

A.

Peptide	Amino acid sequence	No. of residues	Triple letter code
M-C	RAKHGDFSGVASQEGVLSE	19	Arg-Ala-Lys-His-Gly-Asp-Phe-Ser-Gly-Val-Ala-Ser-Gln-Glu-Gly-Val-Leu-Ser-Glu
N-N	PLEPKFSIALPPELSVVE	18	Pro-Leu-Glu-Pro-Lys-Phe-Ser-Ile-Ala-Leu-Pro-Pro-Glu-Leu-Ser-Val-Val-Glu
N-C	RKKFPPPSFYMPLLVSSD	18	Arg-Lys-Lys-Phe-Pro-Pro-Pro-Ser-Phe-Tyr-Met-Pro-Leu-Leu-Val-Ser-Ser-Asp

B.

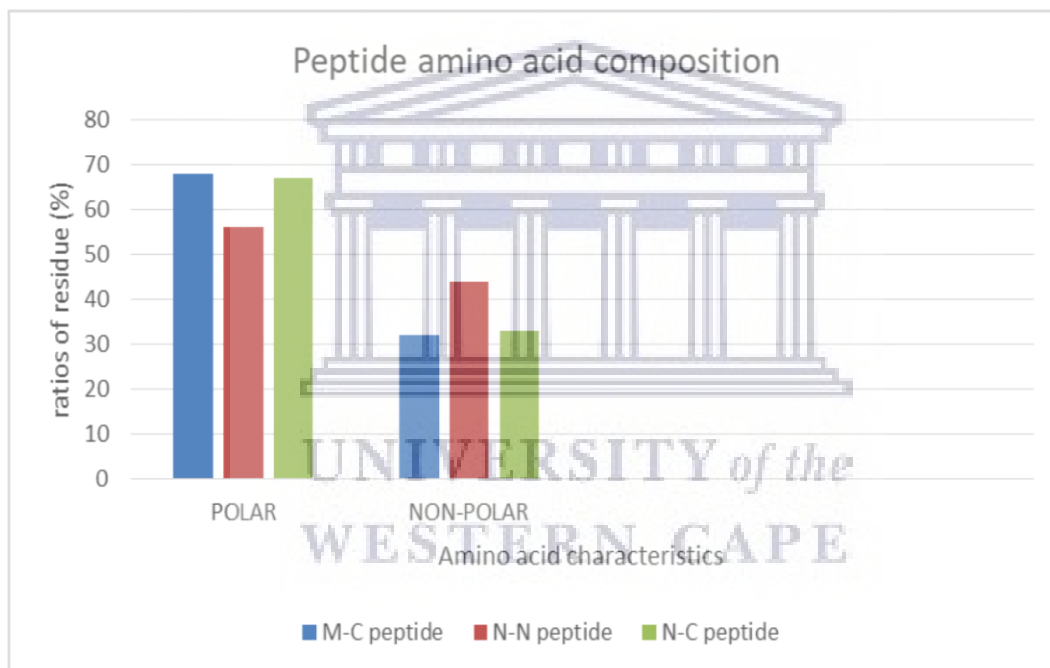


FIGURE 4.2. SCREENING SYNTHETIC PEPTIDES FOR ANTIGEN SUITABILITY. (A) THE SELECTED IMMUNOGENIC PEPTIDE ANTIGEN SEQUENCES FOR HCoV-NL63 M AND N. THE RESPECTIVE PEPTIDE SEQUENCES ARE DENOTED IN BOTH THEIR TRIPLE LETTER AND SINGLE-LETTER CODES. THE NUMBER OF RESIDUES IN EACH PEPTIDE IS SHOWN. CHARGED RESIDUES ARE INDICATED BY ORANGE BOXES. (B) POLAR VS. NON-POLAR RATIOS OF AAS IN EACH SPECIFIC ANTIGENIC PEPTIDE. SUITABLE ANTIGENIC SEQUENCES SHOULD BE MADE UP OF LESS THAN 50% NON-POLAR (HYDROPHOBIC) RESIDUES.

4.1.2. Antigenic peptide suitability screening

When designing and selecting specific peptide antigens, a few basic criteria are required, which improve the likelihood of the specific sequence being experimentally antigenic. These criteria are discussed below.

The ideal antigenic peptide length is 15 – 20 AAs. In order to enhance the specificity of the resulting antibody, it is vital to select a sequence, which is similar in size to a typical antibody epitope. A peptide sequence that is too long, no longer represents a single epitope and will increase the ratio of poly-specific antibodies. A peptide under 15 AAs may be too short and may result in the development of non-specific antibodies. Our peptide antigen sequences, including MC, NN, and NC, are appropriate at 18 – 19 AAs in length (Figure 4.2). Less than 50% of the peptide residues should be non-polar (hydrophobic). Antigenic peptides need to be made up of both hydrophilic and hydrophobic AAs; if a peptide contains too many hydrophobic residues, it is likely to be a sequence buried within the protein structure and, therefore, inaccessible for antibody binding (Dyson et al., 2006; Malleshappa Gowder et al., 2014). Figure 4.2 (B.) indicates that all the peptides comprised of less than 50% non-polar residues. There should be one charged residue per every five AAs in the peptide sequence – charged residues are the least likely to be buried or inaccessible within the protein structure (Wampler, 1996). Each of our selected peptide sequences has an appropriate dispersion of charged residues, indicated by the orange boxes in figure 4.2 (A.). Antigenic peptides should contain multiple glycine (Gly) and/or proline (Pro) residues. These AAs are commonly found in secondary protein structures known as ‘turns’ (Krieger et al., 2005). As turns represent structurally exposed protein sequences, a higher frequency of Pro and Gly residues may serve as further indicators of surface accessibility. Our MC peptide contained multiple Gly residues, and the N-N and N-C peptides each included multiple Pro residues. Our specific N peptide sequences were selected based on their higher proportion of Pro residues relative to other N-epitope sequences (Figure 4.1). In figure 4.2. we observe that each of our synthetic peptide antigens fulfills the basic criteria for an antigenic epitope and may serve as immunising antigens for antibody production.

4.1.3. Enhancing peptide immunogenicity

Peptides by themselves (while complex enough) are not large enough to be immunogenic, and it is necessary to increase their size by conjugation methods. Commonly-used protein conjugation partners include keyhole limpet hemocyanin (KLH) and BSA (Coligan et al., 2005; Hansen, 2015). Some carrier proteins are unsuitable for immunisation. Moreover, even when conjugated to a large carrier protein, some peptides are still weak immunogens and do not elicit a good antibody response. In order to increase the immunogenicity of our peptide antigens, we made use of an alternative conjugation method

known as MAP technology. This method uses an artificially branched lysine backbone to attach multiple peptide chains to a single core. The core can support up to eight branches for peptide-binding, making the molar ratio of peptide antigen to lysine core higher in the resultant MAP. The larger number of presented peptide sequences increases the size and molecular weight (MW) of the antigen, thereby conferring immunogenicity to the previously unconjugated, 'non-immunogenic' peptides. MAPs have been previously shown to be strong immunogens, able to induce an effective memory immune response (Chai et al., 1992; Joshi et al., 2013; Kim & Pau, 2001; Niederhafner et al., 2005; Rosa et al., 1995; Sadler & Tam, 2002; Saravanan et al., 2004).

Adjuvants can be defined as compounds that improve the immunogenicity of a vaccine formulation when added. The use of an adjuvant is important in vaccination as they serve to activate the innate arm of the host immune response, improving the quality of the adaptive immune response to the antigen. Adjuvants do this in various ways, including antigen delivery systems, host immune potentiation, and mucosal immunity activation (Apostólico et al., 2016). The adjuvants we used in our immunisations was Freund's Complete and Incomplete adjuvant (CFA and IFA). Freund's adjuvants are water-in-oil emulsions that function as a carrier for the associated antigens. By continuously releasing the specific antigen from the site of inoculation, much slower than it would be introduced to the host system if the antigen was injected alone, the emulsion-adjuvant aids in increasing the antigen lifespan and stimulating a persistent, strong host immune response (Goto & Akama, 1982; Müssener et al., 1995; Salk & Laurent, 1952) (Apostólico et al., 2016). CFA also contains heat-inactivated *Mycobacterium tuberculosis* (*M. tuberculosis*). The bacteria attracts innate immune cells such as macrophages and APCs (dendritic cells) to the inoculation site (Freund, 1947, 1956; Freund & McDermott, 1942). The side effects of the adjuvant used must be weighed against its efficacy *in vivo*. The strong immune response often induced by CFA can lead to granulomatous lesions or necrosis at the injection site (Apostólico et al., 2016). For this reason, CFA was only used for the initial immunisations, and animals were monitored for any adverse effects. IFA, which does not contain *M. tuberculosis*, was used for every subsequent animal immunisation. Our experimental animals received the highest recommended volume dosage in a mouse animal model, which is 100µL (protein antigen). Antigen-adjuvant emulsions were injected intra-peritoneally as this is the recommended route of administration for a larger volume of antigen (M. Leenaars & Hendriksen, 2005)(Bomford, 1980; Hendriksen & Hau, 2003; Leenaars et al., 1999; van Zutphen et al., 1996).

4.1.4. HCoV-NL63 N-specific peptides are strong inducers of mouse polyclonal antibody response

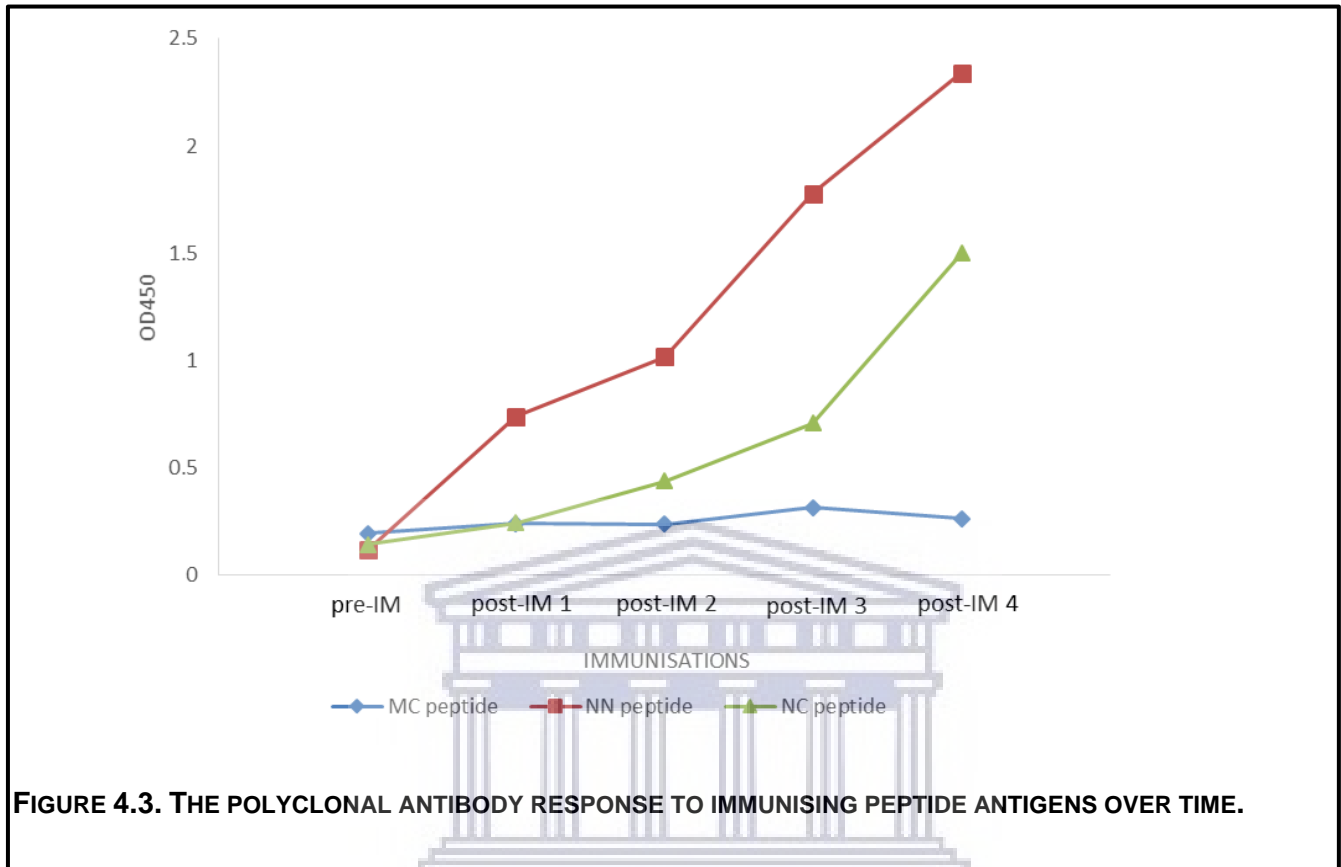


FIGURE 4.3. THE POLYCLONAL ANTIBODY RESPONSE TO IMMUNISING PEPTIDE ANTIGENS OVER TIME.

Mouse serum was collected prior to each immunisation, i.e., pre-immunisation (pre-IM), post-immunisation 1 (post-IM 1), post-immunisation 2 (post-IM 2), post-immunisation 3 (post-IM 3) and post-immunisation 4 (post-IM 4) (see Figure 4.3. above). Sera were diluted (1:1600, v/v) in a diluent. Each data point represents the mean of a duplicate measurement.

4.1.4.1. The production of polyclonal antisera against HCoV-NL63 peptide antigens

The immune system functions to protect the host organism against foreign antigens. The complex immune system has two arms – innate immunity and adaptive immunity. Antibody production is an integral part of the humoral response in adaptive immunity as antibodies are highly targeted immune molecules effective at antigen clearance (Chaplin, 2010). When a host becomes infected with a virus, the immune system produces antibodies specific for epitopes on viral structural proteins/components. Surface-exposed or highly expressed structural virus proteins are frequently selected as targets in therapeutic antibody development, and these protein subunits are considered antigenic (Ahangarzadeh et al., 2020; Murin et al., 2019; Shirkoohi et al., 2010). The CoV N protein is highly antigenic and has been used for specific antibody generation against various CoVs, including SARS-CoV, MERS-CoV,

HCoV-229E, HCoV-NL63, IBV, porcine epidemic diarrhoea virus (PEDV), and TGEV (Burbelo, Riedo, Morishima, Rawlings, Smith, Das, Strich, Chertow, Davey Jr, et al., 2020; Chang et al., 2004; Juan Zhang, 2011; Sastre et al., 2011; Yamaoka et al., 2016; Yang et al., 2019). During CoV infection, N is the most expressed structural subunit (Chan, K. et al., 2005; Chan, P. K. et al., 2005; Ren et al., 2004). Along with anti-S, anti-N antibodies have also been used to detect infection in patient samples, as well as in infected cells (Wu et al., 2004). It was, therefore, expected that our N-specific peptides would likely serve as good antigens.

CoV M protein is also highly expressed during infection, and anti-M rabbit PABs have previously been used to detect M protein in convalescent SARS-CoV patient samples, as well as in infected animal sera. Highly immunogenic epitopes are present within SARS-CoV M, and M-subunits can stimulate strong antibody responses in immunised rabbits (He, Y., Zhou, Y., et al., 2005). M is a highly hydrophobic, multi-pass membrane protein. Furthermore, alternate topologies have been reported for CoV M protein, indicating a species-specific variation in the number of transmembrane domains (Naskalska et al., 2019). This specific peptide sequence was selected in anticipation that it represents the only surface-exposed CTD within the HCoV-NL63 M protein. Given the characteristics of this protein, it was not known what type of PAB immune response to expect to this M-specific peptide antigen in our immunised mice.

As indicated in our immunisation timeline, the second immunisations were administered six weeks after the first round. Immunisation protocols for antibody production often make use of a similar initial booster immunisation timeline. This extended period between the initial antigen exposure and re-exposure is given to allow for the primary antibody response to be raised, and to then decline for antigen clearance, and the development of specific memory B cells. Upon secondary exposure/immunisation, the antigen is re-presented to its cognate “primed” B cell (memory B cell), inducing rapid clonal expansion and the secretion of antibodies. Over time, through this process of re-immunisation and re-presentation of cognate antigen, B cell receptor (paratope) sequences are optimised to produce antibodies with maximal antigen-binding affinity. Therefore, the second and subsequent responses to an antigen are faster and more specific/stronger than the response at initial exposure (Janeway et al., 2001).

An increase in PAB specificity is seen over time against the N peptide antigens (Figure 4.3). While higher PAB specificity is attained sooner against NN at post-IM4, both anti-NN and anti-NC PABs are highly specific and sensitive to their peptide antigens. In addition to confirming the efficacy of N-peptide antigens, these results indicate that our peptide-immunisation regime is effective for raising a strong PAB immune response in a mouse model. Anti-M PABs do not exhibit a similar increase in PAB specificity over time, and at post-IM 4, the binding of PABs to the immunising MC peptide antigen was not significantly higher than baseline level (pre-IM). While the M protein is very hydrophobic and

contains a high ratio of non-polar AA residues, the selected MC peptide contains an appropriate hydrophobic residues ratio (< 50%, see Figure 4.2.) to be considered a possible antigenic epitope. It is possible that the MC peptide is a poor immunogen, and that the PABs generated after immunisation do not recognise the linear epitope sequence presented by the peptide antigen. Alternatively, if the MC peptide adopts an unusual conformation when bound to the plate, this may result in partial or complete masking of the linear epitope within the peptide. In this case, antibody binding can be hindered or even inhibited. To assess the reason for low binding affinity to the MC peptide immunogen, and determine if anti-M PABs are able to recognise the linear M-epitope in denatured protein antigen, proteins were analysed by denaturing SDS-PAGE and Western blotting (see section 4.1.6 “Polyclonal antibodies are specific and sensitive to their full-length protein antigens”). The PAB antibody response for each mouse to their respective immunising antigens is examined next.



4.1.5. Polyclonal antibodies (PABs) recognise their immunising peptide antigens by indirect ELISA

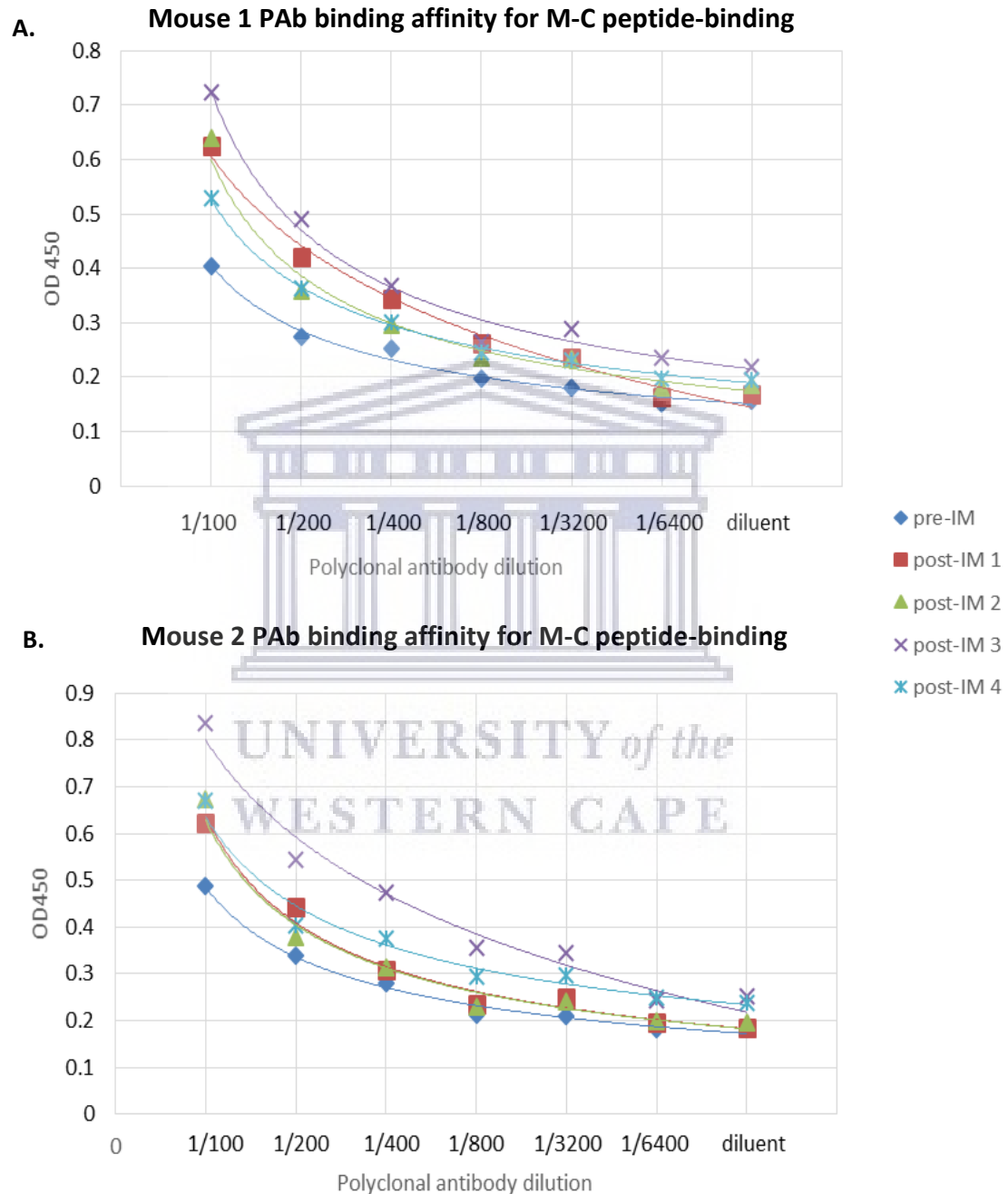


FIGURE 4.4. ANTI-M POLYCLONAL TITRATION CURVE, BINDING AGAINST IMMUNISING PEPTIDE ANTIGEN. (A) POLYCLONAL ANTIBODY BINDING FOR MOUSE 1. PRE-IMMUNE AND POST IMMUNE 1 – 4 SERA WERE TITRATED AND SCREENED BY INDIRECT ELISA AGAINST PEPTIDE ANTIGEN AT 1 μ G/ML. (B) POLYCLONAL ANTIBODY BINDING FOR MOUSE 2.

4.1.5.1. Anti-M PABs exhibit low binding specificity and sensitivity to MC peptide

In order to examine the relative anti-M PAb specificity dynamics throughout our immunisation timeline, the binding of PABs in pre-immune and post-immune 1 – 4 mouse sera were measured over a wide range of antibody dilutions. Figure 4.4. shows a relative yet significant drop in anti-PAb specificity at post-IM 4. It is known that the response to any given antigen varies slightly from host to host (Goldsby et al., 2000). However, in both M-immunised mice, the same general trend in anti-M PAb specificity is seen over time. The antigen-localisation-dose-time and structure concept suggests that, in addition to the structure of the antigen, the immunising dosage, and timing of immunisations, the localisation of antigen in the host are an important determining factor for B and T cell reactivity patterns (Zinkernagel, 2000). The localisation of immunisation in relation to the host lymphoid tissues directly affects antigen presentation to circulatory B and T cells. To be immunologically relevant, a minimal effective dose of immunising antigen must reach the secondary lymphoid tissues and remain for a sufficient amount of time (Ochsenbein et al., 1999; Ohashi et al., 1991; Zinkernagel, 1996; Zinkernagel et al., 1997). Antigens that persist in large amounts for an extended period, lead to the deletion of T cells (Ehl et al., 1998; Moskophidis et al., 1993; Webb et al., 1990). T cell interactions are important in the proliferation and differentiation of B cells. As such, if T cell numbers decrease significantly, it stands to reason that the activity of local B cells will be negatively impacted (Janeway Jr et al., 2001; Zinkernagel, 2000). After the first immunisation, subsequent immunisations were administered with IFA. The viscosity of the oil in water emulsion adjuvant aids in forming localised deposits of antigen at the site of inoculation. In this way, the timing of antigen release is extended, and antigen exposure is modulated. Immunisations 1 and 2 were administered six weeks apart. Immunisations 2 to 4 were administered only one week apart within a three-week period. At each immunisation, the mice were given the highest recommended antigen dosage volume (100µL). In addition to the large dose of antigen, the short amount of time between immunisations 2 to 4 and the 'extended antigen release' afforded by using IFA are all factors which may have caused the persistence of large amounts of peptide antigen in the secondary lymphoid organs. This antigen persistence may have lead to a decrease in T cell availability and a resultant decrease in B cell activity and observed antibody specificity. To compensate for the decrease in anti-M PAb specificity exhibited at post-IM 4, two weeks were allowed before administering a final booster immunisation comprised of only peptide antigen (no adjuvant).

All anti-M PAb titration curves exhibited a sharp decrease in antigen specificity as sera are further diluted to 1:6400, indicating that the anti-M PABs are not highly sensitive in binding MC peptide antigen. This pattern was exhibited in both mice. Antigenic epitopes are generally surface-exposed sequences within the protein, and as such, the prediction of folded protein structure is directly related to antigenic peptide sequence prediction. The protein-folding problem refers to a set of investigative questions designed to elucidate the following: (1) how is the 3D-folded structure of a complete protein determined

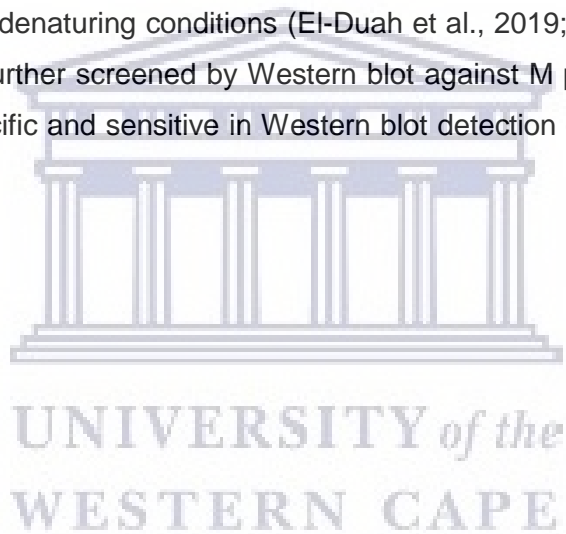
by a linear AA code? (2) How are proteins able to fold so quickly? (3) Is it possible to design an algorithm, which is able to predict protein-folding structure correctly? (Dill & MacCallum, 2012). A few chemical and physical factors have been identified as important causal determinants of protein folding (Berman et al., 2002; Dill, 1990). These include hydrogen bonds, Van der Waals forces, protein backbone stoichiometric preferences, as well as respective polar and hydrophobic interactions (Dill & MacCallum, 2012; Kamtekar et al., 1993). The dynamic loss of chain entropy as a polypeptide compacted into its folded state also plays a role in the resulting folding pattern (Dill, 1985; Ponder & Case, 2003). The possible structural permutations of a native protein are infinite, as determined by the variability of AA residues present in a long polypeptide sequence. For certain small proteins, there have been success in predicting native protein structure by analysing the physiochemical properties of the constituent AA residues (Lindorff-Larsen et al., 2011; Raval et al., 2012). This method loses accuracy as the size of the protein of interest is increased as more interacting domains are present in the polypeptide.

The low binding ability of our anti-M PABs to peptide antigen may indicate that PABs do not recognise the linear epitope sequence. Our antigenic peptides contain a high level of AA variability, and it is not known exactly what structural conformation each peptide adopts as isolated subunits of a whole protein sequence. It is expected that peptides and full-length proteins would adopt different folding patterns based solely on the difference in number and variation of residues. The *in vitro* peptide conformation (in immunised animals) may differ from plate-bound peptide antigen conformation (used for ELISA screening of antibodies). The peptide antigen may have an unexpected secondary conformation when used as a coating antigen for ELISA, which could potentially also mask the linear epitope partially or entirely, hindering/preventing antibody binding. Most B cell epitopes are continuous/conformational epitopes, meaning that only in a native state through folding does the epitope sequence become apparent and exposed for antibody binding (Van Regenmortel, 2009). In these cases, when the protein of interest is denatured, it often leads to the loss of epitope recognition by the antibody. In this study, we screened out anti-M and anti-N antibodies against both native (ELISA) and denatured (Western blot) protein antigens to determine the versatility of the antibodies in structural protein detection. Using peptides as representative molecules for native proteins is common in antibody generation against viral proteins (Trier et al., 2019).

Various computer-based programs exist that are able to predict antigenic sites within a given protein with up to 75% *in vitro* accuracy (Pellequer† & Westhof, 1993). The method by Kolaskar and Tongaonkar used in this study uses a database, including the outcomes of experimentally observed immunogenic epitopes, improving the robustness of epitope identification through also including continuous epitope sequences. This method has a 75% accurate prediction rate (Kolaskar &

Tongaonkar, 1990; Rice et al., 2000; Womble, 2000). Although advances in solving protein structures and predicting structural conformations have been made in recent years, it is not yet possible to predict a complete folded protein structure with a 100% accuracy based on only the AA composition/sequence (Dill & MacCallum, 2012). Our antigenic peptides contain a high variability of AAs, and as such, many structural conformations may be reached by each respective peptide. Differences in peptide and protein sequence folding affect epitope presentation and subsequent antibody binding. There also exists the possibility of differential peptide folding *in vitro* during animal immunisations versus when the antigen is plate-bound for screening antibodies (ELISA). If there is a difference in structural presentation of the epitope, the same antibody may exhibit higher affinity for a specific antigen type. This would explain any differential specificity found to be exhibited by the anti-M and anti-N mouse antibodies.

Peptides corresponding to the CTD of HCoV-NL63 M have previously been demonstrated as effective immunogens in immunised rabbits. These anti-M PABs showed specific recognition of full-length M protein by Western blotting in denaturing conditions (El-Duah et al., 2019; Naskalska et al., 2019). As such, the anti-M PABs were further screened by Western blot against M protein antigen (see section 4.1.6.1 “Anti-M PABs are specific and sensitive in Western blot detection of full-length HCoV-NL63 M protein”).



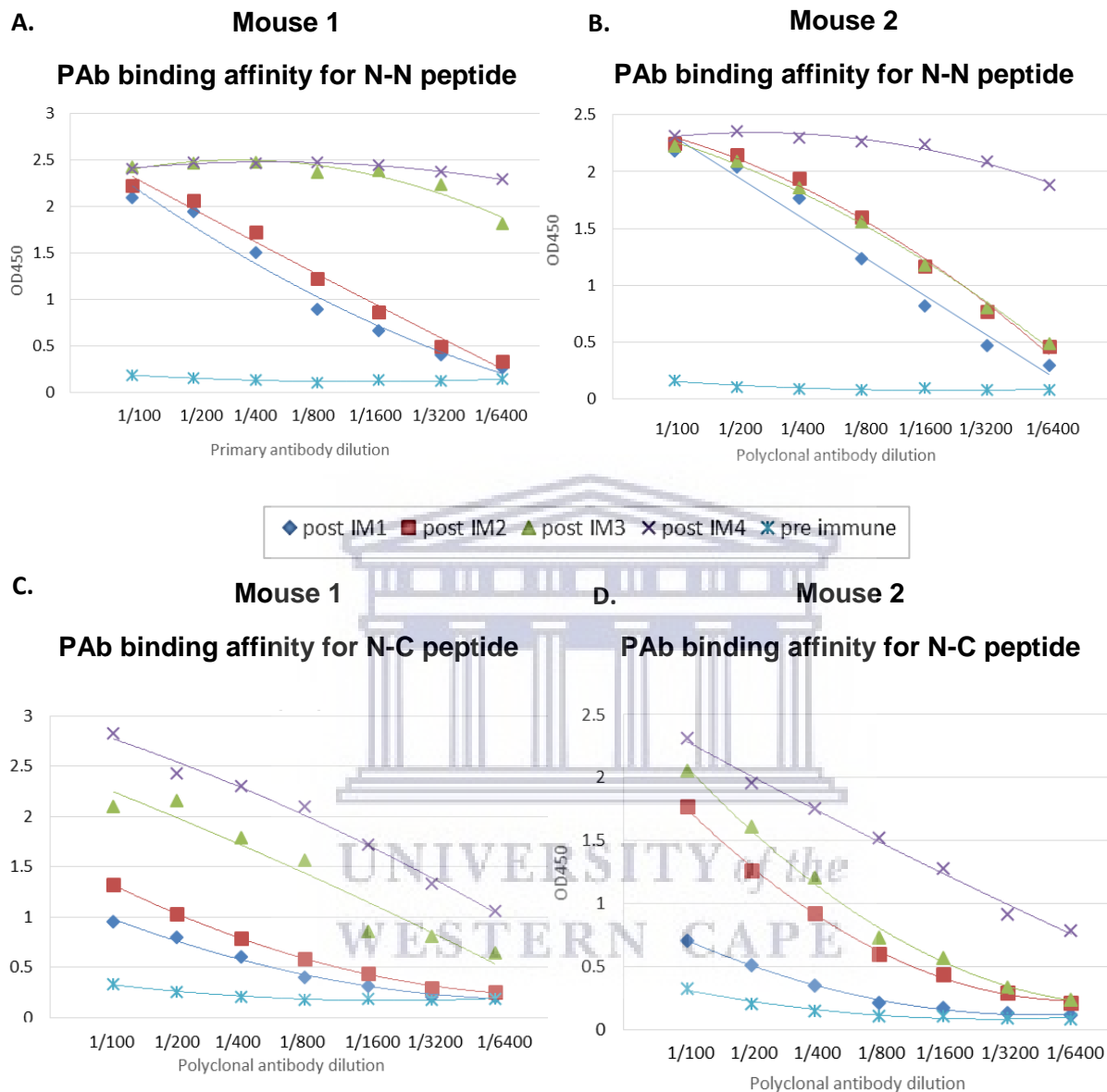


FIGURE 4.5. MOUSE SERUM ANTI-N EXHIBITS HIGH PEPTIDE ANTIGEN SPECIFICITY. (A,C) POLYCLONAL ANTIBODY BINDING FOR MOUSE 1. PRE-IMMUNE AND POST IMMUNE 1 – 4 SERA WERE TITRATED AND SCREENED BY INDIRECT ELISA AGAINST PEPTIDE ANTIGENS AT 1 μ G/ML. (B,D) POLYCLONAL ANTIBODY BINDING FOR MOUSE 2.

4.1.5.2. Anti-N PABs are highly specific and sensitive to N peptides

Both N-immunised mice exhibited strong PAB responses to both peptide antigens immediately following the initial immunisation. The PAB specificity to NN peptide increases significantly following the first immunisations, and this high anti-NN specificity is retained following every immunisation. This retention of PAB specificity over a wide range of PAB dilutions (1:100 to 1:6400) is indicative of high sensitivity developed to the NN peptide antigen.

At post-IM 4, there is a curve plateau of the PAB binding titration against NN peptide (see Figure 4.5 A and B.). The retained specificity of PABs at the highest dilution of 1:6400 is an indication that the optimal binding specificity and sensitivity have been attained for anti-NN PABs in both animals. There is no similar plateau seen in the NC PAB titration curve. At post-IM 4, anti-NC PABs have not yet reached maximal binding affinity in the immunised mice (see Figures 4.5. C and D). It is reasonable to assume that PAB specificity would be increased by an additional immunisation following the same trend. As such, N-immunised mice received booster injections two weeks after the fourth immunisation, following the same protocol as M-booster immunisations. Booster injections contained peptide only, with no adjuvant.

4.1.5.3. Does the NN peptide represent more immunodominant epitope?

Our antigenic N peptides are derived from different regions of the HCoV-NL63 structural N protein. The peptides are N-terminally (NN) and centrally located (NC) within the N sequence. The antibody response to the terminal N peptide is more specific and sensitive than the response to the central N peptide. This is in line with strong antigenic epitope sequences often being located within terminal regions of polypeptides. Protein termini are generally solvent-exposed and available for antibody binding, and less likely to be buried within the folded protein structure (Ramaraj et al., 2012). Anti-N PAB binding indicates that the NN antigenic peptide presents the immunodominant epitope between the two N-peptides.

4.1.6. Polyclonal antibodies are specific and sensitive to their full-length protein antigens

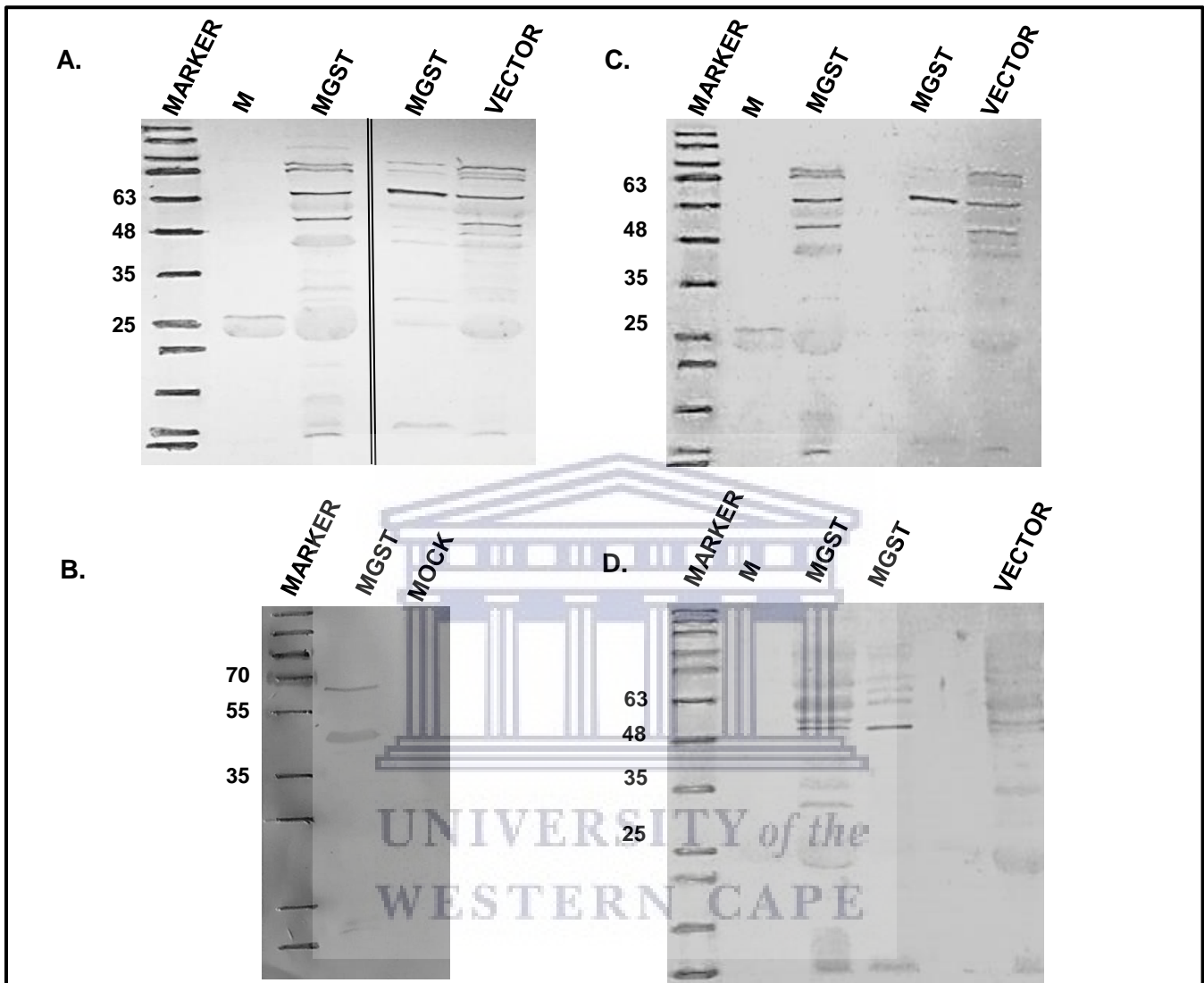


FIGURE 4.6. WESTERN BLOT SCREENING OF ANTI-M POLYCLONAL ANTIBODIES AGAINST FULL-LENGTH HCoV-NL63 MEMBRANE (M) PROTEIN. (A, B) ANTI-M POST-IMMUNE 3 SERA WERE USED AT 1:500 TO DETECT M PROTEIN, PURIFIED M ALONGSIDE MGST FUSION PROTEIN EXPRESSED IN *E. COLI*. THE INSOLUBLE CELL FRACTION AND UNINDUCED (MOCK) EXPRESSION LYSATE WAS ALSO SCREENED FOR M EXPRESSION (C) ANTI-M P.I.3 SERA AT 1:1000 TO DETECT M PROTEIN, PURIFIED M ALONGSIDE MGST FUSION PROTEIN EXPRESSED IN *E. COLI*. THE INSOLUBLE CELL FRACTION AND UI EXPRESSION LYSATE WAS ALSO SCREENED FOR M EXPRESSION. (D) ANTI-GST PRIMARY ANTIBODY USED AT 1:1000 TO SCREEN FOR MGST FUSION PROTEIN. THE INSOLUBLE CELL FRACTION AND UI EXPRESSION LYSATE WAS ALSO SCREENED FOR M EXPRESSION.

In this research study, peptide antigens specific to each of the proteins of interest were used, namely the HCoV-NL63 M and N proteins. The goal was to develop antibodies with a binding affinity specific for these structural proteins when expressed in the UWC Molecular Biology and Virology Research Laboratory's *in vitro* systems in order to characterise these CoV structural components further experimentally. To assess if using these peptide antigens as immunising agents resulted in the production of protein-specific antibodies, mouse PI sera with high specificity to peptide antigens were used to detect full-length protein antigens expressed in either a bacterial (*E.Coli*), insect (Sf9) or mammalian (Cos7) cell line.

4.1.6.1. Anti-M PABs are specific and sensitive in Western blot detection of full-length HCoV-NL63 M protein

The intended use for the anti-peptide antibodies was the detection of full-length proteins in the expression systems. As such, our generated PABs needed to be screened preliminarily against their respective protein antigens. To assess the cause of low anti-M PAB binding affinity for the M peptide, PAB binding was characterised to the denatured, expressed M protein. The denaturing of the protein antigen allowed the M-epitope to be linearly presented in the protein structure. This is congruent with the antibodies being raised against a linear peptide antigen. Post-immune 3 (PI3) mouse serum exhibited the highest specificity for MC peptide antigen and was used at different dilutions to detect full-length M protein (Figure 4.6.). HCoV-NL63 M was expressed as a GST fusion protein in *BL21 E.Coli* cells. Anti-M PABs detected purified M protein at approximately 26kDa (lane 2). This is consistent with the estimated expected size of HCoV-NL63 M (Naskalska et al., 2018). PABs also detected MGST fusion protein specifically in the whole cell lysate, at the expected size of approximately 50kDa (HCoV-NL63 M is expected at 26kDa; GST is expected at 21 – 28kDa). In Figure 4.6. C and D above, polyclonal antisera were further diluted for use at 1:1000 in order to decrease non-specific antibody binding (background, extra bands) in the MGST expression lysate. A duplicate blot exposed to anti-GST primary antibody was run alongside the anti-M PAB blot to confirm the specific detection of MGST fusion protein. This anti-GST blot confirmed the presence of the fusion protein at the same size. Furthermore, anti-GST does not detect purified M protein (lane 2 in both blots). The anti-M PABs exhibited a high binding affinity for HCoV-NL63 M protein, capable of sensitive and specific detection of crude and purified M samples at a serum dilution of 1:1000. Anti-peptide rabbit polyclonals have been raised against HCoV-NL63 M. The M specific synthetic peptides corresponded to AA 181-195 and AA 211-226 of the M sequence. Rabbits are commonly used for PAB production due to their small size and relative ease of housing and handling, as well as their ability to generate high titre serum antibody (Naskalska et al., 2019; Ringler & Newcomer, 2014). To the best of the author's knowledge, this is the first report of an anti-peptide mouse polyclonal antibody specific for the HCoV-NL63 M protein.

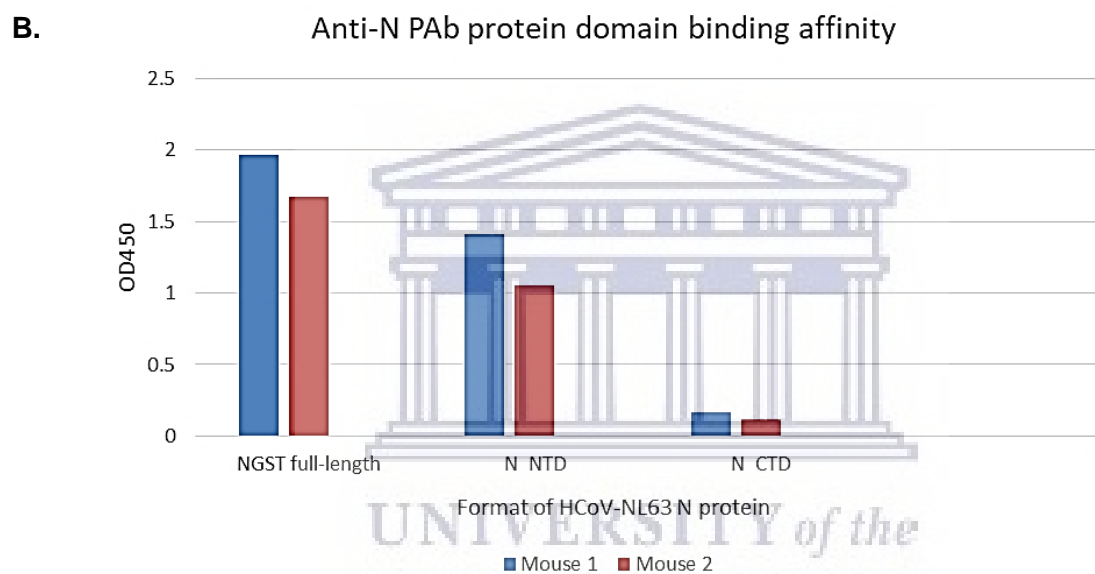
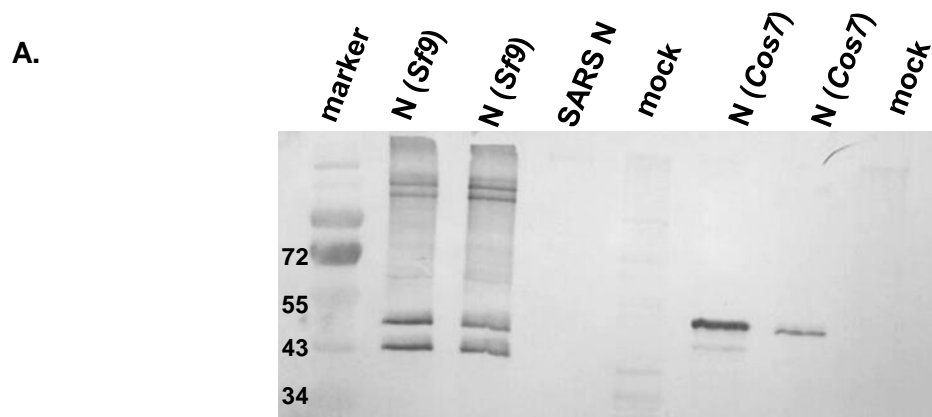


FIGURE 4.7. ANTI-N POLYCLONAL ANTIBODY SCREENING AGAINST HCoV-NL63 NUCLEOCAPSID (N) PROTEIN ANTIGENS. (A) PI 4 MOUSE ANTISERA AT 1:1000 USED TO DETECT N PROTEIN EXPRESSED IN Sf9 INSECT CELLS AND Cos7 MAMMALIAN CELLS. ANTI-N PABS WERE ALSO SCREENED AGAINST SARS-CoV N PROTEIN EXPRESSED IN Sf9 CELLS. ONLY Sf9 AND Cos7 'MOCK' EXPRESSION LYSATES WERE SCREENED ALONGSIDE N PROTEIN LYSATES. (B) POST-IMMUNE 4 (PI 4) MOUSE ANTISERA AT 1:500 SCREENED BY INDIRECT ELISA AGAINST FULL-LENGTH N AND TRUNCATED FORMS OF THE N PROTEIN REPRESENTING THE NTD AND CTD.

4.1.6.2. Anti-N PABs are specific to the N-terminal domain (NTD) of HCoV-NL63 N (indirect ELISA)

The anti-N PABs exhibited high specificity and sensitivity to both the NN and NC peptides (Figure 4.7. above). Poly-specific polyclonal antibody response was expected due to the dual antigen immunisation in the N mice. In order to gain a better understanding of the N protein domain affinity of the PABs, anti-M PABs were screened at 1:1000 by indirect ELISA. PABs were screened for binding against purified NGST fusion proteins (previously confirmed by size by Coomassie staining; not shown) representing the full-length HCoV-NL63 N protein, as well as NTD and CTD truncated forms of HCoV-NL63 N (see Figure 4.7. A). The anti-N PABs in the serum of mouse 1 exhibited slightly more specific binding to N protein antigens than mouse 2. In both N-immunised mice, anti-N PABs showed specificity to the N protein NTD and full-length N. Antibody binding to the N protein CTD was not detected. A stark contrast is noted between the high specificity of PAB binding to NC peptide and the lack of specific binding to the N-CTD protein antigen. In this research study, the NC peptide was derived from a centrally located N-domain and did not represent a peptide sequence found within the N protein CTD. Therefore, it is expected that the anti-PABs do not bind N-CTD protein fragment. In downstream hybridoma screening and cloning, hybridoma antibodies were screened against peptide antigens, as well as full-length N protein.

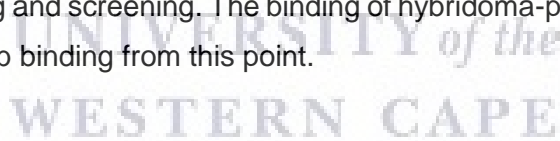
4.1.6.3. Anti-N PABs are specific and sensitive in Western blot detection HCoV-NL63 N protein, exhibiting no cross-reactivity with SARS-CoV N

To further screen the specificity of the anti-N PABs, the author and co-researchers ran whole cell lysates expressing HCoV-NL63 N in two different eukaryotic cell lines (Sf9 insect and Cos7 mammalian) on SDS-PAGE. Total proteins were transferred to PVDF and probed with anti-N PABs at 1:1000 dilution. Highly specific detection of full-length HCoV-NL63 N protein can be seen at the expected size of approximately 50 kDa (see Figure 4.7. A) (Berry et al., 2012; Naskalska et al., 2018). The expressed N protein was seen migrating as two bands at approximately 50kDa and slightly lower at around 43kDa, which may be due to protein degradation/truncation in denaturing conditions. This has been observed before for other expressed CoV full-length N proteins (Fang et al., 2013; Naskalska et al., 2018; Zhou & Collisson, 2000). Antibodies were able to bind N expressed in both *in vitro* systems. This is interesting since while both eukaryotic systems can express native-like structure proteins, there are differences in the co- and post-translational machinery and processing in mammalian vs insect cells (McKenzie & Abbott, 2018; Tripathi & Shrivastava, 2019). These differences can, in theory, lead to slightly variant forms of a given full-length protein being expressed (Zitzmann et al., 2017). The binding of the anti-N PABs across both species expression systems proves their robust detection ability, as any variance that may be present in the two forms of N protein does not negatively affect PAB binding. Furthermore, the

anti-N PAbs showed no cross-reactivity with the related SARS-CoV N protein (previously confirmed expression by laboratory colleague; result not shown here) expressed in insect cells. This may indicate that the PAbs have application in species-specific HCoV diagnostics.

Anti-peptide PAbs specific to HCoV-NL63 M protein have previously been produced in rabbits. These donated antibodies (produced and donated by Lia van der Hoek, Department of Medical Microbiology, University of Amsterdam) have been used to detect HCoV-NL63 M in various experimental applications, including Western blotting and IF (El-Duah et al., 2019; Naskalska et al., 2019). It is inferred that PAbs specific for HCoV-NL63 N have been made as MAbs specific to N have been isolated by murine hybridoma generation (Sastre et al., 2011). There is also a commercially available anti-HCoV-NL63 N protein mouse mAb (produced in Ingenasa, Spain). Monitoring the PAb response to antigen prior to hybridoma generation is an expected procedure; however, this data is not reported in the article by Sastre et al. (2011). Also, the immunising antigen used to generate those anti-N antibodies was full-length recombinant N protein. In this research study, specific synthetic peptide antigens were used for animal immunisation. Here we have managed to isolate and characterise the binding affinity of anti-peptide PAbs raised in mice against two of the major HCoV-NL63 structural components. To the best of the author's knowledge, there is no available similar published data, which showcases murine PAb binding to peptide and full-length protein antigens. The data further supports synthetic peptides as effective antigens for viral protein antibody production in mice (Lee et al., 2016).

For the purpose of this study, the highest specific PAb sera were used as a positive control in downstream hybridoma cloning and screening. The binding of hybridoma-produced antibodies was then screened in comparison to PAb binding from this point.



4.1.7. Antibody production by hybridomas

A. M-C mouse 1

Plate number	Positive well
1	H4
5	E2

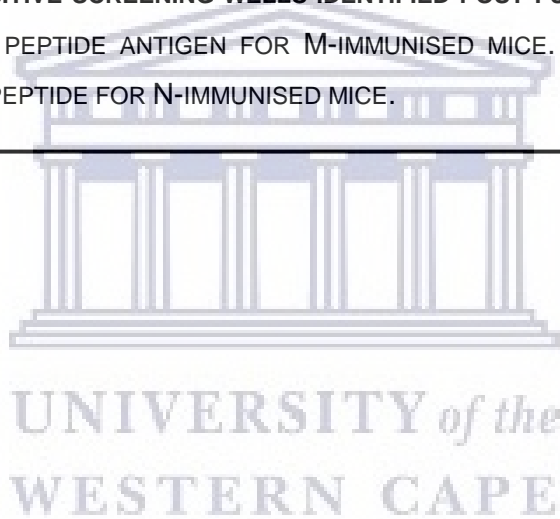
M-C mouse 2

Plate number	Positive well
5	F2
5	E11

B. N-N/N-C mouse

Plate number	Positive well
2	H8
3	D10
4	D11
5	A11

FIGURE 4.8. THE ORIGINAL POSITIVE SCREENING WELLS IDENTIFIED POST-FUSION. (A) WELLS SCREENING POSITIVE AGAINST IMMUNISING PEPTIDE ANTIGEN FOR M-IMMUNISED MICE. (B) WELLS THAT SCREENED POSITIVE AGAINST IMMUNISING PEPTIDE FOR N-IMMUNISED MICE.



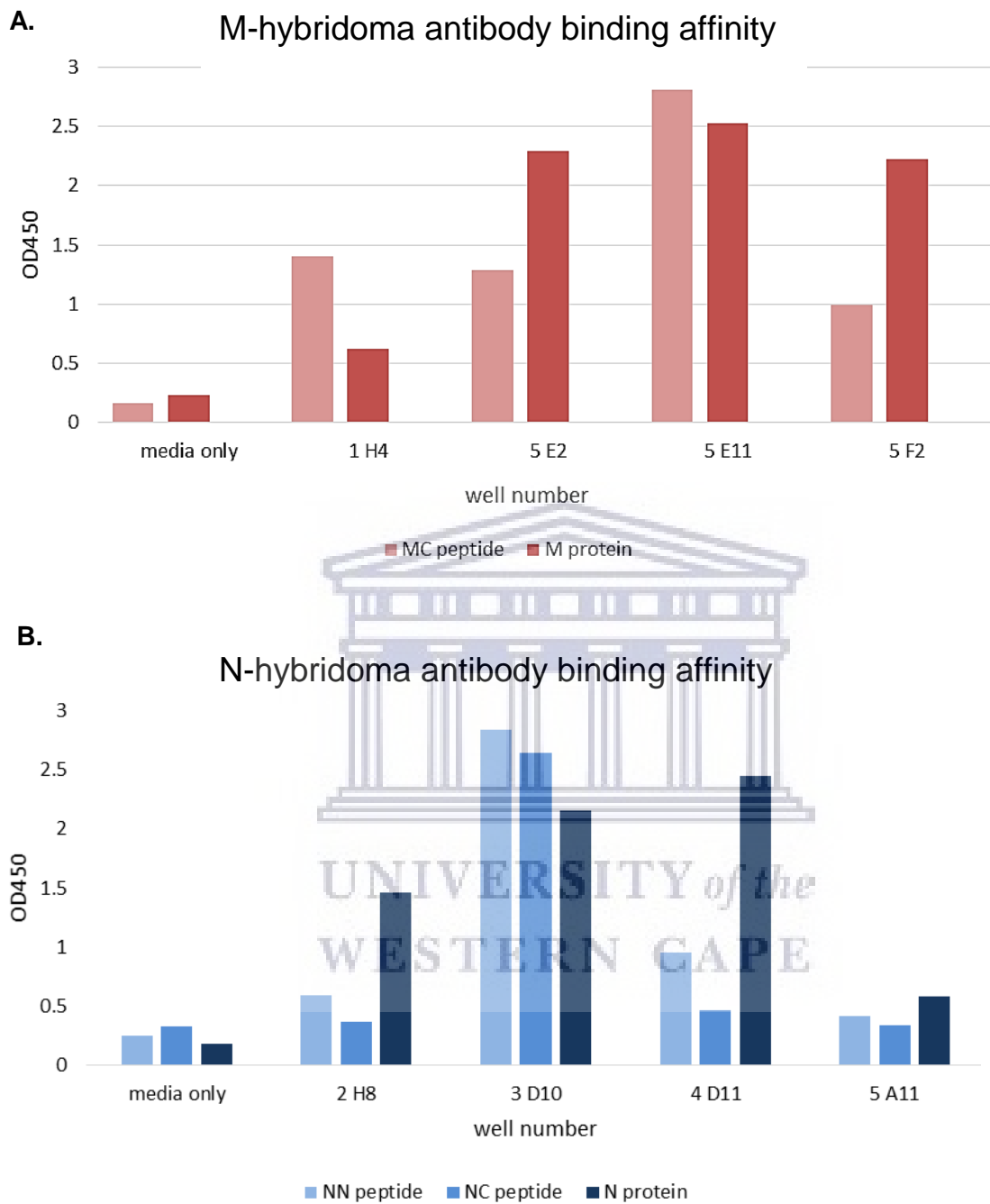


FIGURE 4.9. THE BINDING AFFINITY OF ANTI-M AND ANTI-N HYBRIDOMA-SECRETED ANTIBODIES ISOLATED FROM THE INITIAL POSITIVE CELL LINES. (A) ANTI-N BINDING SPECIFICITY TO PEPTIDE (1 μ G/ML) AND PROTEIN ANTIGEN (0.1 μ G/ML). (B) ANTI-N BINDING SPECIFICITY TO PEPTIDE (1 μ G/ML) AND PROTEIN ANTIGEN (0.1 μ G/ML).

4.1.7.1. Initial screens indicate positive hybrid cell lines

After cell fusion, hybridomas are isolated from the heterogenous plated cell solution by the addition of HAT – hypoxanthine (H), aminopterin (A), and thymidine (T) – media supplement. Positive hybridoma selection is accomplished by aminopterin, which blocks the *de novo* DNA nucleotide synthesis pathway. This inhibition forces cells to make use of the salvage pathway for nucleotide synthesis and DNA replication, which is done in the presence of H and T. Myeloma cells cannot utilise the salvage pathway because they lack a specific enzyme – hypoxanthine-guanine phosphoribosyltransferase (HGPRT). As such, unfused myelomas will not replicate in the presence of HAT. Chimeric hybridoma cells encode a functional HGPRT enzyme, inherited from the splenic parent cell. Unfused B cells will not replicate in cell culture and survive HAT selection (Szybalski, 1992). Following fusion and cell selection by HAT growth media, the supernatants from hybridoma cells were screened for specificity to their respective peptide and protein antigens. The hybridoma cell lines with positive screening antibodies are indicated for all experimental animals in Figure 4.8. Anti-M antibodies all exhibited specificity for the cognate MC peptide when screened by indirect ELISA (see Figure 4.9. A). Of the four isolated hybridoma lines, three bound the full-length M protein antigen with high specificity, including 5E2, 5E11, and 5F2. Protein affinity binding was significantly higher than peptide affinity for 5E2 and 5F2 antibodies. M-hybridoma lines 1H4, 5E2, 5E11, and 5F2 were maintained for limiting dilution cloning.

Chapter 3 stated that the first N-immunised mouse hybridoma cells were contaminated and died before HAT selection and initial screening could be done. A Balb/C mouse was given a single immunisation (identical to previous first round immunisations), and the animal was sacrificed 72 hours post-immunisation. The harvested spleen cells were boosted *in vitro* in the same manner as all previously processed splenocyte cultures. Fusion with myeloma cells was carried out as previously described. Three hybridoma lines produced anti-N antibodies capable of high specific binding to full-length N protein when screened by indirect ELISA (see Figure 4.9. B). Following the initial ELISA screening, N hybridoma cell lines 2H8 and 4D11 died. During B cell fusion with myeloma cells, forming a new stable cellular genome requires successful genetic recombination between the two cell types. These may have been genetically unstable cell lines, as cells died after removing HAT/HT supplement from cell culture media. N hybridoma lines 3D10 and 5A11 were maintained for limiting dilution cloning.

No clear preference in affinity for either N-peptide was observed in the binding of hybridoma-secreted Abs. While the B cell population in N-immunised mice was expected to produce Abs directed at each respective peptide epitope (NN and NC), a clonal B cell was expected to exhibit mono-specific binding to a single epitope. This lack of preferential binding to a single peptide epitope may be as a result of one of two things, namely 1) either at this stage the hybridoma populous in each well was not yet homogenous and, therefore, two different (or multiple) specific Abs were present in the cell media, or

2) Abs exhibited high non-specific binding to the NC peptide. This question could only be answered by further screening as hybridoma cells were cloned to ensure pure cell lines, each secreting a specific mAb.

The indirect ELISA results showcased the binding specificity of the hybridoma-secreted antibodies against their corresponding immunising peptide antigens and full-length proteins. This serves as confirmation that the anti-M and anti-N antibodies can bind their protein epitope presented in a linear (peptide) and non-linear (protein) conformation. Anti-M and anti-N were intended for use in a variety of protein expression experiments, and the ability to bind non-denatured protein target increased the utility of the antibodies in downstream applications.

4.1.8. Hybridoma antibodies are specific to their denatured protein antigens



FIGURE 4.10. ANTI-M HYBRIDOMA-SECRETED ANTIBODIES BIND FULL-LENGTH HCoV-NL63 M EXPRESSED AS A GST-FUSION PROTEIN. CELL CULTURE SUPERNATANTS FROM THE ORIGINAL HYBRIDOMA COLONY WELLS 1H4, 5E2, 5E11, AND 5F2 WERE SCREENED UNDILUTED AGAINST WHOLE CELL EXPRESSION LYSATES OF RECOMBINANT HCoV-NL63 MEMBRANE PROTEIN.

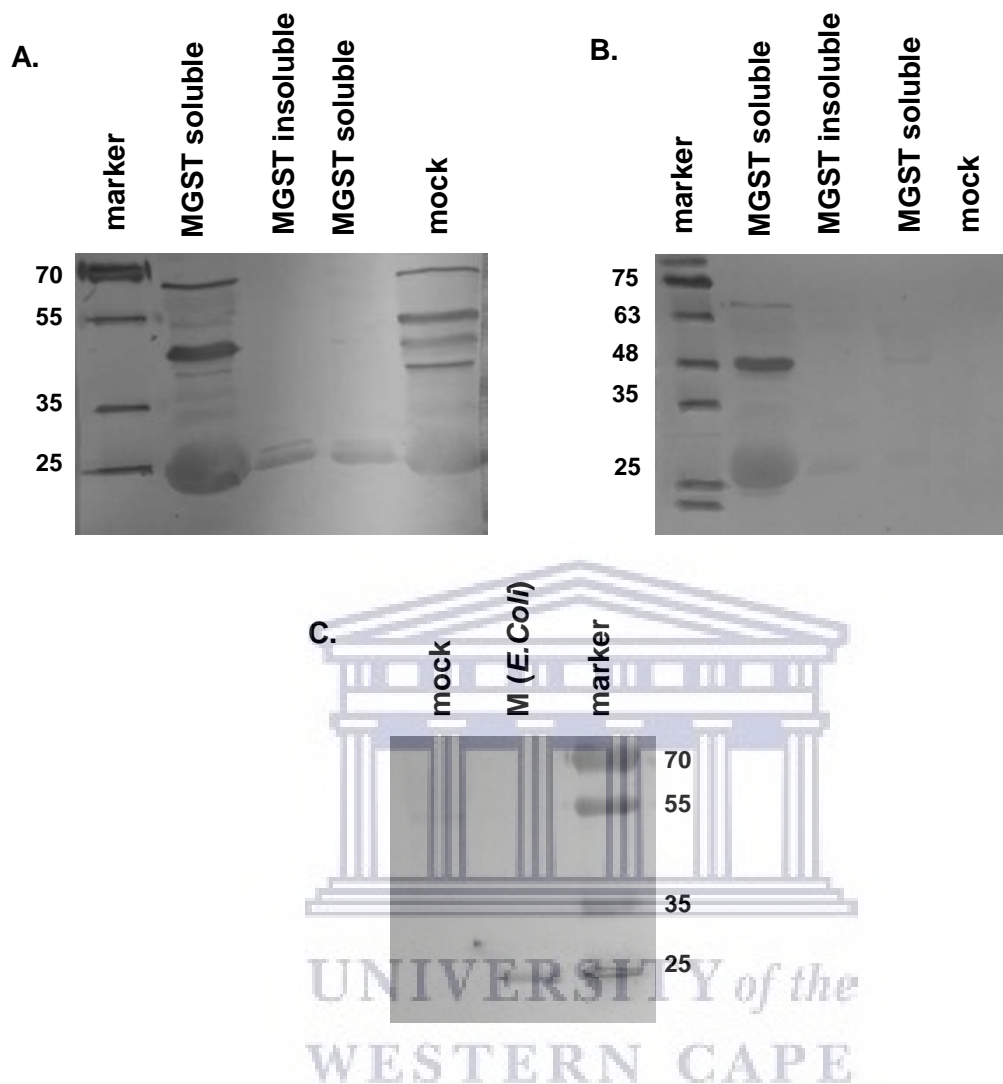


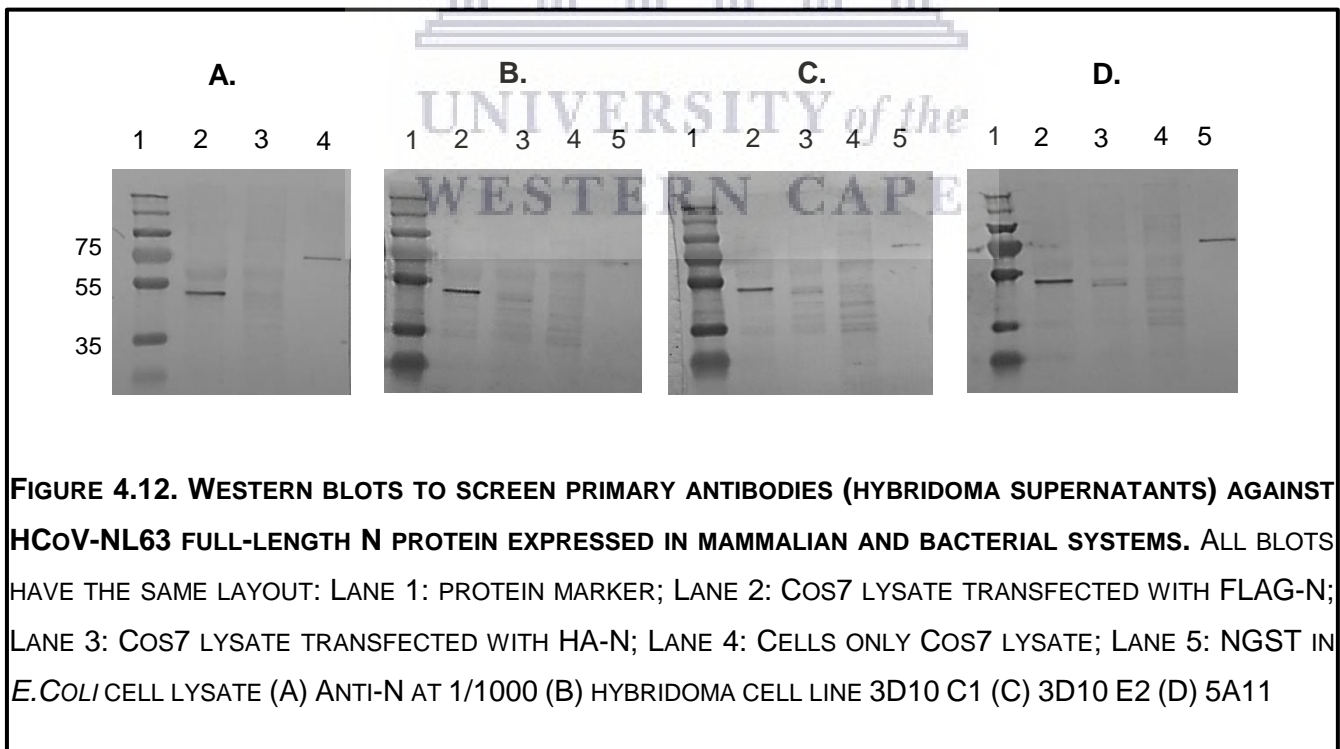
FIGURE 4.11. HYBRIDOMA LINE 5F2 SECRETES HCoV-NL63 M-SPECIFIC MABS. (A.) WESTERN BLOT SCREENING ANTI-M MABS IN 5F2 CELL SUPERNATANT (UNDILUTED) AGAINST HCoV-NL63 FULL-LENGTH M PROTEIN EXPRESSED AS A GST FUSION PROTEIN IN *E. COLI* CELLS. (B.) WESTERN BLOT SCREENING ANTI-M MABS IN 5F2 CELL SUPERNATANT (DILUTED 1:50) AGAINST HCoV-NL63 FULL-LENGTH M PROTEIN EXPRESSED AS A GST FUSION PROTEIN IN *E. COLI* CELLS. (C.) WESTERN BLOT SCREENING ANTI-M MABS IN 5F2 CELL SUPERNATANT (DILUTED 1:100) AGAINST HCoV-NL63 FULL-LENGTH M PROTEIN EXPRESSED IN *E. COLI* CELLS.

4.1.8.1. Anti-M antibodies specifically bind HCoV-NL63 M protein

This research study has shown that M-hybridoma antibodies can bind non-denatured M protein by indirect ELISA. To further characterise anti-M protein binding, supernatants were screened from each positive hybridoma line against full-length MGST fusion protein by Western blot. In Figure 4.10 above, undiluted cell supernatants specifically detect MGST at approximately 50kDa. A lower MW band at around 26kDa may represent spontaneously cleaved M protein (cleaved during cell lysis). A high amount of background staining and non-specific bands were detected in all four Western blots, which can likely be attributed to a supraoptimal antibody concentration. The strongest and most specific M binding signal (least background) was detected by 5F2 antibodies. To determine the antibody dilution needed for optimal M binding, 5F2 supernatant was screened against expressed M protein at different dilutions.

4.1.8.2. 5F2 detects purified and crude HCoV-NL63 M under denaturing conditions on Western blot

The 5F2 hybridoma line produced antibodies that exhibit specific binding to the M protein at a 1:50 dilution (Figure 4.11). Purified M (TEV-cleaved) was also explicitly detected with the anti-M PAb sera at 1:100 dilution. HCoV-NL63 M protein was detected at approximately 26kDa. This purified protein sample was used in the downstream screening of hybridoma-secreted antibodies.



4.1.8.3. N-hybridoma clone antibodies bind N protein across different (species) expression systems

While it is of interest to know which peptide binds hybridoma antibodies more specifically, the goal was to develop antibodies specific to the full-length proteins used within the ambit of this research study. As such, the initial Western blot screening of anti-N hybridoma-secreted antibodies was done against mammalian expressed full-length N, as well as a bacterial-expressed NGST fusion protein. Undiluted cell supernatants were harvested and used to screen N-expression samples. The clonal hybridoma lines 3D10C1 and 3D10E2 produced antibodies, which exhibit specific and robust detection of HCoV-NL63 N. Hybridoma 5A11 was not tolerant of limiting dilution cloning and did not survive at such cell density. However, this cell line exhibited strong growth at normal culture conditions and was maintained to analyse secreted antibodies. The antibodies produced by 5A11 also showed specific and robust binding to our N protein expressed across two different cell species. The specificity of the crude anti-N antibodies is comparable to that of the commercially purchased anti-N mouse mAb (see Figure 4.12. A above).

4.1.9. Generating clonal hybridoma cell lines

4.1.9.1. Successful isolation of M-hybridoma clones

TABLE 4.1. THE ISOLATION OF M-HYBRIDOMA CLONE 5E11G7A5A3 BY LIMITING DILUTION CLONING. WELLS, WITH THE HIGHEST SPECIFICITY AND AFFINITY AS DETERMINED BY ELISA, WERE SELECTED FOR CLONING. WELLS, WITH AN OD450 HIGHER THAN THE POSITIVE CONTROL, WERE DESIGNATED AS POSITIVE WELLS. CHOSEN WELLS WERE FURTHER CLONED INTO 47 NEW WELLS. THE PERCENTAGE OF POSITIVE WELLS AFTER CLONING REPRESENTS THE NUMBER OF POSITIVE WELLS EXPRESSED AS A PERCENTAGE OF PLATED WELLS FROM THE PREVIOUS SCREENING.

Clone	Number of wells plated	Number of wells with growth selected for screening	Number of wells that screened positive	Percentage of positive wells (%)	OD450 of well selected for cloning
5E11G7A5A3					
Post-fusion (1 st screen)	96	96	2	2.08	2.81
Post-cloning 1 (2 nd screen)	47	6	6	100	2.45
Post-cloning 2 (3 rd screen)	47	7	2	28.57	0.57
Post-cloning 3 (4 th screen)	47	28	22	81.48	1.12
Summary	237	137	32	23.36	1.74 (average OD450)

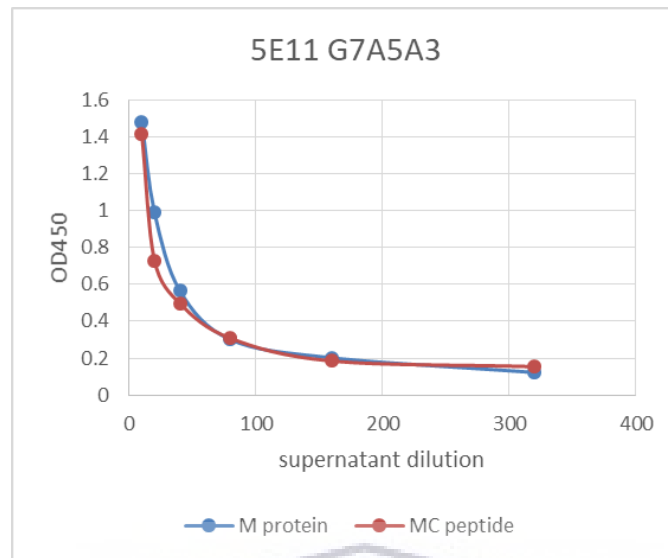


FIGURE 4.13. INDIRECT ELISA OF ANTI-M 5E11G7A5A3 mAb AFFINITY FOR BOUND MC PEPTIDE ANTIGEN AND BOUND PURIFIED HCoV-NL63 M PROTEIN (PURIFIED M, 10 μ G/ML). THE GRAPH REPRESENTS A COMPARISON OF THE ANTI-M BINDING AFFINITY FOR BOTH ANTIGEN TYPES. EACH DATA POINT REPRESENTS THE MEAN OF A DUPLICATE MEASUREMENT.

TABLE 4.2. THE ISOLATION OF M-HYBRIDOMA CLONE 5E11G7G8H8 BY LIMITING DILUTION CLONING. WELLS, WITH THE HIGHEST SPECIFICITY AND AFFINITY AS DETERMINED BY ELISA, WERE SELECTED FOR CLONING. WELLS, WITH AN OD450 HIGHER THAN THE POSITIVE CONTROL, WERE DESIGNATED AS POSITIVE WELLS. CHOSEN WELLS WERE FURTHER CLONED INTO 47 NEW WELLS. THE PERCENTAGE OF POSITIVE WELLS AFTER CLONING REPRESENTS THE NUMBER OF POSITIVE WELLS EXPRESSED AS A PERCENTAGE OF PLATED WELLS FROM THE PREVIOUS SCREENING.

Clone	Number of wells plated	Number of wells with growth selected for screening	Number of wells that screened positive	Percentage of positive wells (%)	OD450 of well selected for cloning
5E11G7G8H8					
Post-fusion (1 st screen)	96	96	2	2.08	2.81
Post-cloning 1 (2 nd screen)	47	6	6	100	2.45
Post-cloning 2 (3 rd screen)	47	7	2	28.57	0.79
Post-cloning 3 (4 th screen)	47	14	10	71.42	1.07
Summary	237	123	20	16.26	1.78 (average OD450)

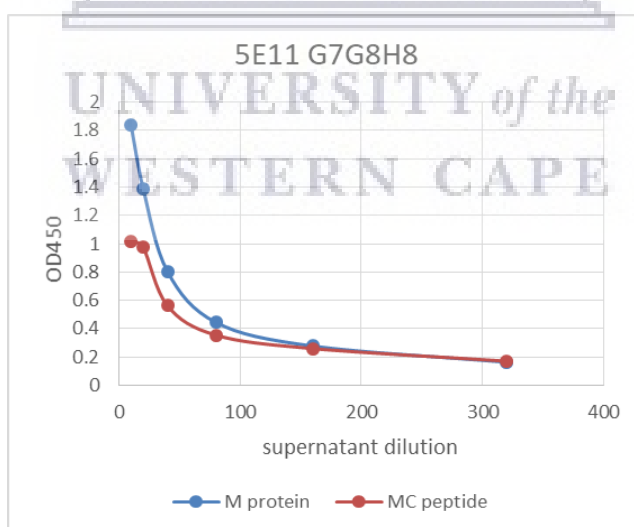


FIGURE 4.14. INDIRECT ELISA OF ANTI-M 5E11G7G8H8 mAb AFFINITY FOR BOUND MC PEPTIDE ANTIGEN AND BOUND PURIFIED HCoV-NL63 M PROTEIN (PURIFIED M, 10µg/mL). THE GRAPH REPRESENTS A COMPARISON OF THE ANTI-M BINDING AFFINITY FOR BOTH ANTIGEN TYPES. EACH DATA POINT REPRESENTS THE MEAN OF A DUPLICATE MEASUREMENT.

TABLE 4.3. THE ISOLATION OF M-HYBRIDOMA CLONE 5E11D10H7D12 BY LIMITING DILUTION CLONING. WELLS, WITH THE HIGHEST SPECIFICITY AND AFFINITY AS DETERMINED BY ELISA, WERE SELECTED FOR CLONING. WELLS, WITH AN OD450 HIGHER THAN THE POSITIVE CONTROL, WERE DESIGNATED AS POSITIVE WELLS. CHOSEN WELLS WERE FURTHER CLONED INTO 47 NEW WELLS. THE PERCENTAGE OF POSITIVE WELLS AFTER CLONING REPRESENTS THE NUMBER OF POSITIVE WELLS EXPRESSED AS A PERCENTAGE OF PLATED WELLS FROM THE PREVIOUS SCREENING.

Clone	Number of wells plated	Number of wells with growth selected for screening	Number of wells that screened positive	Percentage of positive wells (%)	OD450 of well selected for cloning
5E11D10H7D12					
Post-fusion (1 st screen)	96	96	2	2.08	2.81
Post-cloning 1 (2 nd screen)	47	6	6	100	2.01
Post-cloning 2 (3 rd screen)	47	4	3	75	0.76
Post-cloning 3 (4 th screen)	47	31	26	83.87	1.19
Summary	237	137	37	27.01	1.69 (average OD450)

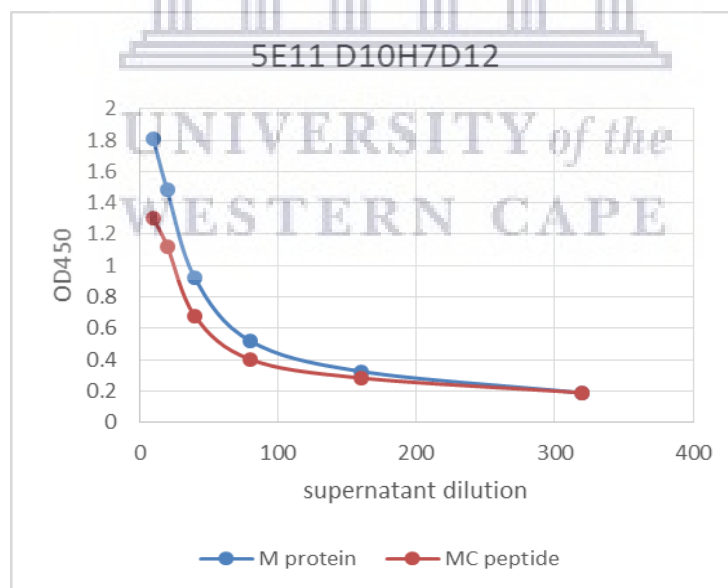


FIGURE 4.15. INDIRECT ELISA OF ANTI-M 5E11D10H7D12 MAB AFFINITY FOR BOUND MC PEPTIDE ANTIGEN AND BOUND PURIFIED HCoV-NL63 M PROTEIN (PURIFIED M, 10 μ G/ML). THE GRAPH REPRESENTS A COMPARISON OF THE ANTI-M BINDING AFFINITY FOR BOTH ANTIGEN TYPES. EACH DATA POINT REPRESENTS THE MEAN OF A DUPLICATE MEASUREMENT.

TABLE 4.4. THE ISOLATION OF M-HYBRIDOMA CLONE 5E11D10B7A4 BY LIMITING DILUTION CLONING. WELLS, WITH THE HIGHEST SPECIFICITY AND AFFINITY AS DETERMINED BY ELISA, WERE SELECTED FOR CLONING. WELLS WITH AN OD450 HIGHER THAN THE POSITIVE CONTROL, WERE DESIGNATED AS POSITIVE WELLS. CHOSEN WELLS WERE FURTHER CLONED INTO 47 NEW WELLS. THE PERCENTAGE OF POSITIVE WELLS AFTER CLONING REPRESENTS THE NUMBER OF POSITIVE WELLS EXPRESSED AS A PERCENTAGE OF PLATED WELLS FROM THE PREVIOUS SCREENING.

Clone	Number of wells plated	Number of wells with growth selected for screening	Number of wells that screened positive	Percentage of positive wells (%)	OD450 of well selected for cloning
5E11D10B7A4					
Post-fusion (1 st screen)	96	96	2	2.08	2.81
Post-cloning 1 (2 nd screen)	47	6	6	100	2.01
Post-cloning 2 (3 rd screen)	47	4	3	75	1.23
Post-cloning 3 (4 th screen)	47	13	10	76.92	1.24
Summary	237	119	21	17.65	1.82 (average OD450)

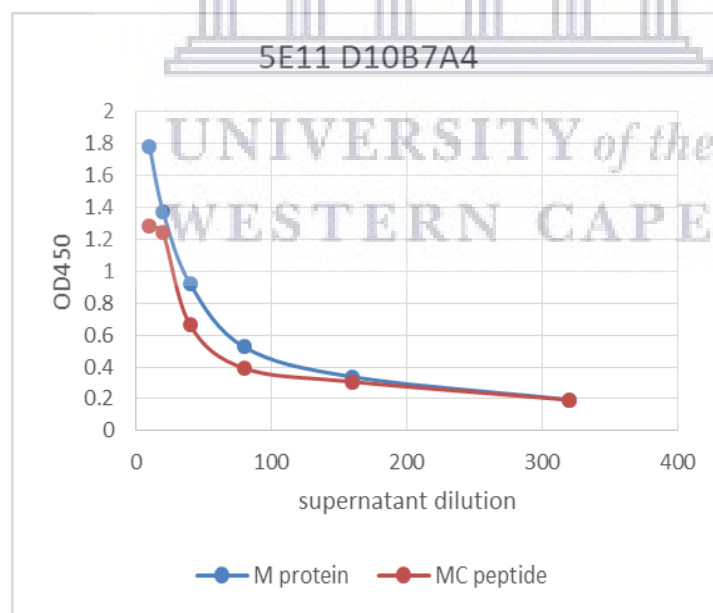


FIGURE 4.16. INDIRECT ELISA OF ANTI-M 5E11D10B7A4 MAB AFFINITY FOR BOUND MC PEPTIDE ANTIGEN AND BOUND PURIFIED HCoV-NL63 M PROTEIN (PURIFIED M, 10 μ G/ML). THE GRAPH REPRESENTS A COMPARISON OF THE ANTI-M BINDING AFFINITY FOR BOTH ANTIGEN TYPES. EACH DATA POINT REPRESENTS THE MEAN OF A DUPLICATE MEASUREMENT.

TABLE 4.5. THE ISOLATION OF M-HYBRIDOMA CLONE 5F2F12F10E3 BY LIMITING DILUTION CLONING. WELLS, WITH THE HIGHEST SPECIFICITY AND AFFINITY AS DETERMINED BY ELISA, WERE SELECTED FOR CLONING. WELLS, WITH AN OD450 HIGHER THAN THE POSITIVE CONTROL, WERE DESIGNATED AS POSITIVE WELLS. CHOSEN WELLS WERE FURTHER CLONED INTO 47 NEW WELLS. THE PERCENTAGE OF POSITIVE WELLS AFTER CLONING REPRESENTS THE NUMBER OF POSITIVE WELLS EXPRESSED AS A PERCENTAGE OF PLATED WELLS FROM THE PREVIOUS SCREENING.

Clone	Number of wells plated	Number of wells with growth selected for screening	Number of wells that screened positive	Percentage of positive wells (%)	OD450 of well selected for cloning
5F2F12F10E3					
Post-fusion (1 st screen)	96	96	2	2.08	0.99
Post-cloning 1 (2 nd screen)	47	4	4	100	1.87
Post-cloning 2 (3 rd screen)	47	3	1	33.3	0.55
Post-cloning 3 (4 th screen)	47	37	37	100	0.7
Summary	237	140	44	31.43	1.02 (average OD450)

4.1.9.2. Anti-M mAbs are specific to full-length M protein antigen

Four clonal lines were originally isolated for anti-M antibody production. During the first round of limiting dilution cloning, one of those lines died. After round two of cloning, 5E2 clones no longer screened positive against protein antigen. The surviving two lines (5E11 and 5F2) were subjected to three rounds of cloning at a limiting dilution (one cell/well) to ensure the generation of pure clonal hybridoma cell lines. As our immunogens were peptide antigens, the screening of antibodies against the native protein antigen was essential to ensure that the antibodies are able to detect full-length expressed protein. Following cloning, the supernatants of growing cells were screened against purified M protein, and the highest positive wells were further cloned (Table 4.1 - 4.5.). At the conclusion of limiting dilution cloning, supernatants from final hybridoma lines were screened by indirect ELISA against the M peptide and protein antigens (Figure 4.13 - 4.16.) Positive clonal cell lines were also frozen and stocks stored at -80°C, concurrently to hybridoma cloning. When screening, all colonies (all wells) were screened at the same time.

To the best of the author's knowledge, this is the first time a mAb to the HCoV-NL63 M protein has been produced. Polyclonal anti-CoV M antibodies generated in rabbits have been published in multiple research experiments. Rabbits are generally the top choice for the production of polyclonals because

of their size and amount of serum that can be collected (Hanly et al., 1995; Leenaars & Hendriksen, 2005). There is no commercially available anti-HCoV-NL63-M mAb or published data to date on producing a mouse mAb specific for HCoV-NL63 M protein. This antibody will detect M protein in future expression, localisation, and interaction studies with the major structural proteins of HCoV-NL63. Detecting M specifically could also help obtain a more complete picture of M's role in HCoV-NL63 virion assembly.



4.1.9.3. Successful isolation of N-hybridoma clones

TABLE 4.6. THE ISOLATION OF N-HYBRIDOMA CLONE 3D10E2A6C2 BY LIMITING DILUTION CLONING. WELLS, WITH THE HIGHEST SPECIFICITY AND AFFINITY AS DETERMINED BY ELISA, WERE SELECTED FOR CLONING. WELLS, WITH AN OD450 HIGHER THAN THE POSITIVE CONTROL, WERE DESIGNATED AS POSITIVE WELLS. CHOSEN WELLS WERE FURTHER CLONED INTO 47 NEW WELLS. THE PERCENTAGE OF POSITIVE WELLS AFTER CLONING REPRESENTS THE NUMBER OF POSITIVE WELLS EXPRESSED AS A PERCENTAGE OF PLATED WELLS FROM THE PREVIOUS SCREENING.

Clone	Number of wells plated	Number of wells with growth selected for screening	Number of wells that screened positive	Percentage of positive wells (%)	OD450 of well selected for cloning
3D10E2A6C2					
Post-fusion (1 st screen)	96	96	1	1.04	2.16
Post-cloning 1 (2 nd screen)	47	18	12	66.67	2.78
Post-cloning 2 (3 rd screen)	47	4	3	75	2.61
Post-cloning 3 (4 th screen)	47	38	38	100	2.21
Summary	237	156	54	34.62	2.44 (average OD450)

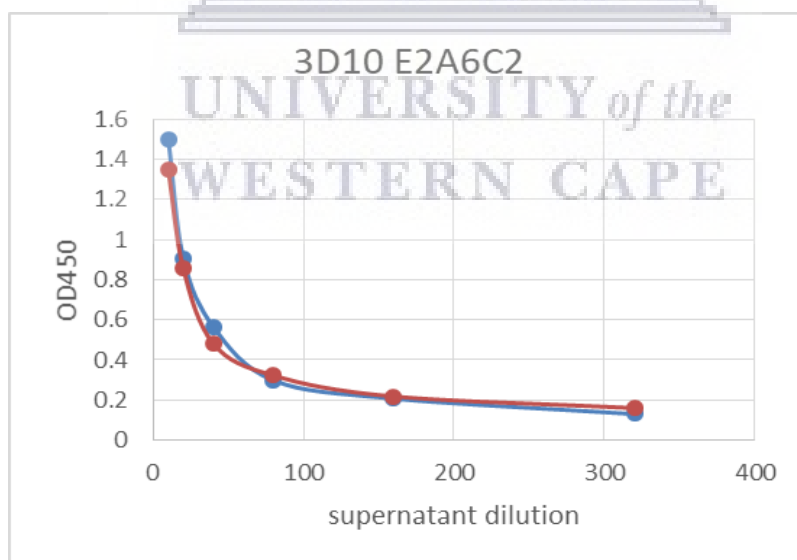


FIGURE 4.17. INDIRECT ELISA OF ANTI-N MAB PRODUCED BY CLONE 3D10E2A6C2 FOR BOUND NN PEPTIDE ANTIGEN AND BOUND PURIFIED HCoV-NL63 N PROTEIN (PURIFIED N, 10 μ G/ML). THE GRAPH REPRESENTS A COMPARISON OF THE ANTI-N BINDING AFFINITY FOR BOTH ANTIGEN TYPES. EACH DATA POINT REPRESENTS THE MEAN OF A DUPLICATE MEASUREMENT.

TABLE 4.7. THE ISOLATION OF N HYBRIDOMA CLONE 3D10C1E2D1 BY LIMITING DILUTION CLONING. WELLS, WITH THE HIGHEST SPECIFICITY AND AFFINITY AS DETERMINED BY ELISA, WERE SELECTED FOR CLONING. WELLS, WITH AN OD450 HIGHER THAN THE POSITIVE CONTROL, WERE DESIGNATED AS POSITIVE WELLS. CHOSEN WELLS WERE FURTHER CLONED INTO 47 NEW WELLS. THE PERCENTAGE OF POSITIVE WELLS AFTER CLONING REPRESENTS THE NUMBER OF POSITIVE WELLS EXPRESSED AS A PERCENTAGE OF PLATED WELLS FROM THE PREVIOUS SCREENING.

Clone	Number of wells plated	Number of wells with growth selected for screening	Number of wells that screened positive	Percentage of positive wells (%)	OD450 of well selected for cloning
3D10C1E2D1					
Post-fusion (1 st screen)	96	96	1	1.04	2.16
Post-cloning 1 (2 nd screen)	47	18	12	66.67	2.75
Post-cloning 2 (3 rd screen)	47	14	11	78.57	2.67
Post-cloning 3 (4 th screen)	47	16	13	81.25	1.35
Summary	237	144	37	25.69	2.23 (average OD450)

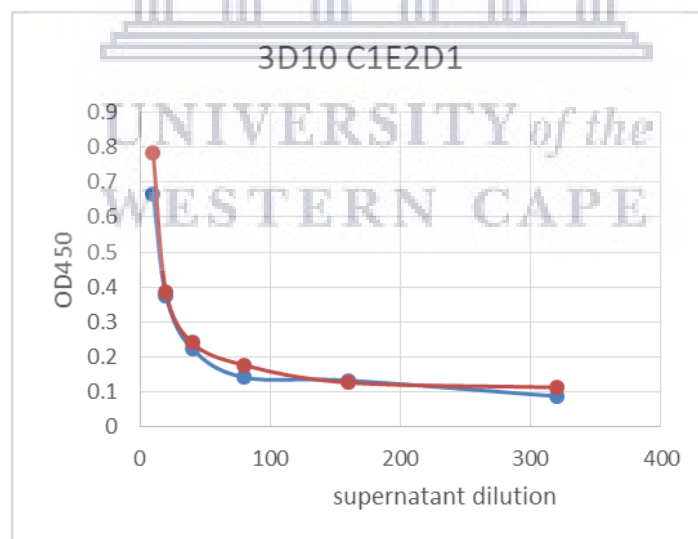


FIGURE 4.18. INDIRECT ELISA OF ANTI-N MAB PRODUCED BY CLONE 3D10C1E2D1 FOR BOUND NN PEPTIDE ANTIGEN AND BOUND PURIFIED HCoV-NL63 N PROTEIN (PURIFIED N, 10µg/ML). THE GRAPH REPRESENTS A COMPARISON OF THE ANTI-M BINDING AFFINITY FOR BOTH ANTIGEN TYPES. EACH DATA POINT REPRESENTS THE MEAN OF A DUPLICATE MEASUREMENT.

TABLE 4.8. THE ISOLATION OF N HYBRIDOMA CLONE 3D10C1A6A12 BY LIMITING DILUTION CLONING. WELLS, WITH THE HIGHEST SPECIFICITY AND AFFINITY AS DETERMINED BY ELISA, WERE SELECTED FOR CLONING. WELLS, WITH AN OD450 HIGHER THAN THE POSITIVE CONTROL, WERE DESIGNATED AS POSITIVE WELLS. CHOSEN WELLS WERE FURTHER CLONED INTO 47 NEW WELLS. THE PERCENTAGE OF POSITIVE WELLS AFTER CLONING REPRESENTS THE NUMBER OF POSITIVE WELLS EXPRESSED AS A PERCENTAGE OF THE NUMBER OF PLATED WELLS FROM THE PREVIOUS SCREENING.

Clone	Number of wells plated	Number of wells with growth selected for screening	Number of wells that screened positive	Percentage of positive wells (%)	OD450 of well selected for cloning
3D10C1A6A12					
Post-fusion (1 st screen)	96	96	1	1.04	2.16
Post-cloning 1 (2 nd screen)	47	18	12	66.67	2.75
Post-cloning 2 (3 rd screen)	47	14	11	78.57	1.4
Post-cloning 3 (4 th screen)	47	19	12	63.16	1.7
Summary	237	147	36	24.49	2.0 (average OD450)

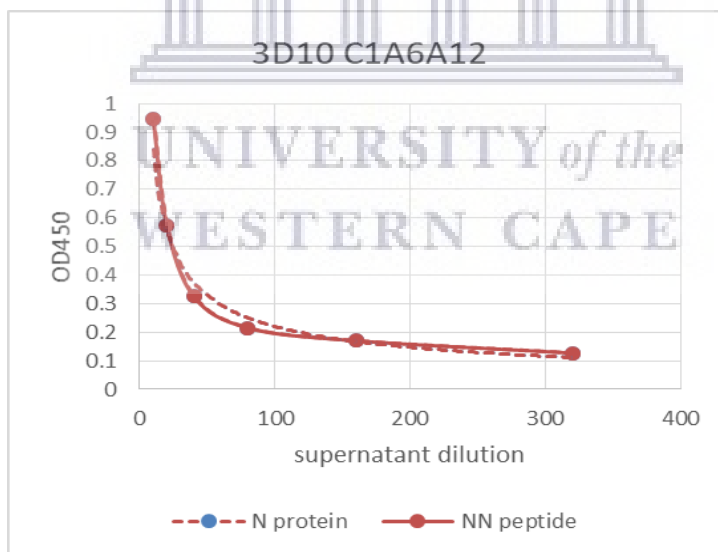


FIGURE 4.19. INDIRECT ELISA OF ANTI-N MAb PRODUCED BY CLONE 3D10C1A6A12 FOR BOUND NN PEPTIDE ANTIGEN AND BOUND PURIFIED HCoV-NL63 N PROTEIN (PURIFIED N, 10µg/ML). THE GRAPH REPRESENTS A COMPARISON OF THE ANTI-M BINDING AFFINITY FOR BOTH ANTIGEN TYPES. EACH DATA POINT REPRESENTS THE MEAN OF A DUPLICATE MEASUREMENT.

4.1.10. Monoclonal antibodies are specific to native HCoV-NL3 M and N

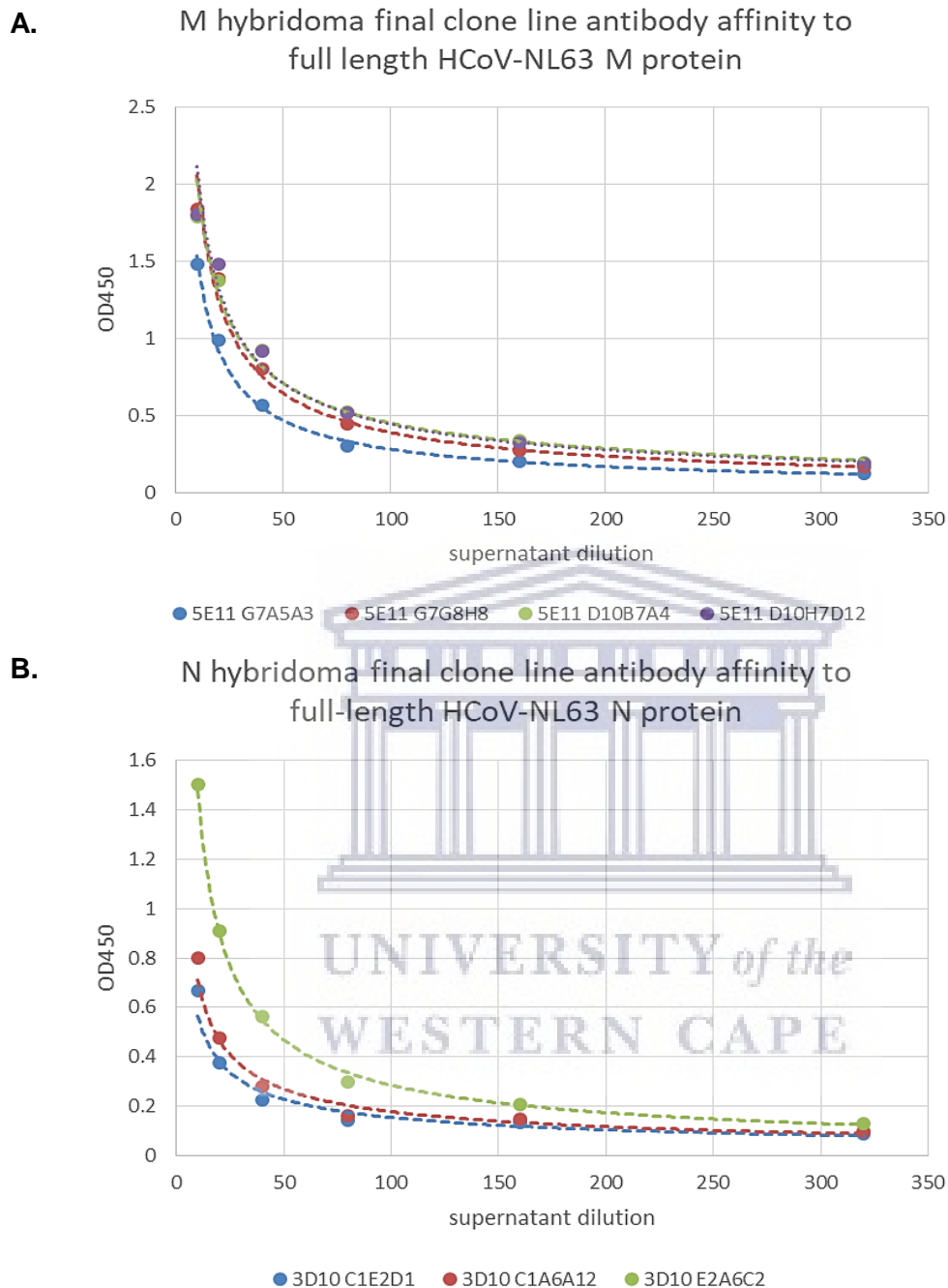
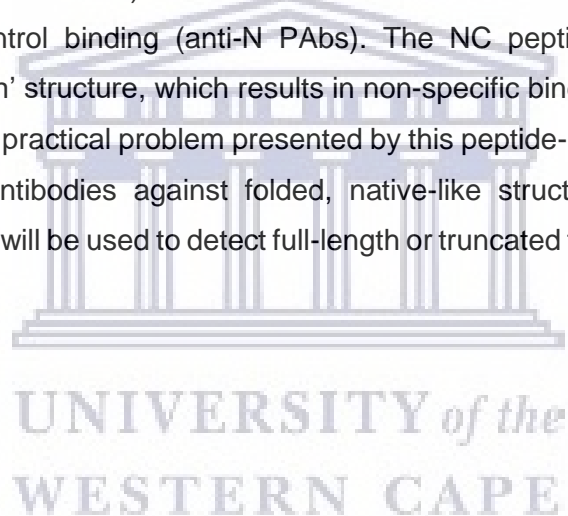


FIGURE 4.20. BINDING ASSAY OF ANTI-M AND ANTI-N MABS AGAINST FOLDED FULL-LENGTH PROTEIN ANTIGENS. (A) FINAL CLONAL M-HYBRIDOMA LINE SUPERNATANTS SCREENED OVER A RANGE OF DILUTIONS AGAINST FULL-LENGTH PURIFIED HCoV-NL63 M PROTEIN. (B) FINAL CLONAL N-HYBRIDOMA LINE SUPERNATANTS SCREENED OVER A RANGE OF DILUTIONS AGAINST FULL-LENGTH PURIFIED HCoV-NL63 N PROTEIN.

The final M-hybridoma clones all exhibited a similar binding pattern against full-length M when screened against native protein structure in an indirect ELISA (Figure 4.20 A.). These mAbs bind M specifically at a dilution of about 1/30. When examining antibody binding in the N hybridoma lines, 3D10E2A6 exhibited the highest binding specificity against N protein (Figure 4.20 B.). The slight differences in binding patterns between the three final N clones may also be explained by a difference in cell growth rate between the different lines. As cells were concurrently cultured, cell media from all the lines was harvested on the same day. Also, dilute antibodies, like in this case (in culture medium), are not stable in solution; therefore, antibodies could not be stored for longer than 24 hours at 4°C. These mAbs bind full-length N specifically at a dilution of approximately 1/20. The anti-N mAbs exhibited high non-specific binding to NC peptide. In the final screening, the NC binding was excluded because results (ELISA OD450s, not shown) indicate that all antibodies show much higher than expected specific binding to every clonal line antibody. With N protein and NN peptide-binding, we see at least a variation in antigen specificity between lines (Figure 4.20 B.). No such variation is seen for NC binding, and all binding is very high above positive control binding (anti-N PAbs). The NC peptide may adopt an unusual secondary confirmation or 'turn' structure, which results in non-specific binding of the anti-N antibodies (Dill & MacCallum, 2012). The practical problem presented by this peptide-binding affinity question was resolved by screening the antibodies against folded, native-like structure proteins. In the future application of the antibodies, it will be used to detect full-length or truncated forms of expressed proteins.



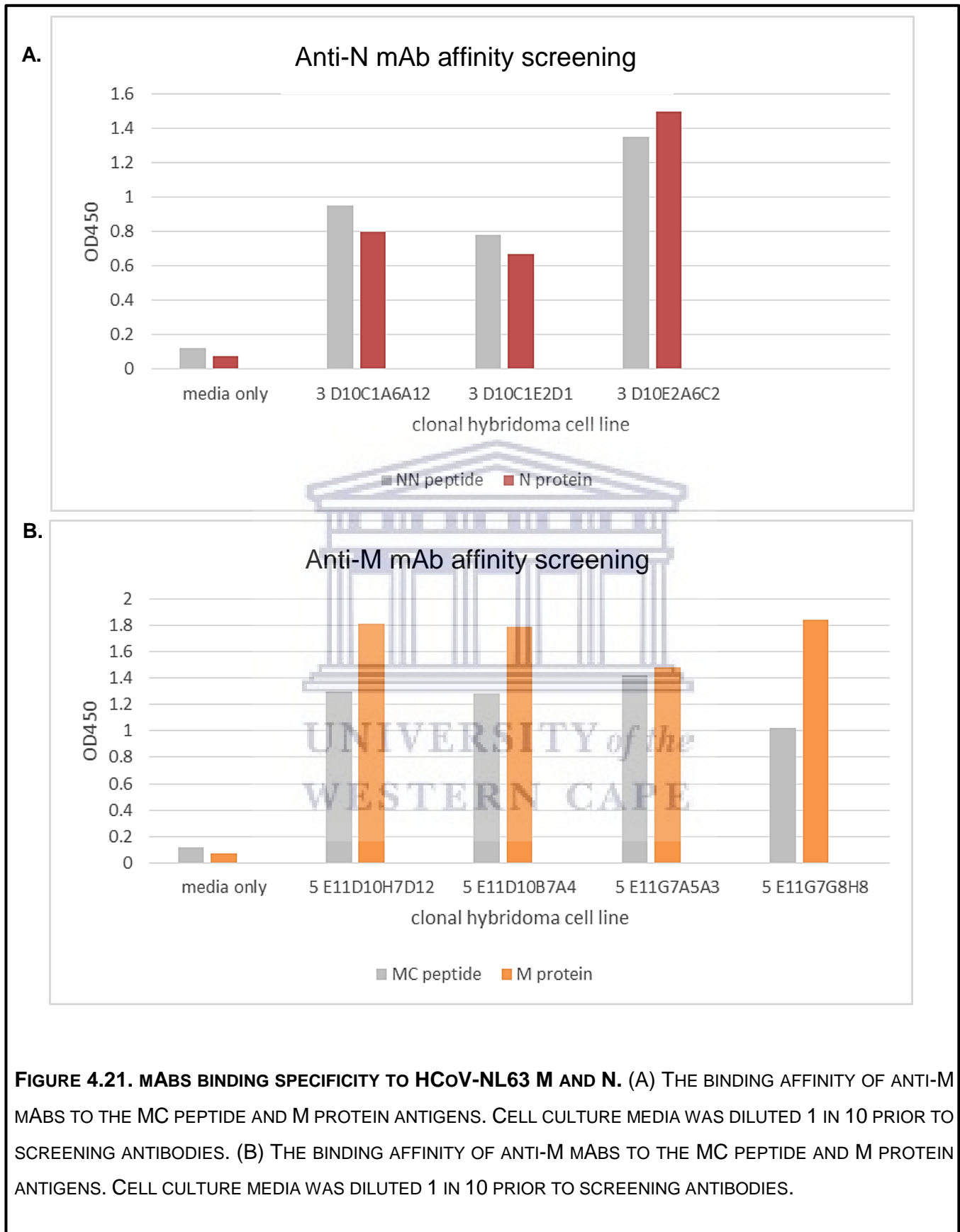


FIGURE 4.21. MABS BINDING SPECIFICITY TO HCoV-NL63 M AND N. (A) THE BINDING AFFINITY OF ANTI-M MABS TO THE MC PEPTIDE AND M PROTEIN ANTIGENS. CELL CULTURE MEDIA WAS DILUTED 1 IN 10 PRIOR TO SCREENING ANTIBODIES. (B) THE BINDING AFFINITY OF ANTI-M MABS TO THE MC PEPTIDE AND M PROTEIN ANTIGENS. CELL CULTURE MEDIA WAS DILUTED 1 IN 10 PRIOR TO SCREENING ANTIBODIES.

4.1.11. Hybridoma-secreted mAbs in crude cell supernatants exhibit specific binding to M and N protein antigens

After isolating clonal hybridoma cell lines, antibodies in culture supernatant from each final clone were further diluted 1:10 and screened to ensure the retention of antigen specificity. Figures 4.21 A and B graphically depicts how the binding specificity of the mAbs was characterised to the cognate peptide and native protein antigens. Considering the hybridoma lines secreting antibodies against M (Figure 4.21 B.), 5E11D10H7D12 exhibits the relative highest specific binding to both the protein and peptide antigens. G7G8 also binds M with high affinity; however, MC peptide affinity is lowered in G7G8. A mAb which is able to bind its epitope across various formats is preferred, and as such, 5E11D10H7D12 would be a more applicable mAb for further affinity purification methods. Considering the anti-N hybridomas, 3D10E2A6C2 exhibits specific binding to both antigens – linear and folded (Figure 4.21 A.). Whole protein immunisation also allows for antibody production to conformational epitopes (only available when protein is in a folded, mature, processed state). Full-length protein introduces the host to the entire range of available epitopes within the protein antigen. The peptide antigen immunogens provided a short antigenic epitope sequence, eliminating the risk of antibodies being generated to a large variety of predicted antigenic determinants within the full-length N protein. The binding of the mAbs is then specific to the short sequences presented by the applicable peptide/s. Results indicate that the antibodies recognised and bonded their specific epitopes even when presented within the folded protein.

Here it is confirmed that the anti-M and anti-N mAbs detect their specific full-length protein antigens in a native-like folded form. As previously stated, the ability of an antibody to recognise its epitope within the native-like conformation of a folded protein is a highly desirable characteristic for a mAb, as it broadens the application platform for the antibody. The hybridoma-produced antibodies were able to bind their epitope within their immunogenic peptide sequence in the denatured form of the full-length protein and folded protein. Antibody binding was specific for the expressed protein antigens. Unpurified antibodies in cell culture supernatants were not at a high concentration, which may explain the early drop in antigen specificity as supernatant dilution increased. The same trend was exhibited by both M and N antibodies, indicating a lowered sensitivity. In order to be used in a different downstream application such as Western blotting, antibody sensitivity is essential. Thus, mAbs will require molecular weight cut-off (MWCO) concentration and affinity purification to increase antibody concentration and improve sensitivity before use in applications other than ELISA.

4.1.11.1. Freezing of hybridoma cells

Once clonal hybridoma lines that produced anti-HCoV-NL63 M and N mAbs were obtained, cells were frozen in cryomedia and stored at -80°C. As cells were being sub-cultured for supernatant collection, all hybridoma cell lines that screened positive throughout for M or N-specific antibodies, were preserved in freezing media and stored at -80°C.

4.1.12. The development of CoV-specific antibodies

Generating antibodies against the proteins of specific viruses is necessary for viral research, as well as diagnostics and antiviral therapeutics (Petherick, 2020). Being able to differentiate, quantitate, and visualise different structural components of a virus during infection is essential in understanding the complex viral replicative cycle.

Antibodies have been or are being developed against known highly pathogenic HCoVs, including SARS-CoV and MERS-CoV, and most recently, SARS-CoV-2 (Elshabrawy et al., 2012; Liu et al., 2006; Park, B. K. et al., 2019; Zhou & Zhao, 2020). Each of these viruses has been responsible for human outbreaks in recent years, with the SARS-CoV-2 Covid-19 pandemic still ongoing. A major avenue of antiviral research and vaccine development involves generating 'neutralising' antibodies (NAbs) against major viral proteins. Neutralising antibodies target structural proteins on the virion surface in order to inhibit the attachment of the virus to host cell (Klasse, 2014).

In the current context of the Covid-19 global pandemic, several approaches are being exploited for antiviral CoV research and development, including antibody treatment. NAbs are currently being widely developed and assayed for activity against pandemic-causing viral agents (Baum et al., 2020; Ejemel et al., 2020; Hansen et al., 2020; Pinto et al., 2020). As NAbs have the potential to inhibit infection and can, therefore, be adapted for prophylactic vaccine development, these are highly attractive as antiviral strategies. Over the past few decades, the increased research effort into producing antiviral MAbs for vaccines has led to many advancements in mapping Ab-epitopes, hybridoma platform technology, and the development of humanised MAbs (Abbott et al., 2014; Lu et al., 2020; Zaroff & Tan, 2019). Subunit (protein) vaccine platforms, which target portions of the S protein receptor-binding domain (RBD), present the lowest safety risk to the host; however, these exhibit varying levels of immunogenicity, and as such, the dosage must be optimised relative to the adjuvant used as well as the route of vaccine administration (Lan et al., 2014; Lan et al., 2015; Ma, Li, et al., 2014; Ma, Wang, et al., 2014; Tai et al., 2016; Tang et al., 2015; Zhang et al., 2016). As the CoV S protein is considered the major protein involved in host cell attachment and entry, anti-CoV antibodies have generally targeted the S protein to inhibit the initial interaction between the virus and host cell. Most S protein antibodies are directed to the RBD of S as this is the region which complexes with the host cell receptor (Song et al., 2018; Wang et al., 2013). The SARS-CoV S protein and the S protein RBD have been demonstrated as primary

targets for NAbs developed in infected humans, non-human primates, and mice (Kumar et al., 2013). The structure of both SARS- (ACE2) and MERS- (DPP4) receptor host binding complex has been elucidated, allowing for the development/generation of specific NAbs. RBD-specific antibodies have been shown as effective antagonists to binding SARS and MERS S protein at ACE2 and DPP4, respectively (Coughlin et al., 2009; Lu et al., 2013; Wang et al., 2013). Multiple review articles have been published examining the importance of NAbs and their protective capacity against SARS-CoV infection (Coughlin & Prabhakar, 2012; Prabakaran et al., 2009; Zhang et al., 2005; Zhu et al., 2013). Designed against the S1 region of SARS-CoV Spike protein, the human monoclonal antibody (hmAb) 80R inhibits SARS-CoV infection *in vitro* (Sui et al., 2004). Immortalised B cells isolated from a convalescent SARS patient produced a mAb (S3.1) capable of neutralising infection in a mouse model (Traggiai et al., 2004). A mAb specific for the S protein RBD (AA 317-518) called m396, was shown to be 100 per cent effective in protecting against infection by various SARS-CoV strains during the 2002 – 2003 pandemic. In addition, in a murine model, m396 offers complete protection against viral challenge with the SARS-CoV strain isolated during the first outbreak, as well as against the GD03 strain isolated from the index patient of the second SARS-CoV outbreak (Sui et al., 2005; Yang et al., 2005; Zhu et al., 2007). In combination, these anti-S mAbs may have potential as a subunit vaccine anti-SARS-CoV therapy/treatment. Potent NAbs against MERS-CoV have been produced (Park, B. K. et al., 2019; Widjaja et al., 2019). Using phage display, a strong neutralising mAb, m336, has been isolated. The m336 epitope lies in a region, which overlaps the S protein RBD (Ying et al., 2014). Other mAbs termed 'MERS-4' and 'MERS-27' showed a strong synergistic inhibition of interaction between MERS-S and the host DPP4 receptor *in vitro* (Jiang et al., 2014). Another group managed to identify multiple Nabs, which bound specifically at different epitopes within the S-RBD/DPP4 interface region, effectively inhibiting MERS-CoV infection *in vitro* (Tang et al., 2014). B cells from a convalescent MERS-CoV patient allowed for the generation of an anti-S mAb, LCA60, which showed strong neutralising activity against S protein binding *in vitro* and *in vivo*. This antibody was developed using Cellclone technology (Corti et al., 2016). Another emergent mAb production technology, Veloclmmune, has been used to generate non-competing hmAbs capable of blocking MERS-CoV infection in a mouse model (Pascal et al., 2015). A recombinant protein vaccine encoding a partial MERS-CoV RBD fused with human antibody F_c region (S377-588-F_c) induces the production of NAbs in mice, providing significant protection against MERS-CoV infection (Tang et al., 2015). Intravenously administered human NAbs are able to confer complete protection against MER-CoV infection in a variety of human dipeptidyl peptidase 4 (hDPP4)-transgenic animal models with no adverse compatibility issues (Qiu et al., 2016). Currently, there are more than 20 NAbs proven effective against MERS-CoV in various *in vitro* and *in vivo* models (Xu et al., 2019). The attempted generation of neutralising antibodies specific to SARS-CoV-2 has been underway since the beginning of the global pandemic. SARS-CoV-2 S protein is shown

to interact with the same host receptor as the closely related SARS-CoV S, with both making use of the angiotensin-converting enzyme 2 (ACE2) receptor molecule found on the surface of human airway epithelial cells (Shang et al., 2020; Wrapp et al., 2020). An RBD-specific hmAb has been generated by immortalising B cells isolated from SARS-CoV-2 infected patients. Two hmAbs, P2C-1F11 and P2B-2F6, were shown potent neutralisation action against SARS-CoV-2 infection. These antibodies showed no cross-reactivity with the RBD of MERS-CoV S protein or SARS-CoV S protein (Ju et al., 2020). Transgenic mice encoding chimeric human-rat Ig have been used to generate mAbs specific to the S2-S1 region of SARS-CoV. Analysing cross-reactivity, multiple hybridoma lines antibodies were shown to react to the S2 and S1 subunits of both SARS-CoV and SARS-CoV-2. Owing to the very species-specific nature of the S protein RBD sequence, it is speculated that this type of cross-reactive mAb may interact with S protein at a binding region outside of the usual RBD (Wang, Y. et al., 2020). The immunisation of mice with a SARS-CoV-S protein RBD fragment allowed for the generation of hybridomas producing anti-S mAbs capable of detecting SARS-CoV-2 S protein *in vitro*. These mAbs are specific to the S-RBD, and were shown to decrease the rate of infection with SARS-CoV-2 pseudovirions in mammalian cell culture (Antipova et al., 2020). These S- and RBD-directed mAbs are promising therapeutic candidates.

During the SARS-CoV epidemic in 2002/03, many SARS patients developed a strong neutralising antibody response, which correlated with improved disease outcomes. The convalescent plasma containing neutralising anti-SARS antibodies could be considered as passive immunotherapy in the case of a viral re-emergence or experimental exposure (Cheng et al., 2005; He, Y., Lu, H., et al., 2005). Passive immunotherapy with antibodies found in convalescent patient plasma may be the most effective way of directly combatting SARS-CoV-2 infection in Covid-19 patients (Kruse, 2020). Convalescent plasma therapy has been effectively used against numerous viruses, including the parvovirus, H1N1, measles virus, Ebola virus, and SARS-CoV (Cheng et al., 2005; Marano et al., 2016; Van Griensven et al., 2016). There have been a few reports on the use of convalescent plasma to treat SARS-CoV-2 in the current Covid-19 pandemic (Shen et al., 2020). Convalescent patient antibodies provide the most immunologically relevant information on neutralising epitopes within viral structural proteins. The elucidation of antibody paratope sequences and unravelling of binding interactions between CoV S protein and ACE2 and DPP4 receptors, together with the recent advancements in hybridoma technology, have made it possible to produce humanised antibodies with highly specific immunodominant epitopes. These type of antibodies may be crucial in protecting against the most prevalent strains of circulating SARS-CoV-2 (Liu et al., 2020; Zhou & Zhao, 2020). Peripheral B cells present difficulty in isolation as the numbers of circulating cells are low (Traggiai et al., 2004). However, given the high number of recovered Covid-19 patients now present globally, there should at present be ample opportunity for the isolation of B cells to produce human hybridoma lines secreting anti-SARS-

CoV-2 NABs. Current research also indicates that plasma must be collected within three months after diagnosis as the high plasma NAb response is not long-lived (Harvala et al., 2020). When considering the development of anti-CoV antibody treatment, it would be prudent to select NABs binding epitopes from as many variant strains of SARS-CoV-2 as is possible (Zhou & Zhao, 2020). In this way, combination treatment with non-competing antibodies may provide the best chance of protection against multiple circulating strains or perhaps from emergent strains with minor mutations.

4.1.13. CoV antibody generation for non-therapeutic use

There are a wide variety of uses for molecule-specific binding agents such as antibodies. While NABs have been the main focus of therapeutic CoV intervention, numerous other antibodies against SARS-CoV and MERS-CoV proteins have been produced for purposes other than vaccine research and development. These include those designed for species-specific viral detection assays or the differentiation of virus-specific structural proteins, or for identifying protein-specific mutations in virus strains (Fukushi et al., 2018; Goo et al., 2020). Many of these antibodies could potentially be used diagnostically to identify infectious pathogens in patient samples (Al-Amri & Hashem, 2020; Lee et al., 2010).

While antibodies generated against the CoV S protein are the most used in viral diagnostics, both the M and N proteins are highly expressed during infection. The CoV N protein exhibits high antigenicity, and SARS-CoV N has also been a target for antibodies generated during natural infection (Flego et al., 2005; He, Q. et al., 2005; Lee et al., 2010). Antibodies against M and N may be useful for viral protein research, in expression characterisation studies, including functional and structural viral protein analyses, and monitoring protein production within the viral life cycle in infected cells. Anti-MERS M antibodies have been developed which are able to bind infected cells *in vitro* (Park, Byoung Kwon et al., 2019). Anti-M and –N antibodies could therefore potentially also be useful in a clinical setting, with infected samples.

4.1.13.1. Antibodies to endemic HCoVs

The lower pathogenic HCoVs persist within the human population, and seroprevalence to these viruses is high (Zhou et al., 2013). These endemic HCoVs includes HCoV-OC43, HCoV-229E, HCoV-HKU-1, and HCoV-NL63. Sastre *et al.* developed a DAS-ELISA to differentiate between the N proteins of two HCoVs, namely *alphacoronaviruses* NL63 and 229E (Sastre et al., 2011). They obtained three murine mAbs specific to the NL63 N protein. Anti-N mAbs that were cross-reactive with NL63 and 229E N protein were also obtained. The immunogen used was N protein expressed in *E.Coli*. The selected discriminating antibodies did not show any cross-reactivity with N protein from other endemic *betacoronaviruses* HCoV-OC43 and HCoV-HKU1, or against N of another *alphacoronavirus*, PEDV. This highlights the species-specific binding of the antibody and the high level of sequence variation

within CoV N proteins. For HCoV-229E N protein, a specific mAb has been generated – mAb 1E7. The NL63 anti-N mAbs were named 1B12, 2D4, and 2E6 (Sastre et al., 2011). PABs to the N protein of HCoV-OC43 have previously been generated in rabbits. The stimulating antigen was recombinant purified OC43-N protein (Liang et al., 2013). There is no available published data on the generation of anti-HCoV-HKU1 antibodies. Interestingly, there is some evidence to suggest that HCoV infection and immune resolution may offer a level of cross-species protection against infection by HCoVs from within the same genogroup. The examination of seroprevalence to the *alphacoronaviruses* HCoV-NL63 and -229E indicates that an immune response to NL63 infection in children may elicit protective immunity against 229E (seroconversion to 229E occurs only in the absence of NL63 seropositivity). Moreover, infection by OC43 seems to offer protection against infection by another *betacoronavirus*, HKU1. Interestingly, the reverse was not true, as 229E infection did not protect against NL63 infection, nor did HKU1 infection protect against HCoV-NL63. Much is to be learned about the complex nature of the human immune response to CoVs (Dijkman et al., 2012).

The mAbs developed here are specific for the HCoV-NL63 M and N proteins, respectively. To the best of the author's knowledge, this is the first report on the generation of mouse anti-peptide mAbs against these respiratory viral structural proteins. Our anti-N antibodies may have a diagnostic application, as no cross-reactivity is seen with SARS-CoV N protein. Anti-N would have to be screened for cross-specificity to other endemic HCoVs to determine the degree of species-specificity exhibited by this antibody (e.g., screening against related *alphacoronaviruses*).

Since 2018, the WHO has recognised the need for increased research and development effort in emerging HCoVs (Mehand et al., 2018). The current pandemic has provided the impetus for a major shift towards CoV surveillance in human populations. Beyond this global outbreak and its severe consequences, the future emergence and re-emergence of HCoVs may be another reality we have to face. Endemic HCoVs may prove highly relevant in the near future of CoV research and development of an effective treatment or protective antiviral. This group of viruses, including HCoV-NL63, are known to persist within the global human population. HCoV-NL63 shows seasonal prevalence and is globally distributed with various populations exhibiting high seroprevalence to this and other endemic HCoVs (Khan et al., 2020; Nickbakhsh et al., 2020; Otieno et al., 2020; Zhou et al., 2013). Monitoring the mutational divergence within NL63 strains and other endemic HCoVs may provide clues as to the evolutionary impact of this prolonged human exposure (increase in recombination opportunities) on the CoV viral genome and preferred genetic mutations (that occur through viral mutation over time). It has been speculated that the novel SARS-CoV-2 may become a seasonal type of flu or respiratory disease. As such, an increased research effort into the population infection dynamics of endemic HCoVs may offer insight as to what we could expect from another persisting human pathogen. Recently, researchers

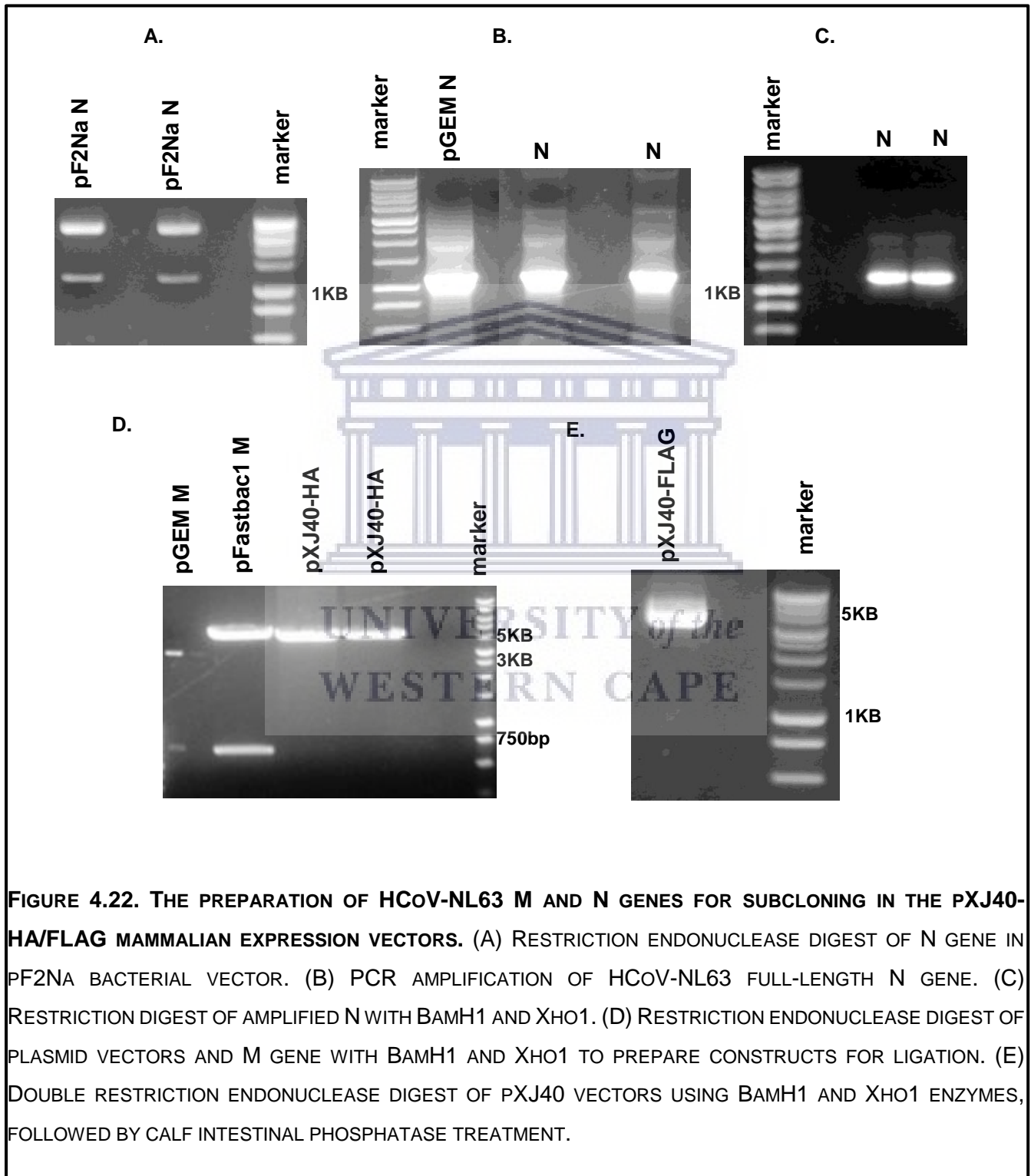
have also increased investigative efforts into the relationship between the immune response to SARS-CoV-2 and the four endemic HCoVs (Hicks et al., 2020; Huang, A. T. et al., 2020; Ma et al., 2020). Immune-reactive T cell binding to SARS-CoV-2 has been observed in samples isolated from seropositive patients for HCoV-OC43 and HCoV-NL63 (Grifoni et al., 2020; Ma et al., 2020).

HCoV-NL63-specific antibodies may also have relevant application in diagnostics. Exposure to HCoV-NL63 occurs already during childhood. As such, it may be relevant for NL63 and other low-pathogenic HCoVs to become a part of routine testing in respiratory infection screening in children. In those patients with an active infection (replicating virus), both the N and M proteins should be highly expressed and detectable by antibody (El-Duah et al., 2019; He, Y., Zhou, Y., et al., 2005; Lehmann et al., 2008; Pohl-Koppe et al., 1995). Here multiple hybridoma lines were produced, which secrete mAbs specific to our proteins of interest, HCoV-NL63 M and N proteins, respectively. To the author's knowledge, this is the first murine mAb generated against HCoV-NL63 M. Furthermore, no published work could be found on the generation of a mAb specific for HCoV-NL63 M protein. As such, there is no commercially available mAb to detect untagged NL63 M. Here a hybridoma cell line producing NL63-M-specific mAbs has been generated, capable of detecting full-length NL63 M protein. According to the author's knowledge, there is a single commercially available mAb specific for the HCoV-NL63 N protein (used as our control in Western blots previously used by (Zuwała et al., 2015)). The anti-N antibodies were shown to detect N with a specificity comparable to this purified mAb. The mAbs will be used in future experiments in the UWC Molecular Biology and Virology Research Laboratory, which will assess the interactions of the major structural proteins of HCoV-NL63. Structural protein expression in multiple *in vitro* systems, localisation studies, protein-protein interactions, and VLP assembly for HCoV-NL63 will be evaluated.

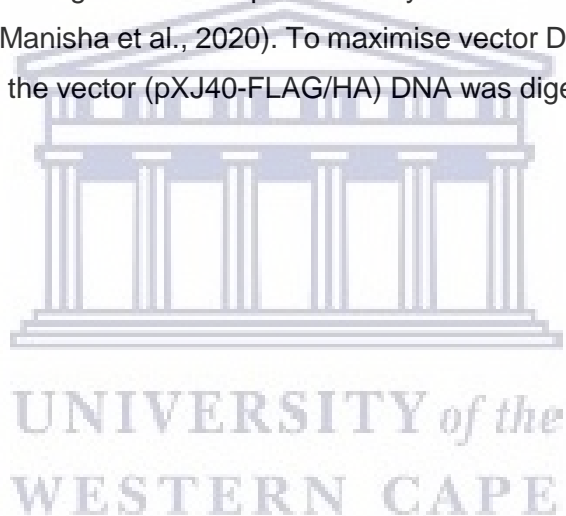
As all four endemic HCoVs exhibit high seroprevalence in the human population, it is useful to differentiate between these four CoV species. Specific antibodies, capable of discriminating each endemic HCoV species, would be an invaluable tool in monitoring epidemiological distribution patterns of each circulating HCoV, as well as assessing the relative impact of these endemic HCoVs on global health. It may also become important to monitor the prevalence and epidemiological characteristics of these persistent/circulating HCoVs. These results could provide information on human populations that exhibit the highest seasonal prevalence and seroprevalence to endemic HCoVs. These viruses have the highest level of opportunity for recombination. HCoV-NL63 diverged from its closest CoV relative HCoV-229E over 500 years ago (Pyrce et al., 2006). A recent study indicates that this endemic HCoV is continuously evolving while circulating persistently in the human population, and is capable of causing severe lower respiratory tract infection (Wang, Y. et al., 2020). HCoVs are now more than ever in our history, being revised and considered important emerging human pathogens.

4.2. Assessing *in vitro* interaction between the M and N structural proteins of HCoV-NL63

4.2.1. Preparation of the M and N genes and pXJ40 vectors for cloning



The HCoV-NL63 full-length M gene was subcloned from a pFastbac1-M expression construct, generated by the author, encoding BamH1 and Xho1 cut sites flanking the M gene (see Section 4.4.1). These sites are also compatible with cloning in the pXJ40-HA/FLAG MCS, and as such, M was released from pFastbac1 with compatible sticky end sites for cloning in pX40 (Figure 4.22. D.). The HCoV-NL63 full-length N gene was previously cloned in a bacterial pF2Na expression vector in the UWC Molecular Biology and Virology Research Laboratory. To confirm the presence and integrity of the gene construct, a restriction digest was performed with a Flexi™ enzyme blend to release the cloned gene fragment from the pF2Na Flexi Vector. In Figure 4.22 A, the full-length N gene is confirmed at approximately 1200bp (GenBank ID: DQ846901.1). For subcloning into a new mammalian expression vector pXJ40-HA/-FLAG, and to amplify the amount of target gene the author and co-researchers have to work with, N was amplified, and new, compatible restriction enzyme cut sites BamH1 and Xho1 were incorporated flanking the gene termini (Figure 4.22 B and C). The pXJ40-FLAG/HA vectors were accordingly digested with BamH1 and Xho1 enzymes to generate compatible sticky ends. Linearised pXJ40 vector DNA is approximately 5000bp in size (Manisha et al., 2020). To maximise vector DNA concentration in the final purified gel product, 4 – 5µg of the vector (pXJ40-FLAG/HA) DNA was digested by restriction enzymes (Figure 4.22 D and E).



4.2.2. Generating the pXJ40-HCoV-NL63 M and pXJ40-HCoV-NL63 N expression constructs

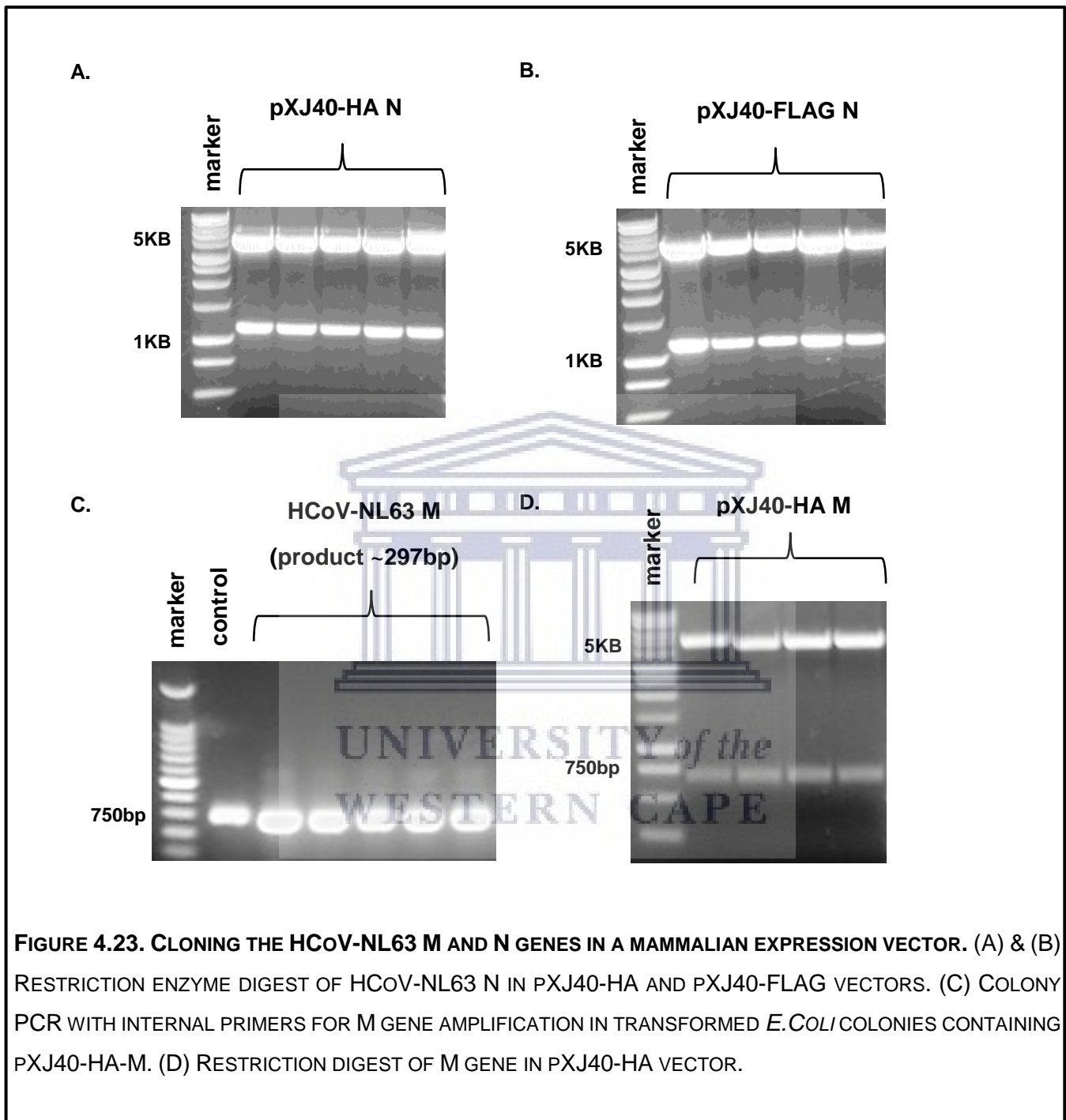


FIGURE 4.23. CLONING THE HCoV-NL63 M AND N GENES IN A MAMMALIAN EXPRESSION VECTOR. (A) & (B) RESTRICTION ENZYME DIGEST OF HCoV-NL63 N IN pXJ40-HA AND pXJ40-FLAG VECTORS. (C) COLONY PCR WITH INTERNAL PRIMERS FOR M GENE AMPLIFICATION IN TRANSFORMED *E. COLI* COLONIES CONTAINING pXJ40-HA-M. (D) RESTRICTION DIGEST OF M GENE IN pXJ40-HA VECTOR.

4.2.2.1. Confirmation of successful clones – pXJ40-FLAG/HA-N and pXJ40-HA-M

The pXJ40 vectors used were a kind donation from Prof. Y. Tan from the Department of Microbiology and Immunology at the National University of Singapore. This mammalian plasmid expression vector includes the following features: A human cytomegalovirus (hCMV) promoter that induces high expression levels of the recombinant gene; a T7 bacteriophage promoter that allows transcription of the cloned gene; an MCS encoding numerous common enzyme recognition sites, facilitating cloning convenience even for multiple DNA sequences; A BSM13+ sequence that functions as an origin of replication (ori); an antibiotic resistance gene (Ampicillin), which allows for the selection of cells containing transformed plasmid vector; An SV40 polyadenylation sequence that facilitates increased recombinant protein expression; as well as an HA or FLAG N-terminus epitope tag that aids in the identification and purification of the recombinant protein (Manisha et al., 2020).

Mammalian expression constructs for HCoV-NL63 M and N were generated successfully. Figure 4.23 graphically depicts the release of the N (1123bp) and M (681bp) genes from their respective pXJ40 vectors (5000bp). The pXJ40 expression construct encodes N-terminal epitope tags HA and FLAG, respectively. Fusion tags are often used to simplify the detection of recombinant *in vitro* protein expression. The expressed recombinant N proteins are fused at their N-termini with either -FLAG or -HA. The expressed M protein is fused with an N-terminal HA tag. These relatively short, linear motifs do not generally interfere with the functional properties of the heterologous expressed protein of interest (Kimple et al., 2013).



4.2.3. The *in vitro* expression of HCoV-NL63 M and N proteins in a mammalian system

4.2.3.1. Cos7 lysate quantitation

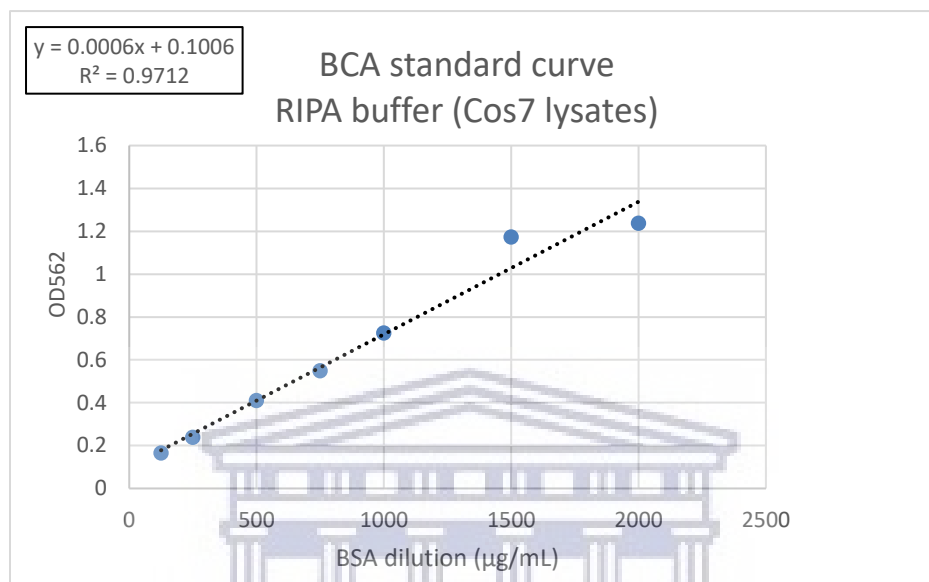


FIGURE 4.24. THE DETERMINATION OF WHOLE CELL PROTEIN LYSATE CONCENTRATIONS OF COS7 CELLS TRANSFECTED WITH PXJ40 M AND N CONSTRUCTS. BCA PROTEIN (BSA) STANDARD CURVE. THE LINE EQUATION (OUTLINED BOX) IS USED TO CALCULATE LYSATE PROTEIN CONCENTRATIONS FOR COS7 HCOV-NL63 M EXPRESSION LYSATES.

TABLE 4.9. COS7 TRANSFECTED LYSATE PROTEIN CONCENTRATIONS

	1µg total DNA	2µg total DNA	4µg total DNA
LYSATE SAMPLE	TOTAL PROTEIN CONCENTRATION (µg/mL)		
NL63 HA-M 48 hours	1207	1114	1123
NL63 HA-M + FLAG-N	-	1285	1094
NL63 FLAG-N	-	1166	1151

4.2.3.2. Optimising the expression of HCoV-NL63 M and N in a mammalian system

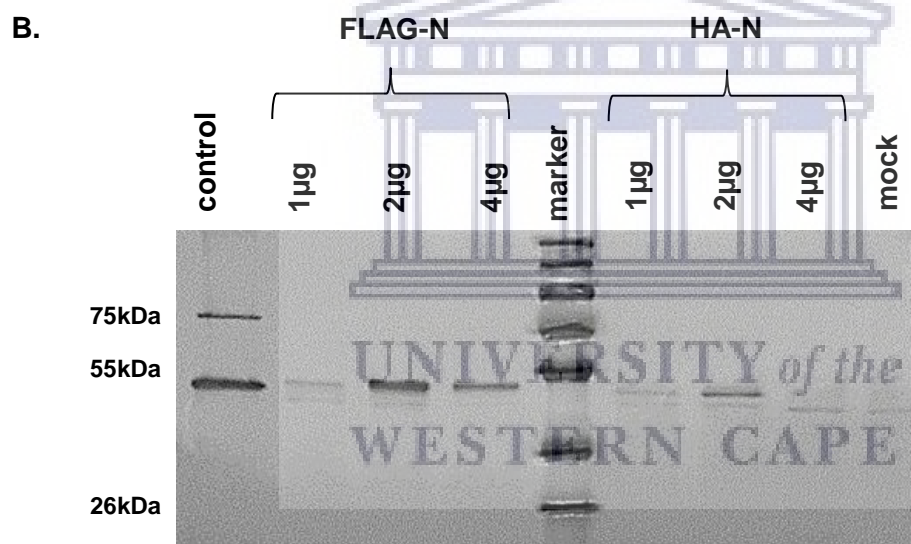
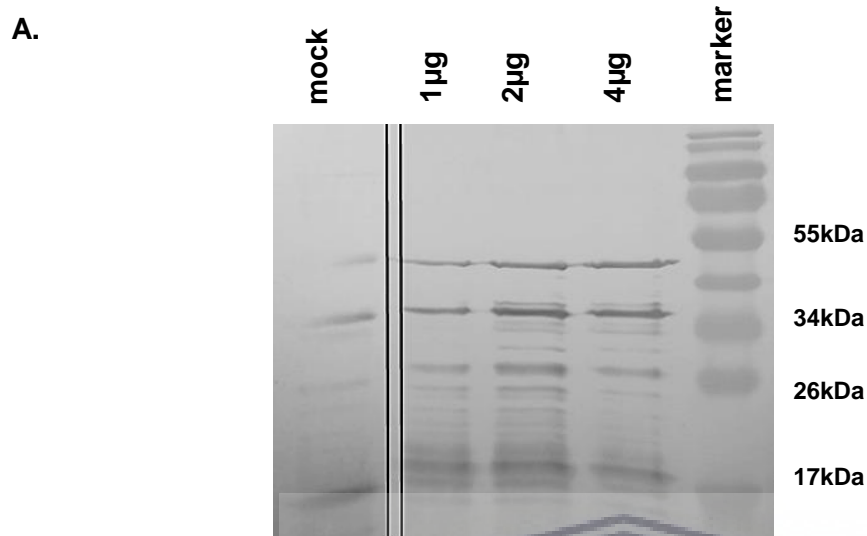


FIGURE 4.25. OPTIMISING THE EXPRESSION OF HCoV-NL63 M AND N PROTEINS IN A MAMMALIAN CELL SYSTEM. (A) WESTERN BLOT SCREENING OF COS7 LYSATES TRANSFECTED WITH PXJ40-HA-M. THE POSITIVE 'CONTROL' IS GST-HA (EXPRESSED IN COS7). (B) WESTERN BLOT SCREENING COS7 LYSATES TRANSFECTED WITH PXJ40-FLAG/HA-HCoV-NL63 N. THE POSITIVE 'CONTROL' IS PARTIALLY CLEAVED NGST FUSION PROTEIN (EXPRESSED IN *E. COLI*).

4.2.3.3. HCoV-NL63 M migrates as multiple bands in a mammalian cell system

The cell line chosen for the transient expression of heterologous proteins is important as not all expression systems will express fully folded and properly modified proteins. When expressing recombinant proteins, the similar environment of a mammalian cell ensures that there is a functional expression of the exogenous protein. This higher eukaryotic cell provides a lipid environment, molecular protein chaperones, and all the post-translational modification machinery required to produce fully folded recombinant proteins, identical to native viral proteins. The transient expression of the proteins is much less time-consuming than creating stable cell lines expressing the said protein. Transient expression is commonly achieved *in vitro* by forming cationic DNA-lipid complexes and uptake of these into the cells. While all mammalian cell lines are expected to provide good environments for the expression of native structure proteins, certain cell lines such as human embryonic kidney cells (HEK293), monkey kidney fibroblast cells (Cos7), baby hamster kidney cells (BHK-21), and Chinese hamster ovary cells (CHO) are routinely used for exogenous protein expression (Andréll & Tate, 2013). The transfection efficiency is impacted by the size of the plasmid, as well as the amount and ratio of transfection reagent to DNA. The Cos7 mammalian cell line used for N expression is an immortalised cell line that has been widely used for recombinant protein expression (Aruffo, 2002; Horthongkham et al., 2007). The cell line is derived from a CV-1 African green monkey kidney fibroblast line, and Cos7 was developed in 1981 by transforming CV-1 cells with a mutated simian virus 40 (SV40) encoding wild-type tumour antigen (Gluzman, 1981; Knibbs et al., 2003).

Transfection efficiency is impacted by the size of the plasmid, as well as the amount and ratio of transfection reagent to DNA. In order to optimise the expression levels of M in Cos7 cells, 1µg, 2µg, and 4µg DNA were used for transfection. Following Cos7 transfection, whole cell expression lysates were quantified (Figure 4.24; Table 4.9) in order to standardise the amount of total protein ran on SDS-PAGE to 30µg for each assayed sample (Figure 4.25.). HCoV-NL63 M protein is optimally expressed using 2µg pXJ40-HA-M DNA. HA-M migrates as multiple bands, including a band present at around 20kDa, which is the previously confirmed size of HCoV-NL63 M protein (Naskalska et al., 2018). Higher MW proteins are also observed at approximately 27kDa, 36kDa and 50kDa. These likely represent incompletely denatured M dimers. M is known to form dimers and homomultimers *in vitro* (Tseng et al., 2010). The detection of these higher MW proteins by anti-HA antibody does not appear non-specific (due to supraoptimal antibody concentration), as using a higher primary antibody dilution (higher than 1:500) results in the loss of antibody activity in detecting all HA-tagged protein of interest.

4.2.3.4. Fully processed N is expressed as a 50kDa polypeptide

HCoV-NL63 N protein has previously been expressed *in vitro* in bacterial-, mammalian-, and insect cells (Berry et al., 2012; Naskalska et al., 2018; Zuwała et al., 2015). Terminal truncated fragments of N have also been expressed. The dimerisation of full-length, expressed N protein has been reported, with oligomerisation driven by the CTD of N (Szelazek et al., 2017). Insect cells have also been used to express N during HCoV-NL63 VLP generation (Naskalska et al., 2018). The expression of N in the *in vitro* Cos7 system was confirmed by a Western blot using an anti-N specific mAb. In Figure 4.25, N is observed at around 50kDa. Both the FLAG- and HA epitope tags add approximately 1kDa to the size of expressed protein (Hopp et al., 1988; Zhao et al., 2013). Expression of N was performed with 1µg, 2µg, and 4µg DNA. As the amount of total protein was standardised to 30µg/lane, expression levels of N can be compared across lanes. FLAG-N was optimally expressed using 4µg pXJ40-FLAG-N DNA, and HA-N showed the highest relative expression level when using 2µg pXJ40-HA-N DNA. As a positive control (lane 1) bacterially expressed, purified N/NGST protein was run alongside the Cos7 expression lysates (previously confirmed and used for antibody screening). N was detected at approximately 50kDa, which agrees with the size observed previously for this full-length protein (Berry et al., 2012; Naskalska et al., 2018). The NGST fusion protein was approximately 70 – 75kDa in size, which was the expected approximate size of the fusion protein made up of N (50kDa) and GST (21-28kDa). The blot was also treated with an anti-actin primary antibody. β-actin is a housekeeping protein expression/loading control. β-actin was detected across all Cos7 lysate lanes at the expected 42kDa. As β-actin is a mammalian cell control, it was not detected in the lane containing bacterially expressed N (lane 2). Binding with anti-actin Ab was examined through re-exposure following the completion of the anti-N Western blot, and as such, anti-actin binding did not interfere with N detection signal. In the previous antibody results (see Section 4.1) full-length N protein was also detected at approximately 50kDa (polyclonal and monoclonal anti-M primary antibodies).

4.2.3.5. The post-translational processing of viral proteins

The post-translational processing of viral proteins is implicit in intracellular signal transduction (Casino et al., 2009; Gao & Stock, 2010; Graves & Krebs, 1999; Gray et al., 2016; Hazelbauer & Lai, 2010; Stewart, 2010; Weston & Davis, 2007). Viral protein post-translational modifications (PTMs) have been of great interest to researchers as the existence of an additional level of viral protein activation (epi-functional) 'control' opens a new avenue for antiviral research and therapeutics. It has been shown that viral proteins undergo multiple PTMs at different infection stages (Bretana et al., 2012). In the coevolution of viruses and hosts, constant selective pressure is exerted on both groups. However, due to the significantly reduced replication time of viruses (compared to hosts), and exaggerated virion progeny number (also compared to hosts), virus populations often exhibit (measurable) changes in response to selective pressures (Keck et al., 2015). Viruses must be able to adapt to changes in the

host cell environment, and viral mechanisms of sensing and reacting to environmental changes include ligand recognition, altering protein conformation or protein PTMs (Gruenke et al., 2002; Hoover et al., 2016; Matsuyama & Taguchi, 2002; Schievano et al., 2004; Wang, 2002). Previously unknown PTMs continue to be uncovered, along with novel roles for known PTMs in protein function and cell metabolism. Over 200 PTMs have been identified, and the most well-characterised of these modifications include phosphorylation, glycosylation, acetylation, SUMOylation, ubiquitination, and methylation, among others (Duan & Walther, 2015).

4.2.3.6. Glycosylation of the CoV M protein

The M protein is glycosylated within the N-terminal ectodomain. *Alpha*- and *Gamma*-coronavirus M proteins, as well as SARS-CoV-M, are N-glycosylated (N-linked oligosaccharides). *Betacoronavirus* M proteins are O-glycosylated (O-linked oligosaccharides) (Cavanagh & Davis, 1988; Jacobs et al., 1986; Nal et al., 2005; Niemann et al., 1984; Oostra et al., 2006; Stern & Sefton, 1982). The MHV M protein is unique as it is both N-glycosylated and O-glycosylated (Yamada et al., 2000). The glycosylation of the M protein may be linked to a CoV's ability to induce an interferon response within infected cells. It is unclear whether there is a difference in the IFN-inducing abilities of N-glycosylated vs O-glycosylated M proteins. However, the complete lack of glycosylation of the M protein results in a significantly reduced ability to activate an IFN- α response (Baudoux et al., 1998; de Haan et al., 2003). The HCoV-NL63 M protein is predicted to be N-glycosylated at three residues (AA positions 3, 19, and 188) within the 226 AA protein sequence (Gupta et al., 2004). NetOGlyc4.0 predicts M to be O-glycosylated at four putative sites (AA positions 63, 88, 99, and 116) (Steentoft et al., 2013). It is expected that glycosylation alters the size of the mature protein (Gross et al., 1989; Unal et al., 2008). Each N-linked glycosylation is predicted to add approximately 2.5kDa to the overall size of the protein. Different glycosylation states have been reported previously for HCoV-NL63 M, migrating as multiple bands of different sizes under denaturing conditions (El-Duah et al., 2019; Naskalska et al., 2019).

Viruses make use of host cell glycosylation pathways to modify viral proteins on the virion surface. The glycosylation of viral proteins plays a role in protein stability, antigenicity, and evading host cell defenses (Vigerust & Shepherd, 2007). N-linked glycosylation of viral E proteins can promote the correct folding and trafficking of the protein by utilising host folding factors and protein chaperones. Altering the sequence of a protein glycosylation site can greatly impact virus transmissibility and survival (Land & Braakman, 2001; Meunier et al., 1999; Slater-Handshy et al., 2004). Changing the glycosylation status of a protein can also alter receptor-protein interactions. N-linked glycosylation has been shown to be important for many viruses on proteins that function in viral pathogenesis evasion of the host immune system (Vigerust & Shepherd, 2007). Several emerging viruses, including SARS-CoV, express major proteins that are glycosylated, and the glycosylation profile of these proteins is a determinant of

structure and function (Abe et al., 2004; Klenk et al., 2002; Londrigan et al., 2011; Slater-Handshy et al., 2004; Vigerust, 2011).

4.2.3.7. CoV N protein production and processing

Protein phosphorylation is the addition of a phosphate group, by a kinase, to a serine/threonine or tyrosine residue in the protein sequence. Serine-, threonine-, and tyrosine-kinases are responsible for the attachment, respectively. This reaction is reversible and ATP-dependent (Keck et al., 2015). Phosphorylation is the most commonly occurring PTM, and it is estimated that 30% of all human (and fly and yeast) proteins are phosphorylated (Mann et al., 2002; Schweiger & Linial, 2010). The phosphorylation of endogenous eukaryotic proteins is important for cell survival and basic function, protein-protein interactions, and protein localisation (Keck et al., 2015). Research has revealed a high degree of sequence homology between virally encoded kinases and eukaryotic host cell kinases, reinforcing the ability of viruses to take control of host cell kinase machinery (Keck et al., 2015). The phosphorylation of viral proteins by host kinases has been reported for both positive-strand and negative-strand RNA viruses (Lenard, 1999)(Keck et al., 2015). Many aspects of the virus life cycle are regulated by protein phosphorylation of structural and non-structural viral proteins (Jakubiec & Jupin, 2007; Lenard, 1999). Phosphoproteins can be phosphorylated at multiple residues. The specific site and number of phosphorylation events are known to differentially regulate protein function (ref). Phosphorylation reactions are catalysed by phosphatases, and the addition of a single phosphor group adds approximately 1kDa to the overall size of the protein. The phosphorylation of a protein generally also induces a change in charge of the protein. This shift in charge can alter protein conformation, as well as molecular activity and function in response to cellular environmental changes (Canova & Molle, 2014; Keck et al., 2015; Yang et al., 2009). The viral nucleoprotein is one of the most abundantly expressed viral proteins during infection with an enveloped virus. The N protein is involved in multiple activities in the infected cell, including viral RNA and protein synthesis, encapsidation of the viral genome, as well as host immune modulation (Ni & Cheng Kao, 2013). The nucleic acid binding role of the N protein is impacted by the protein's phosphorylation status (increases repulsive forces between (-) nucleic acid backbone and (+) phosphate groups) (Boyle et al., 1991; Mayrand et al., 1993). The phosphorylation of the N protein plays a role throughout RNA virus infection, including virus entry, RNA-N protein interaction, viral transcription, and virion structure and assembly (Hoover & Kao, 2016). Phosphorylation occurs at a higher rate in less conserved areas in a given protein sequence. These are analogous with the IDRs in the CoV N protein (Wright & Dyson, 2015). The phospho-dependent shift in charge and protein conformation within an IDR in the N protein may impact the interactions between N and other viral and host proteins (Groban et al., 2006). Phosphorylation sites have been identified in *Alphacoronaviruses* TGEV N- and IBV N proteins (Calvo et al., 2005; Chen et al., 2005). There is evidence to suggest that phosphorylation of IBV N aids in the protein's ability to recognise viral RNA

(Fung & Liu, 2018). Here we express the N protein, another *Alphacoronavirus*, HCoV-NL63. The HCoV-NL63 N protein is predicted to be phosphorylated at multiple residues such as serine-, threonine-, and tyrosine residues (Blom et al., 1999). The N proteins of *Betacoronaviruses* MHV and SARS-CoV are also phosphorylated (Surjit et al., 2005; (White et al., 2007; Wu et al., 2009). The phosphorylation status of the MHV N protein may be relevant in regulating viral replication (Wu et al., 2014). SARS-CoV N protein is known to be phosphorylated at multiple serine residues in the serine/arginine enriched region in the central domain of N. The domain in this region drives N protein oligomerisation, another important viral protein interaction, which is impacted by phosphorylation (He, R. et al., 2004; Peng et al., 2008; Surjit et al., 2005; Zakhartchouk et al., 2005). Phosphorylation of SARS-CoV N is also required for efficient viral replication as the inactivation of a kinase responsible for phosphorylating N results in suppressing virus replication (Wu et al., 2009). Phosphorylation increases the size of the N protein, and the phosphorylation status of this major structural protein may be directly linked to virion assembly and maturation (Hogue, 1995; Jayaram et al., 2005; Stohlman et al., 1983). The immunoreactivity of the SARS-CoV N protein is also dependent on phosphorylation (McCormick & Khapersky, 2017; Shin et al., 2007).

Other modifications of N within eukaryotic expression systems include protein proteolytic cleavage, ADP-ribosylation, and SUMOylation (Eleouet et al., 1998; Grunewald et al., 2018; Li et al., 2005). The TGEV, IBV, and SARS-CoV N proteins have shown to be proteolytically cleaved during infection. This cleavage seems to be a natural consequence of CoV-induced apoptosis. It is presumed that the CoV N protein competes as a caspase substrate in order to slow down cell death and extend the duration of virion release (Diemer et al., 2008; Eléouët et al., 2000; Fung et al., 2014; Liao et al., 2013). ADP-ribosylation is the covalent attachment of single or multiple ADP-ribose groups to a protein. It has been found that the N proteins of MHV, SARS-CoV, and MERS-CoV are all ADP-ribosylated in the host cell during CoV infection (Grunewald et al., 2018).

When expressing a viral protein *in vitro*, it is important to consider that PTMs may alter the size or conformation of the final, fully processed protein. The cell machinery processing capabilities differ across species, and while bacterial cells are able to produce folded proteins, protein glycosylation and phosphorylation of eukaryotic proteins fall outside of the range of abilities of bacterial cell machinery (Brown et al., 2017; Ding et al., 2017; Dumont et al., 2016; Jenkins et al., 2008). As CoV N is a phosphoprotein, it is expected that HCoV-NL63 is phosphorylated when expressed in mammalian cells. In Figure 4.25 B, bacterially- and mammalian-expressed N protein are observed at the same size of approximately 50kDa. This result indicates that the post-translational processing of HCoV-NL63 N protein does not significantly alter the full-length protein size.

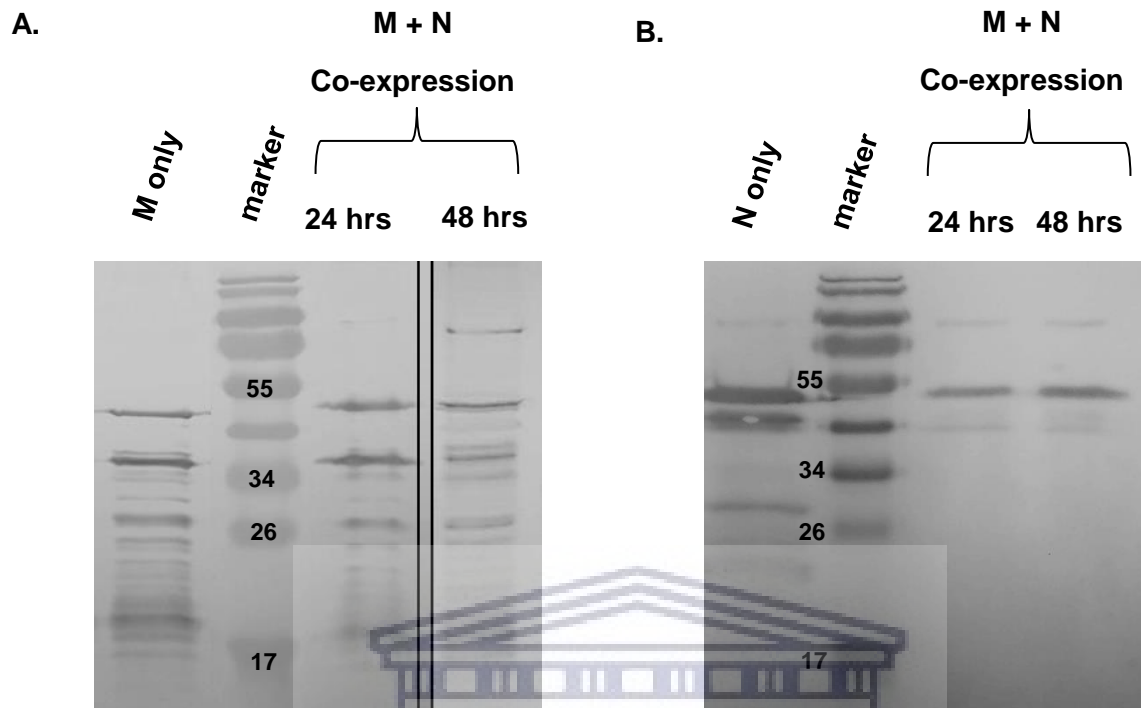


FIGURE 4.26. THE CO-EXPRESSION OF HCoV-NL63 M AND N PROTEINS IN A COS7 CELL LINE. (A) WESTERN BLOT OF COS7 LYSATES TRANSFECTED WITH M ONLY AND WITH M AND N USING ANTI-HA PRIMARY ANTIBODY. (B) WESTERN BLOT OF COS7 LYSATES TRANSFECTED WITH N ONLY AND WITH M AND N USING ANTI-FLAG PRIMARY ANTIBODY.

UNIVERSITY of the
WESTERN CAPE

4.2.4. Lower MW N protein is not present during co-expression

Both M and N protein were present in the co-expression Cos7 lysates at 24 hours and 48 hours post-transfection. When N was expressed alone, two protein bands were detected at approximately 43kDa and 50kDa, respectively. We have previously shown that HCoV-NL63 N protein is expressed at approximately 50kDa in prokaryotic and eukaryotic cell systems. Therefore, the lower MW protein band observed is not a result of differential phosphorylation states. The migration of N in multiple bands has been previously reported and can be attributed to denaturing/truncation of the N protein in denaturing conditions cells by (Fang et al., 2013; Naskalska et al., 2018; Zhou & Collisson, 2000). Interestingly, when HCoV-NL63 M and N are co-expressed, only a 50kDa N protein is present in the cell lysate. N is clearly expressed at a higher level when expressed alone (all lanes were standardised to 30µg total protein), indicating that less N protein is produced in the cell when HCoV-NL63 M and N are co-expressed. The co-expression may strain cell machinery, now allocating resources preferentially to two

different structural proteins. More cell resources are required to transcribe and translate/express two exogenous proteins. This is the first time that HCoV-NL63 M and N have been co-expressed in a mammalian cell system.

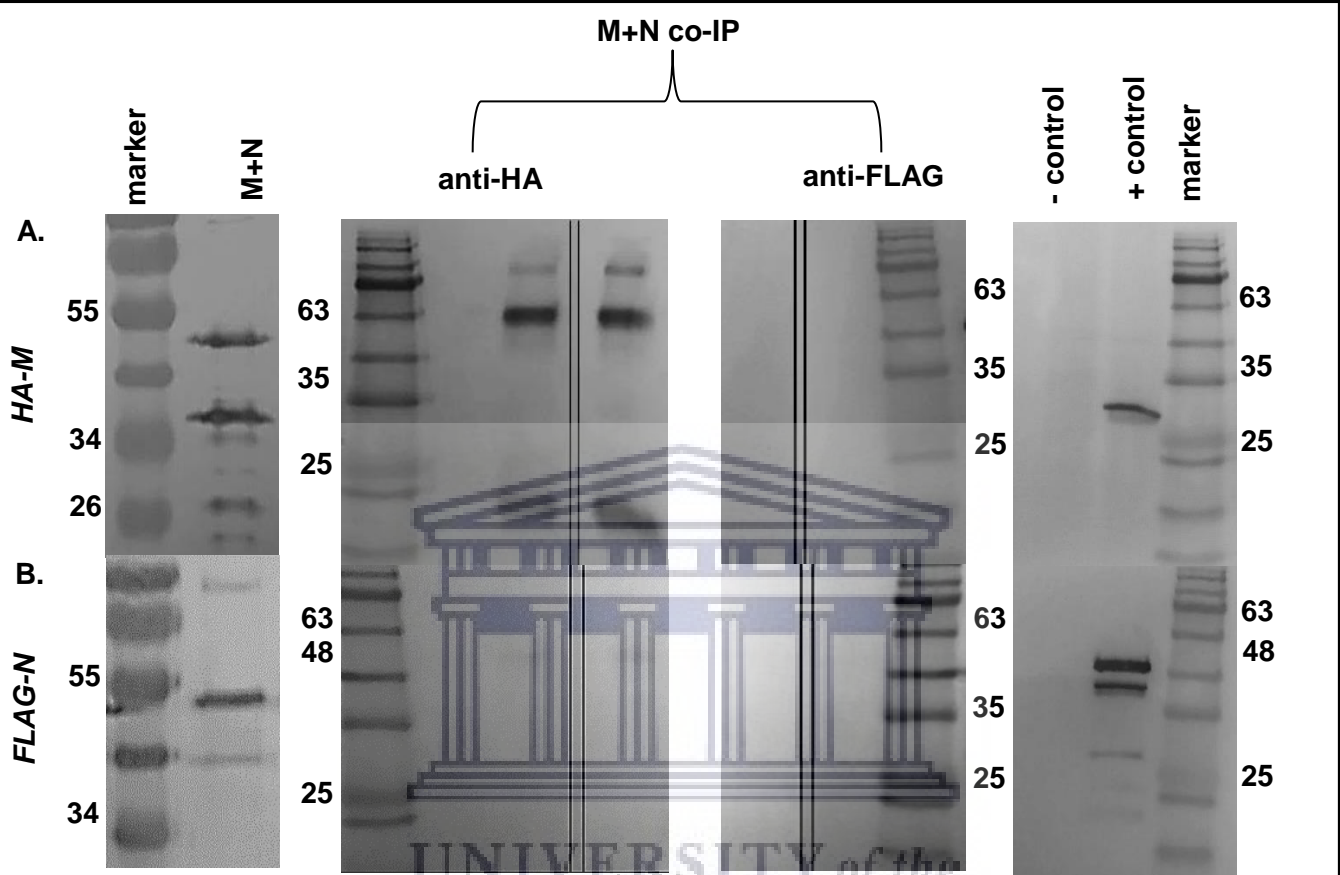


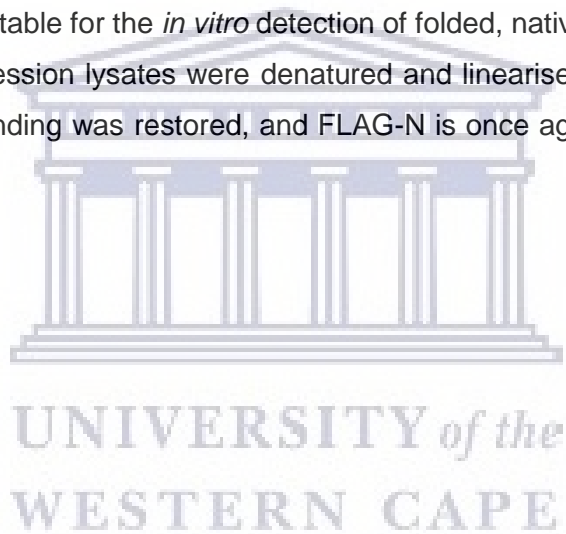
FIGURE 4.27. WESTERN BLOT ANALYSIS OF Cos7 HCoV-NL63 M AND N EXPRESSION LYSATES AND CO-IMMUNOPRECIPITATION (CO-IP) PROTEIN INTERACTION PARTNERS. (A) HA ANTIBODY DETECTION OF HA-M IN CO-EXPRESSION LYSATE AND CO-IP SAMPLES. THE '+ CONTROL' IS GST-HA EXPRESSED IN Cos7 CELLS. (B) FLAG ANTIBODY DETECTION OF FLAG-N IN CO-EXPRESSION LYSATE AND CO-IP SAMPLES. THE '+ CONTROL' IS FLAG-N EXPRESSED ALONE IN Cos7 CELLS.

4.2.5. HCoV-NL63 M and N proteins exhibit interaction in a mammalian *in vitro* system

There is previously reported evidence for the *in vitro* interaction of HCoV-NL63 M and N proteins. Naskalska *et al* found that M and N exhibited co-localisation to a certain degree when overexpressed in insect cells by (Naskalska et al., 2018). The author investigated the possible M-N *in vitro* interaction when HCoV-NL63 M and N proteins were co-expressed for 48 hours in a mammalian cell system. The respective tagged proteins were also expressed alone for 48 hours. M and N were detected by anti-HA and anti-OctA (FLAG) primary antibodies, respectively. Co-expression lysates were probed with both anti-HA and anti-FLAG. To assay for interaction protein interaction partners, co-immunoprecipitation (co-IP) was performed with anti-FLAG and anti-HA antibodies in order to establish if M and N proteins interact stably at 48 hours post-transfection. IP protein samples were examined for the presence of N, and M. Cos7 expressed GST-HA and FLAG-N were used as positive controls in the Western blots screening respective IP protein samples. In Figure 4.27. above, we observe that HA-M protein is precipitated out of the lysate by anti-HA. HA-tagged HCoV-NL63 M protein is seen once again migrating as multiple bands, including the expected M monomer at approximately 26kDa, as well as higher MW proteins at around 60kDa and 100kDa. These higher MW bands may represent M protein homomultimers that were incompletely denatured when processing expression samples. CoV M protein is known to form higher-order M complexes when expressed alone. These complexes accumulate in the Golgi apparatus (Locker et al., 1995). SARS-CoV M protein can assimilate into homomultimeric structures in the form of VLPs when expressed *in vitro* in the absence of any other viral subunits. This indicates that M-M interactions are not dependent on the presence of viral gRNA or any additional structural protein (Tseng et al., 2010). Here the author has demonstrated that M self-complexes in higher MW multimers when expressed alone and co-expressed with N protein. These results support the evidence for HCoV-NL63 M protein self-assembly being independent of other viral components. As M samples are denatured at 45 – 50°C and not at boiling temperature, it is possible that stable multimeric protein structures do not completely denature and run as higher MW compounds on SDS-PAGE. While FLAG-N is co-expressed with HA-M, a very low level of FLAG-N is also precipitated out of the lysate by anti-HA. This may indicate that HA-M and FLAG-N form a stable interaction when expressed together in Cos7 cells. The buffer used to prepare cell lysates was RIPA buffer. This particularly buffer formulation was chosen to ensure solubilisation of the M protein in buffer. The use of a less stringent buffer that does not contain ionic detergents would result in an insoluble cell membrane fraction that would require processing at high temperature for denaturation and analysis. CoV M protein undergoes thermal aggregation at high temperatures, rendering samples unable to be used for gel resolution cells by (Naskalska et al., 2018). For this reason, it was necessary to use a cell lysis buffer that increases the amount of M protein in the soluble cell fraction. In this research study's analysis, it

was then expected to observe only stable *in vitro* interaction. The very low amount of FLAG-N was observed as HA-M interaction (HA-IP).

In the FLAG co-IP samples, no HA- or FLAG-tagged proteins were observed. The lack of FLAG-tagged protein detection was not due to a loss in FLAG antibody reactivity as the positive control FLAG-N is detected in the whole cell lysate. It is suspected that some factor interfered with antibody binding to tagged protein *in vitro* during interaction and co-IP. PTMs of proteins can alter protein and antibody activity. A common PTM, which occurs in mammalian cells, is known as sulfation (Yang et al., 2015; Yeoh & Bayliss, 2018). The FLAG epitope tag contains a tyrosine residue that has been previously shown to be targeted for sulfation by host cell machinery (Choe & Farzan, 2009). Sulfation of this tag results in lowered FLAG antibody binding and recognition of tagged proteins in mammalian cells, although protein expression levels are maintained (Hunter et al., 2016; Schmidt et al., 2012; Tan et al., 2013). It has been previously shown that sulfation occurs in Cos7 cells (Leitinger et al., 1994). The FLAG antibody may not be suitable for the *in vitro* detection of folded, native structure tagged proteins. When whole cell protein expression lysates were denatured and linearised in the presence of strong detergents, FLAG antibody binding was restored, and FLAG-N is once again clearly detected (Figure 4.27, FLAG-N '+ control' lane).



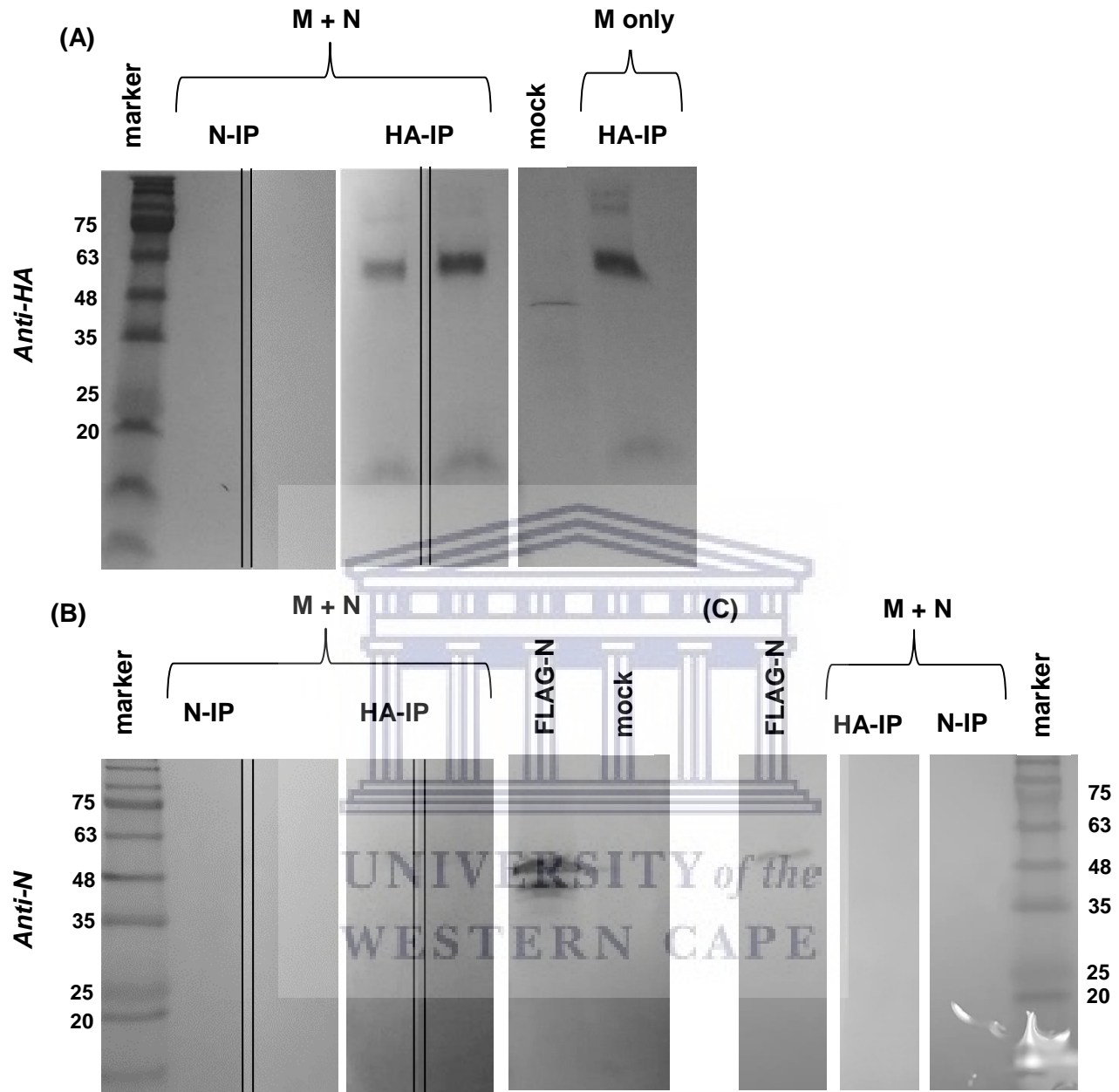


FIGURE 4.28. THE INTERACTION OF HCoV-NL63 M AND N IN A NON-STRINGENT/ NON-DENATURING LYSIS BUFFER SYSTEM. (A) HA-ANTIBODY DETECTION OF HA-M IN CO-EXPRESSION LYSATE AND CO-IP SAMPLES, DENATURED AT 45°C FOR 30 MINUTES. (B) FLAG-ANTIBODY DETECTION OF FLAG-N IN CO-EXPRESSION LYSATE AND CO-IP SAMPLES, DENATURED AT 45°C FOR 30 MINUTES. (C) FLAG-ANTIBODY DETECTION OF FLAG-N IN CO-EXPRESSION LYSATE AND CO-IP SAMPLES, DENATURED AT 95°C FOR 10 MINUTES

To investigate how the use of a stringent RIPA buffer used for cell lysis and IP may have impacted the *in vitro* detection of M and N protein interactions, *Cos7* expression experiments were performed again, this time using both a non-stringent buffer and RIPA buffer system. After probing M and M+N co-expression lysates with anti-HA, HA-M was detected in mono- and multi-meric forms at approximately 20, 60 and 100kDa (Figure 4.28 A.). The 60kDa trimeric form of M protein was the most relatively abundant form of M present under these denaturing conditions. When expressed alone, HA-M was also detected in the same pattern of different homomultimers. Interestingly when expressed alone, there was an additional higher MW M protein complex present at approximately 120kDa. The CoV M protein is responsible for directing virion assembly, and is known to self-complex through interactions at multiple sites (Neuman et al., 2011). Here we observed higher MW HCoV-NL63 M-complexes in various stages of denaturation, including its monomeric form, providing evidence for HCoV-NL63 M protein self-assembly when expressed alone and co-expressed with N protein. HA-M immunoprecipitation in non-stringent/non-denaturing buffer (Figure 4.28) revealed similar expression levels to HA-M processed in denaturing RIPA buffer (figure 30). The HA-tagged HCoV-NL63 M protein could therefore be extracted out of the mammalian cell membrane without the need for a stringent buffer. This was advantageous as it allowed for the examination of M protein-protein interactions without interference/bond disruption by denaturing conditions during the protein extraction and purification stages. No M was detected in co-expression samples precipitated with anti-N, consistent with our previous results.

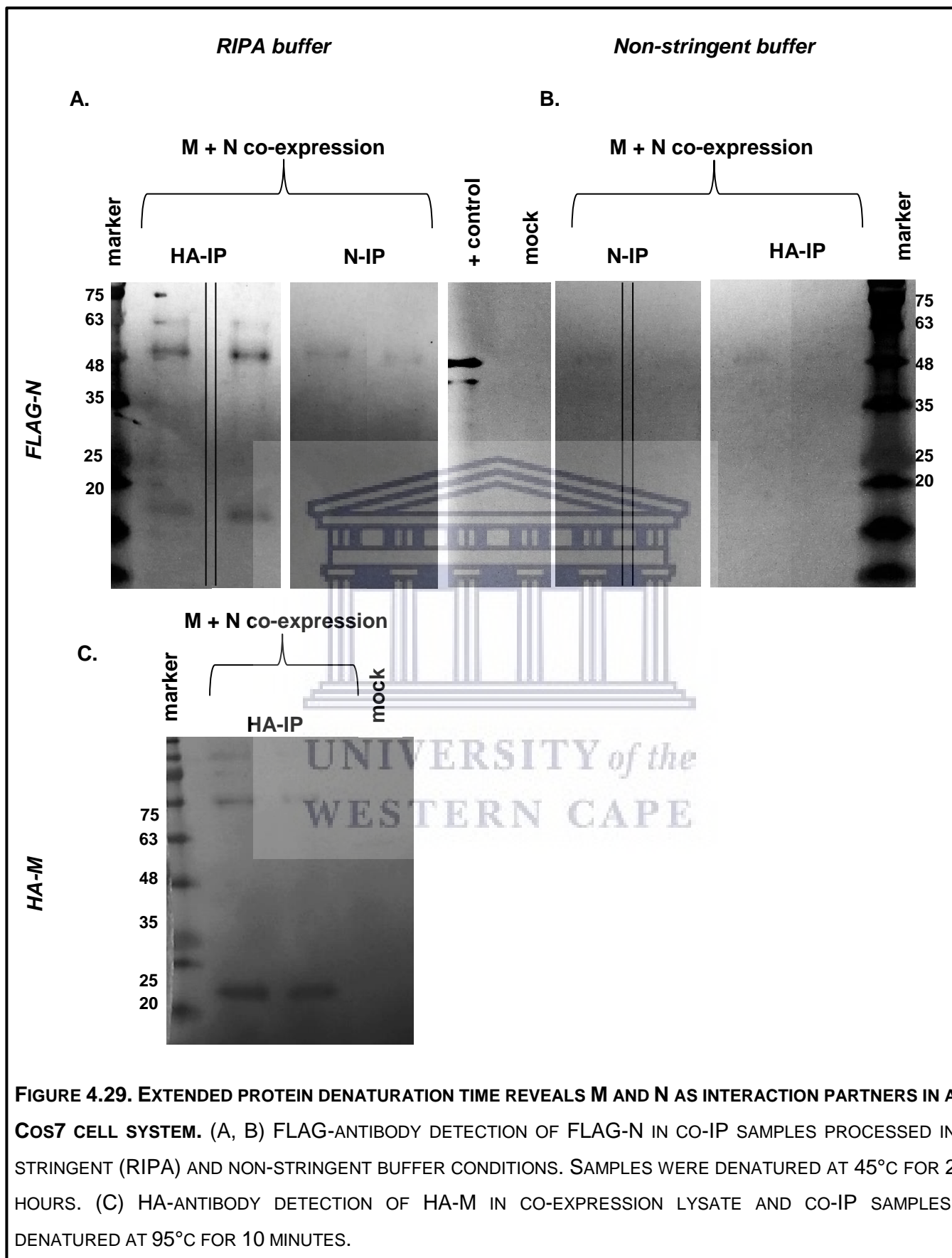
Figure B above shows a very faint detection of FLAG-N, precipitated out of M+N co-expression lysates with the anti-HA antibody. This suggests that FLAG-N was complexed to HA-M *in vitro* and was thereby precipitated out by the antibody specific for the M protein construct. No FLAG-N was detected in N-IP samples. The anti-N monoclonal antibody that was used to purify N out of the cell lysate has been previously shown to specifically bind HCoV-NL63 N protein in its denatured and non-denatured protein form, by western blotting as well as *in vitro* (section 4.1, 4.3). It is therefore unlikely that this antibody was unable to purify N protein out from whole cell lysate. This in conjunction with the quantified protein concentrations in the N-IP purified samples and the standardised amount of protein loaded across all lanes, points to a problem in N protein detection rather than purification.

To determine if a high denaturation temperature would improve the detection and visualisation of N, co-IP samples were denatured at 95°C (figure C). High temperature denaturation was only done for N protein detection, as HCoV-NL63 M protein has previously been shown to aggregate at higher temperatures (Naskalska et al., 2018). No FLAG-N was detected in HA-IP or N-IP co-expression samples. Denaturing N at a high temperature did not improve the detection of N protein.

In the previous expression experiment (figure 30), lysates were probed/precipitated with an anti-FLAG monoclonal antibody specific to the N protein epitope tag. It was speculated that FLAG-tag sulfation in

the cell may have interfered with antibody binding *in vitro*. To overcome sulfation as an antibody-binding hindrance, the subsequent round of Cos7 expression lysates were precipitated using an N protein-specific monoclonal antibody. The results indicate that purified FLAG-N was difficult to detect in both FLAG-IP and N-IP co-expression samples.





In a further attempt to denature purified N protein to improve detection, co-IP protein samples were denatured for an extended time period of 2 hours at a lower temperature of 45°C. This extended denaturation allowed for the successful detection of FLAG-N in both HA- and N-IP samples (Figure 4.29 A.). The presence of FLAG-N in the HA-IP samples suggests that N was purified out of the cell lysate in complex with HA-M. In figure C above we observe HA-M protein in various multimeric forms, co-purified with FLAG-N (above) from the same M+N co-expression lysate. Protein samples processed in stringent RIPA buffer were denatured and analysed alongside non-stringent buffer samples to investigate which buffer system is preferable to characterize the M-N protein-protein interaction.

FLAG/N-IP samples require an extended denaturation time to allow for antibody binding and detection. Purified FLAG-N, expressed alone or in complex with M may be unstable and/or adopt an unusual conformation that is resistant to denaturation, making the protein/s difficult to detect with an N-specific antibody. HA-M was similarly undetectable in samples purified with the anti-N (N-IP). When the M-N complex was precipitated out of the cell lysate via the HA antibody, FLAG-N was more easily denatured and detected (Figure 4.29 A.). More FLAG-N was seen in the HA-IP samples than in the N-IP purified samples. HA-M was also easily detected in these HA-IP samples (Figure 4.29 C.). Once again various multimeric M protein complexes were observed, but this time with a higher relative amount of M-monomer. Previous shorter denaturation times showed higher order M-multimers, with M-trimers being the most abundant protein form. The result in C above is in line with an extended denaturation time increasing HA-M self-complex denaturation. Due to unknown conformational issues with purified full-length N protein when expressed alone or co-expressed with M, the analysis of the M-N complex via the N protein or protein tag proved challenging. While FLAG-N was detected in co-IP samples in both buffer types, a higher level of N protein was detected in RIPA buffer samples (Figure 4.29 A, B.). This indicates that the more stringent, denaturing conditions provided by the anionic detergents in RIPA buffer may have aided in denaturing the M-N protein complex and improving N detection by specific antibody-binding. HA-M is detectable in HA-IP samples at 24 and 48 hours post transfection (PT) (figure C). A more denatured form of M protein is detected, indicated by the higher relative amount of M-monomer, with less higher order M-homomultimers observed in the sample. The confirmation of HCoV-NL63 M and N proteins as interaction partners when expressed in mammalian cells, even under denaturing conditions (RIPA buffer), is indicative of a strong native M-N interaction.

Here for the first time, the HCoV-NL63 M and N proteins have been co-expressed in a mammalian cell system. The specific expression system was relevant to native protein structure and enabled the evaluation of protein function in its completely-processed native form. M and N have been demonstrated as *in vitro* interaction partners through the co-purification/co-immunoprecipitation of HA-M and FLAG-N out of the same expression lysate by only HA-tag affinity purification. M-N complexes were resistant

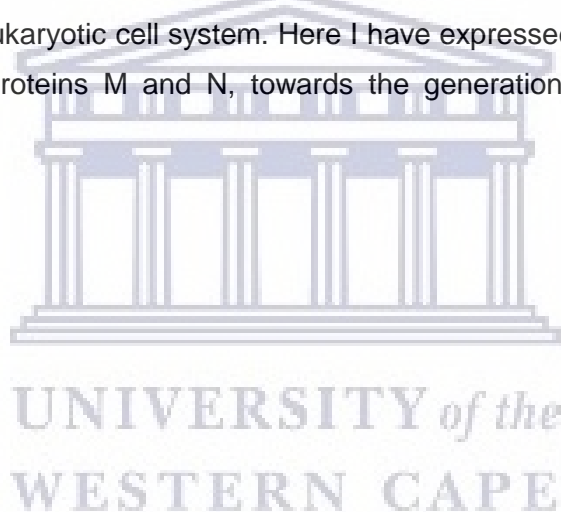
to denaturation under standard conditions and required an extended 2 hour denaturation at a lower temperature of 45°C in order to be detected by western blot – this resistance to denaturation seems to be driven by the N protein. Even expressed alone, N was not detected under extended denaturing conditions. HCoV-NL63 M protein form homomultimeric structures when expressed alone and in complex with N protein; The *in vitro* interaction of HCoV-NL63 M and N in a mammalian cell system was resistant to disruption/degradation even under stringent lysis buffer conditions (in the presence of denaturing detergents), indicating a stable protein-protein interaction between M and N in the host cell, occurring independently of other viral components.t

4.2.5.1. Interactions between CoV M and N proteins

The interaction of CoV M and N proteins is important in the viral replication cycle and necessary for infectious virion morphogenesis (Neuman et al., 2011). The highly studied SARS-CoV M and N have been shown to interact *in vitro* through the respective protein carboxy-termini. Disruption of the M-N interaction by acidification increased salt concentration, or the addition of divalent cations suggests that this protein-protein interaction involves electrostatic forces (Fang et al., 2005; He, Runtao et al., 2004; Luo et al., 2006). Previous genetic and biochemical studies have shown that in other CoVs, M-N interactions also occur via the CTDs of the respective structural CoV proteins (Escors, Ortego, & Enjuanes, 2001; Kuo & Masters, 2002). Domain 3 of the CoV N protein has been shown to have an excess of acidic AAs. Mutagenesis studies have revealed a pair of essential aspartate residues within domain 3 of N, and this CTD interacts with the M protein CTD. The N protein CTD 3 is sufficient for incorporation into the virion through interaction with M protein (Hurst et al., 2005; Masters et al., 2006). As the HCoV-NL63 structural proteins in this analysis were tagged at their N-termini, these fusion tags were unlikely to interfere (physically/structurally) with possible M-N interactions *in vitro*.

In this analysis a stable association was observed between HCoV-NL63 M and N in an *in vitro* mammalian system. These results provide clear evidence that the M and N structural components of HCoV-NL63, similar to other CoVs, exhibit *in vitro* protein-protein interactions. Some evidence suggests that the CoV M-N interaction requires additional viral factors, as M and N were shown to not interact unless M protein is bound first to viral RNA (Hurst et al., 2005). The MHV N protein is only recruited/bound by the M protein (for virion formation) if N is already bound to gRNA (Baric et al., 1988; Cologna et al., 2000; Narayanan et al., 2000). The MHV M and N proteins do not associate/interact when co-expressed without any other viral components. It was previously indicated that the CoV M protein interacts directly with viral RNA (Sturman et al., 1980), and this was confirmed by another analysis in which the M protein-viral RNA interaction, in turn, initiated the interaction between the M and N. The M-N interaction stabilises the M-gRNA interaction (Hurst et al., 2005), as well as the N-RNA complex (Escors, Ortego, Laude, et al., 2001; Fehr & Perlman, 2015). The MHV-RNA contains a

'packing signal', sufficient for incorporation into the virion during assembly. This signal is only present in genomic viral RNA and not sgRNA transcripts (de Haan et al., 2002; Narayanan et al., 2000). BCoV also contains this signal within its gRNA (de Haan, C. A. et al., 1998)(Bos, Luytjes, Meulen, Koerten, & Spaan, 1996). During virus assembly, CoV RNA is 'packaged' by the N protein in order to form the virion's nucleoprotein core. The M protein interaction with viral gRNA may initiate this viral RNA packaging (Hurst et al., 2005). The CoV M protein not only directs envelope formation, it appears that the interactions carried out by M protein also play an important role in the viral RNA N protein interactions that lead to the virion core formation. Co-expressing M and N with additional NL63 viral components such as gRNA or other major structural proteins, may result in a stronger, more detectable, stable interaction between full-length M and N proteins in a mammalian cell system. The author and co-researchers aim to develop NL63 virus-like particles (VLPs) in the laboratory, towards examining structural protein interactions and the relative effects on the host cell cycle, as well as protein subcellular localisation patterns when expressed alone or together. There is currently no report on the production of NL63 VLPs in an optimal eukaryotic cell system. Here I have expressed and confirmed interactions of 2 major NL63 structural proteins M and N, towards the generation of HCoV-NL63 VLPs in a mammalian host cell system.



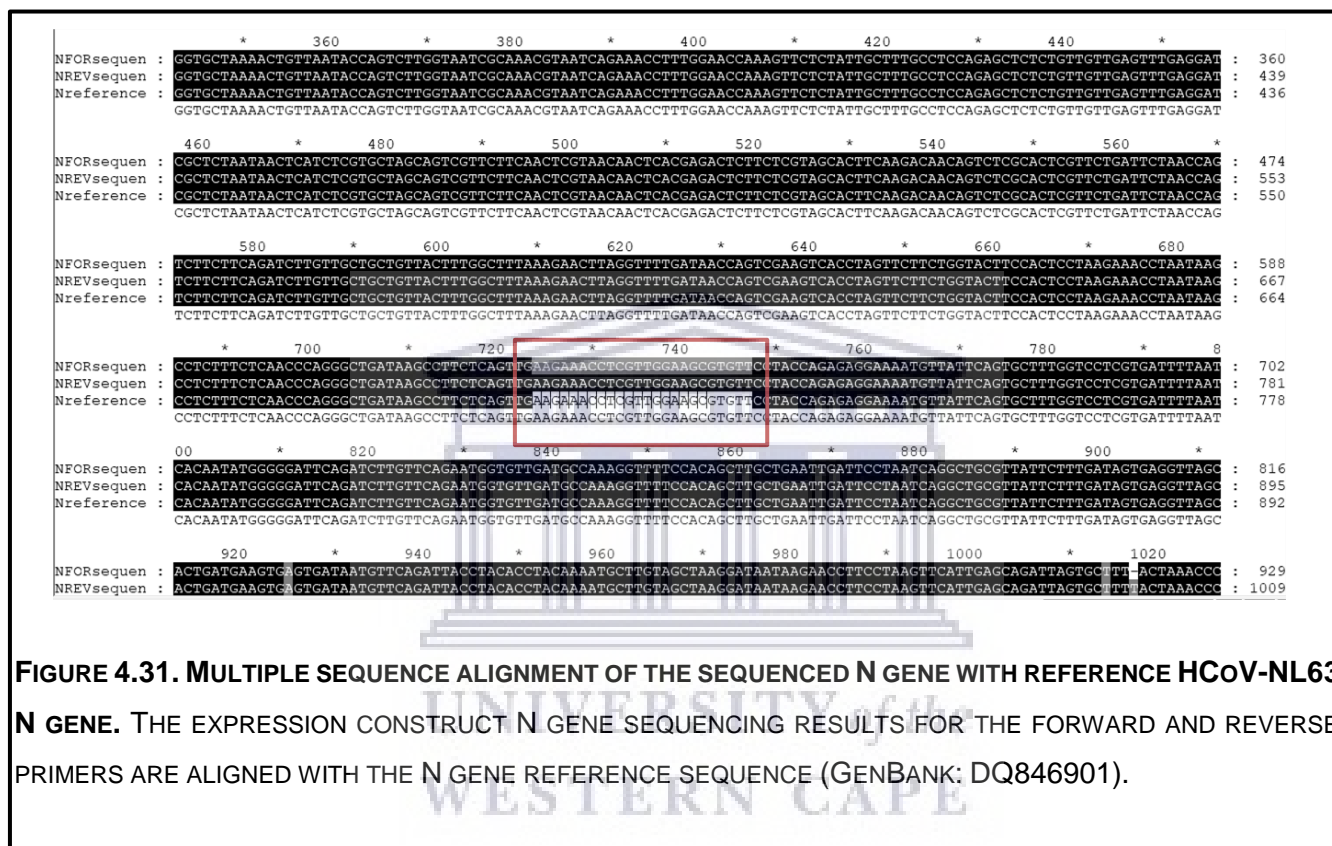
4.3. An *in vitro* localisation study on the HCoV-NL63 N protein

4.3.1. Subcellular localisation of the HCoV-NL63 N protein



4.3.1.1. Confirming the presence of pat4/pat7 classic nuclear localisation signal (NLS) in HCoV-NL63 N gene/protein

In Figure 4.30 (A) above the single-letter AA sequence of the N protein is shown. Figure 4.31 below shows the pat4/7 NLS (indicated by an orange box). The DNA/nucleotide code corresponding to the pat4/7 NLS is highlighted in grey within the full-length N gene sequence. The NLS is found at nucleotide position 693 to 719.

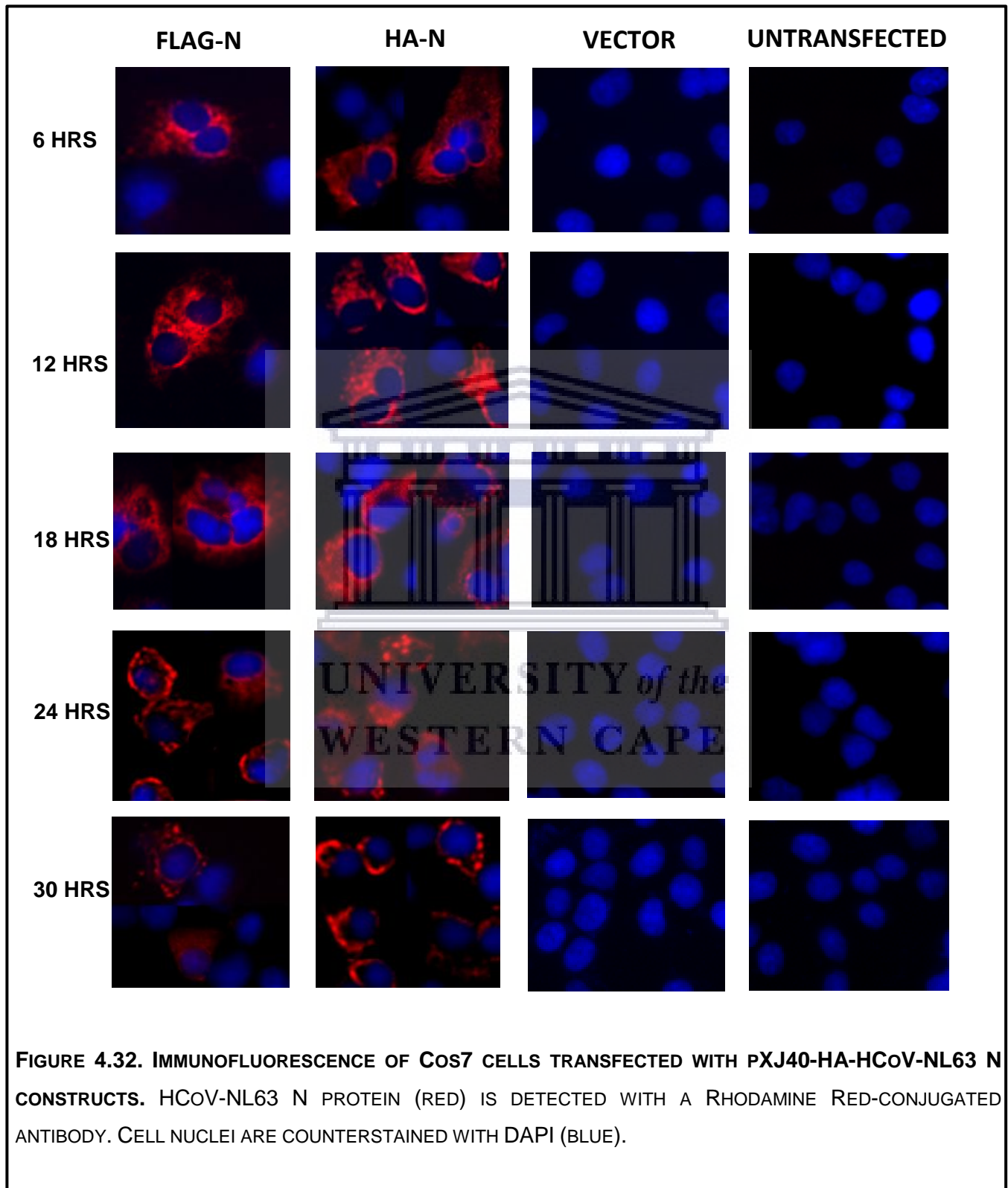


During PCR amplification, the addition of free nucleotides can sometimes lead to errors in incorporation, causing mutations in the amplification product. The larger the target sequence, the higher the number of mutations there are likely to be in the sequence (there are no proofreading enzymes functional in a PCR reaction as *in vivo*). Much of the time, these mutations are missense/silent mutations, which means that they still encode the same AA and do not lead to a mutated polypeptide. Following PCR amplification of the full-length N, the purified DNA samples were sequenced. The analysed sequence was then aligned with the ref N sequence using an alignment algorithm (ClustalX and GeneDoc) to check the correctness of the gene sequence. Figure 4.31. above shows a multiple sequence alignment of the forward ('NFORsequence') and reverse ('NREVsequence') sequences along with the reference sequence ('Nreference', GenBank ID: DQ846901). The sequence identity of the amplified N and ref N

is 99%. The highlighted area in the sequence above (Figure 4.31) is the classic pat4/7 NLS. In the full-length N clone, the NLS is intact, and the coding sequence is unaltered/not mutated. Therefore, the N gene should encode the same signal as the reference N (sequence from virus isolate) and should be functional *in vivo* if necessary.



4.3.2. Subcellular localisation of N protein in Cos7 cells by immunofluorescence (IF)



4.3.2.1. Native N protein exhibits perinuclear and cytoplasmic localisation in Cos7 cells

CoV nucleoproteins and those of the closely related arteriviruses have been shown to localise to the cytoplasm, nucleus, and nucleolus of the host cell (Hiscox et al., 2001; Ning et al., 2003; Tijms et al., 2002; Wurm et al., 2001). Some of these N proteins can also bind nucleolar-associated proteins (Chen et al., 2002; Yoo et al., 2003). The nucleolus is involved in cell growth and synthesis of ribosomal subunits (Andersen et al., 2005; Lam et al., 2005). The localisation of the CoV N protein to the host cell nucleolus may be a property of many CoVs. This subcellular localisation pattern may function to disrupt nucleolar function. The N protein may also associate with RNA subunits as part of an effort to exercise control host cell protein synthesis machinery (Hiscox et al., 2001). The SARS-CoV N protein sequence contains nuclear localisation signals within the NTD and CTD, and a nucleolar retention signal (NoRS) within the linker domain. The pat7 bipartite NLS in the SARS-CoV CTD has been shown to have some activity, but it does not seem to be the dominant signal directing N transport. It is speculated that there is a cytoplasmic retention signal within N that may override activity from this pat7 NLS (You et al., 2005).

Although the HCoV-NL63 N protein contains an intact pat4 and pat7 NLS, the full-length protein does not localise to the nucleus, or for that matter, does it exhibit any localisation pattern other than cytoplasmic. It is presumed that CoV N proteins receive multiple signals related to localisation and that the subcellular localisation pattern is modulated through these signals (Rowland et al., 2005). In this analysis, full-length N protein is seen exhibiting a cytoplasmic subcellular distribution. There does not seem to be a difference in the distribution pattern between HA- and FLAG-tagged N proteins. This is congruent with both epitope tags being fused to at the N-terminus of N. Previous analyses reported on HCoV-NL63 N localising to the cytoplasm. In the same analysis, the N protein is also localised during virus infection, and in both transfection and infection, there is a similar subcellular localisation pattern for the HCoV-NL63 N protein (Zuwała et al., 2015). The protein tags used in this study were short epitope tags, FLAG, and HA. Each of these is approximately 1kDa in size. The small size of the tags used is unlikely to alter the structure or functionality of the N protein, meaning that the N protein in this analysis should follow a similar localisation pattern to wild-type HCoV-NL63 N. Zuwała *et al* showed that untagged N protein and C-terminally tagged N protein did not show a significant difference in localisation LLCMK2 cells (Zuwała et al., 2015). Additionally, we have shown that N-terminus tagged N protein exhibited a similar localisation pattern to the two aforementioned types of expressed N protein. Together, these results indicate that there is no implicit involvement of other viral proteins in the subcellular localisation of N in the host cell. The HCoV-NL63 N protein has been localised *in vitro* in 293TACE2+ cells and LLCMK2 cells (Zuwała et al., 2015). Here we expressed and localised HCoV-NL63 N in a Cos7 mammalian cell line. Previously HCoV-NL63 N subcellular localisation was only examined at 24 hours post-transfection in LLCMK2 cells (Zuwała et al., 2015). The aim was to establish whether or not N shuttles back and forth between the cytoplasmic and nuclear regions over time during

protein synthesis and maturation within the host cell. To this end, in this analysis, N localisation is characterised at 6, 12, 18, 24, and 30 hours PT. N exhibited cytoplasmic localisation at all time points; there was no other observable changes in the subcellular localisation pattern. The results indicate that N does not exhibit any nucleo-cytoplasmic trafficking when overexpressed *in vitro*, and that the identified pat4/7 NLSs are either inactive or overruled by alternative signals.

4.3.2.2. The functionality of protein NLSs

NLSs are classified into four general categories. The first two categories include the classic mono- and bi-partite type NLSs. The third category comprises NLSs consisting of polar/charged AAs interspersed between nonpolar AAs. An example of this type of NLS is the yeast homeodomain, which contains the protein MATalpha2. Several viral proteins possess atypical NLSs, consisting of arginine-rich domains (Timani et al., 2005; Zheng et al., 2005). NLSs are often found at or near the terminal ends of the polypeptide sequence. This is most likely since NLSs need to be exposed in order to be available for interaction with transporter proteins (Gharakhanian et al., 1987; Lyons et al., 1987). Other factors that may impact the function of an NLS include the 3D structure of the native protein and the species or cell type from which the protein is derived (Boulikas, 1993). Phosphorylation of a protein is used within the cell to expose hidden NLSs, as in the case of NF- κ B, whereby only after processing (cleavage) and unmasking of the NLS, the protein can translocate into the nucleus (Shirakawa & Mizel, 1989). The SV40 large T antigen NLS has been shown to be non-functional when located within a PK region that is not exposed to the molecule's surface (Roberts, 1989). In order to be recognised as a functional target sequence, the NLS must be necessary for the transport of the protein into the nucleus. This means that any deletion or mutation within the sequence would prevent localisation to the nucleus. It was confirmed that the NLS was intact at the DNA sequence level (Figure 4.31.).

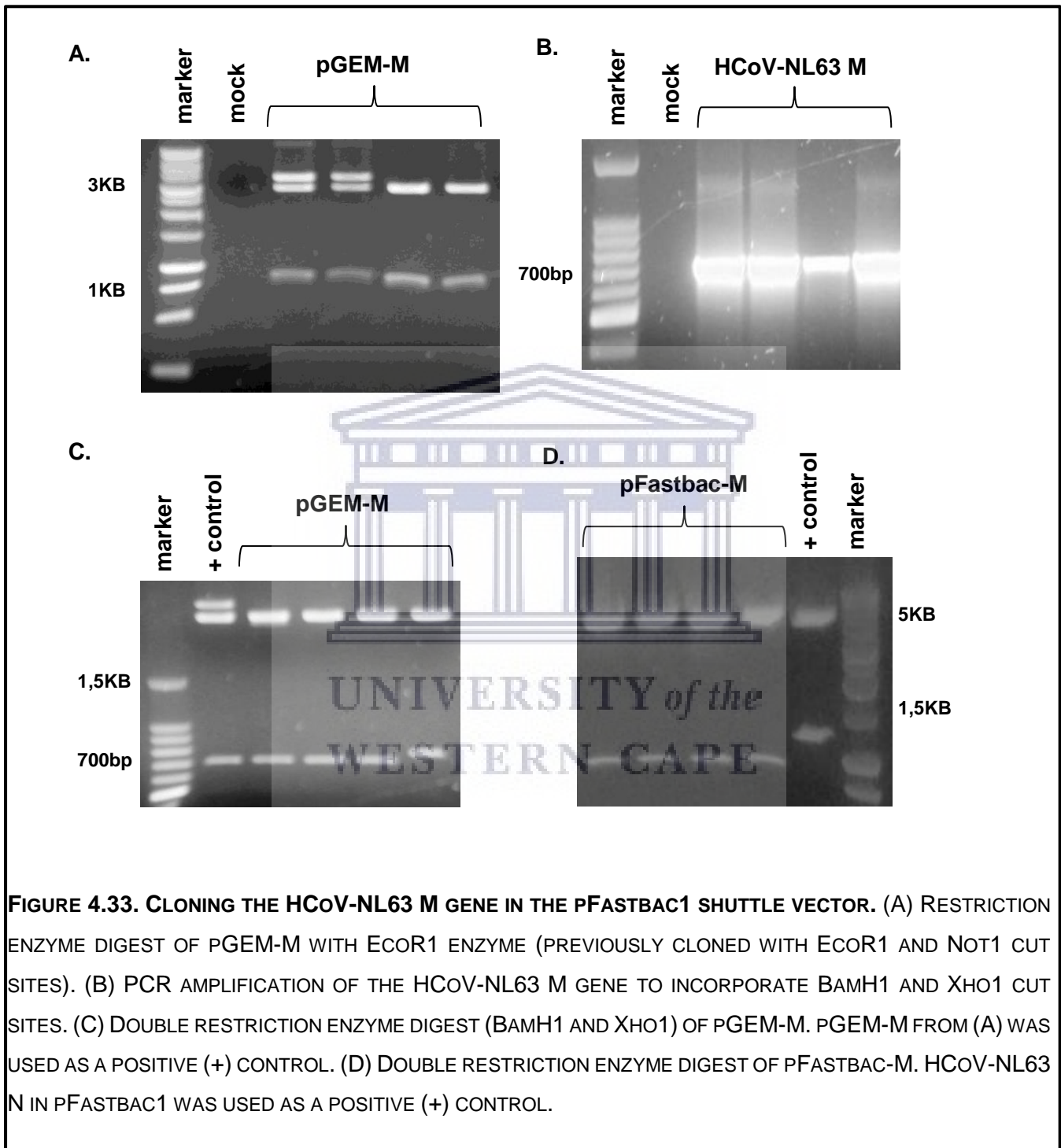
It is possible that a protein, which does not have its own NLS, may enter the nucleus through co-transport with another protein that has a functional NLS (Zheng et al., 2005). Many cytoplasmic proteins possess motifs that fulfil the requirements for a classic NLS. These proteins are usually associated with M proteins or large structures within the cell cytoplasm, making them unavailable for nuclear transport. Other proteins such as transmembrane, luminal endoplasmic reticulum and extracellular proteins, which encode NLS-like sequences, do not localise to the nucleus. It is suggested that the N-terminal hydrophobic region of these proteins transported and processed through the endoplasmic reticulum, serve to direct the protein away from the nuclear and cytoplasmic areas regardless of their NLS-like sequence. Therefore, the NTD or transmembrane domain is stronger determinants of the protein's subcellular localisation (Boulikas, 1994). A difference exhibited between the NLS peptide sequence of nuclear proteins and those NLS-like sequences found in many non-nuclear proteins is the presence of two bulky AAs such as tyrosine and phenylalanine within the latter. Bulky AA residues are not generally

found in the hexapeptide motifs of NLSs. Also, some NLS-like sequences possess one or more aspartic/glutamic acid residues, an unfavourable characteristic within functional NLSs (Boulikas, 1993). Some proteins that do not localise to the nucleus also contain classic NLSs within their sequence. The reasons for these are still to be elucidated (Cokol et al., 2000). It should be noted that a single protein may contain more than one NLS, and these may be involved in different pathways or respond to different signals. This indicates the complex nature of nuclear localisation within the cell (Lange et al., 2007). Both SARS-CoV and SARS-CoV-2 contain multiple protein localisation signals within their sequences. SARS-CoV N exhibits only cytosolic localisation with a lack of nucleocytoplasmic trafficking despite the protein's many signal sequences (Wu et al., 2020; Wulan et al., 2015; You et al., 2007; You et al., 2005). Similarly to SARS-CoV N, HCoV-NL63 N protein exhibits only cytoplasmic subcellular localisation within a mammalian cell.



4.4. The expression of HCoV-NL63 M protein in a baculovirus system

4.4.1. Cloning the HCoV-NL63 M gene into the pFastbac1 shuttle vector



4.4.1.1. Confirmation of successful clones – pFastbac1-M

M gene was cloned with Eco and Not restriction sites. Downstream pFastbac1 vector MCS does not include a Not1 site, so new restriction enzyme recognition sites had to be incorporated. First, the author checked M gene integrity in previously cloned pGEM-M constructs (see Figure 4.33. A). Full-length HCoV-NL63 M was then amplified with new cut sites (BamH1 and Xho1) flanking the 3' and 5' ends (Figure 4.33. B). Figure 4.33. C and D graphically depict the full-length M gene (680bp) cloned in the pGEM shuttle vector (3KB) and subcloned into the pFastbac1 bacmid shuttle vector (5KB).



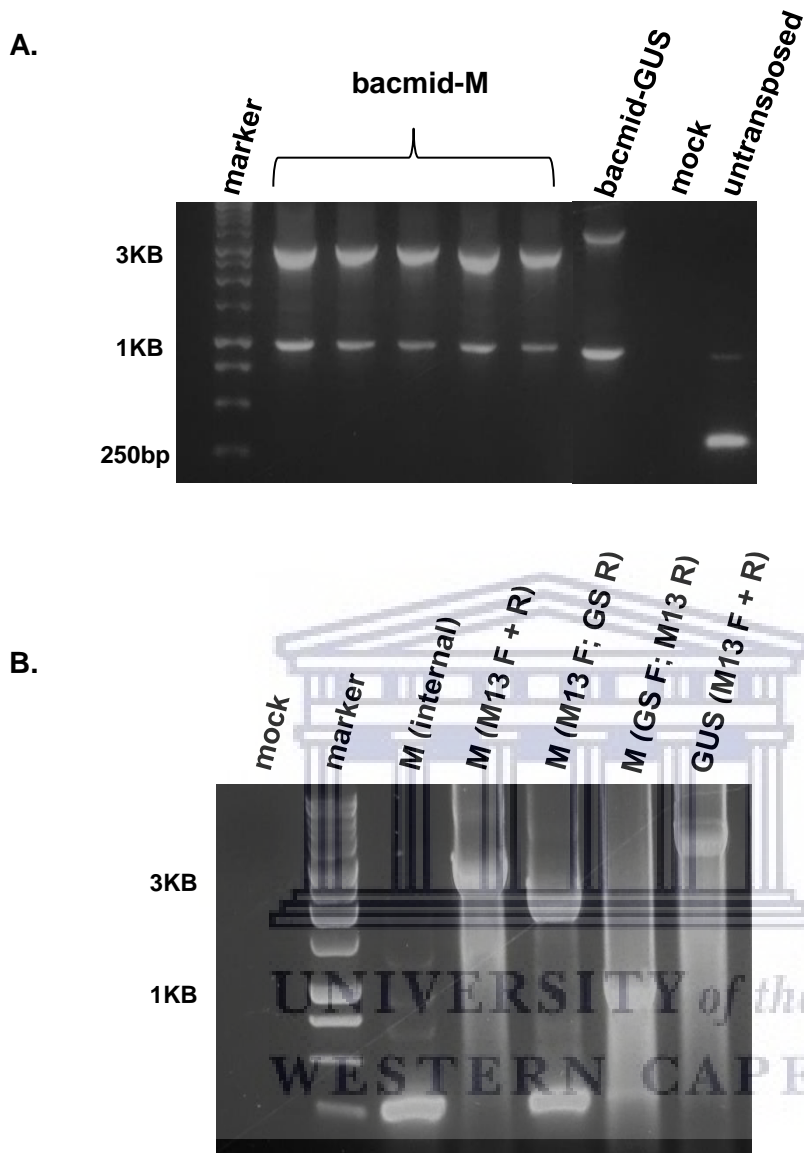


FIGURE 4.34. PCR AMPLIFICATION OF THE TRANSPOSED BACMID. (A) USING M13 PRIMERS. pFASTBAC-GUS (APPROX. 4.2KB); UNTRANSPOSED BACMID (EXPECTED AT APPROXIMATELY 300BP). (B) PCR WITH DIFFERENT PRIMER PAIRS AND COMBINATION PRIMERS TO CONFIRM THE ORIENTATION OF THE HCoV-NL63 M GENE IN THE RECOMBINANT BACMID. PCR OF BACMID-M WITH GS FOR AND GS REV PRIMERS; LANE 4: PCR OF BACMID-M WITH M13 FOR AND M13 REV PRIMERS; LANE 5: PCR OF BACMID-M WITH M13 FOR AND GS REV; LANE 6: PCR OF BACMID-M WITH GS FOR AND M13 REV PRIMERS; LANE 7: PCR OF BACMID-GUS WITH M13 FOR AND REV PRIMERS.

4.4.2. Generation of the recombinant bacmid-HCoV-NL63 M expression construct

Confirming the transposition and correct orientation of the HCoV-NL63 M gene within the recombinant bacmid by PCR is important to ensure the purity and integrity of the viral DNA prior to cell transfection. Combination primer pairs were used in the PCR, along with two different annealing temperatures in order to obtain an optimal and specific amplification reaction with primers from two different primer pairs. The GS primers that were used in combination with the M13 primers were internal M primers. As amplifying the full-length M gene proved difficult after the initial amplification from the template DNA, internal primers were designed to confirm the presence of the M gene. These primers were also designed to function at an annealing temperature close to that of the M13 primers. The internal M primers bind at 302-321bp (FOR) and 579-598bp (REV). The estimated band sizes for the combination PCR were calculated as follows:



M13 forward; M13 reverse = 3000bp
M13 forward; GS reverse = 2247bp
GS forward; M13 reverse = 958bp
GS forward; GS reverse = 300bp
GUS control – M13 forward; M13 reverse = 4300bp

In Figure 4.32. B, the appropriate amplified bands can be seen at the expected sizes in each lane. This confirms the purity of the recombinant DNA. A non-specific band is observed at 1000bp across all lanes, including the empty bacmid vector. This is most likely non-specific amplification by M13 primers at another site in the bacmid. This band is considered negligible as it appears in all experimental lanes (not in water blank-no contamination).

4.4.2.1. The advantages of using a baculovirus expression system

Nowadays, the Bac-to-Bac system is one of the most widely-used *in vitro* systems for the expression of recombinant proteins (Kost & Condreay, 1999; O'Reilly et al., 1994; Possee et al., 2019; Possee, 1997). The recombinant baculovirus insect *in vitro* expression system is relatively easy to scale down or up in production volume, even to industrial-scale volumes (Ikonomou et al., 2003). The techniques are rapid, and it is relatively simple to isolate and purify a recombinant virus containing the protein/s of interest (Ciccarone et al., 1998). The cells used to express recombinant baculoviruses (insect or mammalian) possess the cellular machinery to correctly fold, modify, and transport the newly synthesised proteins. The baculovirus system can also produce soluble, multi-protein complexes (Jarvis, 1997; Luckow & Summers, 1988; Possee, 1993). Although the co- and post-translational processing capabilities of

insect and mammalian cells are similar in nature, modifications in insect cells are not necessarily equal to those in mammalian cell lines (e.g., Glycosylation) (Kost et al., 2005). The baculovirus system allows single and multiple proteins to be expressed at one time in the cell. In the cases of co-expression, each recombinant baculovirus can express single or multiple proteins (gene constructs/expression cassettes). Using different MOIs allows for the optimisation of the expression ratio of proteins for VLP generation and release (Berger et al., 2004; Kost et al., 2005).



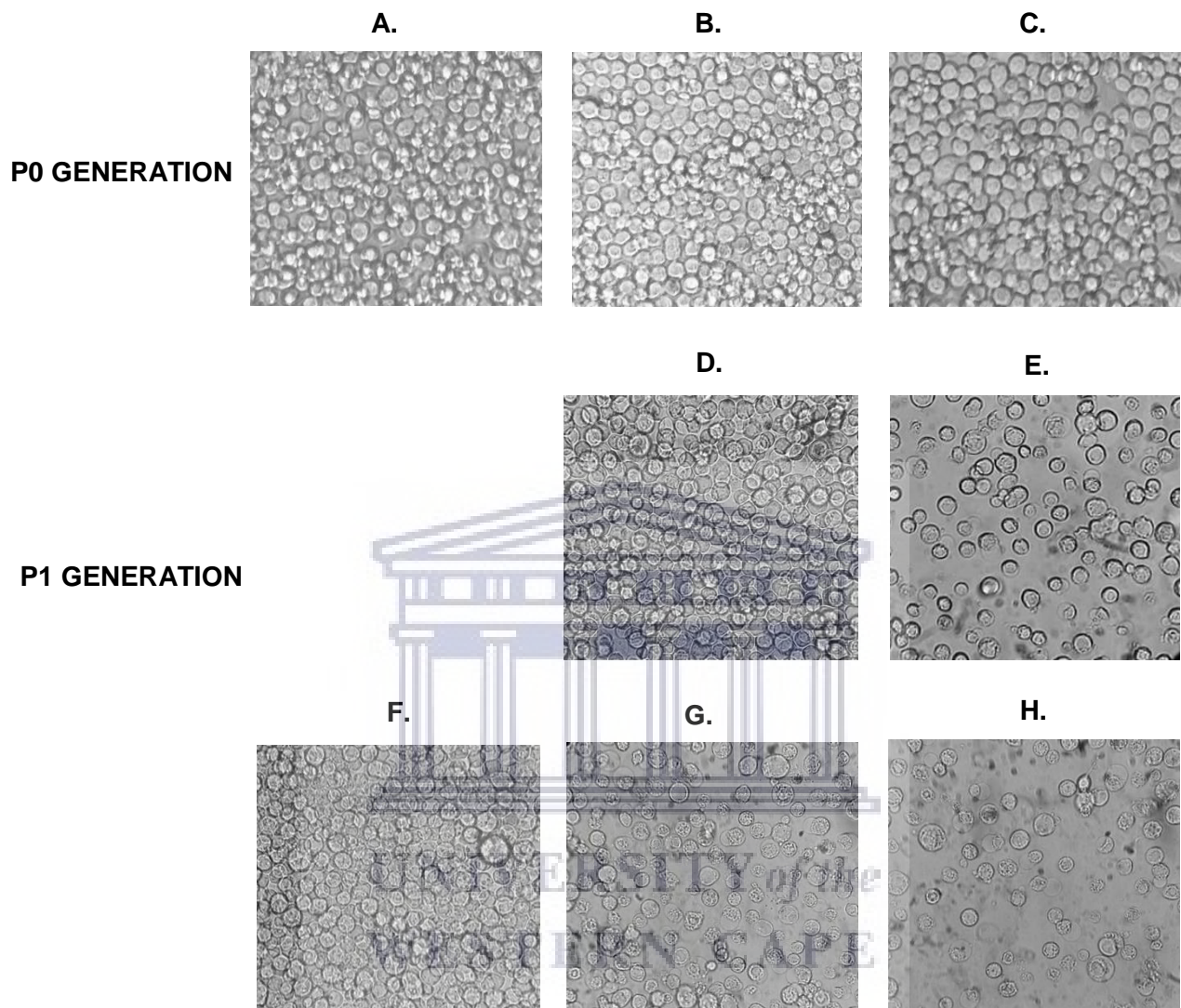


FIGURE 4.35. P0 AND P1 GENERATION OF BACULOVIRUS STOCK IN TRANSFECTED Sf9 CELLS AT 400X MAGNIFICATION AT 96 – 120 HOURS POST-TRANSFECTION/INFECTION. (A) CELLS ONLY 96 HOURS PT; (B) MOI 0.1 96 HOURS PT; (C) MOI 0.1 120 HOURS PT (D) CELLS ONLY 96 HOURS PI; (E) MOI 0.1 96 HOURS PI; (F) CELLS ONLY 120 HOURS PI; (G,H) MOI 0.1 120 HOURS PI.

4.4.3. The generation of a high titre recombinant baculovirus stock expressing HCoV-NL63 M

4.4.3.1. Infection of Sf9 cells and amplification of viral titre – P2 generation

No significant changes in cell growth (in comparison to cells only) are exhibited in transfected samples when generating P0 viral stock (top figures). The initial concentration/titre of virus stock is generally low, and a lack in CPE is seen in the cells (Figure 4.35. B, C). To increase viral titre and generate a stock with an appropriately high titre for use in expression studies, P0 stock was used to infect fresh Sf9 cells (Figure 4.35 E, G, H) above shows visible differences in cell growth and cell death in the infected samples vs the uninfected control. At 96 hours PI, infected cells exhibit membrane blebbing, a common characteristic of apoptosis (Wyllie et al., 1980; Zhang et al., 2018). Vacuolisation, another common feature of programmed cell death, can also be seen in most of the cells (see Figure 4.33. B at 120 hours PI). There are very few live cells still present in baculovirus M infected samples. At 120 hours, uninfected cells are still actively growing. Some HCoVs are known to induce apoptosis in specific infected cell types. SARS-CoV has been shown to cause apoptosis in infected patient cells and culture immortalised cells (Peiris et al., 2003; Yan et al., 2004). HCoV-229E causes apoptosis in dendritic cells (antigen-presenting cells (APCs)), an important immune cell type, which functions in antigen presentation and pathogen recognition (Mesel-Lemoine et al., 2012).

An increase in cell apoptosis has been reported previously for insect cells infected with a recombinant baculovirus expressing SARS-CoV M. The CPE exhibited by infected cells included cell shrinkage, nuclear condensation, increased cytotoxicity, and cell death (Lai et al., 2006).

4.4.3.2. Baculoviruses as eukaryotic expression vectors

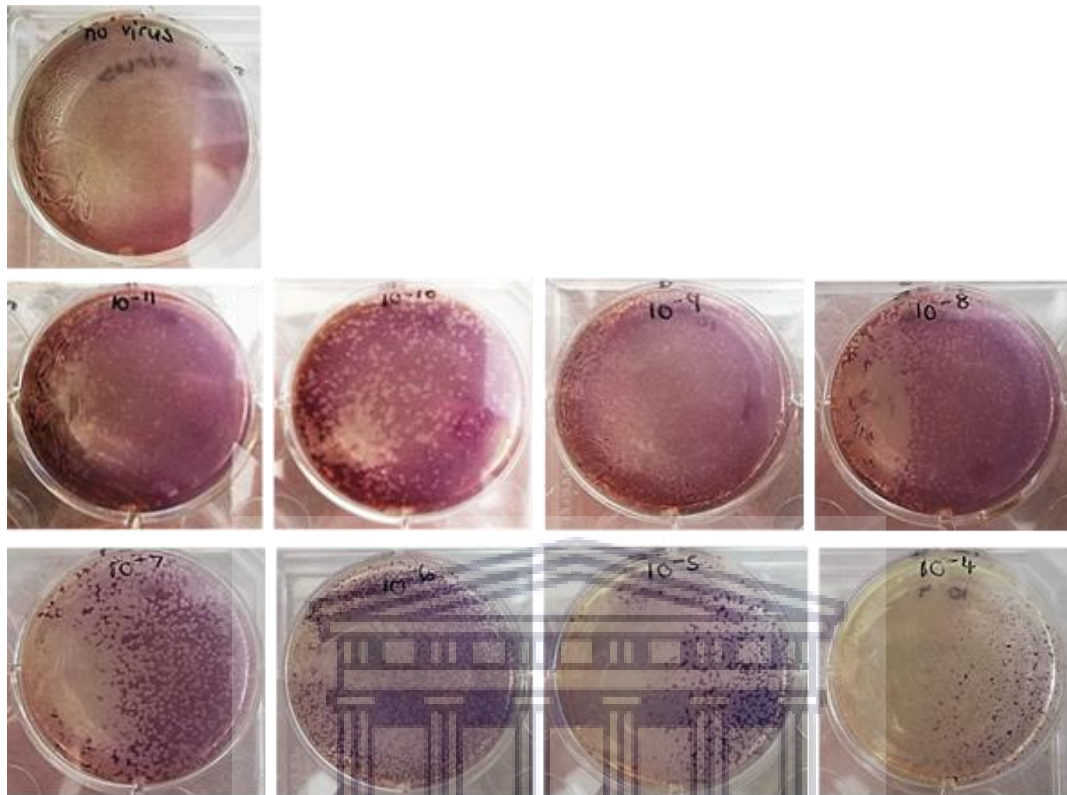
Recombinant baculoviruses have been used since 1983 for expressing exogenous proteins (Hitchman et al., 2009; Smith, Gale E. et al., 1983; Smith, G E et al., 1983). Baculoviruses are highly pathogenic to insects, particularly to those of the order *Lepidoptera*. These viruses were first studied for their potential use in biological pest control, and research revealed a biphasic virus life cycle with a unique characteristic: Following the budding of infectious virions, baculo-infected cells undergo a stage of significantly increased/robust protein expression (Volkman & LE, 1977; Volkman et al., 1976). Certain advancements in insect cell culture technology and insect virus propagation *in vitro* have led to the widespread use of the Bac expression vector system. The development of continuous Lepidopteran cultures led to the generation of adherent (Sf9) and suspension (Sf21) insect cells (Lynn, 2001). Growth reagents specific to insect cell culture have also become commercially available (Kost et al., 2005). The development of transfer vectors, methods to increase the yield of recombinant viruses, and improvements in recombinant virus isolation techniques (Airenne et al., 2003; Laitinen et al., 2005) are

all factors that have played a role in making the Bac-to-Bac system a routinely-used laboratory expression system. The recombinant baculovirus genome has also been used to express proteins under the control of a mammalian promoter, allowing the expression of proteins in mammalian cell lines (Kost et al., 2005).

4.4.3.3. Functionality of recombinant baculovirus expressed M proteins

Baculovirus systems have been used to express a wide range of mammalian, membrane-bound proteins in Sf9 insect cells (Dale et al., 1996). FLAG-tagged GluR-D glutamate receptor subunits have been expressed in Sf21 cells to similar expression levels as native, untagged GluR-D (Kuusinen et al., 1995). Phospholamban, a transmembrane phosphoprotein, as well as a functionally active cardiac calcium pump, have been expressed in Sf21 cells (Autry & Jones, 1998). His-tagged membrane-bound human 3β -hydroxysteroid dehydrogenase type 1 (3β -HSD1) enzyme has been overexpressed in a baculovirus system (Huang et al., 2000). A type 1 rabbit ryanodine receptor (RyR1) from skeletal muscle has been functionally expressed in insect Sf21 cells (Antaramian et al., 2001). Muscarinic M2 acetylcholine receptors have been expressed in Sf9 cells (Weill et al., 1997). The baculovirus system has been used to efficiently overexpress a variety of G protein-coupled receptors in insect cells. These include subtypes of muscarinic-, dopaminergic-, serotonin-, opioid-, or adrenergic receptors (Grisshammer & Tateu, 1995; Massotte, 2003; Warne et al., 2003). Glycoprotein B of the pseudorabies virus (PrV) has been expressed in recombinant baculovirus-infected Sf9 cells (SERENA et al., 2015).





$$\text{Viral titre} \left(\frac{\text{pfu}}{\text{mL}} \right) = \text{number of plaques} \times \text{dilution factor} \times \left(\frac{1}{\text{mL of inoculum/well}} \right)$$

$$\text{P2 viral titre} = 103 \times 10^{11} \times \left(\frac{1}{1} \right) = 1.03 \times 10^{13} \text{ pfu/mL}$$

FIGURE 4.36. PLAQUE ASSAY TO DETERMINE VIRUS TITRE OF P2 BACULOVIRAL M STOCK. (A) PLAQUE ASSAY STAINED WITH MTT (50µg/ML). AN UNINFECTED CONTROL ('NO VIRUS') WELL IS SHOWN ALONGSIDE WELLS INFECTED WITH A RANGE OF WORKING STOCK DILUTIONS (10⁻⁴ TO 10⁻¹¹). (B) CALCULATION OF OUR P2 BACULOVIRUS HCOV-NL63 M STOCKS.

4.4.4. Plaque assay of P2 stock – Calculating viral titre

When propagating a newly produced recombinant virus, the virus plaque assay allows for the isolation and pure viral clones. These can then be amplified within the host system, which in this case, was Sf9 cells. The virus stock can then be quantified or tited by another virus plaque assay.

A monolayer of cells is infected with a virus stock of unknown concentration/titre during a viral plaque assay. The stock is serially diluted before using it to infect populations of cells at different dilutions. Infected cells are covered in a semi-solid plaquing growth medium in order to prevent the virus from spreading randomly throughout the population by movement through the liquid media. Following the infection and immobilisation of cells, individual plaques will start to develop. These plaques are zones of dead cells/no growth which, due to the agarose restriction, usually form outward from a single infected cell. As infected cells continue to lysis and spread the virus to adjacent immobilised cells, the plaque diameter will increase in size. After 2 – 14 days (virus-dependent), individual plaques can be visualised with a standard bright field microscope. For improved visualisation for counting plaques, stains such as neutral red or crystal violet can stain the plaquing media and thereby, make plaques more easily visible. Crystal violet is added to viral plaques after removing the plaquing overlay and allows for the visualisation of small plaques in the presence of mixed viral morphologies. Neutral red stain can be added to the plaquing media and cells days prior to counting plaques. This can allow for the real-time monitoring of plaque formation, which can be useful when working with an uncharacterised virus with unknown infection kinetics.

However, staining with neutral red does not allow for the picking (isolation) and propagating stained viral plaques, as neutral red is known to have mutagenising effects on DNA (Matrosovich et al., 2006; Shurtleff et al., 2012). MTT (3-(4, 5-Dimethylthiazol-2-yl)-2, 5-diphenyltetrazolium bromide) is non-damaging to the virus and can be used for staining and isolating viral plaques. In Figure 4.36 above, baculoviral plaques were stained with MTT to enable plaque visualisation and counting. MTT is a yellow-coloured stain, which turns dark blue upon contact with live cells. Plaques appear as clearing in the monolayer, and these can be picked and propagated for further amplification (Klebe & Harriss, 1984). In this analysis, MTT was used to perform viral plaque staining. The major advantage of using the viral plaque assay is determining the number of infectious viral particles in a given stock sample. This information is used in downstream virus infection analyses (Baer & Kehn-Hall, 2014; Cooper, 1962; Dulbecco & Vogt, 1953).

4.4.5. The expression of recombinant HCoV-NL63 M protein in an insect cell line

4.4.5.1. Sf9 protein lysate quantitation

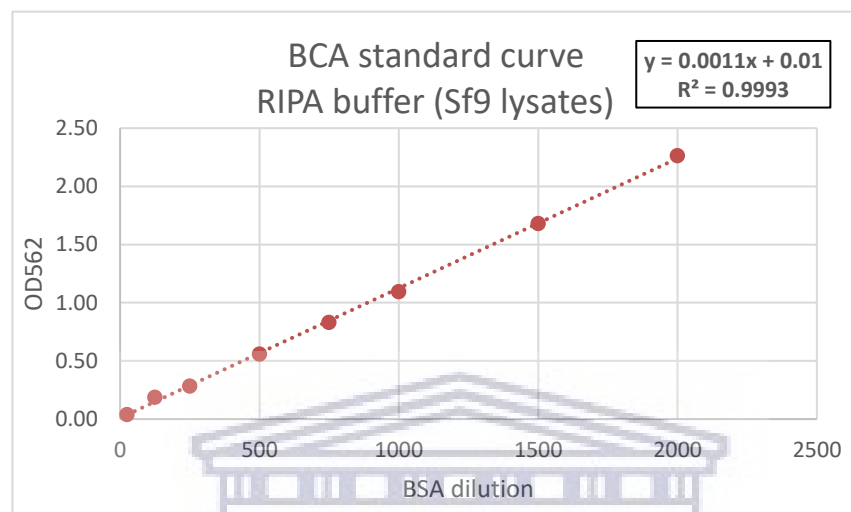


FIGURE 4.37. THE DETERMINATION OF WHOLE CELL PROTEIN LYSATE CONCENTRATIONS OF Sf9 CELLS INFECTED WITH A RECOMBINANT BACULOVIRUS EXPRESSING HCoV-NL63 M PROTEIN. THE STANDARD CURVE AND LINE EQUATION GENERATED USING BSA AT DIFFERENT CONCENTRATIONS (0 – 2000µg/mL) IS SHOWN DILUTED IN Sf9 CELL LYSIS BUFFER. THE LINE EQUATION IS USED BELOW TO DETERMINE THE PROTEIN CONCENTRATION IN EACH SAMPLE.

TABLE 4.10. WHOLE CELL LYSATE PROTEIN CONCENTRATIONS OF BACULO-M INFECTED Sf9 CELLS

	MOI 1	MOI 5	MOI 10	MOI 20
LYSATE SAMPLE	TOTAL PROTEIN CONCENTRATION (µg/mL)			
24 hours	794	776	776	758
48 hours	1176	1240	1221	1112
72 hours	1640	1567	1503	1385
96 hours	1567	1585	1540	1458

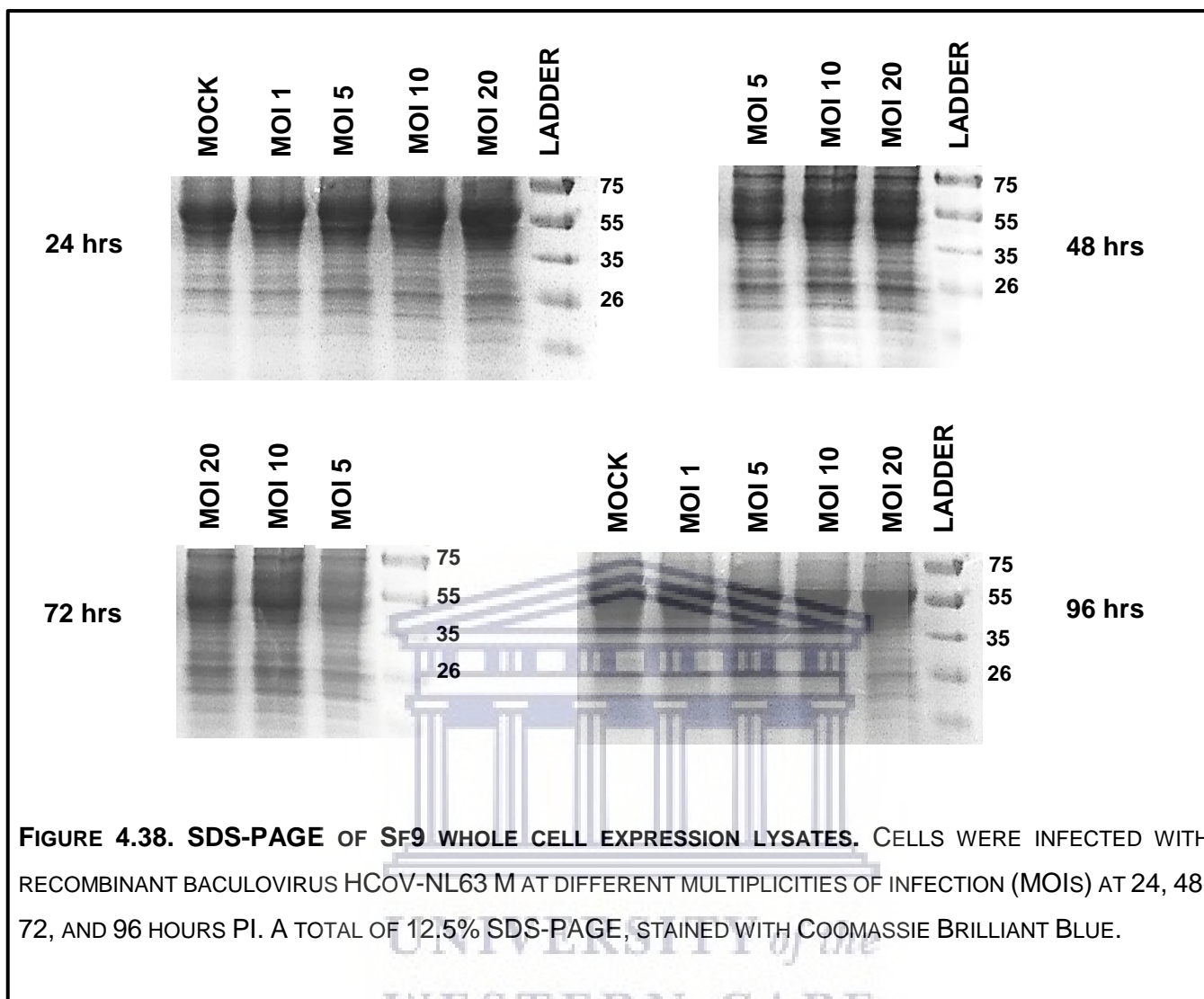


FIGURE 4.38. SDS-PAGE OF Sf9 WHOLE CELL EXPRESSION LYSATES. CELLS WERE INFECTED WITH RECOMBINANT BACULOVIRUS HCoV-NL63 M AT DIFFERENT MULTIPLICITIES OF INFECTION (MOIS) AT 24, 48, 72, AND 96 HOURS PI. A TOTAL OF 12.5% SDS-PAGE, STAINED WITH COOMASSIE BRILLIANT BLUE.

4.4.5.2. Optimisation of HCoV-NL63 M expression

In order to standardise the amount of protein loaded on to the gel for each sample, Sf9 expression lysates were quantified (Figure 4.37, Table 10). In Figure 4.38, at 48 and 72 hours PI, there is a band detected at approximately 25kDa. As these are stained whole cell lysates, there may be a cellular protein expressed at the same size as the previously confirmed size of M. The uninfected cells at 24 hours and 96 hours exhibit a marked decrease in the expression level of the protein at 26kDa. This protein band of interest is visibly more pronounced in MOI 5, 10, and 20 samples at 24- and 96 hours compared to the uninfected cell control. This may indicate that at 24- and 96 hours PI, HCoV-NL63 M is expressed in Sf9 cells. Furthermore, at 48- and 72 hours PI, the 26kDa protein band is accompanied by a band running slightly higher in the gel. This differential expression of M protein agrees with the previously observed HCoV-NL63 M migrating as two protein bands, reflecting two different M-

glycosylation states (Naskalska et al., 2018). The higher MW protein band is not observed at 24- and 96 hours PI, even in lanes where the 26kDa band is stronger than the uninfected control (MOI 5, 10, and 20). While the upper half of the gel is highly stained due to many higher MW cellular proteins at 48- and 72 hours, a protein band is present at approximately 50kDa. As previously stated, M was denatured at a lower temperature of 45 – 50°C and not boiled, in order to prevent thermal aggregation of the protein (Naskalska et al., 2018). This may have resulted in incomplete denaturation of the M protein homodimer, leading to the presence of higher MW HCoV-NL63 M protein (El-Duah et al., 2019; Naskalska et al., 2019).

HCoV-NL63 full-length M protein is expected at approximately 26kDa (Naskalska et al., 2018). The M protein in this analysis runs slightly slower on the gel than the predicted size. This may be due to protein glycosylation in the insect cell host system. The same has been reported in a baculovirus insect system for the SARS-CoV M protein, where the expected 25kDa M protein migrated slower in the gel and was detected at 30kDa (Mortola & Roy, 2004). It is unknown to what degree glycosylation of the HCoV-NL63 M protein will affect its size in kDa. The baculovirus system has been used to assess HCoV-NL63 virus-like particle formation in High Five (HF) insect cells (Sf9 cells were used for infection and amplification initially). The S, M, and E proteins of HCoV-NL63 were expressed and co-infected/co-expressed in insect cells. Their study showed M on a Western blot at around 20kDa (12% SDS-PAGE). This study also confirmed thermal aggregation of the CoV M protein when trying to denature it at a high temperature, as has been previously noted about SARS CoV M protein but not about other CoV M proteins. The co-infection of HF insect cells with recombinant baculoviruses encoding the NL63 M and E proteins, respectively, led to the formation and secretion of NL63 (Naskalska et al., 2018).

The M protein is first observed at 48 hours PI, and can also be visualised in the 72-hour PI lysates (see Figure 4.36.). At 24 hours PI, the M protein band is not yet seen and at 96 hours PI, the M protein band is once again absent. The expression of HCoV-NL63 M protein seems to occur after 24 hours PI and is no longer present (visualised) by 96 hours PI. It is possible that at 96 hours, the level of M expression was below the detection range of the Coomassie stain. Insect cell cultures were infected with a range of virus stock concentrations, including MOI 1, 5, 10, and 20. The highest expression level of M was detected at MOI 10 and 20 at 72 hours PI. The expression level does not seem to differ significantly between MOI 5, 10, and 20 at 48 hours PI.

Baculoviruses are double-stranded DNA viruses that infect the insect species *Lepidoptera*. *Autographica californica* multiple nucleopolyhedrovirus is the best-characterised baculovirus, and is known to have a distinct, two-phase life cycle. The budded virus type is released from the host cell between the early and late phase of baculovirus infection. These virions are encased with host-derived envelope membranes and are able to spread in and infect other cells. The occluded virus type is

produced during the very late phase of infection when the viral protein polyhedrin (P_{PH}) accumulates and forms occlusion bodies in the host cell. The highly active *polh* promoter controls PPH expression in the baculovirus-infected cell (O'Reilly et al., 1994; Zitzmann et al., 2017). During the early infection phase, viral synthesis may be initiated (30 minutes to 6 hours post-infection). The late phase of infection involves the expression of genes involved in virus assembly. During this phase, recombinant baculovirus particles are produced and released (18 – 24 hours post-infection). In the very late phase of infection (20 – 36 hours post-infection) in the wild-type baculovirus, the P_{PH} promoter is activated, and occlusion-derived virions are formed (Luckow et al., 1993). Within the recombinant baculovirus, the M protein was under the control of the P_{PH} promoter and is thus, expressed between late and very late-stage infection in the host cells. As infection kinetics differ between wild-type baculovirus and the recombinant viruses generated to express heterologous viral proteins, the timing of the stages of infection are altered.

4.4.5.3. Differences in eukaryotic glycosylation systems

Protein glycosylation occurs in eukaryotic systems, including insect and mammalian cells (Shi & Jarvis, 2007). Current data suggests that the first half of the N-glycosylation is the same in both insect and mammalian systems. This includes the initial transfer of N-glycans and trimming of glycans by glycosidases. The intermediate, high-mannose N-glycan products produced by each system are, therefore, identical. Furthermore, it is notable that there are sites on some proteins, which require oligosaccharide additions of this type (no further modification) (Kornfeld & Kornfeld, 1985; Shi & Jarvis, 2007). Further 'trimming' processing in both systems can result in forming one of two common paucimannose intermediate molecules. The elongation reactions, which occur with these trimmed intermediates, differ between insect and mammalian cells. In mammalian cells, the intermediate N-glycan can be modified and elongated into a variety of possible N-glycans. Branching and elongation are mediated by glycosyltransferases (Kornfeld & Kornfeld, 1985). In insect cells such as the Sf9 cell line used in this analysis, further elongation of the intermediates is not possible/does not occur. The final N-glycans produced in the insect system are the 'intermediate' high-mannose or paucimannose structures (Shi & Jarvis, 2007). Therefore, the HCoV-NL63 M glycoprotein in this Sf9 system was expected to be N-glycosylated by the above-mentioned saccharide structures. The specific impact of the differing glycosylation systems on the size of the final protein is not yet elucidated. The difference in the glycosylation of proteins in insect cells and higher eukaryotic cells is important in terms of protein antigenicity and biosafety. A few types of insect cells can produce core α -1, 3-fucosylated glycans, and these have been shown to cause allergic sensitivity in humans. Insect-processed N-glycans lack terminal sialic acids, which are only produced in mammalian cells. Terminal sialic acid residues are needed to inhibit the clearance of glycoproteins in mammals. Therefore, recombinant protein antigens intended for vaccine research or development should be produced in higher eukaryotic cells, not in

insect cells, without modifications. There are only a few insect cells/tissues that can produce complex, terminally sialylated N-glycans. The membrane glycoproteins expressed in most insect cell systems, including Sf9, Sf21, and HF cells, are modified with paucimannose side chains that lack terminal sialylation. Therefore, it was expected that the M protein expressed here would not be glycosylated in a manner consistent with mammalian expressed HCoV-NL63 M protein. Insect and mammalian *in vitro* systems generally produce various N-glycan structures, namely trimmed high mannose-, complex-, or hybrid structures. The overall percentage of complex or hybrid N-glycan structures is low within insect cells, and these structures are non-sialylated (Shi & Jarvis, 2007). It has not been shown how the differential glycosylation systems of insect versus mammalian cells may affect protein size or charge migration.



Chapter 5: General conclusions

Murine anti-peptide antibodies were produced for the first time against the HCoV-NL63 M and N structural proteins. Poly-specific polyclonal anti-N antibodies were raised, while anti-M polyclonal antibodies were mono-specific. Anti N PABs showed robust detection of full-length N expressed in 3 different *in vitro* expression systems including bacterial, insect and mammalian cells. The polyclonal antibodies against both the M and N proteins are not only specific in binding their respective peptide antigens; the antibodies also bind the corresponding full-length protein with high specificity and sensitivity. Monoclonal antibodies were generated for both M and N. The anti-M and –N monoclonal antibodies produced by clonal hybridoma lines are shown to be specific to their appropriate immunizing peptides as well as denatured and folded HCoV-NL63-protein antigens. Here for the first time, the HCoV-NL63 Membrane and Nucleocapsid proteins were successfully co-expressed in a mammalian cell system. This is relevant to native protein structure and enables the evaluation of protein function in completely-processed native form. M and N have been demonstrated as *in vitro* interaction partners through the co-purification/co-immunoprecipitation of HA-M and FLAG-N out of the same expression lysate by only HA-tag affinity purification. HCoV-NL63 M-N protein complexes are resistant to denaturation under standard conditions and require an extended 2 hour denaturation at a lower temperature of 45°C in order to be detected by western blot – this resistance to denaturation seems to be driven by the N protein. Even expressed alone, N is not detected by a specific N-antibody under extended denaturing conditions. HCoV-NL63 M protein forms homomultimeric structures when expressed alone and in complex with N protein. The *in vitro* interaction of HCoV-NL63 M and N in a mammalian cell system is stable and resistant to disruption/degradation even in a stringent lysis buffer system (in the presence of anionic/denaturing detergents). The results obtained here provide insight in to the structural dynamics and interactions of 2 of the major virion components. The Nucleocapsid protein associates with the genome to form the nucleoprotein core of the HCoV-NL63 virion. CoV N is found to localize either to the cytoplasm and nucleus/nucleolus or only to the cytoplasm, depending on CoV species/genogroup. Zuwala *et al* 2015 (Zuwala *et al.*, 2015) was the first to describe the cytoplasmic localisation of the HCoV-NL63 Nucleocapsid protein in mammalian cells. Here we examined the possibility of nuclear-cytoplasmic shuttling of N during early protein synthesis to maturation. Expressing HCoV-NL63 N over an expression time-course, we found that N was expressed from as early as 6 hours post-transfection, and only subcellular localisation is observed at 6, 12, 18, 24 and 30 hours PT. The HCoV-NL63 N protein remains localised to the perinuclear-cytoplasmic region, and exhibits no nuclear-shuttling over time when expressed alone in an *in vitro* mammalian system. The pat4/pat7 NLS present within the N sequence (confirmed in sequencing of clone DNA) may be inactive, alternatively the subcellular localization of N maybe be modulated by numerous intracellular localization

signals. The SARS-CoV N protein also exhibits cytoplasmic localisation although it has numerous classic trafficking signals including NLSs (Wulan et al., 2015; You et al., 2007; You et al., 2005). It is understood that during CoV infection, other viral components and even cellular proteins may influence the subcellular trafficking of the Nucleocapsid. Our results together with those previously found with HCoV-NL63 subcellular localization (Zuwała et al., 2015) indicate that within the N protein there likely exists multiple putative protein trafficking signal sequences.

The HCoV-NL63 Membrane protein is a triple-membrane spanning 226AA protein. M is the director of CoV virion assembly, crucial when studying viral assembly. Here we have optimised M expression in a baculovirus system, which is a system commonly used for generating virus-like particles (VLPs) in research and therapeutics (Aucoin et al., 2007; Krammer et al., 2010; Meghrouf et al., 2005; Mena & Kamen, 2011; Thompson et al., 2016). Recombinant baculoviruses encoding full length M were purified, amplified and titred. *Sf9* (*Spodoptera frugiperda*) cells were infected with different concentrations of virus and it was determined that HCoV-NL63 M protein was expressed from 48 to 72 hours post-infection (PI). This is consistent with our recombinant protein being expressed during very late stage baculovirus-infection, and also with the optimal expression time for NL63 M found previously in *HF* (High Five, *Trichoplusia ni*, ATCC:CRL-7701) insect cells by (Naskalska et al., 2018).

Scientists deconstruct viruses into their subunits in order to better understand viral replication and pathogenesis. Protein subunits provide a platform to evaluate viruses in non-infectious forms, with molecular biology and viral proteomics allowing for broader access to virology research worldwide. Studying CoV structural proteins has helped us better understand virus-neutralising targets, elucidate conserved CoV protein/enzyme targets, and characterize viral protein interactions and virus-host protein interactions. These types of studies help reveal the multifunctional roles of individual proteins in the complex virus life cycle and, importantly, how the host immune response is impacted by various viral components.

HCoV-NL63 is an endemic HCoV which exhibits a high seroprevalence in the global population and has been associated with respiratory disease ranging from asymptomatic infections to severe acute illness. Fatalities associated with HCoV-NL63 infection have been reported (Mayer et al., 2016)(Oosterhof et al., 2010). Endemic HCoVs are important in the current context of the global SARS-CoV-2/Covid-19 pandemic. At present there is some evidence for a link between the immune response to endemic HCoVs and cross-protection against novel SARS-CoV-2 (Loos et al., 2020; Ma et al., 2020; Raoult et al., 2020). The epidemiological data on seasonal HCoVs may be invaluable tools in the increased research efforts towards understanding CoVs and how they impact the global human population. Individuals with an immune response or immune memory to endemic HCoVs are in theory ubiquitous, offering us the most robust data on the CoV immune response in humans. It has been speculated that

the novel SARS-CoV-2 may adopt a seasonal infection pattern, similar to the 4 endemic HCoVs (Audi et al., 2020; Neher et al., 2020; Shaman & Galanti, 2020). Epidemiology and evolutionary mutational studies on endemic HCoVs may give us an idea of what could be expected from SARS-CoV-2 within the global population in the future. Prior to the 2002/03 SARS-CoV outbreak, CoVs were not considered a significant threat to human health. However, CoVs have always been medically relevant in the context of animal health and much of what is known about CoVs has been learned through veterinary virology. Animal CoVs cause severe disease in a wide range of hosts including poultry, livestock and domestic animals (Lai & Holmes, 2001; Vijgen et al., 2005). Among the 7 human CoVs identified to date, SARS-CoV, MERS-CoV and SARS-CoV-2 stand out as highly pathogenic causal agents in recent human epidemics and pandemics. Other human CoVs are known to cause milder respiratory symptoms. The global disease burden of these endemic HCoVs is unknown, as many infections are subclinical, but nevertheless these lower pathogenic viruses have demonstrated the ability of CoVs to persist within a population (Zlateva et al., 2013). *Alphacoronavirus* HCoV-NL63 shares a host receptor with highly-pathogenic *betacoronaviruses* SARS-CoV and SARS-CoV-2 (Hofmann et al., 2005; Li et al., 2003; Shang et al., 2020). Virulence is not high and HCoV-NL63 infection generally occurs with milder symptoms, although it is able to cause both upper and lower respiratory tract infections. While there have been reports of fatal cases in immunocompromised patients, this virus is also capable of causing severe pneumonia and bronchitis in otherwise healthy individuals (Mayer et al., 2016; Oosterhof et al., 2010; Wang, Y. et al., 2020). HCoV-NL63 remains a clinically-important human pathogen with a seemingly dynamic pathogenesis. HCoV-NL63 exposure and infection is fairly common during early life (before 10yrs of age) and the virus persists in the population, causing seasonal infections (Raoult et al., 2020). Evidence suggests that HCoV-NL63 has been infecting humans for almost 1000 years, and a recent study has shown that different sub-genotypes of this virus exist in the population, showcasing the mutational adaptability of this endemic HCoV to maintain viral fitness in the environment (Wang, Y. et al., 2020).

Considering the broad range of mammalian host species susceptible to CoV infection (potential animal reservoirs), the persistent nature of circulating CoVs in the environment, as well as the adaptation propensity for this family of viruses, the emergence of novel HCoVs from animal reservoirs/sources may be inevitable, and it is important that we learn as much as we can about all known HCoVs. Various anti-CoV compounds have shown efficacy *in vitro* and *in vivo*. Since the start of the covid-19 pandemic, there have been close to 200 anti-SARS-CoV-2 vaccines in different stages of development and clinical trials (Krammer, 2020). Currently, 58 vaccine formulations are in some stage of human clinical trials, and 3 have been approved for use. Many countries including Britain, India, Russia and the United States of America (USA) have already begun immunising citizens with a chosen SARS-CoV-2 vaccine (Corum et al., 2020). Attempts at vaccines have focused mainly on protective immunity (antibodies), and various

vaccine platforms have targeted antigenic regions within the CoV Spike protein - mainly the variable RBD and associated regions of the SARS-CoV-, MERS-CoV- and SARS-CoV-2 S proteins (Kim et al., 2014; Malczyk et al., 2015; Polack et al., 2020; ter Meulen et al., 2004; Tian et al., 2020; Traggiati et al., 2004; Voysey et al., 2021; Widge et al., 2020). Use of these non-conserved viral targets may render anti-CoV vaccines more specific, limiting the cross-species protection and broad-anti CoV activity, which is required from a CoV vaccine. HCoV antiviral research may be better directed towards developing a pan-CoV inhibitor, targeting a common instead of species-specific trait, such as a virally-encoded protease that is necessary for CoV replication (Kim et al., 2016; Rathnayake et al., 2020; Zhou et al., 2015). While this type of anti-CoV approach may serve as a post-infection treatment option, it could potentially be very useful during future CoV outbreaks to prevent virus transmission and bring an end to novel outbreaks. The sudden occurrence of these zoonotic pathogens in our population, the high rate of mutation and the relatively short time-span of an outbreak are all factors that make a targeted vaccine development very challenging. SARS-CoV-2 has and continues to have a massive impact on the global human population, across all economic, health and social sectors (Cohen, 2020; Donthu & Gustafsson, 2020; Haleem et al., 2020; Hiscott et al., 2020; Javed et al., 2020; Lenzen et al., 2020; Li, H. et al., 2020). The emergence of another highly pathogenic HCoV not even 20 years since the last SARS-CoV epidemic highlights the need for a HCoV vaccine, and this pandemic has caused a global upsurge in CoV research (Lammers et al., 2020; Thelwall, 2020; Wiersinga et al., 2020; Zhou et al.). While future zoonotic transmission or spillover events may be unavoidable, good healthcare intervention practices together with a pan-CoV antiviral agent to reduce viral load affected populations as well as to halt further virus spread, we should be able to manage and minimize future CoV zoonotic threats. There is now a greater-than-ever-before need for research into the epidemiology of HCoVs as well as their zoonotic origins, so we may learn and develop possible ways of reducing the chances of animal to human transmission in global practices.

Summary and future perspectives

- Expression of *HCoV-NL63 Membrane (M)* and *Nucleocapsid (N)* proteins has been characterised. A bacterial and mammalian expression vector/cell system has been optimised to allow for further evaluation of these expressed viral proteins *in vitro*.
- Polyclonal and monoclonal antibodies specific to *HCoV-NL63* major structural subunits *M* and *N* were generated for the first time in a mouse model. Antibodies were able to specifically bind full length protein antigens and were used to characterize *Membrane* and *Nucleocapsid* protein expression in pro- and eu-karyotic cell systems.
- Full length *HCoV-NL63 M* and *N* were successfully co-expressed in a mammalian cell system. In our system there is a stable interaction exhibited between these 2 structural proteins after 24 hours of co-expression.
- The subcellular localization pattern of *HCoV-NL63 N* protein was examined during protein synthesis and maturation in a mammalian host cell. *HCoV-NL63 N* exhibited no nuclear-cytoplasmic shuttling.
- A recombinant baculovirus has been generated that encodes *HCoV-NL63 M*. Expression of full length *M* was assayed in infected insect cells. Preliminary SDS-PAGE expression results indicate the presence of *M* at 48-72 hours post-infection.

Myself and other laboratory colleagues are currently working on cloning and expressing the necessary structural proteins for the generation of HCoV-NL63 virus-like particles (VLPs). Each of these proteins will be cloned in multiple systems so that we may optimise the expression of non-infectious VLPs in both our mammalian and insect *in vitro* systems. Furthermore under the larger umbrella project we aim to develop and optimise *in vitro* expression systems for the expression/characterization of the structural proteins of HCoV-NL63. For a variety of analyses, full length and truncated forms of the M, E and N core CoV proteins will be expressed across different species including bacterial, insect and mammalian cells. In our attempt to enrich the body of information available on this distinct HCoV and its protein subunit functionality, we intend to examine the expression, localisation patterns and protein-protein interactions of native-like HCoV-NL63 proteins.

Hybridoma-secreted monoclonal anti-M and anti-N antibodies must be purified and re-tested across different experimental platforms/methods, including Immunofluorescence (IF), co-immunoprecipitation (Co-IP) and western blotting. If functional for IF, the antibodies can be used in protein localisation studies (*Cos7* and *Sf9* cells) as well as structural virus studies like HCoV-NL63 VLP generation in a mammalian *in vitro* system. Immunoprecipitation of M and N using anti-N and anti-M antibodies together with anti-FLAG and anti-HA probes under non-denaturing conditions (Native-PAGE), over the

same time course, could reveal if transient, non-stable interactions occur between the co-expressed structural CoV proteins. Improved visualisation of the HCoV-NL63 M glycoprotein in polyacrylamide gel may be achieved by enrichment staining such as silver staining or periodic acid shift (PAS) staining. Our expression and co-expression studies serve as the first set of experiments towards evaluating HCoV-NL63 M and N protein interactions in a higher eukaryotic system.



References

- Abbott, W. M., Damschroder, M. M., & Lowe, D. C. (2014). Current approaches to fine mapping of antigen-antibody interactions. *Immunology*, 142(4), 526-535. doi: 10.1111/imm.12284
- Abdul-Rasool, S., & Fielding, B. C. (2010). Understanding Human Coronavirus HCoV-NL63. *The Open Virology Journal*, 4, 76-84. doi: 10.2174/1874357901004010076
- Abduljalil, J. M., & Abduljalil, B. M. (2020). Epidemiology, genome, and clinical features of the pandemic SARS-CoV-2: a recent view. *New Microbes and New Infections*, 35, 100672. doi: <https://doi.org/10.1016/j.nmni.2020.100672>
- Abe, Y., Takashita, E., Sugawara, K., Matsuzaki, Y., Muraki, Y., & Hongo, S. (2004). Effect of the addition of oligosaccharides on the biological activities and antigenicity of influenza A/H3N2 virus hemagglutinin. *Journal of Virology*, 78(18), 9605-9611. doi: 10.1128/jvi.78.18.9605-9611.2004
- Adams, M. J., & Carstens, E. B. (2012). Ratification vote on taxonomic proposals to the International Committee on Taxonomy of Viruses (2012). *Archives of Virology*, 157(7), 1411-1422. doi: 10.1007/s00705-012-1299-6
- Afrasiabi, S., Pourhajibagher, M., Raoofian, R., Tabarzad, M., & Bahador, A. (2020). Therapeutic applications of nucleic acid aptamers in microbial infections. *Journal of Biomedical Science*, 27(1), 6. doi: 10.1186/s12929-019-0611-0
- Ahangarzadeh, S., Payandeh, Z., Arezumand, R., Shahzamani, K., Yarian, F., & Alibakhshi, A. (2020). An update on antiviral antibody-based biopharmaceuticals. *International Immunopharmacology*, 86, 106760-106760. doi: 10.1016/j.intimp.2020.106760
- Airenne, K. J., Peltomaa, E., Hytönen, V. P., Laitinen, O. H., & Ylä-Herttuala, S. (2003). Improved generation of recombinant baculovirus genomes in *Escherichia coli*. *Nucleic Acids Research*, 31(17), e101-e101.
- Al-Amri, S. S., & Hashem, A. M. (2020). *Qualitative and Quantitative Determination of MERS-CoV S1-Specific Antibodies Using ELISA* (Vol. 2099): Humana, New York, NY.
- Andersen, J. S., Lam, Y. W., Leung, A. K., Ong, S. E., Lyon, C. E., Lamond, A. I., & Mann, M. (2005). Nucleolar proteome dynamics. *Nature*, 433(7021), 77-83. doi: 10.1038/nature03207
- Anderson, E. J., Roupael, N. G., Widge, A. T., Jackson, L. A., Roberts, P. C., Makhene, M., . . . Pruijssers, A. J. (2020). Safety and immunogenicity of SARS-CoV-2 mRNA-1273 vaccine in older adults. *New England Journal of Medicine*, 383(25), 2427-2438.
- Andréll, J., & Tate, C. G. (2013). Overexpression of membrane proteins in mammalian cells for structural studies. *Molecular Membrane Biology*, 30(1), 52-63. doi: 10.3109/09687688.2012.703703

- Angeletti, R. (1999). Design of useful peptide antigens. *Journal of Biomolecular Techniques: JBT*, 10(1), 2.
- Angelini, M. M., Akhlaghpour, M., Neuman, B. W., & Buchmeier, M. J. (2013). Severe acute respiratory syndrome coronavirus nonstructural proteins 3, 4, and 6 induce double-membrane vesicles. *MBio*, 4(4), e00524-00513. doi: 10.1128/mBio.00524-13
- Antaramian, A., Butanda-Ochoa, A., Vazquez-Martinez, O., Díaz-Muñoz, M., & Vaca, L. (2001). Functional expression of recombinant type 1 ryanodine receptor in insect cells. *Cell Calcium*, 30(1), 9-17.
- Antipova, N. V., Larionova, T. D., Shakhparonov, M. I., & Pavlyukov, M. S. (2020). Establishment of murine hybridoma cells producing antibodies against spike protein of SARS-CoV-2. *International Journal of Molecular Sciences*, 21(23), 9167. doi: 10.1101/2020.08.29.272963
- Apostólico, J. d. S., Lunardelli, V. A. S., Coirada, F. C., Boscardin, S. B., & Rosa, D. S. (2016). Adjuvants: Classification, Modus Operandi, and Licensing. *Journal of Immunology Research*, 2016, 1459394-1459394. doi: 10.1155/2016/1459394
- Arevalo, M. T., Wong, T. M., & Ross, T. M. (2016). Expression and Purification of Virus-like Particles for Vaccination. *Journal of Visualized Experiments : JoVE*(112), 54041. doi: 10.3791/54041
- Arndt, A. L., Larson, B. J., & Hogue, B. G. (2010). A Conserved Domain in the Coronavirus Membrane Protein Tail Is Important for Virus Assembly. *Journal of Virology*, 84(21), 11418-11428. doi: 10.1128/jvi.01131-10
- Aruffo, A. (2002). Transient Expression of Proteins Using COS Cells. *Current Protocols in Molecular Biology*, 60(1), 16.12.11-16.12.17. doi: 10.1002/0471142727.mb1612s60
- Assenberg, R., Wan, P. T., Geisse, S., & Mayr, L. M. (2013). Advances in recombinant protein expression for use in pharmaceutical research. *Current Opinion in Structural Biology*, 23(3), 393-402.
- Aucoin, M. G., Jacob, D., Chahal, P. S., Meghrou, J., Bernier, A., & Kamen, A. A. (2007). Virus-like particle and viral vector production using the baculovirus expression vector system/insect cell system: adeno-associated virus-based products. *Methods in Molecular Biology*, 388, 281-296. doi: 10.1007/978-1-59745-457-5_14
- Audi, A., Allbrahim, M., Kaddoura, M., Hijazi, G., Yassine, H. M., & Zaraket, H. (2020). Seasonality of Respiratory Viral Infections: Will COVID-19 Follow Suit? *Frontiers in Public Health*, 8(576). doi: 10.3389/fpubh.2020.567184
- Autry, J. M., & Jones, L. R. (1998). High-Level Coexpression of the Canine Cardiac Calcium Pump and Phospholamban in Sf21 Insect Cells. *Annals of the New York Academy of Sciences*, 853(1), 92-102.

- Baer, A., & Kehn-Hall, K. (2014). Viral concentration determination through plaque assays: using traditional and novel overlay systems. *Journal of Visualized Experiments (JoVE)*(93), e52065-e52065. doi: 10.3791/52065
- Bailey-Elkin, B. A., Knaap, R. C., Johnson, G. G., Dalebout, T. J., Ninaber, D. K., van Kasteren, P. B., . . . Mark, B. L. (2014). Crystal structure of the Middle East respiratory syndrome coronavirus (MERS-CoV) papain-like protease bound to ubiquitin facilitates targeted disruption of deubiquitinating activity to demonstrate its role in innate immune suppression. *The Journal of Biological Chemistry*, 289(50), 34667-34682. doi: 10.1074/jbc.M114.609644
- Balboni, A., Battilani, M., & Prosperi, S. (2012). The SARS-like coronaviruses: the role of bats and evolutionary relationships with SARS coronavirus. *New Microbiology*, 35(1), 1-16.
- Bárcena, M., Oostergetel, G. T., Bartelink, W., Faas, F. G., Verkleij, A., Rottier, P. J., . . . Bosch, B. J. (2009). Cryo-electron tomography of mouse hepatitis virus: insights into the structure of the coronavirus. *Proceedings of the National Academy of Sciences*, 106(2), 582-587.
- Baric, R. S., Nelson, G. W., Fleming, J. O., Deans, R. J., Keck, J. G., Casteel, N., & Stohlman, S. A. (1988). Interactions between coronavirus nucleocapsid protein and viral RNAs: implications for viral transcription. *Journal of Virology*, 62(11), 4280-4287.
- Baudoux, P., Carrat, C., Besnardeau, L., Charley, B., & Laude, H. (1998). Coronavirus pseudoparticles formed with recombinant M and E proteins induce alpha interferon synthesis by leukocytes. *Journal of Virology*, 72(11), 8636-8643.
- Baum, A., Fulton, B. O., Wloga, E., Copin, R., Pascal, K. E., Russo, V., . . . Kyratsous, C. A. (2020). Antibody cocktail to SARS-CoV-2 spike protein prevents rapid mutational escape seen with individual antibodies. *Science*, 369(6506), 1014-1018. doi: 10.1126/science.abd0831
- Becares, M., Pascual-Iglesias, A., Nogales, A., Sola, I., Enjuanes, L., & Zuniga, S. (2016). Mutagenesis of Coronavirus nsp14 Reveals Its Potential Role in Modulation of the Innate Immune Response. *Journal of Virology*, 90(11), 5399-5414. doi: 10.1128/JVI.03259-15
- Berger, I., Fitzgerald, D. J., & Richmond, T. J. (2004). Baculovirus expression system for heterologous multiprotein complexes. *Nature Biotechnology*, 22(12), 1583-1587.
- Berman, H. M., Battistuz, T., Bhat, T. N., Bluhm, W. F., Bourne, P. E., Burkhardt, K., . . . Jain, S. (2002). The protein data bank. *Acta Crystallographica Section D: Biological Crystallography*, 58(6), 899-907.
- Berrow, N. S., Büssow, K., Coutard, B., Diprose, J., Ekberg, M., Folkers, G., . . . Peleg, Y. (2006). Recombinant protein expression and solubility screening in *Escherichia coli*: a comparative study. *Acta Crystallographica Section D: Biological Crystallography*, 62(10), 1218-1226.

- Berry, M., Manasse, T.-L., Tan, Y.-J., & Fielding, B. C. (2012). Characterisation of human coronavirus-NL63 nucleocapsid protein. *African Journal of Biotechnology*, 11(75), 13962-13968.
- Bhardwaj, K., Guarino, L., & Kao, C. C. (2004). The Severe Acute Respiratory Syndrome Coronavirus Nsp15 Protein Is an Endoribonuclease That Prefers Manganese as a Cofactor. *Journal of Virology*, 78(22), 12218-12224. doi: 10.1128/jvi.78.22.12218-12224.2004
- Biswas, A., Bhattacharjee, U., Chakrabarti, A. K., Tewari, D. N., Banu, H., & Dutta, S. (2020). Emergence of Novel Coronavirus and COVID-19: whether to stay or die out? *Critical Reviews in Microbiology*, 46(2), 182-193. doi: 10.1080/1040841X.2020.1739001
- Blom, N., Gammeltoft, S., & Brunak, S. (1999). Sequence and structure-based prediction of eukaryotic protein phosphorylation sites. *Journal of Molecular Biology*, 294(5), 1351-1362. doi: 10.1006/jmbi.1999.3310
- Bomford, R. (1980). The comparative selectivity of adjuvants for humoral and cell-mediated immunity. I. Effect on the antibody response to bovine serum albumin and sheep red blood cells of Freund's incomplete and complete adjuvants, alhydrogel, Corynebacterium parvum, Bordetella pertussis, muramyl dipeptide and saponin. *Clinical and Experimental Immunology*, 39(2), 426.
- Bos, E. C. W., Luytjes, W., Meulen, H. V. D., Koerten, H. K., & Spaan, W. J. M. (1996). The Production of Recombinant Infectious DI-Particles of a Murine Coronavirus in the Absence of Helper Virus. *Virology*, 218(1), 52-60. doi: https://doi.org/10.1006/viro.1996.0165
- Boscarino, J. A., Logan, H. L., Lacny, J. J., & Gallagher, T. M. (2008). Envelope Protein Palmitoylations Are Crucial for Murine Coronavirus Assembly. *Journal of Virology*, 82(6), 2989-2999. doi: 10.1128/jvi.01906-07
- Bosch, B. J., de Haan, C., Smits, S., & Rottier, P. (2005). Spike protein assembly into the coronavirus: Exploring the limits of its sequence requirements. *Virology*, 334(2), 306-318. doi: 10.1016/j.virol.2005.02.001
- Boulikas, T. (1993). Nuclear localization signals (NLS). *Critical Reviews in Eukaryotic Gene Expression*, 3(3), 193-227.
- Boulikas, T. (1994). Putative nuclear localization signals (NLS) in protein transcription factors. *Journal of Cellular Biochemistry*, 55(1), 32-58.
- Bouvet, M., Debarnot, C., Imbert, I., Selisko, B., Snijder, E. J., Canard, B., & Decroly, E. (2010). In vitro reconstitution of SARS-coronavirus mRNA cap methylation. *Public Library of Science (PLOS) Pathogens*, 6(4), e1000863. doi: 10.1371/journal.ppat.1000863
- Bouvet, M., Imbert, I., Subissi, L., Gluais, L., Canard, B., & Decroly, E. (2012). RNA 3'-end mismatch excision by the severe acute respiratory syndrome coronavirus nonstructural protein

- nsp10/nsp14 exoribonuclease complex. *Proceedings of the National Academy of Sciences of the United States of America (PNAS)*, 109(24), 9372-9377. doi: 10.1073/pnas.1201130109
- Bouvet, M., Lugari, A., Posthuma, C. C., Zevenhoven, J. C., Bernard, S., Betzi, S., . . . Morelli, X. (2014). Coronavirus Nsp10, a critical co-factor for activation of multiple replicative enzymes. *The Journal of Biological Chemistry*, 289(37), 25783-25796. doi: 10.1074/jbc.M114.577353
- Boyle, W. J., Smeal, T., Defize, L. H. K., Angel, P., Woodgett, J. R., Karin, M., & Hunter, T. (1991). Activation of protein kinase C decreases phosphorylation of c-Jun at sites that negatively regulate its DNA-binding activity. *Cell*, 64(3), 573-584. doi: 10.1016/0092-8674(91)90241-P
- Braakman, I., & Van Anken, E. (2000). Folding of viral envelope glycoproteins in the endoplasmic reticulum. *Traffic*, 1(7), 533-539.
- Bretana, N. A., Lu, C.-T., Chiang, C.-Y., Su, M.-G., Huang, K.-Y., Lee, T.-Y., & Weng, S.-L. (2012). Identifying protein phosphorylation sites with kinase substrate specificity on human viruses. *PloS one*, 7(7).
- Brierley, I., Digard, P., & Inglis, S. C. (1989). Characterization of an efficient coronavirus ribosomal frameshifting signal: Requirement for an RNA pseudoknot. *Cell*, 57(4), 537-547. doi: [https://doi.org/10.1016/0092-8674\(89\)90124-4](https://doi.org/10.1016/0092-8674(89)90124-4)
- Brisco, P., Creswell, D., Ekenberg, S., Towne, J., Holmes, D., Hurst, R., . . . Storts, D. (1996). Wizard® Plus SV Minipreps DNA Purification System: The Next Generation in Miniprep Purification. *Promega Notes Magazine*, 59(10).
- Brockway, S. M., Clay, C. T., Lu, X. T., & Denison, M. R. (2003). Characterization of the Expression, Intracellular Localization, and Replication Complex Association of the Putative Mouse Hepatitis Virus RNA-Dependent RNA Polymerase. *Journal of Virology*, 77(19), 10515-10527. doi: 10.1128/jvi.77.19.10515-10527.2003
- Brown, C. W., Sridhara, V., Boutz, D. R., Person, M. D., Marcotte, E. M., Barrick, J. E., & Wilke, C. O. (2017). Large-scale analysis of post-translational modifications in E. coli under glucose-limiting conditions. *BMC Genomics*, 18(1), 1-21.
- Brucz, K., Miknis, Z. J., Schultz, L. W., & Umland, T. C. (2007). Expression, purification and characterization of recombinant severe acute respiratory syndrome coronavirus non-structural protein 1. *Protein Expression and Purification*, 52(2), 249-257. doi: 10.1016/j.pep.2006.11.005
- Burbelo, P. D., Riedo, F. X., Morishima, C., Rawlings, S., Smith, D., Das, S., . . . Cohen, J. I. (2020). Detection of nucleocapsid antibody to SARS-CoV-2 is more sensitive than antibody to spike protein in COVID-19 patients. *MedRxiv, Preprint*.
- Burbelo, P. D., Riedo, F. X., Morishima, C., Rawlings, S., Smith, D., Das, S., . . . Cohen, J. I. (2020). Sensitivity in Detection of Antibodies to Nucleocapsid and Spike Proteins of Severe Acute

- Respiratory Syndrome Coronavirus 2 in Patients With Coronavirus Disease 2019. *The Journal of Infectious Diseases*, 222(2), 206-213. doi: 10.1093/infdis/jiaa273
- Cabeça, T. K., & Bellei, N. (2012). Human coronavirus NL-63 infection in a Brazilian patient suspected of H1N1 2009 influenza infection: description of a fatal case. *J Clin Virol*, 53(1), 82-84. doi: 10.1016/j.jcv.2011.09.006
- Calvo, E., Escors, D., Lopez, J., Gonzalez, J., Alvarez, A., Arza, E., & Enjuanes, L. (2005). Phosphorylation and subcellular localization of transmissible gastroenteritis virus nucleocapsid protein in infected cells. *Journal of General Virology*, 86(8), 2255-2267.
- Canova, M. J., & Molle, V. (2014). Bacterial serine/threonine protein kinases in host-pathogen interactions. *The Journal of Biological Chemistry*, 289(14), 9473-9479. doi: 10.1074/jbc.R113.529917
- Cascella, M., Rajnik, M., Cuomo, A., Dulebohn, S. C., & Di Napoli, R. (2020). Features, evaluation and treatment coronavirus (COVID-19) *Statpearls [internet]*: StatPearls Publishing.
- Casino, P., Rubio, V., & Marina, A. (2009). Structural Insight into Partner Specificity and Phosphoryl Transfer in Two-Component Signal Transduction. *Cell*, 139(2), 325-336. doi: 10.1016/j.cell.2009.08.032
- Castilho, A., Bohorova, N., Grass, J., Bohorov, O., Zeitlin, L., Whaley, K., . . . Steinkellner, H. (2011). Rapid High Yield Production of Different Glycoforms of Ebola Virus Monoclonal Antibody. *PLoS ONE*, 6(10), e26040. doi: 10.1371/journal.pone.0026040
- Cavanagh, D., & Davis, P. J. (1988). Evolution of Avian Coronavirus IBV: Sequence of the Matrix Glycoprotein Gene and Intergenic Region of Several Serotypes. *Journal of General Virology*, 69(3), 621-629. doi: https://doi.org/10.1099/0022-1317-69-3-621
- Chai, S. K., Clavijo, P., Tam, J. P., & Zavala, F. (1992). Immunogenic properties of multiple antigen peptide systems containing defined T and B epitopes. *The Journal of Immunology*, 149(7), 2385-2390.
- Chakraborty, I., & Maity, P. (2020). COVID-19 outbreak: Migration, effects on society, global environment and prevention. *Science of The Total Environment*, 728, 138882. doi: https://doi.org/10.1016/j.scitotenv.2020.138882
- Chan, K., Cheng, V., Woo, P., Lau, S., Poon, L., Guan, Y., . . . Peiris, J. (2005). Serological responses in patients with severe acute respiratory syndrome coronavirus infection and cross-reactivity with human coronaviruses 229E, OC43, and NL63. *Clinical and Diagnostic Laboratory Immunology*, 12(11), 1317-1321.
- Chan, P. K., Liu, E. Y., Leung, D. T., Cheung, J. L., Ma, C., Tam, F. C., . . . Lim, P. L. (2005). Evaluation of a recombinant nucleocapsid protein-based assay for Anti-SARS-CoV IgG detection. *Journal of Medical Virology*, 75(2), 181-184.

- Chang, M.-S., Lu, Y.-T., Ho, S.-T., Wu, C.-C., Wei, T.-Y., Chen, C.-J., . . . Yang, Y.-C. (2004). Antibody detection of SARS-CoV spike and nucleocapsid protein. *Biochemical and Biophysical Research Communications*, 314(4), 931-936. doi: 10.1016/j.bbrc.2003.12.195
- Chang, R.-Y., & Brian, D. A. (1996). cis Requirement for N-specific protein sequence in bovine coronavirus defective interfering RNA replication. *Journal of Virology*, 70(4), 2201-2207.
- Chaplin, D. D. (2010). Overview of the immune response. *The Journal of Allergy and Clinical Immunology*, 125(2 Suppl 2), S3-S23. doi: 10.1016/j.jaci.2009.12.980
- Cheever, F. S., Daniels, J. B., & et al. (1949). A murine virus (JHM) causing disseminated encephalomyelitis with extensive destruction of myelin. *Journal of Experimental Medicine*, 90(3), 181-210. doi: 10.1084/jem.90.3.181
- Chen, C.-J., Sugiyama, K., Kubo, H., Huang, C., & Makino, S. (2004). Murine Coronavirus Nonstructural Protein p28 Arrests Cell Cycle in G0/G1 Phase. *Journal of Virology*, 78(19), 10410-10419. doi: 10.1128/jvi.78.19.10410-10419.2004
- Chen, C.-Y., Chang, C.-k., Chang, Y.-W., Sue, S.-C., Bai, H.-I., Riang, L., . . . Huang, T.-h. (2007). Structure of the SARS coronavirus nucleocapsid protein RNA-binding dimerization domain suggests a mechanism for helical packaging of viral RNA. *Journal of Molecular Biology*, 368(4), 1075-1086.
- Chen, H., Gill, A., Dove, B. K., Emmett, S. R., Kemp, C. F., Ritchie, M. A., . . . Hiscox, J. A. (2005). Mass spectroscopic characterization of the coronavirus infectious bronchitis virus nucleoprotein and elucidation of the role of phosphorylation in RNA binding by using surface plasmon resonance. *Journal of Virology*, 79(2), 1164-1179.
- Chen, H., Wurm, T., Britton, P., Brooks, G., & Hiscox, J. A. (2002). Interaction of the coronavirus nucleoprotein with nucleolar antigens and the host cell. *Journal of virology*, 76(10), 5233-5250. doi: 10.1128/jvi.76.10.5233-5250.2002
- Chen, Y., Cai, H., Pan, J. a., Xiang, N., Tien, P., Ahola, T., & Guo, D. (2009). Functional screen reveals SARS coronavirus nonstructural protein nsp14 as a novel cap N7 methyltransferase. *Proceedings of the National Academy of Sciences of the United States of America (PNAS)*, 106(9), 3484-3489. doi: 10.1073/pnas.0808790106
- Chen, Y., Liu, Q., & Guo, D. (2020). Emerging coronaviruses: Genome structure, replication, and pathogenesis. *Journal of Medical Virology*, 92(4), 418-423. doi: 10.1002/jmv.25681
- Cheng, Y., Wong, R., Soo, Y., Wong, W., Lee, C., Ng, M., . . . Cheng, G. (2005). Use of convalescent plasma therapy in SARS patients in Hong Kong. *European Journal of Clinical Microbiology and Infectious Diseases*, 24(1), 44-46.
- Choe, H., & Farzan, M. (2009). Chapter 7. Tyrosine sulfation of HIV-1 coreceptors and other chemokine receptors. *Methods in Enzymology*, 461, 147-170.

- Chou, P. Y., & Fasman, G. D. (1977). Secondary structural prediction of proteins from their amino acid sequence. *Trends in Biochemical Sciences*, 2(6), 128-131.
- Chou, P. Y., & Fasman, G. D. (1979). Prediction of beta-turns. *Biophysical Journal*, 26(3), 367-383. doi: 10.1016/S0006-3495(79)85259-5
- Ciccarone, V. C., Polayes, D. A., & Luckow, V. A. (1998). Generation of Recombinant Baculovirus DNA in E.coli Using a Baculovirus Shuttle Vector. In U. Reischl (Ed.), *Molecular Diagnosis of Infectious Diseases* (pp. 213-235). Totowa, NJ: Humana Press.
- Cohen, S. (2020). Psychosocial vulnerabilities to upper respiratory infectious illness: Implications for susceptibility to coronavirus disease 2019 (COVID-19). *Perspectives on Psychological Science*, 16(1), 161-174. doi: 10.1177/1745691620942516
- Cokol, M., Nair, R., & Rost, B. (2000). Finding nuclear localization signals. *EMBO Reports*, 1(5), 411-415.
- Coleman, C. M., & Frieman, M. B. (2014). Coronaviruses: important emerging human pathogens. *Journal of Virology*, 88(10), 5209-5212.
- Coligan, J. E., Bierer, B. E., Margulies, D. H., Shevach, E. M., & Strober, W. (2005). *Short protocols in immunology: a compendium of methods from current protocols in immunology*. Hoboken, N.J.: John Wiley & Sons, ©2005.
- Cologna, R., Spagnolo, J. F., & Hogue, B. G. (2000). Identification of nucleocapsid binding sites within coronavirus-defective genomes. *Virology*, 277(2), 235-249. doi: 10.1006/viro.2000.0611
- Compeer, E. B., & Uhl, L. F. K. (2020). Antibody response to SARS-CoV-2 — sustained after all? *Nature Reviews Immunology*, 20(10), 590-590. doi: 10.1038/s41577-020-00423-9
- Compton, S., Rogers, D., Holmes, K., Fertsch, D., Remenick, J., & McGowan, J. (1987). In vitro replication of mouse hepatitis virus strain A59. *Journal of Virology*, 61(6), 1814-1820.
- Cooper, P. (1962). The plaque assay of animal viruses *Advances in virus research* (Vol. 8, pp. 319-378): Elsevier.
- Corman, V. M., Muth, D., Niemeyer, D., & Drosten, C. (2018). Chapter Eight - Hosts and Sources of Endemic Human Coronaviruses. In M. Kielian, T. C. Mettenleiter & M. J. Roossinck (Eds.), *Advances in Virus Research* (Vol. 100, pp. 163-188): Academic Press.
- Cornillez-Ty, C. T., Liao, L., Yates, J. R., Kuhn, P., & Buchmeier, M. J. (2009). Severe Acute Respiratory Syndrome Coronavirus Nonstructural Protein 2 Interacts with a Host Protein Complex Involved in Mitochondrial Biogenesis and Intracellular Signaling. *Journal of Virology*, 83(19), 10314-10318. doi: 10.1128/jvi.00842-09
- Corse, E., & Machamer, C. E. (2000). Infectious Bronchitis Virus E Protein Is Targeted to the Golgi Complex and Directs Release of Virus-Like Particles. *Journal of Virology*, 74(9), 4319-4326.

- Corse, E., & Machamer, C. E. (2003). The cytoplasmic tails of infectious bronchitis virus E and M proteins mediate their interaction. *Virology*, 312(1), 25-34. doi: [https://doi.org/10.1016/S0042-6822\(03\)00175-2](https://doi.org/10.1016/S0042-6822(03)00175-2)
- Corti, D., Passini, N., Lanzavecchia, A., & Zambon, M. (2016). Rapid generation of a human monoclonal antibody to combat Middle East respiratory syndrome. *Journal of Infection and Public Health*, 9(3), 231-235. doi: <https://doi.org/10.1016/j.jiph.2016.04.003>
- Corum, J., Grady, D., Wee, S.-L., & Zimmer, C. (2020). Coronavirus vaccine tracker. Retrieved 10 January 2021 <https://www.nytimes.com/interactive/2020/science/coronavirus-vaccine-tracker.html>
- Coughlin, M. M., Babcook, J., & Prabhakar, B. S. (2009). Human monoclonal antibodies to SARS-coronavirus inhibit infection by different mechanisms. *Virology*, 394(1), 39-46. doi: <https://doi.org/10.1016/j.virol.2009.07.028>
- Coughlin, M. M., & Prabhakar, B. S. (2012). Neutralizing human monoclonal antibodies to severe acute respiratory syndrome coronavirus: target, mechanism of action, and therapeutic potential. *Reviews in Medical Virology*, 22(1), 2-17.
- COVID-19 alert Coronavirus disease. (2020). https://www.google.com/search?ei=tcgBYOenO-6X1fAPu9Wt8Ak&q=covid+19+stats&oq=covid+19+stats&gs_lcp=CgZwc3ktYWIQAzIFCAAQyQMMyBQgAEJIDMgUIABCSAzICCAAYBQgAEJECMgIIADICCAAYAggAMgIIADICCAA6CAqHEBYQHRAeOgoIABCxAXCDARAKUO8NWlgRYLgXaABwAHgAgAH4AogB8weSAQUyLTEuMp_gBAKABAaoBB2d3cy13aXrAAQE&sclient=psy-ab&ved=0ahUKEwin1urGs57uAhXuSxUIHbtqC54Q4dUDCA0&uact=5
- Crawford, K. H., Dingens, A. S., Eguia, R., Wolf, C. R., Wilcox, N., Logue, J. K., . . . Bloom, J. D. (2020). Dynamics of neutralizing antibody titers in the months after SARS-CoV-2 infection. *Journal of Infectious Diseases*, *jiaa618*. doi: 10.1093/infdis/jiaa618
- Cunningham, C. H., & Stuart, H. O. (1947). Cultivation of the virus of infectious bronchitis of chickens in embryonated chicken eggs. *American Journal Veterinary Research*, 8(27), 209-212.
- D'Arienzo, M., & Coniglio, A. (2020). Assessment of the SARS-CoV-2 basic reproduction number, $R(0)$, based on the early phase of COVID-19 outbreak in Italy. *Biosafety and Health*, 2(2), 57-59. doi: 10.1016/j.bsheal.2020.03.004
- Dale, W. E., Textor, J. A., Mercer, R. W., & Simchowitz, L. (1996). Expression and Characterization of the Human Erythrocyte Anion Exchanger in a Baculovirus/Sf-9 Cell System. *Protein Expression and Purification*, 7(1), 1-11. doi: <https://doi.org/10.1006/prep.1996.0001>
- de Haan, C. A., Kuo, L., Masters, P. S., Vennema, H., & Rottier, P. J. (1998). Coronavirus particle assembly: primary structure requirements of the membrane protein. *Journal of Virology*, 72(8), 6838-6850.

- de Haan, C. A., Roestenberg, P., de Wit, M., de Vries, A. A., Nilsson, T., Vennema, H., & Rottier, P. J. (1998). Structural requirements for O-glycosylation of the mouse hepatitis virus membrane protein. *Journal of Biological Chemistry*, 273(45), 29905-29914.
- de Haan, C. A., Smeets, M., Vernooij, F., Vennema, H., & Rottier, P. J. (1999). Mapping of the coronavirus membrane protein domains involved in interaction with the spike protein. *Journal of Virology*, 73(9), 7441-7452.
- de Haan, C. A., Volders, H., Koetzner, C. A., Masters, P. S., & Rottier, P. J. (2002). Coronaviruses maintain viability despite dramatic rearrangements of the strictly conserved genome organization. *Journal of Virology*, 76(24), 12491-12502.
- de Haan, C. A. M., de Wit, M., Kuo, L., Montalto-Morrison, C., Haagmans, B. L., Weiss, S. R., . . . Rottier, P. J. M. (2003). The glycosylation status of the murine hepatitis coronavirus M protein affects the interferogenic capacity of the virus in vitro and its ability to replicate in the liver but not the brain. *Virology*, 312(2), 395-406. doi: [https://doi.org/10.1016/S0042-6822\(03\)00235-6](https://doi.org/10.1016/S0042-6822(03)00235-6)
- de Haan, C. A. M., Vennema, H., & Rottier, P. J. M. (2000). Assembly of the Coronavirus Envelope: Homotypic Interactions between the M Proteins. *Journal of Virology*, 74(11), 4967-4978. doi: 10.1128/jvi.74.11.4967-4978.2000
- De Vries, A. A., Horzinek, M. C., Rottier, P. J., & De Groot, R. J. (1997). The genome organization of the Nidovirales: similarities and differences between arteri-, toro-, and coronaviruses. *Seminars in Virology*, 8(1), 33-47.
- Decroly, E., Debarnot, C., Ferron, F., Bouvet, M., Coutard, B., Imbert, I., . . . Canard, B. (2011). Crystal Structure and Functional Analysis of the SARS-Coronavirus RNA Cap 2'-O-Methyltransferase nsp10/nsp16 Complex. *Public Library of Science (PLoS) Pathogens*, 7(5), e1002059. doi: 10.1371/journal.ppat.1002059
- Diemer, C., Schneider, M., Seebach, J., Quaas, J., Frösner, G., Schätzl, H. M., & Gilch, S. (2008). Cell type-specific cleavage of nucleocapsid protein by effector caspases during SARS coronavirus infection. *Journal of Molecular Biology*, 376(1), 23-34.
- Dijkman, R., Jebbink, M. F., El Idrissi, N. B., Pirc, K., Müller, M. A., Kuijpers, T. W., . . . van der Hoek, L. (2008). Human coronavirus NL63 and 229E seroconversion in children. *Journal of clinical microbiology*, 46(7), 2368-2373.
- Dijkman, R., Jebbink, M. F., Gaunt, E., Rossen, J. W. A., Templeton, K. E., Kuijpers, T. W., & van der Hoek, L. (2012). The dominance of human coronavirus OC43 and NL63 infections in infants. *Journal of Clinical Virology*, 53(2), 135-139. doi: <https://doi.org/10.1016/j.jcv.2011.11.011>
- Dill, K. A. (1985). Theory for the folding and stability of globular proteins. *Biochemistry*, 24(6), 1501-1509.
- Dill, K. A. (1990). Dominant forces in protein folding. *Biochemistry*, 29(31), 7133-7155.

- Dill, K. A., & MacCallum, J. L. (2012). The Protein-Folding Problem, 50 Years On. *Science*, 338(6110), 1042-1046. doi: 10.1126/science.1219021
- Ding, L., Huang, Y., Du, Q., Dong, F., Zhao, X., Zhang, W., . . . Tong, D. (2014). TGEV nucleocapsid protein induces cell cycle arrest and apoptosis through activation of p53 signaling. *Biochemical and Biophysical Research Communications*, 445(2), 497-503.
- Ding, N., Yang, C., Sun, S., Han, L., Ruan, Y., Guo, L., . . . Zhang, J. (2017). Increased glycosylation efficiency of recombinant proteins in *Escherichia coli* by auto-induction. *Biochemical and Biophysical Research Communications*, 485(1), 138-143.
- Donaldson, E. F., Sims, A. C., Graham, R. L., Denison, M. R., & Baric, R. S. (2007). Murine Hepatitis Virus Replicase Protein nsp10 Is a Critical Regulator of Viral RNA Synthesis. *Journal of Virology*, 81(12), 6356-6368. doi: 10.1128/jvi.02805-06
- Dong, E., Du, H., & Gardner, L. (2020). An interactive web-based dashboard to track COVID-19 in real time. *The Lancet Infectious Diseases*, 20(5), 533-534. doi: 10.1016/S1473-3099(20)30120-1
- Donthu, N., & Gustafsson, A. (2020). Effects of COVID-19 on business and research. *Journal of Business Research*, 117, 284-289. doi: <https://doi.org/10.1016/j.jbusres.2020.06.008>
- Doyle, L. P., & Hutchings, L. M. (1946). A transmissible gastroenteritis in pigs. *Journal of the American Veterinary Medical Association*, 108, 257-259.
- Doytchinova, I. A., & Flower, D. R. (2007). VaxiJen: a server for prediction of protective antigens, tumour antigens and subunit vaccines. *BMC Bioinformatics*, 8(1), 4.
- Drosten, C., Preiser, W., Günther, S., Schmitz, H., & Doerr, H. W. (2003). Severe acute respiratory syndrome: identification of the etiological agent. *Trends in Molecular Medicine*, 9(8), 325-327. doi: 10.1016/s1471-4914(03)00133-3
- Duan, G., & Walther, D. (2015). The roles of post-translational modifications in the context of protein interaction networks. *PLoS Computational Biology*, 11(2), e1004049-e1004049. doi: 10.1371/journal.pcbi.1004049
- Dulbecco, R., & Vogt, M. (1953). *Some problems of animal virology as studied by the plaque technique*. Paper presented at the Cold Spring Harbor symposia on quantitative biology.
- Dumont, J., Ewart, D., Mei, B., Estes, S., & Kshirsagar, R. (2016). Human cell lines for biopharmaceutical manufacturing: history, status, and future perspectives. *Critical Reviews in Biotechnology*, 36(6), 1110-1122.
- Dyson, H. J., Wright, P. E., & Scheraga, H. A. (2006). The role of hydrophobic interactions in initiation and propagation of protein folding. *Proceedings of the National Academy of Sciences*, 103(35), 13057-13061. doi: 10.1073/pnas.0605504103

- Eckerle, L. D., Becker, M. M., Halpin, R. A., Li, K., Venter, E., Lu, X., . . . Stockwell, T. B. (2010). Infidelity of SARS-CoV Nsp14-exonuclease mutant virus replication is revealed by complete genome sequencing. *Public Library of Science (PLoS) Pathogens*, *6*(5), e1000896.
- Edridge, A. W. D., Kaczorowska, J., Hoste, A. C. R., Bakker, M., Klein, M., Loens, K., . . . van der Hoek, L. (2020). Seasonal coronavirus protective immunity is short-lasting. *Nature Medicine*, *26*, 1691-1693. doi: 10.1038/s41591-020-1083-1
- Ehl, S., Aichele, P., Ramseier, H., Barchet, W., Hombach, J., Pircher, H., . . . Zinkernagel, R. M. (1998). Antigen persistence and time of T-cell tolerization determine the efficacy of tolerization protocols for prevention of skin graft rejection. *Nature Medicine*, *4*(9), 1015-1019. doi: 10.1038/2001
- Ejemel, M., Li, Q., Hou, S., Schiller, Z. A., Tree, J. A., Wallace, A., . . . Wang, Y. (2020). A cross-reactive human IgA monoclonal antibody blocks SARS-CoV-2 spike-ACE2 interaction. *Nature Communications*, *11*(1), 4198. doi: 10.1038/s41467-020-18058-8
- El-Duah, P., Meyer, B., Sylverken, A., Owusu, M., Gottula, L. T., Yeboah, R., . . . Drosten, C. (2019). Development of a Whole-Virus ELISA for Serological Evaluation of Domestic Livestock as Possible Hosts of Human Coronavirus NL63. *Viruses*, *11*(1), 43. doi: 10.3390/v11010043
- Eleouet, J.-F., Chilmoczyk, S., Besnardeau, L., & Laude, H. (1998). Transmissible gastroenteritis coronavirus induces programmed cell death in infected cells through a caspase-dependent pathway. *Journal of Virology*, *72*(6), 4918-4924.
- Eléouët, J.-F., Slee, E. A., Saurini, F., Castagné, N., Poncet, D., Garrido, C., . . . Martin, S. J. (2000). The viral nucleocapsid protein of transmissible gastroenteritis coronavirus (TGEV) is cleaved by caspase-6 and-7 during TGEV-induced apoptosis. *Journal of Virology*, *74*(9), 3975-3983.
- Elshabrawy, H. A., Coughlin, M. M., Baker, S. C., & Prabhakar, B. S. (2012). Human Monoclonal Antibodies against Highly Conserved HR1 and HR2 Domains of the SARS-CoV Spike Protein Are More Broadly Neutralizing. *PLoS ONE*, *7*(11), e50366. doi: 10.1371/journal.pone.0050366
- Emini, E. A., Hughes, J. V., Perlow, D., & Boger, J. (1985). Induction of hepatitis A virus-neutralizing antibody by a virus-specific synthetic peptide. *Journal of Virology*, *55*(3), 836-839.
- Escors, D., Camafeita, E., Ortego, J., Laude, H., & Enjuanes, L. (2001). Organization of Two Transmissible Gastroenteritis Coronavirus Membrane Protein Topologies within the Virion and Core. *Journal of Virology*, *75*(24), 12228-12240. doi: 10.1128/jvi.75.24.12228-12240.2001
- Escors, D., Ortego, J., & Enjuanes, L. (2001). The Membrane M Protein of the Transmissible Gastroenteritis Coronavirus Binds to the Internal Core through the Carboxy-Terminus. In E. Lavi, S. R. Weiss & S. T. Hingley (Eds.), *The Nidoviruses: Coronaviruses and Arteriviruses* (pp. 589-593). Boston, MA: Springer US.

- Escors, D., Ortego, J., Laude, H., & Enjuanes, L. (2001). The Membrane M Protein Carboxy Terminus Binds to Transmissible Gastroenteritis Coronavirus Core and Contributes to Core Stability. *Journal of Virology*, 75(3), 1312-1324. doi: 10.1128/jvi.75.3.1312-1324.2001
- Fang, S., Xu, L., Huang, M., Qisheng Li, F., & Liu, D. X. (2013). Identification of two ATR-dependent phosphorylation sites on coronavirus nucleocapsid protein with nonessential functions in viral replication and infectivity in cultured cells. *Virology*, 444(1-2), 225-232. doi: 10.1016/j.virol.2013.06.014
- Fang, X., Gao, J., Zheng, H., Li, B., Kong, L., Zhang, Y., . . . Ye, L. (2007). The membrane protein of SARS-CoV suppresses NF- κ B activation. *Journal of Medical Virology*, 79(10), 1431-1439. doi: 10.1002/jmv.20953
- Fang, X., Ye, L., Timani, K. A., Li, S., Zen, Y., Zhao, M., . . . Wu, Z. (2005). Peptide domain involved in the interaction between membrane protein and nucleocapsid protein of SARS-associated coronavirus. *Journal of Biochemistry and Molecular Biology Research*, 38(4), 381-385. doi: 10.5483/bmbrep.2005.38.4.381
- Fehr, A. R., & Perlman, S. (2015). Coronaviruses: An Overview of Their Replication and Pathogenesis. *Methods in Molecular Biology (Clifton, N.J.)*, 1282, 1-23. doi: 10.1007/978-1-4939-2438-7_1
- Fischer, F., Stegen, C. F., Masters, P. S., & Samsonoff, W. A. (1998). Analysis of constructed E gene mutants of mouse hepatitis virus confirms a pivotal role for E protein in coronavirus assembly. *Journal of Virology*, 72(10), 7885-7894.
- Flego, M., Di Bonito, P., Ascione, A., Zamboni, S., Carattoli, A., Grasso, F., . . . Cianfriglia, M. (2005). Generation of human antibody fragments recognizing distinct epitopes of the nucleocapsid (N) SARS-CoV protein using a phage display approach. *BMC Infectious Diseases*, 5(1), 73. doi: 10.1186/1471-2334-5-73
- Folegatti, P. M., Ewer, K. J., Aley, P. K., Angus, B., Becker, S., Belij-Rammerstorfer, S., . . . Yau, Y. (2020). Safety and immunogenicity of the ChAdOx1 nCoV-19 vaccine against SARS-CoV-2: a preliminary report of a phase 1/2, single-blind, randomised controlled trial. *The Lancet*, 396(10249), 467-478. doi: 10.1016/S0140-6736(20)31604-4
- Forthal, D. N. (2014). Functions of Antibodies. *Microbiology Spectrum*, 2(4), 1-17.
- Freund, J. (1947). Some aspects of active immunization. *Annual Review of Microbiology*, 1(1), 291-308.
- Freund, J. (1956). The mode of action of immunologic adjuvants. *Adv Tuberc Res*, 7, 130-148.
- Freund, J., & McDermott, K. (1942). Sensitization to horse serum by means of adjuvants. *Proceedings of the Society for Experimental Biology and Medicine*, 49(4), 548-553.

- Friedman, N., Alter, H., Hindiyeh, M., Mendelson, E., Shemer Avni, Y., & Mandelboim, M. (2018). Human coronavirus infections in Israel: epidemiology, clinical symptoms and summer seasonality of HCoV-HKU1. *Viruses*, *10*(10), 515.
- Frieman, M., Yount, B., Agnihothram, S., Page, C., Donaldson, E., Roberts, A., . . . Baric, R. S. (2012). Molecular determinants of severe acute respiratory syndrome coronavirus pathogenesis and virulence in young and aged mouse models of human disease. *Journal of Virology*, *86*(2), 884-897. doi: 10.1128/JVI.05957-11
- Fukushi, S., Fukuma, A., Kurosu, T., Watanabe, S., Shimojima, M., Shirato, K., . . . Saijo, M. (2018). Characterization of novel monoclonal antibodies against the MERS-coronavirus spike protein and their application in species-independent antibody detection by competitive ELISA. *Journal of Virological Methods*, *251*, 22-29. doi: <https://doi.org/10.1016/j.jviromet.2017.10.008>
- Fulton, A., Lai, H., Chen, Q., & Zhang, C. (2015). Purification of monoclonal antibody against Ebola GP1 protein expressed in *Nicotiana benthamiana*. *Journal of Chromatography A*, *1389*, 128-132. doi: <https://doi.org/10.1016/j.chroma.2015.02.013>
- Fung, T. S., Liao, Y., & Liu, D. X. (2014). The endoplasmic reticulum stress sensor IRE1 α protects cells from apoptosis induced by the coronavirus infectious bronchitis virus. *Journal of Virology*, *88*(21), 12752-12764.
- Fung, T. S., & Liu, D. X. (2018). Post-translational modifications of coronavirus proteins: roles and function. *Future Virology*, *13*(6), 405-430. doi: 10.2217/fvl-2018-0008
- Gaglia, M. M., Covarrubias, S., Wong, W., & Glaunsinger, B. A. (2012). A common strategy for host RNA degradation by divergent viruses. *Journal of Virology*, *86*(17), 9527-9530.
- Galanti, M., & Shaman, J. (2020). Direct Observation of Repeated Infections With Endemic Coronaviruses. *The Journal of Infectious Diseases*. doi: 10.1093/infdis/jiaa392
- Gannon, J. V., Greaves, R., Iggo, R., & Lane, D. P. (1990). Activating mutations in p53 produce a common conformational effect. A monoclonal antibody specific for the mutant form. *The EMBO Journal*, *9*(5), 1595-1602. doi: 10.1002/j.1460-2075.1990.tb08279.x
- Gao, R., & Stock, A. M. (2010). Molecular strategies for phosphorylation-mediated regulation of response regulator activity. *Current Opinion in Microbiology*, *13*(2), 160-167. doi: 10.1016/j.mib.2009.12.009
- Gao, X., Zhou, H., Wu, C., Xiao, Y., Ren, L., Paranhos-Baccala, G., . . . Wang, J. (2015). Antibody against nucleocapsid protein predicts susceptibility to human coronavirus infection. *J Infect*, *71*(5), 599-602. doi: 10.1016/j.jinf.2015.07.002
- Gao, X., Zhou, H., Wu, C., Xiao, Y., Ren, L., Paranhos-Baccalà, G., . . . Wang, J. (2015). Antibody against nucleocapsid protein predicts susceptibility to human coronavirus infection. *The Journal of Infection*, *71*(5), 599-602. doi: 10.1016/j.jinf.2015.07.002

- Gaunt, E. R., Hardie, A., Claas, E. C., Simmonds, P., & Templeton, K. E. (2010). Epidemiology and clinical presentations of the four human coronaviruses 229E, HKU1, NL63, and OC43 detected over 3 years using a novel multiplex real-time PCR method. *Journal of Clinical Microbiology*, 48(8), 2940-2947.
- Geisse, S., & Henke, M. (2005). Large-scale transient transfection of mammalian cells: a newly emerging attractive option for recombinant protein production. *Journal of Structural and Functional Genomics*, 6(2-3), 165-170.
- Gharakhanian, E., Takahashi, J., & Kasamatsu, H. (1987). The carboxyl 35 amino acids of SV40 Vp3 are essential for its nuclear accumulation. *Virology*, 157(2), 440-448. doi: 10.1016/0042-6822(87)90286-8
- Gluzman, Y. (1981). SV40-transformed simian cells support the replication of early SV40 mutants. *Cell*, 23(1), 175-182.
- Goldsby, R., Kindt, T., & Osborne, B. (2000). Kuby Immunology 4th Edition. W. H: Freeman and Company, New York.
- Goo, J., Jeong, Y., Park, Y.-S., Yang, E., Jung, D.-I., Rho, S., . . . Song, M. (2020). Characterization of novel monoclonal antibodies against MERS-coronavirus spike protein. *Virus Research*, 278, 197863. doi: 10.1016/j.virusres.2020.197863
- Gorbalenya, A. E. (2001). Big Nidovirus Genome. In E. Lavi, S. R. Weiss & S. T. Hingley (Eds.), *The Nidoviruses: Coronaviruses and Arteriviruses* (pp. 1-17). Boston, MA: Springer US.
- Gorbalenya, A. E., Enjuanes, L., Ziebuhr, J., & Snijder, E. J. (2006). Nidovirales: evolving the largest RNA virus genome. *Virus Research*, 117(1), 17-37.
- Gorbalenya, A. E., Koonin, E. V., Donchenko, A. P., & Blinov, V. M. (1989). Coronavirus genome: prediction of putative functional domains in the non-structural polyprotein by comparative amino acid sequence analysis. *Nucleic Acids Research*, 17(12), 4847-4861.
- Goto, N., & Akama, K. (1982). Histopathological studies of reactions in mice injected with aluminum-adsorbed tetanus toxoid. *Microbiology and Immunology*, 26(12), 1121-1132.
- Graves, J. D., & Krebs, E. G. (1999). Protein Phosphorylation and Signal Transduction. *Pharmacology & Therapeutics*, 82(2), 111-121. doi: [https://doi.org/10.1016/S0163-7258\(98\)00056-4](https://doi.org/10.1016/S0163-7258(98)00056-4)
- Gray, D. (2001). Overview of protein expression by mammalian cells. *Current Protocols in Protein Science*, 10(1), 591-5918. doi: 10.1002/0471140864.ps0509s10
- Gray, P., Dunne, A., Brikos, C., Jefferies, C., Doyle, S., & O'Neill, L. (2016). MyD88 adapter-like (Mal) is phosphorylated by Bruton's tyrosine kinase during TLR2 and TLR4 signal transduction. *Journal of Biological Chemistry*, 281(15), 10489-10495. doi: 10.1074/jbc.M508892200

- Grifoni, A., Weiskopf, D., Ramirez, S. I., Mateus, J., Dan, J. M., Moderbacher, C. R., . . . Jadi, R. S. (2020). Targets of T cell responses to SARS-CoV-2 coronavirus in humans with COVID-19 disease and unexposed individuals. *Cell*, *181*(7), 1489-1501.
- Grisshammer, R., & Tateu, C. (1995). Overexpression of integral membrane proteins for structural studies. *Quarterly Reviews of Biophysics*, *28*(3), 315-422.
- Groban, E. S., Narayanan, A., & Jacobson, M. P. (2006). Conformational changes in protein loops and helices induced by post-translational phosphorylation. *PLoS Computational Biology*, *2*(4), e32-e32. doi: 10.1371/journal.pcbi.0020032
- Gross, V., Andus, T., Castell, J., Vom Berg, D., Heinrich, P. C., & Gerok, W. (1989). O- and N-glycosylation lead to different molecular mass forms of human monocyte interleukin-6. *FEBS Letters*, *247*(2), 323-326. doi: 10.1016/0014-5793(89)81361-4
- Gruenke, J. A., Armstrong, R. T., Newcomb, W. W., Brown, J. C., & White, J. M. (2002). New insights into the spring-loaded conformational change of influenza virus hemagglutinin. *Journal of Virology*, *76*(9), 4456-4466. doi: 10.1128/jvi.76.9.4456-4466.2002
- Grunewald, M. E., Fehr, A. R., Athmer, J., & Perlman, S. (2018). The coronavirus nucleocapsid protein is ADP-ribosylated. *Virology*, *517*, 62-68.
- Gupta, R., Jung, E., & Brunak, S. (2004). Prediction of N-glycosylation sites in human proteins. Retrieved 10 April 2020, from <http://www.cbs.dtu.dk/services/NetNGlyc/>
- Habjan, M., Hubel, P., Lacerda, L., Benda, C., Holze, C., Eberl, C. H., . . . Ziebuhr, J. (2013). Sequestration by IFIT1 impairs translation of 2' O-unmethylated capped RNA. *Public Library of Science (PLoS) Pathogens*, *9*(10), e1003663.
- Hagemeijer, M. C., & de Haan, C. A. (2015). Studying the dynamics of coronavirus replicative structures. *Methods in Molecular Biology*, *1282*, 261-269. doi: 10.1007/978-1-4939-2438-7_22
- Hagemeijer, M. C., Ulasli, M., Vonk, A. M., Reggiori, F., Rottier, P. J., & de Haan, C. A. (2011). Mobility and interactions of coronavirus nonstructural protein 4. *Journal of Virology*, *85*(9), 4572-4577. doi: 10.1128/JVI.00042-11
- Haleem, A., Javaid, M., & Vaishya, R. (2020). Effects of COVID-19 pandemic in daily life. *Current Medicine Research and Practice*, *10*(2), 78-79. doi: 10.1016/j.cmrp.2020.03.011
- Hamre, D., & Procknow, J. J. (1966). A new virus isolated from the human respiratory tract. *Proceedings of the Society for Experimental Biology and Medicine*, *121*(1), 190-193.
- Hanly, W. C., Artwohl, J. E., & Bennett, B. T. (1995). Review of polyclonal antibody production procedures in mammals and poultry. *ILAR Journal*, *37*(3), 93-118.
- Hansen, J., Baum, A., Pascal, K. E., Russo, V., Giordano, S., Wloga, E., . . . Kyriatsous, C. A. (2020). Studies in humanized mice and convalescent humans yield a SARS-CoV-2 antibody cocktail. *Science*, *369*(6506), 1010-1014. doi: 10.1126/science.abd0827

- Hansen, P. R. (2015). Peptide-Carrier Conjugation. *Methods in Molecular Biology (Clifton, N.J.)*, 1348, 51-57. doi: 10.1007/978-1-4939-2999-3_6
- Harrison, S. M., Dove, B. K., Rothwell, L., Kaiser, P., Tarpey, I., Brooks, G., & Hiscox, J. A. (2007). Characterisation of cyclin D1 down-regulation in coronavirus infected cells. *FEBS Letters*, 581(7), 1275-1286.
- Harvala, H., Mehew, J., Robb, M. L., Ijaz, S., Dicks, S., Patel, M., . . . Transplant Convalescent Plasma Testing, G. (2020). Convalescent plasma treatment for SARS-CoV-2 infection: analysis of the first 436 donors in England, 22 April to 12 May 2020. *Euro Surveillance : bulletin Europeen sur les maladies transmissibles = European Communicable Disease Bulletin*, 25(28), 2001260. doi: 10.2807/1560-7917.ES.2020.25.28.2001260
- Hazelbauer, G. L., & Lai, W.-C. (2010). Bacterial chemoreceptors: providing enhanced features to two-component signaling. *Current Opinion in Microbiology*, 13(2), 124-132. doi: 10.1016/j.mib.2009.12.014
- He, Q., Du, Q., Lau, S., Manopo, I., Lu, L., Chan, S.-W., . . . Kwang, J. (2005). Characterization of monoclonal antibody against SARS coronavirus nucleocapsid antigen and development of an antigen capture ELISA. *Journal of Virological Methods*, 127(1), 46-53. doi: <https://doi.org/10.1016/j.jviromet.2005.03.004>
- He, R., Dobie, F., Ballantine, M., Leeson, A., Li, Y., Bastien, N., . . . Li, X. (2004). Analysis of multimerization of the SARS coronavirus nucleocapsid protein. *Biochemical and Biophysical Research Communications*, 316(2), 476-483. doi: 10.1016/j.bbrc.2004.02.074
- He, R., Leeson, A., Ballantine, M., Andonov, A., Baker, L., Dobie, F., . . . Li, X. (2004). Characterization of protein-protein interactions between the nucleocapsid protein and membrane protein of the SARS coronavirus. *Virus Research*, 105(2), 121-125. doi: <https://doi.org/10.1016/j.virusres.2004.05.002>
- He, Y., Lu, H., Siddiqui, P., Zhou, Y., & Jiang, S. (2005). Receptor-Binding Domain of Severe Acute Respiratory Syndrome Coronavirus Spike Protein Contains Multiple Conformation-Dependent Epitopes that Induce Highly Potent Neutralizing Antibodies. *The Journal of Immunology*, 174(8), 4908-4915. doi: 10.4049/jimmunol.174.8.4908
- He, Y., Zhou, Y., Siddiqui, P., Niu, J., & Jiang, S. (2005). Identification of immunodominant epitopes on the membrane protein of the severe acute respiratory syndrome-associated coronavirus. *Journal of Clinical Microbiology*, 43(8), 3718-3726.
- Hendricksen, C., & Hau, J. (2003). *Production of polyclonal and monoclonal antibodies* (Vol. 1).
- Hicks, J., Klumpp-Thomas, C., Kalish, H., Shunmugavel, A., Mehalko, J., Denson, J.-P., . . . Sadtler, K. (2020). Serologic cross-reactivity of SARS-CoV-2 with endemic and seasonal

- Betacoronaviruses. *MedRxiv : The Preprint Server for Health Sciences*, 2020.2006.2022.20137695. doi: 10.1101/2020.06.22.20137695
- Hiscott, J., Alexandridi, M., Muscolini, M., Tassone, E., Palermo, E., Soultsioti, M., & Zevini, A. (2020). The global impact of the coronavirus pandemic. *Cytokine & Growth Factor Reviews*, 53, 1-9. doi: 10.1016/j.cytogfr.2020.05.010
- Hiscox, J. A., Cavanagh, D., & Britton, P. (1995). Quantification of individual subgenomic mRNA species during replication of the coronavirus transmissible gastroenteritis virus. *Virus Research*, 36(2-3), 119-130.
- Hiscox, J. A., Wurm, T., Wilson, L., Britton, P., Cavanagh, D., & Brooks, G. (2001). The coronavirus infectious bronchitis virus nucleoprotein localizes to the nucleolus. *Journal of Virology*, 75(1), 506-512.
- Hitchman, R., Possee, R., & King, L. (2009). Baculovirus Expression Systems for Recombinant Protein Production in Insect Cells. *Recent Patents on Biotechnology*, 3(1), 46-54. doi: 10.2174/187220809787172669
- Hofmann, H., Pyrc, K., van der Hoek, L., Geier, M., Berkhout, B., & Pöhlmann, S. (2005). Human coronavirus NL63 employs the severe acute respiratory syndrome coronavirus receptor for cellular entry. *Proc Natl Acad Sci U S A*, 102(22), 7988-7993. doi: 10.1073/pnas.0409465102
- Hogue, B. G. (1995). Bovine coronavirus nucleocapsid protein processing and assembly. *Advances in Experimental Medicine and Biology*, 380, 259-263. doi: 10.1007/978-1-4615-1899-0_41
- Holmes, K. (2001). *Coronaviruses, vol. 1*: Lippincott Williams and Wilkins, Philadelphia, PA.
- Hoover, H., & Kao, C. C. (2016). Phosphorylation of the viral coat protein regulates RNA virus infection. *Virus Adaptation and Treatment*, 8, 13-20. doi: 10.2147/VAAT.S118440
- Hoover, H. S., Wang, J. C., Middleton, S., Ni, P., Zlotnick, A., Vaughan, R. C., & Kao, C. C. (2016). Phosphorylation of the Brome Mosaic Virus Capsid Regulates the Timing of Viral Infection. *Journal of Virology*, 90(17), 7748-7760. doi: 10.1128/jvi.00833-16
- Hopp, T. P., Prickett, K. S., Price, V. L., Libby, R. T., March, C. J., Cerretti, D. P., . . . Conlon, P. J. (1988). A short polypeptide marker sequence useful for recombinant protein identification and purification. *Biotechnology*, 6(10), 1204-1210.
- Horthongkham, N., Srihtrakul, T., Athipanyasilp, N., Siritantikorn, S., Kantakamalakul, W., Poovorawan, Y., & Sutthent, R. (2007). Specific antibody response of mice after immunization with COS-7 cell derived avian influenza virus (H5N1) recombinant proteins. *Journal of Immune Based Therapies and Vaccines*, 5(1), 10. doi: 10.1186/1476-8518-5-10
- Hsin, W.-C., Chang, C.-H., Chang, C.-Y., Peng, W.-H., Chien, C.-L., Chang, M.-F., & Chang, S. C. (2018). Nucleocapsid protein-dependent assembly of the RNA packaging signal of Middle East

- respiratory syndrome coronavirus. *Journal of Biomedical Science*, 25(1), 47. doi: 10.1186/s12929-018-0449-x
- Hu, Y., Wen, J., Tang, L., Zhang, H., Zhang, X., Li, Y., . . . Shi, J. (2003). The M protein of SARS-CoV: basic structural and immunological properties. *Genomics, Proteomics & Bioinformatics*, 1(2), 118-130.
- Huan, C.-c., Wang, Y., Ni, B., Wang, R., Huang, L., Ren, X.-f., . . . Mao, X. (2015). Porcine epidemic diarrhea virus uses cell-surface heparan sulfate as an attachment factor. *Archives of Virology*, 160(7), 1621-1628. doi: 10.1007/s00705-015-2408-0
- Huang, A. T., Garcia-Carreras, B., Hitchings, M. D. T., Yang, B., Katzelnick, L. C., Rattigan, S. M., . . . Cummings, D. A. T. (2020). A systematic review of antibody mediated immunity to coronaviruses: kinetics, correlates of protection, and association with severity. *Nature Communications*, 11(1), 4704. doi: 10.1038/s41467-020-18450-4
- Huang, C., Lokugamage, K. G., Rozovics, J. M., Narayanan, K., Semler, B. L., & Makino, S. (2011). SARS coronavirus nsp1 protein induces template-dependent endonucleolytic cleavage of mRNAs: viral mRNAs are resistant to nsp1-induced RNA cleavage. *PLoS Pathogens*, 7(12), e1002433. doi: 10.1371/journal.ppat.1002433
- Huang, C., Wang, Y., Li, X., Ren, L., Zhao, J., Hu, Y., . . . Cao, B. (2020). Clinical features of patients infected with 2019 novel coronavirus in Wuhan, China. *The Lancet*, 395(10223), 497-506. doi: 10.1016/S0140-6736(20)30183-5
- Huang, S.-H., Su, M.-C., Tien, N., Huang, C.-J., Lan, Y.-C., Lin, C.-S., . . . Lin, C.-W. (2017). Epidemiology of human coronavirus NL63 infection among hospitalized patients with pneumonia in Taiwan. *Journal of Microbiology, Immunology and Infection*, 50(6), 763-770.
- Huang, Y.-W., Lu, M.-L., Qi, H., & Lin, S.-X. (2000). Membrane-Bound Human 3 β -Hydroxysteroid Dehydrogenase: Overexpression with His-Tag Using a Baculovirus System and Single-Step Purification. *Protein Expression and Purification*, 18(2), 169-174. doi: <https://doi.org/10.1006/prep.1999.1180>
- Hulswit, R. J. G., Lang, Y., Bakkers, M. J. G., Li, W., Li, Z., Schouten, A., . . . de Groot, R. J. (2019). Human coronaviruses OC43 and HKU1 bind to 9-O-acetylated sialic acids via a conserved receptor-binding site in spike protein domain A. *Proceedings of the National Academy of Sciences*, 116(7), 2681-2690. doi: 10.1073/pnas.1809667116
- Hunter, M. R., Grimsey, N. L., & Glass, M. (2016). Sulfation of the FLAG epitope is affected by co-expression of G protein-coupled receptors in a mammalian cell model. *Scientific Reports*, 6(1), 27316. doi: 10.1038/srep27316
- Hurst, K. R., Koetzner, C. A., & Masters, P. S. (2013). Characterization of a Critical Interaction between the Coronavirus Nucleocapsid Protein and Nonstructural Protein 3 of the Viral

- Replicase-Transcriptase Complex. *Journal of Virology*, 87(16), 9159-9172. doi: 10.1128/jvi.01275-13
- Hurst, K. R., Kuo, L., Koetzner, C. A., Ye, R., Hsue, B., & Masters, P. S. (2005). A Major Determinant for Membrane Protein Interaction Localizes to the Carboxy-Terminal Domain of the Mouse Coronavirus Nucleocapsid Protein. *Journal of Virology*, 79(21), 13285-13297. doi: 10.1128/jvi.79.21.13285-13297.2005
- Hurst, K. R., Ye, R., Goebel, S. J., Jayaraman, P., & Masters, P. S. (2010). An interaction between the nucleocapsid protein and a component of the replicase-transcriptase complex is crucial for the infectivity of coronavirus genomic RNA. *Journal of Virology*, 84(19), 10276-10288. doi: 10.1128/JVI.01287-10
- Huynh, J., Li, S., Yount, B., Smith, A., Sturges, L., Olsen, J. C., . . . Donaldson, E. F. (2012). Evidence supporting a zoonotic origin of human coronavirus strain NL63. *Journal of Virology*, 86(23), 12816-12825. doi: 10.1128/JVI.00906-12
- Ikonomou, L., Schneider, Y.-J., & Agathos, S. (2003). Insect cell culture for industrial production of recombinant proteins. *Applied Microbiology and Biotechnology*, 62(1), 1-20.
- Imbert, I., Guillemot, J.-C., Bourhis, J.-M., Bussetta, C., Coutard, B., Egloff, M.-P., . . . Canard, B. (2006). A second, non-canonical RNA-dependent RNA polymerase in SARS Coronavirus. *The EMBO Journal*, 25(20), 4933-4942. doi: 10.1038/sj.emboj.7601368
- Imbert, I., Snijder, E. J., Dimitrova, M., Guillemot, J.-C., Lécine, P., & Canard, B. (2008). The SARS-Coronavirus PLnc domain of nsp3 as a replication/transcription scaffolding protein. *Virus Research*, 133(2), 136-148. doi: <https://doi.org/10.1016/j.virusres.2007.11.017>
- Immunomedicine Group - Predicting Antigenic Peptides. (2020). Retrieved 13 May 2020, from <http://imed.med.ucm.es/Tools/antigenic.pl>
- Ivanov, K. A., Hertzog, T., Rozanov, M., Bayer, S., Thiel, V., Gorbalenya, A. E., & Ziebuhr, J. (2004). Major genetic marker of nidoviruses encodes a replicative endoribonuclease. *Proceedings of the National Academy of Sciences of the United States of America (PNAS)*, 101(34), 12694-12699. doi: 10.1073/pnas.0403127101
- Ivanov, K. A., Thiel, V., Dobbe, J. C., van der Meer, Y., Snijder, E. J., & Ziebuhr, J. (2004). Multiple Enzymatic Activities Associated with Severe Acute Respiratory Syndrome Coronavirus Helicase. *Journal of Virology*, 78(11), 5619-5632. doi: 10.1128/jvi.78.11.5619-5632.2004
- Ivanov, K. A., & Ziebuhr, J. (2004). Human Coronavirus 229E Nonstructural Protein 13: Characterization of Duplex-Unwinding, Nucleoside Triphosphatase, and RNA 5'-Triphosphatase Activities. *Journal of Virology*, 78(14), 7833-7838. doi: 10.1128/jvi.78.14.7833-7838.2004

- Jacobs, L., van der Zeijst, B. A., & Horzinek, M. C. (1986). Characterization and translation of transmissible gastroenteritis virus mRNAs. *Journal of Virology*, 57(3), 1010-1015.
- Jakubiec, A., & Jupin, I. (2007). Regulation of positive-strand RNA virus replication: The emerging role of phosphorylation. *Virus Research*, 129(2), 73-79. doi: <https://doi.org/10.1016/j.virusres.2007.07.012>
- Janeway, C., Walport, M., & Travers, P. (2001). Immunobiology, Part III, The Development of Mature Lymphocyte Receptor Repertoires *Immunobiology: The Immune System in Health and Disease. 5th edition*: Garland Science, New York.
- Janeway Jr, C. A., Travers, P., Walport, M., & Shlomchik, M. J. (2001). B-cell activation by armed helper T cells *Immunobiology: The Immune System in Health and Disease. 5th edition*: Garland Science.
- Jarvis, D. L. (1997). Baculovirus Expression Vectors. In L. K. Miller (Ed.), *The Baculoviruses. The Viruses*. (pp. 389-431). Boston, MA: Springer US.
- Javed, B., Sarwer, A., Soto, E. B., & Mashwani, Z.-u.-R. (2020). Impact of SARS-CoV-2 (Coronavirus) Pandemic on Public Mental Health. *Frontiers in Public Health*, 8(292). doi: [10.3389/fpubh.2020.00292](https://doi.org/10.3389/fpubh.2020.00292)
- Jayaram, J., Youn, S., & Collisson, E. W. (2005). The virion N protein of infectious bronchitis virus is more phosphorylated than the N protein from infected cell lysates. *Virology*, 339(1), 127-135.
- Jenkins, N., Murphy, L., & Tyther, R. (2008). Post-translational Modifications of Recombinant Proteins: Significance for Biopharmaceuticals. *Molecular Biotechnology*, 39(2), 113-118. doi: [10.1007/s12033-008-9049-4](https://doi.org/10.1007/s12033-008-9049-4)
- Jiang, L., Wang, N., Zuo, T., Shi, X., Poon, K. M., Wu, Y., . . . Zhang, L. (2014). Potent neutralization of MERS-CoV by human neutralizing monoclonal antibodies to the viral spike glycoprotein. *Science Translational Medicine*, 6(234), 234-259. doi: [10.1126/scitranslmed.3008140](https://doi.org/10.1126/scitranslmed.3008140)
- Jin, X., Chen, Y., Sun, Y., Zeng, C., Wang, Y., Tao, J., . . . Guo, D. (2013). Characterization of the guanine-N7 methyltransferase activity of coronavirus nsp14 on nucleotide GTP. *Virus Research*, 176(1-2), 45-52. doi: [10.1016/j.virusres.2013.05.001](https://doi.org/10.1016/j.virusres.2013.05.001)
- Joshi, V. G., Dighe, V. D., Thakuria, D., Malik, Y. S., & Kumar, S. (2013). Multiple antigenic peptide (MAP): a synthetic peptide dendrimer for diagnostic, antiviral and vaccine strategies for emerging and re-emerging viral diseases. *Indian Journal of Virology : an Official Organ of Indian Virological Society*, 24(3), 312-320. doi: [10.1007/s13337-013-0162-z](https://doi.org/10.1007/s13337-013-0162-z)
- Ju, B., Zhang, Q., Ge, J., Wang, R., Sun, J., Ge, X., . . . Zhang, L. (2020). Human neutralizing antibodies elicited by SARS-CoV-2 infection. *Nature*, 584(7819), 115-119. doi: [10.1038/s41586-020-2380-z](https://doi.org/10.1038/s41586-020-2380-z)

- Juan Zhang, D. W., Yue Li, Qing Zhao, Ailong Huang, Jian Zheng, and Weixian Chen. (2011). SARS Coronavirus Nucleocapsid Protein Monoclonal Antibodies Developed Using a Prokaryotic Expressed Protein. *Hybridoma*, 30(5), 481-485. doi: 10.1089/hyb.2011.0028
- Kadaré, G., & Haenni, A. L. (1997). Virus-encoded RNA helicases. *Journal of Virology*, 71(4), 2583-2590.
- Kamitani, W., Huang, C., Narayanan, K., Lokugamage, K. G., & Makino, S. (2009). A two-pronged strategy to suppress host protein synthesis by SARS coronavirus Nsp1 protein. *Nature Structural & Molecular Biology*, 16, 1134. doi: 10.1038/nsmb.1680
- <https://www.nature.com/articles/nsmb.1680#supplementary-information>
- Kamitani, W., Narayanan, K., Huang, C., Lokugamage, K., Ikegami, T., Ito, N., . . . Makino, S. (2006). Severe acute respiratory syndrome coronavirus nsp1 protein suppresses host gene expression by promoting host mRNA degradation. *Proceedings of the National Academy of Sciences (PNAS)*, 103(34), 12885-12890. doi: 10.1073/pnas.0603144103
- Kamtekar, S., Schiffer, J. M., Xiong, H., Babik, J. M., & Hecht, M. H. (1993). Protein design by binary patterning of polar and nonpolar amino acids. *Science*, 262(5140), 1680-1685.
- Kapke, P. A., Tung, F. Y., Hogue, B. G., Brian, D. A., Woods, R. D., & Wesley, R. (1988). The amino-terminal signal peptide on the porcine transmissible gastroenteritis coronavirus matrix protein is not an absolute requirement for membrane translocation and glycosylation. *Virology*, 165(2), 367-376. doi: 10.1016/0042-6822(88)90581-8
- Ke, Z., Oton, J., Qu, K., Cortese, M., Zila, V., McKeane, L., . . . Briggs, J. A. G. (2020). Structures and distributions of SARS-CoV-2 spike proteins on intact virions. *Nature*, 588, 498–502. doi: 10.1038/s41586-020-2665-2
- Keck, F., Ataey, P., Amaya, M., Bailey, C., & Narayanan, A. (2015). Phosphorylation of Single Stranded RNA Virus Proteins and Potential for Novel Therapeutic Strategies. *Viruses*, 7(10), 5257-5273. doi: 10.3390/v7102872
- Khan, T., Rahman, M., Al Ali, F., Huang, S. S. Y., Sayeed, A., Nasrallah, G. K., . . . Marr, N. (2020). Endemic human coronaviruses induce distinct antibody repertoires in adults and children. *BioRxiv*, 2020.2006.2021.163394. doi: 10.1101/2020.06.21.163394
- Kim, E., Okada, K., Kenniston, T., Raj, V. S., AlHajri, M. M., Farag, E. A. B. A., . . . Gambotto, A. (2014). Immunogenicity of an adenoviral-based Middle East Respiratory Syndrome coronavirus vaccine in BALB/c mice. *Vaccine*, 32(45), 5975-5982. doi: <https://doi.org/10.1016/j.vaccine.2014.08.058>
- Kim, P., & Pau, C.-P. (2001). Comparing tandem repeats and multiple antigenic peptides as the antigens to detect antibodies by enzyme immunoassay. *Journal of Immunological Methods*, 257(1-2), 51-54.

- Kim, Y., Liu, H., Galasiti Kankanamalage, A. C., Weerasekara, S., Hua, D. H., Groutas, W. C., . . . Pedersen, N. C. (2016). Reversal of the progression of fatal coronavirus infection in cats by a broad-spectrum coronavirus protease inhibitor. *PLoS Pathogens*, *12*(3), e1005531.
- Kimple, M. E., Brill, A. L., & Pasker, R. L. (2013). Overview of affinity tags for protein purification. *Current Protocols in Protein Science*, *73*, 9.9.1-9.9.23. doi: 10.1002/0471140864.ps0909s73
- Klasse, P. J. (2014). Neutralization of Virus Infectivity by Antibodies: Old Problems in New Perspectives. *Advances in Biology*, *2014*, 157895. doi: 10.1155/2014/157895
- Klebe, R., & Harriss, J. V. (1984). A technically simple “non-lethal” vital staining procedure for viral plaque and cell transformation assays. *Archives of Virology*, *81*(3-4), 359-362.
- Klenk, H. D., Wagner, R., Heuer, D., & Wolff, T. (2002). Importance of hemagglutinin glycosylation for the biological functions of influenza virus. *Virus Research*, *82*(1-2), 73-75. doi: 10.1016/s0168-1702(01)00389-6
- Klumperman, J., Locker, J. K., Meijer, A., Horzinek, M. C., Geuze, H. J., & Rottier, P. J. (1994). Coronavirus M proteins accumulate in the Golgi complex beyond the site of virion budding. *Journal of Virology*, *68*(10), 6523-6534.
- Knibbs, R. N., Dame, M., Allen, M. R., Ding, Y., Hillegas, W. J., Varani, J., & Stoolman, L. M. (2003). Sustained high-yield production of recombinant proteins in transiently transfected COS-7 cells grown on trimethylamine-coated (hillex) microcarrier beads. *Biotechnology Progress*, *19*(1), 9-13. doi: 10.1021/bp020092r
- Knoll, M. D., & Wonodi, C. (2021). Oxford–AstraZeneca COVID-19 vaccine efficacy. *The Lancet*, *397*(10269), 72-74. doi: 10.1016/S0140-6736(20)32623-4
- Knoops, K., Kikkert, M., van den Worm, S. H. E., Zevenhoven-Dobbe, J. C., van der Meer, Y., Koster, A. J., . . . Snijder, E. J. (2008). SARS-Coronavirus Replication Is Supported by a Reticulovesicular Network of Modified Endoplasmic Reticulum. *Public Library of Science (PLoS) Biology*, *6*(9), e226. doi: 10.1371/journal.pbio.0060226
- Kolaskar, A. S., & Tongaonkar, P. C. (1990). A semi-empirical method for prediction of antigenic determinants on protein antigens. *FEBS Lett*, *276*(1-2), 172-174. doi: 10.1016/0014-5793(90)80535-q
- Konca, C., Korukluoglu, G., Tekin, M., Almis, H., Bucak, I. H., Uygun, H., . . . Bayrakdar, F. (2017). The first infant death associated with human coronavirus NL63 infection. *The Pediatric Infectious Disease Journal*, *36*(2), 231-233.
- Kornfeld, R., & Kornfeld, S. (1985). Assembly of asparagine-linked oligosaccharides. *Annual Review of Biochemistry*, *54*(1), 631-664.

- Kost, T. A., & Condreay, J. P. (1999). Recombinant baculoviruses as expression vectors for insect and mammalian cells. *Current Opinion in Biotechnology*, 10(5), 428-433. doi: [https://doi.org/10.1016/S0958-1669\(99\)00005-1](https://doi.org/10.1016/S0958-1669(99)00005-1)
- Kost, T. A., Condreay, J. P., & Jarvis, D. L. (2005). Baculovirus as versatile vectors for protein expression in insect and mammalian cells. *Nature Biotechnology*, 23(5), 567-575. doi: 10.1038/nbt1095
- Krammer, F. (2020). SARS-CoV-2 vaccines in development. *Nature*, 586 516–527 (2020). doi: 10.1038/s41586-020-2798-3
- Krammer, F., Schinko, T., Palmberger, D., Tauer, C., Messner, P., & Grabherr, R. (2010). Trichoplusia ni cells (High Five TM) are highly efficient for the production of influenza A virus-like particles: a comparison of two insect cell lines as production platforms for influenza vaccines. *Molecular Biotechnology*, 45(3), 226-234.
- Krieger, F., Möglich, A., & Kiefhaber, T. (2005). Effect of Proline and Glycine Residues on Dynamics and Barriers of Loop Formation in Polypeptide Chains. *Journal of the American Chemical Society*, 127(10), 3346-3352. doi: 10.1021/ja042798i
- Kruse, R. L. (2020). Therapeutic strategies in an outbreak scenario to treat the novel coronavirus originating in Wuhan, China. *F1000Research*, 9, 72. doi: 10.12688/f1000research.22211.2
- Ksiazek, T. G., Erdman, D., Goldsmith, C. S., Zaki, S. R., Peret, T., Emery, S., . . . Lim, W. (2003). A novel coronavirus associated with severe acute respiratory syndrome. *New England Journal of Medicine*, 348(20), 1953-1966.
- Kumar, A. (2020). Characterization of Nucleocapsid (N) Protein from Novel Coronavirus SARS-CoV-2. *Preprints 2020*, 2020050413 doi: 10.20944/preprints202005.0413.v1
- Kumar, V., Jung, Y.-S., & Liang, P.-H. (2013). Anti-SARS coronavirus agents: a patent review (2008 – present). *Expert Opinion on Therapeutic Patents*, 23(10), 1337-1348. doi: 10.1517/13543776.2013.823159
- Kuo, L., Hurst-Hess, K. R., Koetzner, C. A., & Masters, P. S. (2016). Analyses of Coronavirus Assembly Interactions with Interspecies Membrane and Nucleocapsid Protein Chimeras. *Journal of Virology*, 90(9), 4357-4368. doi: 10.1128/JVI.03212-15
- Kuo, L., Koetzner, C. A., & Masters, P. S. (2016). A key role for the carboxy-terminal tail of the murine coronavirus nucleocapsid protein in coordination of genome packaging. *Virology*, 494, 100-107. doi: 10.1016/j.virol.2016.04.009
- Kuo, L., & Masters, P. S. (2002). Genetic Evidence for a Structural Interaction between the Carboxy Termini of the Membrane and Nucleocapsid Proteins of Mouse Hepatitis Virus. *Journal of Virology*, 76(10), 4987-4999. doi: 10.1128/jvi.76.10.4987-4999.2002

- Kuo, L., & Masters, P. S. (2010). Evolved variants of the membrane protein can partially replace the envelope protein in murine coronavirus assembly. *Journal of Virology*, *84*(24), 12872-12885. doi: 10.1128/JVI.01850-10
- Kuusinen, A., Arvola, M., Oker-Blom, C., & Keinänen, K. (1995). Purification of recombinant GluR-D glutamate receptor produced in Sf21 insect cells. *European Journal of Biochemistry*, *233*(3), 720-726.
- Lai, C., Chan, Z.-R., Yang, D.-G., Lo, W.-H., Lai, Y.-K., Chang, M. D.-T., & Hu, Y.-C. (2006). Accelerated induction of apoptosis in insect cells by baculovirus-expressed SARS-CoV membrane protein. *FEBS Letters*, *580*(16), 3829-3834. doi: 10.1016/j.febslet.2006.06.003
- Lai, C., Wang, C.-Y., Wang, Y.-H., Hsueh, S.-C., Ko, W.-C., & Hsueh, P.-R. (2020). Global epidemiology of coronavirus disease 2019 (COVID-19): disease incidence, daily cumulative index, mortality, and their association with country healthcare resources and economic status. *International Journal of Antimicrobial Agents*, *55*(4), 105946. doi: <https://doi.org/10.1016/j.ijantimicag.2020.105946>
- Lai, M., & Holmes, K. V. (2001). Coronaviridae: the viruses and their replication *Fields Virology* (Vol. 1, pp. 1163-1185).
- Laitinen, O., Airene, K. J., Hytönen, V. P., Peltomaa, E., Mähönen, A. J., Wirth, T., . . . Schenkwein, D. (2005). A multipurpose vector system for the screening of libraries in bacteria, insect and mammalian cells and expression in vivo. *Nucleic Acids Research*, *33*(4), e42-e42.
- Lam, Y. W., Trinkle-Mulcahy, L., & Lamond, A. I. (2005). The nucleolus. *Journal of Cell Science*, *118*(7), 1335-1337. doi: 10.1242/jcs.01736
- Lammers, J., Crusius, J., & Gast, A. (2020). Correcting misperceptions of exponential coronavirus growth increases support for social distancing. *Proceedings of the National Academy of Sciences*, *117*(28), 16264-16266. doi: 10.1073/pnas.2006048117
- Lan, J., Deng, Y., Chen, H., Lu, G., Wang, W., Guo, X., . . . Tan, W. (2014). Tailoring subunit vaccine immunity with adjuvant combinations and delivery routes using the Middle East respiratory coronavirus (MERS-CoV) receptor-binding domain as an antigen. *PLoS One*, *9*(11), e112602.
- Lan, J., Yao, Y., Deng, Y., Chen, H., Lu, G., Wang, W., . . . Tan, W. (2015). Recombinant Receptor Binding Domain Protein Induces Partial Protective Immunity in Rhesus Macaques Against Middle East Respiratory Syndrome Coronavirus Challenge. *EBioMedicine*, *2*(10), 1438-1446. doi: 10.1016/j.ebiom.2015.08.031
- Land, A., & Braakman, I. (2001). Folding of the human immunodeficiency virus type 1 envelope glycoprotein in the endoplasmic reticulum. *Biochimie*, *83*(8), 783-790. doi: [https://doi.org/10.1016/S0300-9084\(01\)01314-1](https://doi.org/10.1016/S0300-9084(01)01314-1)

- Lang, J., Yang, N., Deng, J., Liu, K., Yang, P., Zhang, G., & Jiang, C. (2011). Inhibition of SARS Pseudovirus Cell Entry by Lactoferrin Binding to Heparan Sulfate Proteoglycans. *PLoS ONE*, 6(8), e23710. doi: 10.1371/journal.pone.0023710
- Lange, A., Mills, R. E., Lange, C. J., Stewart, M., Devine, S. E., & Corbett, A. H. (2007). Classical nuclear localization signals: definition, function, and interaction with importin α . *Journal of Biological Chemistry*, 282(8), 5101-5105.
- Lapps, W., Hogue, B. G., & Brian, D. A. (1987). Sequence analysis of the bovine coronavirus nucleocapsid and matrix protein genes. *Virology*, 157(1), 47-57.
- Laude, H., & Masters, P. S. (1995). The coronavirus nucleocapsid protein *The coronaviridae* (pp. 141-163): Springer.
- Lee, B. S., Huang, J. S., Jayathilaka, L. P., Lee, J., & Gupta, S. (2016). Antibody Production with Synthetic Peptides. *Methods in Molecular Biology*, 1474, 25-47. doi: 10.1007/978-1-4939-6352-2_2
- Lee, C., Hodgins, D., Calvert, J. G., Welch, S.-K. W., Jolie, R., & Yoo, D. (2006). Mutations within the nuclear localization signal of the porcine reproductive and respiratory syndrome virus nucleocapsid protein attenuate virus replication. *Virology*, 346(1), 238-250.
- Lee, H., Lee, B. H., Seok, S. H., Baek, M. W., Lee, H. Y., Kim, D. J., . . . Park, J. H. (2010). Production of specific antibodies against SARS-coronavirus nucleocapsid protein without cross reactivity with human coronaviruses 229E and OC43. *Journal of Veterinary Science*, 11(2), 165-167. doi: 10.4142/jvs.2010.11.2.165
- Leenaars, M., & Hendriksen, C. (2005). Critical Steps in the Production of Polyclonal and Monoclonal Antibodies: Evaluation and Recommendations. *ILAR Journal / National Research Council, Institute of Laboratory Animal Resources*, 46, 269-279. doi: 10.1093/ilar.46.3.269
- Leenaars, P., Hendriksen, C. F., de Leeuw, W. A., Carat, F., Delahaut, P., Fischer, R., . . . Hau, J. (1999). The Production of Polyclonal Antibodies in Laboratory Animals: The report and recommendations of ECVAM workshop 35. *Alternatives to Laboratory Animals*, 27(1), 79-102.
- Lehmann, C., Wolf, H., Xu, J., Zhao, Q., Shao, Y., Motz, M., & Lindner, P. (2008). A line immunoassay utilizing recombinant nucleocapsid proteins for detection of antibodies to human coronaviruses. *Diagnostic Microbiology and Infectious Disease*, 61(1), 40-48.
- Lehmann, K., Gulyaeva, A., Zevenhoven-Dobbe, J. C., Janssen, George M C., Ruben, M., Overkleeft, H. S., . . . Gorbalenya, A. E. (2015). Discovery of an essential nucleotidylating activity associated with a newly delineated conserved domain in the RNA polymerase-containing protein of all nidoviruses. *Nucleic Acids Research*, 43(17), 8416-8434. doi: 10.1093/nar/gkv838

- Leitinger, B., Brown, J. L., & Spiess, M. (1994). Tagging secretory and membrane proteins with a tyrosine sulfation site. Tyrosine sulfation precedes galactosylation and sialylation in COS-7 cells. *Journal of Biological Chemistry*, 269(11), 8115-8121.
- Lenard, J. (1999). Host cell protein kinases in nonsegmented negative-strand virus (mononegavirales) infection. *Pharmacol Ther*, 83(1), 39-48. doi: 10.1016/s0163-7258(99)00016-9
- Lenzen, M., Li, M., Malik, A., Pomponi, F., Sun, Y.-Y., Wiedmann, T., . . . Yousefzadeh, M. (2020). Global socio-economic losses and environmental gains from the Coronavirus pandemic. *PLoS ONE*, 15(7), e0235654. doi: 10.1371/journal.pone.0235654
- Leung, T., Li, C. Y., Lam, W. Y., Wong, G. W., Cheuk, E., Ip, M., . . . Chan, P. K. (2009). Epidemiology and clinical presentations of human coronavirus NL63 infections in hong kong children. *Journal of Clinical Microbiology*, 47(11), 3486-3492.
- Li, C., Wu, H., Yan, H., Ma, S., Wang, L., Zhang, M., . . . Brenchley, J. M. (2008). T cell responses to whole SARS coronavirus in humans. *The Journal of Immunology*, 181(8), 5490-5500.
- Li, F., Xiao, H., Tam, J. P., & Liu, D. (2005). Sumoylation of the nucleocapsid protein of severe acute respiratory syndrome coronavirus. *FEBS Letters*, 579(11), 2387-2396.
- Li, H., Liu, S.-M., Yu, X.-H., Tang, S.-L., & Tang, C.-K. (2020). Coronavirus disease 2019 (COVID-19): current status and future perspective. *International Journal of Antimicrobial Agents*, 55(5), 105951. doi: 10.1016/j.ijantimicag.2020.105951.
- Li, Q., Guan, X., Wu, P., Wang, X., Zhou, L., Tong, Y., . . . Feng, Z. (2020). Early Transmission Dynamics in Wuhan, China, of Novel Coronavirus-Infected Pneumonia. *New England Journal of Medicine*, 382(13), 1199-1207. doi: 10.1056/NEJMoa2001316
- Li, R., Pei, S., Chen, B., Song, Y., Zhang, T., Yang, W., & Shaman, J. (2020). Substantial undocumented infection facilitates the rapid dissemination of novel coronavirus (SARS-CoV-2). *Science*, 368(6490), 489-493.
- Li, T., Wang, L., Wang, H., Li, X., Zhang, S., Xu, Y., & Wei, W. (2020). Serum SARS-COV-2 Nucleocapsid Protein: A Sensitivity and Specificity Early Diagnostic Marker for SARS-COV-2 Infection. *Frontiers in Cellular and Infection Microbiology*, 10(470). doi: 10.3389/fcimb.2020.00470
- Li, W., Moore, M. J., Vasilieva, N., Sui, J., Wong, S. K., Berne, M. A., . . . Greenough, T. C. (2003). Angiotensin-converting enzyme 2 is a functional receptor for the SARS coronavirus. *Nature*, 426(6965), 450-454.
- Liang, F., Lin, L.-C., Ying, T.-H., Yao, C.-W., Tang, T.-K., Chen, Y.-W., & Hou, M.-H. (2013). Immunoreactivity characterisation of the three structural regions of the human coronavirus OC43 nucleocapsid protein by Western blot: Implications for the diagnosis of coronavirus

- infection. *Journal of Virological Methods*, 187(2), 413-420. doi:
<https://doi.org/10.1016/j.jviromet.2012.11.009>
- Liao, Y., Fung, T. S., Huang, M., Fang, S. G., Zhong, Y., & Liu, D. X. (2013). Upregulation of CHOP/GADD153 during coronavirus infectious bronchitis virus infection modulates apoptosis by restricting activation of the extracellular signal-regulated kinase pathway. *Journal of Virology*, 87(14), 8124-8134.
- Lin, Y., Shen, X., Yang, R. F., Li, Y. X., Ji, Y. Y., He, Y. Y., . . . Sun, B. (2003). Identification of an epitope of SARS-coronavirus nucleocapsid protein. *Cell Research*, 13(3), 141-145. doi:
10.1038/sj.cr.7290158
- Lindorff-Larsen, K., Piana, S., Dror, R. O., & Shaw, D. E. (2011). How fast-folding proteins fold. *Science*, 334(6055), 517-520.
- Liu, D. X., Fung, T. S., Chong, K. K.-L., Shukla, A., & Hilgenfeld, R. (2014). Accessory proteins of SARS-CoV and other coronaviruses. *Antiviral Research*, 109, 97-109. doi:
<https://doi.org/10.1016/j.antiviral.2014.06.013>
- Liu, J., Shao, H., Tao, Y., Yang, B., Qian, L., Yang, X., . . . Cheng, X. (2006). Production of an anti-severe acute respiratory syndrome (SARS) coronavirus human monoclonal antibody Fab fragment by using a combinatorial immunoglobulin gene library derived from patients who recovered from SARS. *Clinical and Vaccine Immunology : CVI*, 13(5), 594-597. doi:
10.1128/CVI.13.5.594-597.2006
- Liu, J., Sun, Y., Qi, J., Chu, F., Wu, H., Gao, F., . . . Gao, G. F. (2010). The Membrane Protein of Severe Acute Respiratory Syndrome Coronavirus Acts as a Dominant Immunogen Revealed by a Clustering Region of Novel Functionally and Structurally Defined Cytotoxic T-Lymphocyte Epitopes. *The Journal of Infectious Diseases*, 202(8), 1171-1180. doi: 10.1086/656315
- Liu, L., Celma, C. C. P., & Roy, P. (2008). Rift Valley fever virus structural proteins: expression, characterization and assembly of recombinant proteins. *Virology Journal*, 5, 82-82. doi:
10.1186/1743-422X-5-82
- Liu, L., Wang, P., Nair, M. S., Yu, J., Rapp, M., Wang, Q., . . . Ho, D. D. (2020). Potent neutralizing antibodies against multiple epitopes on SARS-CoV-2 spike. *Nature*, 584(7821), 450-456. doi:
10.1038/s41586-020-2571-7
- Locker, J. K., Opstelten, D. J., Ericsson, M., Horzinek, M. C., & Rottier, P. J. (1995). Oligomerization of a trans-Golgi/trans-Golgi network retained protein occurs in the Golgi complex and may be part of its retention. *Journal of Biological Chemistry*, 270(15), 8815-8821. doi:
10.1074/jbc.270.15.8815

- Locker, J. K., Rose, J. K., Horzinek, M. C., & Rottier, P. J. (1992). Membrane assembly of the triple-spanning coronavirus M protein. Individual transmembrane domains show preferred orientation. *Journal of Biological Chemistry*, 267(30), 21911-21918.
- Lokugamage, K. G., Narayanan, K., Nakagawa, K., Terasaki, K., Ramirez, S. I., Tseng, C. T., & Makino, S. (2015). Middle East Respiratory Syndrome Coronavirus nsp1 Inhibits Host Gene Expression by Selectively Targeting mRNAs Transcribed in the Nucleus while Sparing mRNAs of Cytoplasmic Origin. *Journal of Virology*, 89(21), 10970-10981. doi: 10.1128/JVI.01352-15
- Londrigan, S. L., Turville, S. G., Tate, M. D., Deng, Y.-M., Brooks, A. G., & Reading, P. C. (2011). N-linked glycosylation facilitates sialic acid-independent attachment and entry of influenza A viruses into cells expressing DC-SIGN or L-SIGN. *Journal of Virology*, 85(6), 2990-3000. doi: 10.1128/JVI.01705-10
- Long, Q.-X., Tang, X.-J., Shi, Q.-L., Li, Q., Deng, H.-J., Yuan, J., . . . Huang, A.-L. (2020). Clinical and immunological assessment of asymptomatic SARS-CoV-2 infections. *Nature Medicine*, 26(8), 1200-1204. doi: 10.1038/s41591-020-0965-6
- Loos, C., Atyeo, C., Fischinger, S., Burke, J., Slein, M. D., Streeck, H., . . . Alter, G. (2020). Evolution of Early SARS-CoV-2 and Cross-Coronavirus Immunity. *MSphere*, 5(5), e00622-00620. doi: 10.1128/mSphere.00622-20
- Lu, G., Hu, Y., Wang, Q., Qi, J., Gao, F., Li, Y., . . . Gao, G. F. (2013). Molecular basis of binding between novel human coronavirus MERS-CoV and its receptor CD26. *Nature*, 500(7461), 227-231. doi: 10.1038/nature12328
- Lu, R.-M., Hwang, Y.-C., Liu, I. J., Lee, C.-C., Tsai, H.-Z., Li, H.-J., & Wu, H.-C. (2020). Development of therapeutic antibodies for the treatment of diseases. *Journal of Biomedical Science*, 27(1), 1. doi: 10.1186/s12929-019-0592-z
- Lu, X., Pan, J. a., Tao, J., & Guo, D. (2011). SARS-CoV nucleocapsid protein antagonizes IFN- β response by targeting initial step of IFN- β induction pathway, and its C-terminal region is critical for the antagonism. *Virus Genes*, 42(1), 37-45.
- Luckow, V. A., Lee, S. C., Barry, G. F., & Olins, P. O. (1993). Efficient generation of infectious recombinant baculoviruses by site-specific transposon-mediated insertion of foreign genes into a baculovirus genome propagated in Escherichia coli. *Journal of Virology*, 67(8), 4566-4579.
- Luckow, V. A., & Summers, M. D. (1988). Trends in the Development of Baculovirus Expression Vectors. *BioTechnology*, 6(1), 47-55. doi: 10.1038/nbt0188-47
- Lugari, A., Betzi, S., Decroly, E., Bonnaud, E., Hermant, A., Guillemot, J. C., . . . Lecine, P. (2010). Molecular mapping of the RNA Cap 2'-O-methyltransferase activation interface between severe acute respiratory syndrome coronavirus nsp10 and nsp16. *The Journal of Biological Chemistry*, 285(43), 33230-33241. doi: 10.1074/jbc.M110.120014

- Luo, H., Wu, D., Shen, C., Chen, K., Shen, X., & Jiang, H. (2006). Severe acute respiratory syndrome coronavirus membrane protein interacts with nucleocapsid protein mostly through their carboxyl termini by electrostatic attraction. *The International Journal of Biochemistry & Cell Biology*, 38(4), 589-599.
- Luo, Z., Ang, M. J. Y., Chan, S. Y., Yi, Z., Goh, Y. Y., Yan, S., . . . Liu, X. (2020). Combating the Coronavirus Pandemic: Early Detection, Medical Treatment, and a Concerted Effort by the Global Community. *Research (Washington, D.C.)*, 2020, 6925296-6925296. doi: 10.34133/2020/6925296
- Lynn, D. E. (2001). Novel techniques to establish new insect cell lines. *In Vitro Cellular & Developmental Biology - Animal*, 37(6), 319-321. doi: 10.1007/BF02577564
- Lyons, R., Ferguson, B., & Rosenberg, M. (1987). Pentapeptide nuclear localization signal in adenovirus E1a. *Molecular and Cellular Biology*, 7(7), 2451-2456.
- Ma, C., Li, Y., Wang, L., Zhao, G., Tao, X., Tseng, C.-T. K., . . . Jiang, S. (2014). Intranasal vaccination with recombinant receptor-binding domain of MERS-CoV spike protein induces much stronger local mucosal immune responses than subcutaneous immunization: Implication for designing novel mucosal MERS vaccines. *Vaccine*, 32(18), 2100-2108. doi: <https://doi.org/10.1016/j.vaccine.2014.02.004>
- Ma, C., Wang, L., Tao, X., Zhang, N., Yang, Y., Tseng, C.-T. K., . . . Du, L. (2014). Searching for an ideal vaccine candidate among different MERS coronavirus receptor-binding fragments—the importance of immunofocusing in subunit vaccine design. *Vaccine*, 32(46), 6170-6176.
- Ma, Y., Tong, X., Xu, X., Li, X., Lou, Z., & Rao, Z. (2010). Structures of the N- and C-terminal domains of MHV-A59 nucleocapsid protein corroborate a conserved RNA-protein binding mechanism in coronavirus. *Protein Cell*, 1(7), 688-697. doi: 10.1007/s13238-010-0079-x
- Ma, Y., Wu, L., Shaw, N., Gao, Y., Wang, J., Sun, Y., . . . Rao, Z. (2015). Structural basis and functional analysis of the SARS coronavirus nsp14-nsp10 complex. *Proceedings of the National Academy of Sciences of the United States of America (PNAS)*, 112(30), 9436-9441. doi: 10.1073/pnas.1508686112
- Ma, Z., Li, P., Ji, Y., Ikram, A., & Pan, Q. (2020). Cross-reactivity towards SARS-CoV-2: the potential role of low-pathogenic human coronaviruses. *The Lancet Microbe*, 1(4), e151. doi: 10.1016/S2666-5247(20)30098-7
- Machamer, B. G. H. C. E. (2007). Coronavirus Structural Proteins and Virus Assembly *Nidoviruses* (pp. 179-200).
- Machamer, C. E., Mentone, S. A., Rose, J. K., & Farquhar, M. G. (1990). The E1 glycoprotein of an avian coronavirus is targeted to the cis Golgi complex. *Proceedings of the National Academy of Sciences*, 87(18), 6944-6948. doi: 10.1073/pnas.87.18.6944

- Machery-Nagel. (2020). *Instruction-NucleoBond-PC-BAC*. from <https://www.mn-net.com/media/pdf/e4/c4/67/Instruction-NucleoBond-PC-BAC.pdf>
- Malczyk, A. H., Kupke, A., Prüfer, S., Scheuplein, V. A., Hutzler, S., Kreuz, D., . . . Mühlebach, M. D. (2015). A Highly Immunogenic and Protective Middle East Respiratory Syndrome Coronavirus Vaccine Based on a Recombinant Measles Virus Vaccine Platform. *Journal of Virology*, 89(22), 11654-11667. doi: 10.1128/jvi.01815-15
- Mallesappa Gowder, S., Chatterjee, J., Chaudhuri, T., & Paul, K. (2014). Prediction and Analysis of Surface Hydrophobic Residues in Tertiary Structure of Proteins. *The Scientific World Journal*, 2014, 971258. doi: 10.1155/2014/971258
- Manisha, R., Diaz, Heckman, C., Deters, D., & Jamasbi, R. (2020). *Use of bionanotechnology to decipher the patterns of assemblage and interactions of multi-protein complexes*. (Master of Science), Graduate College of Bowling Green State University Retrieved from <https://citeseerx.ist.psu.edu/viewdoc/download?doi=10.1.1.967.5129&rep=rep1&type=pdf>
- Mann, M., Ong, S.-E., Grønborg, M., Steen, H., Jensen, O. N., & Pandey, A. (2002). Analysis of protein phosphorylation using mass spectrometry: deciphering the phosphoproteome. *Trends in Biotechnology*, 20(6), 261-268.
- Marano, G., Vaglio, S., Pupella, S., Facco, G., Catalano, L., Liunbruno, G. M., & Grazzini, G. (2016). Convalescent plasma: new evidence for an old therapeutic tool? *Blood Transfusion*, 14(2), 152.
- Marra, M. A., Jones, S. J., Astell, C. R., Holt, R. A., Brooks-Wilson, A., Butterfield, Y. S., . . . Chan, S. Y. (2003). The genome sequence of the SARS-associated coronavirus. *Science*, 300(5624), 1399-1404.
- Masse, S., Capai, L., Villechenaud, N., Blanchon, T., Charrel, R., & Falchi, A. (2020). Epidemiology and Clinical Symptoms Related to Seasonal Coronavirus Identified in Patients with Acute Respiratory Infections Consulting in Primary Care over Six Influenza Seasons (2014-2020) in France. *Viruses*, 12(6), 630. doi: 10.3390/v12060630
- Massotte, D. (2003). G protein-coupled receptor overexpression with the baculovirus–insect cell system: a tool for structural and functional studies. *Biochimica et Biophysica Acta (BBA) - Biomembranes*, 1610(1), 77-89. doi: [https://doi.org/10.1016/S0005-2736\(02\)00720-4](https://doi.org/10.1016/S0005-2736(02)00720-4)
- Masters, P. S. (2006). The molecular biology of coronaviruses. *Advances in Virus Research*, 66, 193-292.
- Masters, P. S., Kuo, L., Ye, R., Hurst, K. R., Koetzner, C. A., & Hsue, B. (2006). Genetic and Molecular Biological Analysis of Protein-Protein Interactions in Coronavirus Assembly. *Advances in Experimental Medicine and Biology*, 581, 163-173. doi: 10.1007/978-0-387-33012-9_29

- Mateos-Gómez, P. A., Zuñiga, S., Palacio, L., Enjuanes, L., & Sola, I. (2011). Gene N proximal and distal RNA motifs regulate coronavirus nucleocapsid mRNA transcription. *Journal of Virology*, 85(17), 8968-8980.
- Mathewson, A. C., Bishop, A., Yao, Y., Kemp, F., Ren, J., Chen, H., . . . Jones, I. M. (2008). Interaction of severe acute respiratory syndrome-coronavirus and NL63 coronavirus spike proteins with angiotensin converting enzyme-2. *The Journal of General Virology*, 89(Pt 11), 2741-2745. doi: 10.1099/vir.0.2008/003962-0
- Matrosovich, M., Matrosovich, T., Garten, W., & Klenk, H.-D. (2006). New low-viscosity overlay medium for viral plaque assays. *Virology Journal*, 3(1), 63.
- Matsuyama, S., & Taguchi, F. (2002). Receptor-Induced Conformational Changes of Murine Coronavirus Spike Protein. *Journal of Virology*, 76(23), 11819-11826. doi: 10.1128/jvi.76.23.11819-11826.2002
- Matthes, N., Mesters, J. R., Coutard, B., Canard, B., Snijder, E. J., Moll, R., & Hilgenfeld, R. (2006). The non-structural protein Nsp10 of mouse hepatitis virus binds zinc ions and nucleic acids. *FEBS Letters*, 580(17), 4143-4149. doi: doi:10.1016/j.febslet.2006.06.061
- Mayer, K., Nellessen, C., Hahn-Ast, C., Schumacher, M., Pietzonka, S., Eis-Hübinger, A. M., . . . Wolf, D. (2016). Fatal outcome of human coronavirus NL63 infection despite successful viral elimination by IFN-alpha in a patient with newly diagnosed ALL. *European Journal of Haematology*, 97(2), 208-210. doi: 10.1111/ejh.12744
- Mayrand, S. H., Dwen, P., & Pederson, T. (1993). Serine/threonine phosphorylation regulates binding of C hnRNP proteins to pre-mRNA. *Proceedings of the National Academy of Sciences of the United States of America*, 90(16), 7764-7768. doi: 10.1073/pnas.90.16.7764
- McBride, C. E., Li, J., & Machamer, C. E. (2007). The Cytoplasmic Tail of the Severe Acute Respiratory Syndrome Coronavirus Spike Protein Contains a Novel Endoplasmic Reticulum Retrieval Signal That Binds COPI and Promotes Interaction with Membrane Protein. *Journal of Virology*, 81(5), 2418-2428. doi: 10.1128/jvi.02146-06
- McBride, R., & Fielding, B. (2012). The role of SARS-coronavirus accessory proteins in virus pathogenesis. *Viruses*, 4(11), 2902-2923. doi: 10.3390/v4112902
- McBride, R., Van Zyl, M., & Fielding, B. C. (2014). The coronavirus nucleocapsid is a multifunctional protein. *Viruses*, 6(8), 2991-3018.
- McCormick, C., & Khapersky, D. A. (2017). Translation inhibition and stress granules in the antiviral immune response. *Nature Reviews Immunology*, 17(10), 647.
- McKenzie, E., & Abbott, W. (2018). Expression of recombinant proteins in insect and mammalian cells. *Methods*, 147, 40-49. doi: 10.1016/j.ymeth.2018.05.013

- Meghrou, J., Aucoin, M. G., Jacob, D., Chahal, P. S., Arcand, N., & Kamen, A. A. (2005). Production of recombinant adeno-associated viral vectors using a baculovirus/insect cell suspension culture system: from shake flasks to a 20-L bioreactor. *Biotechnology Progress*, 21(1), 154-160.
- Mehand, M. S., Al-Shorbaji, F., Millett, P., & Murgue, B. (2018). The WHO R&D Blueprint: 2018 review of emerging infectious diseases requiring urgent research and development efforts. *Antiviral Research*, 159, 63-67. doi: 10.1016/j.antiviral.2018.09.009
- Mena, J. A., & Kamen, A. A. (2011). Insect cell technology is a versatile and robust vaccine manufacturing platform. *Expert Review of Vaccines*, 10(7), 1063-1081.
- Menachery, V. D., Debbink, K., & Baric, R. S. (2014). Coronavirus non-structural protein 16: evasion, attenuation, and possible treatments. *Virus Research*, 194, 191-199. doi: 10.1016/j.virusres.2014.09.009
- Menachery, V. D., Gralinski, L. E., Mitchell, H. D., Dinnon, K. H., Leist, S. R., Yount, B. L., . . . Baric, R. S. (2017). Middle East Respiratory Syndrome Coronavirus Nonstructural Protein 16 Is Necessary for Interferon Resistance and Viral Pathogenesis. *mSphere*, 2(6), e00346-00317. doi: 10.1128/mSphere.00346-17
- Menachery, V. D., Yount, B. L., Jr., Josset, L., Gralinski, L. E., Scobey, T., Agnihothram, S., . . . Baric, R. S. (2014). Attenuation and restoration of severe acute respiratory syndrome coronavirus mutant lacking 2'-o-methyltransferase activity. *Journal of Virology*, 88(8), 4251-4264. doi: 10.1128/JVI.03571-13
- Mesel-Lemoine, M., Millet, J., Vidalain, P.-O., Law, H., Vabret, A., Lorin, V., . . . Tangy, F. (2012). A Human Coronavirus Responsible for the Common Cold Massively Kills Dendritic Cells but Not Monocytes. *Journal of Virology*, 86(14), 7577-7587. doi: 10.1128/jvi.00269-12
- Meulenbergh, J. J., Hulst, M. M., de Meijer, E. J., Moonen, P. L., den Besten, A., de Kluyver, E. P., . . . Moormann, R. J. (1993). Lelystad virus, the causative agent of porcine epidemic abortion and respiratory syndrome (PEARS), is related to LDV and EAV. *Virology*, 192(1), 62-72.
- Meunier, J. C., Fournillier, A., Choukhi, A., Cahour, A., Cocquerel, L., Dubuisson, J., & Wychowski, C. (1999). Analysis of the glycosylation sites of hepatitis C virus (HCV) glycoprotein E1 and the influence of E1 glycans on the formation of the HCV glycoprotein complex. *Journal of General Virology*, 80 (Pt 4), 887-896. doi: 10.1099/0022-1317-80-4-887
- Mielech, A. M., Chen, Y., Mesecar, A. D., & Baker, S. C. (2014). Nidovirus papain-like proteases: multifunctional enzymes with protease, deubiquitinating and delSGylating activities. *Virus Research*, 194, 184-190. doi: 10.1016/j.virusres.2014.01.025

- Milewska, A., Kaminski, K., Ciejka, J., Kosowicz, K., Zeglen, S., Wojarski, J., . . . Pyrc, K. (2016). HTCC: Broad Range Inhibitor of Coronavirus Entry. *Public Library of Science (PLoS) One*, 11(6), e0156552. doi: 10.1371/journal.pone.0156552
- Milewska, A., Zarebski, M., Nowak, P., Stozek, K., Potempa, J., & Pyrc, K. (2014). Human coronavirus NL63 utilizes heparan sulfate proteoglycans for attachment to target cells. *Journal of Virology*, 88(22), 13221-13230.
- Minskaia, E., Hertzog, T., Gorbalenya, A. E., Campanacci, V., Cambillau, C., Canard, B., & Ziebuhr, J. (2006). Discovery of an RNA virus 3'→5' exoribonuclease that is critically involved in coronavirus RNA synthesis. *Proceedings of the National Academy of Sciences of the United States of America (PNAS)*, 103(13), 5108-5113. doi: 10.1073/pnas.0508200103
- Mohammadi, H., Sharif, S., Rowland, R. R., & Yoo, D. (2009). The lactate dehydrogenase-elevating virus capsid protein is a nuclear–cytoplasmic protein. *Archives of Virology*, 154(7), 1071-1080.
- Molenkamp, R., van Tol, H., Rozier, B. C., van der Meer, Y., Spaan, W. J., & Snijder, E. J. (2000). The arterivirus replicase is the only viral protein required for genome replication and subgenomic mRNA transcription. *Journal of General Virology*, 81(10), 2491-2496.
- Mortola, E., & Roy, P. (2004). Efficient assembly and release of SARS coronavirus-like particles by a heterologous expression system. *FEBS Letters*, 576(1), 174-178. doi: <https://doi.org/10.1016/j.febslet.2004.09.009>
- Moskophidis, D., Lechner, F., Pircher, H., & Zinkernagel, R. M. (1993). Virus persistence in acutely infected immunocompetent mice by exhaustion of antiviral cytotoxic effector T cells. *Nature*, 362(6422), 758-761. doi: 10.1038/362758a0
- Müller, M. A., van der Hoek, L., Voss, D., Bader, O., Lehmann, D., Schulz, A. R., . . . Niedrig, M. (2010). Human coronavirus NL63 open reading frame 3 encodes a virion-incorporated N-glycosylated membrane protein. *Virology Journal*, 7, 6-6. doi: 10.1186/1743-422X-7-6
- Murin, C. D., Wilson, I. A., & Ward, A. B. (2019). Antibody responses to viral infections: a structural perspective across three different enveloped viruses. *Nature Microbiology*, 4(5), 734-747. doi: 10.1038/s41564-019-0392-y
- Murphy, K., & Weaver, C. (2016). *Janeway's immunobiology* 9 (9th ed.): Garland science.
- Müssener, Å., Klareskog, L., Lorentzen, J., & Kleinau, S. (1995). TNF- α Dominates Cytokine mRNA Expression in Lymphoid Tissues of Rats Developing Collagen-and Oil-Induced Arthritis. *Scandinavian Journal of Immunology*, 42(1), 128-134.
- Nal, B., Chan, C., Kien, F., Siu, L., Tse, J., Chu, K., . . . Altmeyer, R. (2005). Differential maturation and subcellular localization of severe acute respiratory syndrome coronavirus surface proteins S, M and E. *Journal of General Virology*, 86(5), 1423-1434. doi: doi:10.1099/vir.0.80671-0

- Namy, O., Moran, S. J., Stuart, D. I., Gilbert, R. J. C., & Brierley, I. (2006). A mechanical explanation of RNA pseudoknot function in programmed ribosomal frameshifting. *Nature*, *441*(7090), 244-247. doi: 10.1038/nature04735
- <https://www.nature.com/articles/nature04735#supplementary-information>
- Narayanan, K., Huang, C., Lokugamage, K. G., Kamitani, W., Ikegami, T., Tseng, C. K., & Makino, S. (2008). Severe acute respiratory syndrome coronavirus nsp1 suppresses host gene expression, including that of type I interferon, in infected cells. *Journal of Virology*, *82*(9), 4471-4479.
- Narayanan, K., Huang, C., & Makino, S. (2008). SARS coronavirus accessory proteins. *Virus Research* *133*(1), 113-121. doi: 10.1016/j.virusres.2007.10.009
- Narayanan, K., Kim, K. H., & Makino, S. (2003). Characterization of N protein self-association in coronavirus ribonucleoprotein complexes. *Virus Research*, *98*(2), 131-140. doi: <https://doi.org/10.1016/j.virusres.2003.08.021>
- Narayanan, K., Maeda, A., Maeda, J., & Makino, S. (2000). Characterization of the coronavirus M protein and nucleocapsid interaction in infected cells. *Journal of Virology*, *74*(17), 8127-8134.
- Narayanan, K., & Makino, S. (2001). Characterization of nucleocapsid-M protein interaction in murine coronavirus. *Advances in Experimental Medicine and Biology*, *494*, 577-582. doi: 10.1007/978-1-4615-1325-4_85
- Naskalska, A., Dabrowska, A., Nowak, P., Szczepanski, A., Jasik, K., Milewska, A., . . . Pyrc, K. (2018). Novel coronavirus-like particles targeting cells lining the respiratory tract. *PLOS ONE*, *13*(9), e0203489. doi: 10.1371/journal.pone.0203489
- Naskalska, A., Dabrowska, A., Szczepanski, A., Milewska, A., Jasik, K. P., & Pyrc, K. (2019). Membrane Protein of Human Coronavirus NL63 Is Responsible for Interaction with the Adhesion Receptor. *Journal of Virology*, *93*(19), e00355-00319. doi: 10.1128/jvi.00355-19
- Nedialkova, D. D., Ulferts, R., van den Born, E., Lauber, C., Gorbalenya, A. E., Ziebuhr, J., & Snijder, E. J. (2009). Biochemical Characterization of Arterivirus Nonstructural Protein 11 Reveals the Nidovirus-Wide Conservation of a Replicative Endoribonuclease. *Journal of Virology*, *83*(11), 5671-5682. doi: 10.1128/jvi.00261-09
- Neher, R., Dyrdak, R., Druelle, V., Hodcroft, E., & Albert, J. (2020). Potential impact of seasonal forcing on a SARS-CoV-2 pandemic. *Swiss Medical Weekly*, *150*(w20224). doi: 10.4414/smw.2020.20224
- Nelson, G. W., Stohlman, S. A., & Tahara, S. M. (2000). High affinity interaction between nucleocapsid protein and leader/intergenic sequence of mouse hepatitis virus RNA. *Journal of General Virology*, *81*(1), 181-188.

- Neuman, B. W., & Buchmeier, M. J. (2016). Supramolecular architecture of the coronavirus particle. *Advances in Virus Research*, 96, 1-27. doi: 10.1016/bs.aivir.2016.08.005
- Neuman, B. W., Kiss, G., Kunding, A. H., Bhella, D., Baksh, M. F., Connelly, S., . . . Buchmeier, M. J. (2011). A structural analysis of M protein in coronavirus assembly and morphology. *Journal of Structural Biology*, 174(1), 11-22. doi: 10.1016/j.jsb.2010.11.021
- Ng, K. K. S., Arnold, J. J., & Cameron, C. E. (2008). Structure-Function Relationships Among RNA-Dependent RNA Polymerases. *Current Topics in Microbiology and Immunology*, 320, 137-156.
- Nguyen, H. L., Lan, P. D., Thai, N. Q., Nissley, D. A., O'Brien, E. P., & Li, M. S. (2020). Does SARS-CoV-2 Bind to Human ACE2 More Strongly Than Does SARS-CoV? *The Journal of Physical Chemistry. B*, 124(34), 7336-7347. doi: 10.1021/acs.jpcc.0c04511
- Nguyen, V. P., & Hogue, B. G. (1997). Protein interactions during coronavirus assembly. *Journal of Virology*, 71(12), 9278-9284.
- Ni, P., & Cheng Kao, C. (2013). Non-encapsidation activities of the capsid proteins of positive-strand RNA viruses. *Virology*, 446(1-2), 123-132. doi: 10.1016/j.virol.2013.07.023
- Nickbakhsh, S., Ho, A., Marques, D. F., McMenamin, J., Gunson, R. N., & Murcia, P. R. (2020). Epidemiology of seasonal coronaviruses: Establishing the context for COVID-19 emergence. *The Journal of Infectious Diseases*.
- Nicola, M., Alsafi, Z., Sohrabi, C., Kerwan, A., Al-Jabir, A., Iosifidis, C., . . . Agha, R. (2020). The socio-economic implications of the coronavirus pandemic (COVID-19): A review. *International Journal of Surgery (London, England)*, 78, 185-193. doi: 10.1016/j.ijssu.2020.04.018
- Niederhafner, P., Šebestík, J., & Ježek, J. (2005). Peptide dendrimers. *Journal of Peptide Science: An Official Publication of the European Peptide Society*, 11(12), 757-788.
- Niemann, H., Heisterberg-Moutsis, G., Geyer, R., Klenk, H.-D., & Wirth, M. (1984). Glycoprotein E1 of MHV-A59: Structure of the O-Linked Carbohydrates and Construction of Full Length Recombinant cDNA Clones. *Advances in Experimental Medicine and Biology*, 173, 201-213. doi: 10.1007/978-1-4615-9373-7_20
- Nikolai, L. A., Meyer, C. G., Kremsner, P. G., & Velavan, T. P. (2020). Asymptomatic SARS Coronavirus 2 infection: Invisible yet invincible. *International Journal of Infectious Diseases : IJID : official publication of the International Society for Infectious Diseases*, 100, 112-116. doi: 10.1016/j.ijid.2020.08.076
- Ning, Q., Lakatoo, S., Liu, M., Yang, W., Wang, Z., Phillips, M. J., & Levy, G. A. (2003). Induction of prothrombinase fgl2 by the nucleocapsid protein of virulent mouse hepatitis virus is dependent on host hepatic nuclear factor-4 alpha. *Journal of Biological Chemistry*, 278(18), 15541-15549. doi: 10.1074/jbc.M212806200

- Nishikori, S., Hattori, T., Fuchs, S. M., Yasui, N., Wojcik, J., Koide, A., . . . Koide, S. (2012). Broad ranges of affinity and specificity of anti-histone antibodies revealed by a quantitative peptide immunoprecipitation assay. *Journal of Molecular Biology*, 424(5), 391-399.
- O'Reilly, D. R., Miller, L. K., & Luckow, V. A. (1994). *Baculovirus expression vectors: a laboratory manual*: Oxford University Press.
- Ochsenbein, A. F., Klenerman, P., Karrer, U., Ludewig, B., Pericin, M., Hengartner, H., & Zinkernagel, R. M. (1999). Immune surveillance against a solid tumor fails because of immunological ignorance. *Proceedings of the National Academy of Sciences of the United States of America*, 96(5), 2233-2238. doi: 10.1073/pnas.96.5.2233
- Ohashi, P. S., Oehen, S., Buerki, K., Pircher, H., Ohashi, C. T., Odermatt, B., . . . Hengartner, H. (1991). Ablation of "tolerance" and induction of diabetes by virus infection in viral antigen transgenic mice. *Cell*, 65(2), 305-317. doi: 10.1016/0092-8674(91)90164-t
- Ooi, E. E., & Low, J. G. (2020). Asymptomatic SARS-CoV-2 infection. *The Lancet Infectious Diseases*, 20(9), 996-998. doi: 10.1016/S1473-3099(20)30460-6
- Oosterhof, L., Christensen, C., & Sengeløv, H. (2010). Fatal lower respiratory tract disease with human corona virus NL63 in an adult haematopoietic cell transplant recipient. *Bone Marrow Transplantation*, 45(6), 1115-1116.
- Oostra, M., de Haan, C. A. M., de Groot, R. J., & Rottier, P. J. M. (2006). Glycosylation of the severe acute respiratory syndrome coronavirus triple-spanning membrane proteins 3a and M. *Journal of Virology*, 80(5), 2326-2336. doi: 10.1128/JVI.80.5.2326-2336.2006
- Opstelten, D. J., Raamsman, M. J., Wolfs, K., Horzinek, M. C., & Rottier, P. J. (1995). Envelope glycoprotein interactions in coronavirus assembly. *The Journal of Cell Biology*, 131(2), 339-349. doi: 10.1083/jcb.131.2.339
- Organisation, W. H. (2019, March 2019). Update: Middle East respiratory syndrome coronavirus (MERS-CoV). from <https://www.who.int/emergencies/mers-cov/en/>
- Organization, W. H. (2003). Summary table of SARS cases by country, 1 November 2002-7 August 2003= Tableau récapitulatif du nombre de cas de SRAS par pays, 1er novembre 2002—7 août 2003. *The Weekly Epidemiological Record (WER)*, 78(35), 310-311.
- Organization, W. H. (2019). *Middle East respiratory syndrome coronavirus (MERS-CoV)*. Retrieved 14 January 2020, from https://www.who.int/health-topics/middle-east-respiratory-syndrome-coronavirus-mers#tab=tab_1
- Otieno, G. P., Murunga, N., Agoti, C. N., Gallagher, K. E., Awori, J. O., & Nokes, D. J. (2020). Surveillance of endemic human coronaviruses (HCoV-NL63, OC43 and 229E) associated with pneumonia in Kilifi, Kenya. *Wellcome Open Research*, 5, 150. doi: 10.12688/wellcomeopenres.16037.2

- Oudshoorn, D., Rijs, K., Limpens, R. W. A. L., Groen, K., Koster, A. J., Snijder, E. J., . . . Bárcena, M. (2017). Expression and Cleavage of Middle East Respiratory Syndrome Coronavirus nsp3-4 Polyprotein Induce the Formation of Double-Membrane Vesicles That Mimic Those Associated with Coronaviral RNA Replication. *MBio*, 8(6). doi: 10.1128/mBio.01658-17
- Owen, J. A., Punt, J., & Stranford, S. A. (2013). *Kuby immunology*: WH Freeman New York.
- Pang, H., Liu, Y., Han, X., Xu, Y., Jiang, F., Wu, D., . . . Rao, Z. (2004). Protective humoral responses to severe acute respiratory syndrome-associated coronavirus: implications for the design of an effective protein-based vaccine. *Journal of General Virology*, 85(10), 3109-3113. doi: <https://doi.org/10.1099/vir.0.80111-0>
- Papageorgiou, N., Lichiere, J., Baklouti, A., Ferron, F., Sévajol, M., Canard, B., & Coutard, B. (2016). Structural characterization of the N-terminal part of the MERS-CoV nucleocapsid by X-ray diffraction and small-angle X-ray scattering. *Acta Crystallographica Section D: Structural Biology*, 72(2), 192-202.
- Park, B. K., Lee, S. I., Bae, J.-Y., Park, M.-S., Lee, Y., & Kwon, H.-J. (2019). Production of a Monoclonal Antibody Targeting the M Protein of MERS-CoV for Detection of MERS-CoV Using a Synthetic Peptide Epitope Formulated with a CpG–DNA–Liposome Complex. *International Journal of Peptide Research and Therapeutics*, 25(3), 819-826. doi: 10.1007/s10989-018-9731-8
- Park, B. K., Maharjan, S., Lee, S. I., Kim, J., Bae, J. Y., Park, M. S., & Kwon, H. J. (2019). Generation and characterization of a monoclonal antibody against MERS-CoV targeting the spike protein using a synthetic peptide epitope-CpG-DNA-liposome complex. *BMB Reports*, 52(6), 397-402. doi: 10.5483/BMBRep.2019.52.6.185
- Parker, M. M., & Masters, P. S. (1990). Sequence comparison of the N genes of five strains of the coronavirus mouse hepatitis virus suggests a three domain structure for the nucleocapsid protein. *Virology*, 179(1), 463-468.
- Pascal, K. E., Coleman, C. M., Mujica, A. O., Kamat, V., Badithe, A., Fairhurst, J., . . . Kyratsous, C. A. (2015). Pre- and postexposure efficacy of fully human antibodies against Spike protein in a novel humanized mouse model of MERS-CoV infection. *Proceedings of the National Academy of Sciences*, 112(28), 8738-8743. doi: 10.1073/pnas.1510830112
- Payne, S. (2017). Family Coronaviridae. *Viruses*, 149-158. doi: 10.1016/B978-0-12-803109-4.00017-9
- Pei, Y., Hodgins, D. C., Lee, C., Calvert, J. G., Welch, S.-K. W., Jolie, R., . . . Yoo, D. (2008). Functional mapping of the porcine reproductive and respiratory syndrome virus capsid protein nuclear localization signal and its pathogenic association. *Virus Research*, 135(1), 107-114.
- Peiris, J., Lai, S., Poon, L., Guan, Y., Yam, L., Lim, W., . . . Cheung, M. (2003). Coronavirus as a possible cause of severe acute respiratory syndrome. *The Lancet*, 361(9366), 1319-1325.

- Pellequer†, J. L., & Westhof, E. (1993). PREDITOP: A program for antigenicity prediction. *Journal of Molecular Graphics*, 11(3), 204-210. doi: [https://doi.org/10.1016/0263-7855\(93\)80074-2](https://doi.org/10.1016/0263-7855(93)80074-2)
- Peng, T. Y., Lee, K. R., & Tarn, W. Y. (2008). Phosphorylation of the arginine/serine dipeptide-rich motif of the severe acute respiratory syndrome coronavirus nucleocapsid protein modulates its multimerization, translation inhibitory activity and cellular localization. *FEBS Journal*, 275(16), 4152-4163. doi: 10.1111/j.1742-4658.2008.06564.x
- Petherick, A. (2020). Developing antibody tests for SARS-CoV-2. *The Lancet*, 395(10230), 1101-1102. doi: 10.1016/S0140-6736(20)30788-1
- Pinto, D., Park, Y.-J., Beltramello, M., Walls, A. C., Tortorici, M. A., Bianchi, S., . . . Corti, D. (2020). Cross-neutralization of SARS-CoV-2 by a human monoclonal SARS-CoV antibody. *Nature*, 583(7815), 290-295. doi: 10.1038/s41586-020-2349-y
- Pohl-Koppe, A., Raabe, T., Siddell, S. G., & ter Meulen, V. (1995). Detection of human coronavirus 229E-specific antibodies using recombinant fusion proteins. *Journal of Virological Methods*, 55(2), 175-183. doi: [https://doi.org/10.1016/0166-0934\(95\)00041-R](https://doi.org/10.1016/0166-0934(95)00041-R)
- Polack, F. P., Thomas, S. J., Kitchin, N., Absalon, J., Gurtman, A., Lockhart, S., . . . Gruber, W. C. (2020). Safety and Efficacy of the BNT162b2 mRNA Covid-19 Vaccine. *New England Journal of Medicine*, 383(27), 2603-2615. doi: 10.1056/NEJMoa2034577
- Ponder, J. W., & Case, D. A. (2003). Force fields for protein simulations. *Advances in Protein Chemistry*, 66, 27-85.
- Portolano, N., Watson, P. J., Fairall, L., Millard, C. J., Milano, C. P., Song, Y., . . . Schwabe, J. W. (2014). Recombinant protein expression for structural biology in HEK 293F suspension cells: a novel and accessible approach. *JoVE (Journal of Visualized Experiments)*(92), e51897.
- Possee, R., Chambers, A., Graves, L., Aksular, M., & King, L. (2019). Recent Developments in the Use of Baculovirus Expression Vectors. *Current Issues in Molecular Biology*, 34, 215-230. doi: 10.21775/cimb.034.215
- Possee, R. D. (1993). Baculovirus expression vectors — A laboratory manual: by D. R. O'Reilly, L. K. Miller and V. A. Luckow, W. H. Freeman, 1992. UK£39.95 (xiii + 347 pages) ISBN 0 7167 7017 2. *Trends in Biotechnology*, 11(6), 267-268. doi: 10.1016/0167-7799(93)90146-Z
- Possee, R. D. (1997). Baculoviruses as expression vectors. *Current Opinion in Biotechnology*, 8(5), 569-572.
- Posthuma, C. C., Nedialkova, D. D., Zevenhoven-Dobbe, J. C., Blokhuis, J. H., Gorbalenya, A. E., & Snijder, E. J. (2006). Site-Directed Mutagenesis of the Nidovirus Replicative Endoribonuclease NendoU Exerts Pleiotropic Effects on the Arterivirus Life Cycle. *Journal of Virology*, 80(4), 1653-1661. doi: 10.1128/jvi.80.4.1653-1661.2006

- Poutanen, S. M. (2018). Human Coronaviruses. *Principles and Practice of Pediatric Infectious Diseases*, 1148-1152.e1143. doi: 10.1016/B978-0-323-40181-4.00222-X
- Poutanen, S. M., Low, D. E., Henry, B., Finkelstein, S., Rose, D., Green, K., . . . Ayers, M. (2003). Identification of severe acute respiratory syndrome in Canada. *New England Journal of Medicine*, 348(20), 1995-2005.
- Prabakaran, P., Zhu, Z., Xiao, X., Biragyn, A., Dimitrov, A. S., Broder, C. C., & Dimitrov, D. S. (2009). Potent human monoclonal antibodies against SARS CoV, Nipah and Hendra viruses. *Expert Opinion on Biological Therapy*, 9(3), 355-368.
- Principi, N., Bosis, S., & Esposito, S. (2010). Effects of coronavirus infections in children. *Emerging Infectious Diseases*, 16(2), 183.
- Pyrk, K., Berkhout, B., & van der Hoek, L. (2005). Molecular characterization of human coronavirus NL63. *Recent Research in Development of Infection & Immunity*, 3, 25-48.
- Pyrk, K., Berkhout, B., & van der Hoek, L. (2007). The novel human coronaviruses NL63 and HKU1. *Journal of Virology*, 81(7), 3051-3057.
- Pyrk, K., Dijkman, R., Deng, L., Jebbink, M. F., Ross, H. A., Berkhout, B., & Van der Hoek, L. (2006). Mosaic structure of human coronavirus NL63, one thousand years of evolution. *Journal of Molecular Biology*, 364(5), 964-973.
- Pyrk, K., Jebbink, M. F., Berkhout, B., & van der Hoek, L. (2004). Genome structure and transcriptional regulation of human coronavirus NL63. *Virology Journal*, 1(1), 7. doi: 10.1186/1743-422X-1-7
- Qiu, H., Sun, S., Xiao, H., Feng, J., Guo, Y., Tai, W., . . . Zhou, Y. (2016). Single-dose treatment with a humanized neutralizing antibody affords full protection of a human transgenic mouse model from lethal Middle East respiratory syndrome (MERS)-coronavirus infection. *Antiviral Research*, 132, 141-148.
- Qiu, M., Shi, Y., Guo, Z., Chen, Z., He, R., Chen, R., . . . Yang, R. (2005). Antibody responses to individual proteins of SARS coronavirus and their neutralization activities. *Microbes and Infection*, 7(5-6), 882-889. doi: 10.1016/j.micinf.2005.02.006
- Qu, P., Zhang, C., Li, M., Ma, W., Xiong, P., Liu, Q., . . . Huang, Z. (2020). A new class of broadly neutralizing antibodies that target the glycan loop of Zika virus envelope protein. *Cell Discovery*, 6(1), 5. doi: 10.1038/s41421-019-0140-8
- Raamsman, M. J. B., Locker, J. K., de Hooge, A., de Vries, A. A. F., Griffiths, G., Vennema, H., & Rottier, P. J. M. (2000). Characterization of the Coronavirus Mouse Hepatitis Virus Strain A59 Small Membrane Protein E. *Journal of Virology*, 74(5), 2333-2342. doi: 10.1128/jvi.74.5.2333-2342.2000

- Raj, V. S., Osterhaus, A. D., Fouchier, R. A., & Haagmans, B. L. (2014). MERS: emergence of a novel human coronavirus. *Current Opinion in Virology*, 5, 58-62. doi: 10.1016/j.coviro.2014.01.010
- Ramaraj, T., Angel, T., Dratz, E. A., Jesaitis, A. J., & Mumei, B. (2012). Antigen-antibody interface properties: composition, residue interactions, and features of 53 non-redundant structures. *Biochimica et Biophysica Acta*, 1824(3), 520-532. doi: 10.1016/j.bbapap.2011.12.007
- Rancour, D. M., Backues, S. K., & Bednarek, S. Y. (2010). Protein antigen expression in Escherichia coli for antibody production. *Methods in Molecular Biology*, 657, 3-20. doi: 10.1007/978-1-60761-783-9_1
- Raoult, D., Zumla, A., Locatelli, F., Ippolito, G., & Kroemer, G. (2020). Coronavirus infections: Epidemiological, clinical and immunological features and hypotheses. *Cell Stress*, 4(4), 66-75. doi: 10.15698/cst2020.04.216
- Rathnayake, A. D., Zheng, J., Kim, Y., Perera, K. D., Mackin, S., Meyerholz, D. K., . . . Chang, K.-O. (2020). 3C-like protease inhibitors block coronavirus replication in vitro and improve survival in MERS-CoV-infected mice. *Science Translational Medicine*, 12(557), eabc5332. doi: 10.1126/scitranslmed.abc5332
- Ratia, K., Saikatendu, K. S., Santarsiero, B. D., Barretto, N., Baker, S. C., Stevens, R. C., & Mesecar, A. D. (2006). Severe acute respiratory syndrome coronavirus papain-like protease: Structure of a viral deubiquitinating enzyme. *Proceedings of the National Academy of Sciences of the United States of America (PNAS)*, 103(15), 5717-5722. doi: 10.1073/pnas.0510851103
- Raval, A., Piana, S., Eastwood, M. P., Dror, R. O., & Shaw, D. E. (2012). Refinement of protein structure homology models via long, all-atom molecular dynamics simulations. *Proteins: Structure, Function, and Bioinformatics*, 80(8), 2071-2079.
- Reed, M. L., Dove, B. K., Jackson, R. M., Collins, R., Brooks, G., & Hiscox, J. A. (2006). Delineation and modelling of a nucleolar retention signal in the coronavirus nucleocapsid protein. *Traffic*, 7(7), 833-848.
- Ren, A.-X., Xie, Y.-H., Kong, Y.-Y., Yang, G.-Z., Zhang, Y.-Z., Wang, Y., & Wu, X.-F. (2004). Expression, purification and sublocalization of SARS-CoV nucleocapsid protein in insect cells. *Acta Biochimica et Biophysica Sinica*, 36(11), 754-758.
- Ricagno, S., Egloff, M.-P., Ulferts, R., Coutard, B., Nurizzo, D., Campanacci, V., . . . Canard, B. (2006). Crystal structure and mechanistic determinants of SARS coronavirus nonstructural protein 15 define an endoribonuclease family. *Proceedings of the National Academy of Sciences of the United States of America (PNAS)*, 103(32), 11892-11897. doi: 10.1073/pnas.0601708103
- Rice, P., Longden, I., & Bleasby, A. (2000). EMBOSS: the European molecular biology open software suite. *Trends in Genetics : TIG*, 16(6), 276-277.

- Richard, M., Knauf, S., Lawrence, P., Mather, A. E., Munster, V. J., Müller, M. A., . . . Kuiken, T. (2017). Factors determining human-to-human transmissibility of zoonotic pathogens via contact. *Current Opinion in Virology*, 22, 7-12. doi: 10.1016/j.coviro.2016.11.004
- Ringler, D. H., & Newcomer, C. E. (2014). *The biology of the laboratory rabbit* (2nd ed.): Academic Press.
- Risco, C., Antón, I. M., Suñé, C., Pedregosa, A. M., Martín-Alonso, J. M., Parra, F., . . . Enjuanes, L. (1995). Membrane protein molecules of transmissible gastroenteritis coronavirus also expose the carboxy-terminal region on the external surface of the virion. *Journal of Virology*, 69(9), 5269-5277.
- Roberts, B. (1989). Nuclear location signal-mediated protein transport. *Biochimica et Biophysica Acta (BBA) - Gene Structure and Expression*, 1008(3), 263-280. doi: [https://doi.org/10.1016/0167-4781\(89\)90016-X](https://doi.org/10.1016/0167-4781(89)90016-X)
- Rodrigues, R. L., Menezes, G. D. L., Saivish, M. V., Costa, V. G. D., Pereira, M., Moreli, M. L., & Silva, R. A. D. (2019). Prediction of MAYV peptide antigens for immunodiagnostic tests by immunoinformatics and molecular dynamics simulations. *Scientific Reports*, 9(1), 13339. doi: 10.1038/s41598-019-50008-3
- Rogers, T. F., Zhao, F., Huang, D., Beutler, N., Burns, A., He, W.-t., . . . Burton, D. R. (2020). Isolation of potent SARS-CoV-2 neutralizing antibodies and protection from disease in a small animal model. *Science*, 369(6506), 956-963. doi: 10.1126/science.abc7520
- Rosa, C., Osborne, S., Garetto, F., Griva, S., Rivella, A., Calabresi, G., . . . Bonelli, F. (1995). Epitope mapping of the NS4 and NS5 gene products of hepatitis C virus and the use of a chimeric NS4-NS5 synthetic peptide for serodiagnosis. *Journal of Virological Methods*, 55(2), 219-232.
- Rota, P. A., Oberste, M. S., Monroe, S. S., Nix, W. A., Campagnoli, R., Icenogle, J. P., . . . Chen, M.-h. (2003). Characterization of a novel coronavirus associated with severe acute respiratory syndrome. *Science*, 300(5624), 1394-1399.
- Rottier, P. (1995). *The Coronaviridae*: Plenum Press, New York.
- Rottier, P., Brandenburg, D., Armstrong, J., van der Zeijst, B., & Warren, G. (1984). Assembly in vitro of a spanning membrane protein of the endoplasmic reticulum: the E1 glycoprotein of coronavirus mouse hepatitis virus A59. *Proceedings of the National Academy of Sciences of the United States of America*, 81(5), 1421-1425. doi: 10.1073/pnas.81.5.1421
- Rottier, P. J. M., Welling, G. W., Welling-Wester, S., Niesters, H. G. M., Lenstra, J. A., & Van der Zeijst, B. A. M. (1986). Predicted membrane topology of the coronavirus protein E1. *Biochemistry*, 25(6), 1335-1339. doi: 10.1021/bi00354a022
- Rowland, R., Kervin, R., Kuckleburg, C., Sperlich, A., & Benfield, D. A. (1999). The localization of porcine reproductive and respiratory syndrome virus nucleocapsid protein to the nucleolus of

- infected cells and identification of a potential nucleolar localization signal sequence. *Virus Research*, 64(1), 1-12.
- Rowland, R. R. R., Chauhan, V., Fang, Y., Pekosz, A., Kerrigan, M., & Burton, M. D. (2005). Intracellular localization of the severe acute respiratory syndrome coronavirus nucleocapsid protein: absence of nucleolar accumulation during infection and after expression as a recombinant protein in vero cells. *Journal of Virology*, 79(17), 11507-11512. doi: 10.1128/JVI.79.17.11507-11512.2005
- Rubin, E. J., & Longo, D. L. (2020). SARS-CoV-2 Vaccination — An Ounce (Actually, Much Less) of Prevention. *New England Journal of Medicine*, 383(27), 2677-2678. doi: 10.1056/NEJMe2034717
- Rucinski, S. L., Binnicker, M. J., Thomas, A. S., & Patel, R. (2020). Seasonality of Coronavirus 229E, HKU1, NL63, and OC43 From 2014 to 2020. *Mayo Clinic Proceedings*, 95(8), 1701-1703. doi: <https://doi.org/10.1016/j.mayocp.2020.05.032>
- Sadler, K., & Tam, J. P. (2002). Peptide dendrimers: applications and synthesis. *Reviews in Molecular Biotechnology*, 90(3-4), 195-229.
- Sagar, M., Reifler, K., Rossi, M., Miller, N. S., Sinha, P., White, L., & Mizgerd, J. P. (2020). Recent endemic coronavirus infection is associated with less severe COVID-19. *The Journal of Clinical Investigation*, 131(1), e143380. doi: 10.1172/JCI143380
- Saha, S., & Raghava, G. P. S. (2004). *BcePred: prediction of continuous B-cell epitopes in antigenic sequences using physico-chemical properties*. Paper presented at the International Conference on Artificial Immune Systems.
- Sakai, Y., Kawachi, K., Terada, Y., Omori, H., Matsuura, Y., & Kamitani, W. (2017). Two-amino acids change in the nsp4 of SARS coronavirus abolishes viral replication. *Virology*, 510, 165-174. doi: <https://doi.org/10.1016/j.virol.2017.07.019>
- Salk, J. E., & Laurent, A. M. (1952). The use of adjuvants in studies on influenza immunization i. measurements in monkeys of the dimensions of antigenicity of virus-mineral oil emulsions. *Journal of Experimental Medicine*, 95(5), 429-447.
- Saravanan, P., Kataria, J., & Rasool, T. (2004). Detection of Infectious bursal disease virus by ELISA using an antipeptide antibody raised against VP3 region. *Acta Virologica*, 48(1), 39-45.
- Sarna, M., Lambert, S. B., Sloots, T. P., Whiley, D. M., Alsaleh, A., Mhango, L., . . . Ware, R. S. (2018). Viruses causing lower respiratory symptoms in young children: findings from the ORChID birth cohort. *Thorax*, 73(10), 969-979. doi: 10.1136/thoraxjnl-2017-210233
- Sastre, P., Dijkman, R., Camuñas, A., Ruiz, T., Jebbink, M. F., van der Hoek, L., . . . Rueda, P. (2011). Differentiation between human coronaviruses NL63 and 229E using a novel double-

- antibody sandwich enzyme-linked immunosorbent assay based on specific monoclonal antibodies. *Clin Vaccine Immunol*, 18(1), 113-118. doi: 10.1128/cvi.00355-10
- Sawicki, S. G., Sawicki, D. L., Younker, D., Meyer, Y., Thiel, V., Stokes, H., & Siddell, S. G. (2005). Functional and Genetic Analysis of Coronavirus Replicase-Transcriptase Proteins. *Public Library of Science (PLOS) Pathogens*, 1(4), e39. doi: 10.1371/journal.ppat.0010039
- Schaecher, S. R., & Pekosz, A. (2009). SARS Coronavirus Accessory Gene Expression and Function. *Molecular Biology of the SARS-Coronavirus*, 153-166. doi: 10.1007/978-3-642-03683-5_10
- Schagat, T., Friedman-Ohana, R., Otto, P., Hartnett, J., & Slater, M. (2008). KRX autoinduction protocol: a convenient method for protein expression. *Promega Notes*, 98, 16-18.
- Schelle, B., Karl, N., Ludewig, B., Siddell, S. G., & Thiel, V. (2006). Nucleocapsid protein expression facilitates coronavirus replication. *Advances in Experimental Medicine and Biology*, 581, 43-48.
- Schievano, E., Calisti, T., Menegazzo, I., Battistutta, R., Peggion, E., Mammi, S., . . . Loregian, A. (2004). pH-Dependent conformational changes and topology of a herpesvirus translocating peptide in a membrane-mimetic environment. *Biochemistry*, 43(29), 9343-9351. doi: 10.1021/bi0496438
- Schmidt, P. M., Sparrow, L. G., Attwood, R. M., Xiao, X., Adams, T. E., & McKimm-Breschkin, J. L. (2012). Taking down the FLAG! How insect cell expression challenges an established tag-system. *PLoS One*, 7(6), e37779.
- Schweiger, R., & Linial, M. (2010). Cooperativity within proximal phosphorylation sites is revealed from large-scale proteomics data. *Biology Direct*, 5(1), 6.
- SERENA, M. S., METZ, G. E., PANELI, C. J., LARSEN, A. E., ASPITIA, C., PALACIOS, M., . . . ECHEVERRIA, M. G. (2015). *Development of an AGID based on baculovirus expressed Pseudorabies virus glycoprotein B*. Paper presented at the IMMUNOCOLOMBIA 2015 - 11th Congress of the Latin American Association of Immunology, Medellin, Colombia. Abstract retrieved from http://www.frontiersin.org/Journal/FullText.aspx?f=35&name=immunology&ART_DOI=10.3389/conf.fimmu.2015.05.00236
- Shaman, J., & Galanti, M. (2020). Will SARS-CoV-2 become endemic? *Science*, 370(6516), 527-529. doi: 10.1126/science.abe5960
- Shang, J., Ye, G., Shi, K., Wan, Y., Luo, C., Aihara, H., . . . Li, F. (2020). Structural basis of receptor recognition by SARS-CoV-2. *Nature*, 581(7807), 221-224. doi: 10.1038/s41586-020-2179-y
- Sharma, A., Tiwari, S., Deb, M. K., & Marty, J. L. (2020). Severe acute respiratory syndrome coronavirus-2 (SARS-CoV-2): a global pandemic and treatment strategies. *International*

Journal of Antimicrobial Agents, 56(2), 106054-106054. doi:
10.1016/j.ijantimicag.2020.106054

- Shen, C., Wang, Z., Zhao, F., Yang, Y., Li, J., Yuan, J., . . . Xing, L. (2020). Treatment of 5 critically ill patients with COVID-19 with convalescent plasma. *Jama*, 323(16), 1582-1589.
- Shi, X., & Jarvis, D. L. (2007). Protein N-glycosylation in the baculovirus-insect cell system. *Current Drug Targets*, 8(10), 1116-1125. doi: 10.2174/138945007782151360
- Shin, G.-C., Chung, Y.-S., Kim, I.-S., Cho, H.-W., & Kang, C. (2007). Antigenic characterization of severe acute respiratory syndrome-coronavirus nucleocapsid protein expressed in insect cells: The effect of phosphorylation on immunoreactivity and specificity. *Virus Research*, 127(1), 71-80.
- Shirakawa, F., & Mizel, S. B. (1989). In vitro activation and nuclear translocation of NF-kappa B catalyzed by cyclic AMP-dependent protein kinase and protein kinase C. *Molecular and Cellular Biology*, 9(6), 2424-2430.
- Shirkoochi, R., Endo, R., Ishiguro, N., Teramoto, S., Kikuta, H., & Ariga, T. (2010). Antibodies against structural and nonstructural proteins of human bocavirus in human sera. *Clinical and Vaccine Immunology : CVI*, 17(1), 190-193. doi: 10.1128/CVI.00355-09
- Shurtleff, A. C., Biggins, J. E., Keeney, A. E., Zumbrun, E. E., Bloomfield, H. A., Kuehne, A., . . . Olinger, G. G. (2012). Standardization of the filovirus plaque assay for use in preclinical studies. *Viruses*, 4(12), 3511-3530.
- Siddell, S., Wege, H., Barthel, A., & ter Meulen, V. (1981). Intracellular Protein Synthesis and the inVitro Translation of Coronavirus JHM mRNA. *Advances in Experimental Medicine and Biology*, 142, 193-207. doi: 10.1007/978-1-4757-0456-3_17
- Siddell, S. G. (1995). The Coronaviridae. In S. G. Siddell (Ed.), *The Coronaviridae* (pp. 1-10). Boston, MA: Springer US.
- Siu, Y. L., Teoh, K. T., Lo, J., Chan, C. M., Kien, F., Escriou, N., . . . Nal, B. (2008). The M, E, and N Structural Proteins of the Severe Acute Respiratory Syndrome Coronavirus Are Required for Efficient Assembly, Trafficking, and Release of Virus-Like Particles. *Journal of Virology*, 82(22), 11318-11330. doi: 10.1128/jvi.01052-08
- Slater-Handshy, T., Droll, D. A., Fan, X., Di Bisceglie, A. M., & Chambers, T. J. (2004). HCV E2 glycoprotein: mutagenesis of N-linked glycosylation sites and its effects on E2 expression and processing. *Virology*, 319(1), 36-48. doi: 10.1016/j.virol.2003.10.008
- Smith, E. C., Sexton, N. R., & Denison, M. R. (2014). Thinking Outside the Triangle: Replication Fidelity of the Largest RNA Viruses. *Annual Review of Virology*, 1(1), 111-132. doi: 10.1146/annurev-virology-031413-085507

- Smith, G. E., Fraser, M. J., & Summers, M. D. (1983). Molecular Engineering of the *Autographa californica* Nuclear Polyhedrosis Virus Genome: Deletion Mutations Within the Polyhedrin Gene. *Journal of Virology*, *46*(2), 584-593.
- Smith, G. E., Summers, M. D., & Fraser, M. J. (1983). Production of human beta interferon in insect cells infected with a baculovirus expression vector. *Molecular and Cellular Biology*, *3*(12), 2156-2165. doi: 10.1128/mcb.3.12.2156
- Snijder, E. J., Bredenbeek, P. J., Dobbe, J. C., Thiel, V., Ziebuhr, J., Poon, L. L. M., . . . Gorbalenya, A. E. (2003). Unique and Conserved Features of Genome and Proteome of SARS-coronavirus, an Early Split-off From the Coronavirus Group 2 Lineage. *Journal of Molecular Biology*, *331*(5), 991-1004. doi: [https://doi.org/10.1016/S0022-2836\(03\)00865-9](https://doi.org/10.1016/S0022-2836(03)00865-9)
- Snijder, E. J., Decroly, E., & Ziebuhr, J. (2016). *The Nonstructural Proteins Directing Coronavirus RNA Synthesis and Processing* (Vol. 96).
- Song, W., Gui, M., Wang, X., & Xiang, Y. (2018). Cryo-EM structure of the SARS coronavirus spike glycoprotein in complex with its host cell receptor ACE2. *PLoS pathogens*, *14*(8), e1007236.
- Sørensen, H. P. (2010). Towards universal systems for recombinant gene expression. *Microbial Cell Factories*, *9*(1), 27.
- Spencer, K.-A., Osorio, F. A., & Hiscox, J. A. (2007). Recombinant viral proteins for use in diagnostic ELISAs to detect virus infection. *Vaccine*, *25*(30), 5653-5659. doi: 10.1016/j.vaccine.2007.02.053
- Spencer, R., & Lee, J. (2006). Large noncoding RNAs in mammalian gene dosage regulation *COLD SPRING HARBOR MONOGRAPH SERIES* (Vol. 43, pp. 595).
- Steentoft, C., Vakhrushev, S. Y., Joshi, H. J., Kong, Y., Vester-Christensen, M. B., Schjoldager, K. T., . . . Clausen, H. (2013). Precision mapping of the human O-GalNAc glycoproteome through SimpleCell technology. *EMBO Journal*, *32*(10), 1478-1488. doi: 10.1038/emboj.2013.79
- Stern, D. F., & Sefton, B. M. (1982). Coronavirus proteins: structure and function of the oligosaccharides of the avian infectious bronchitis virus glycoproteins. *Journal of Virology*, *44*(3), 804-812.
- Stertz, S., Reichelt, M., Spiegel, M., Kuri, T., Martínez-Sobrido, L., García-Sastre, A., . . . Kochs, G. (2007). The intracellular sites of early replication and budding of SARS-coronavirus. *Virology*, *361*(2), 304-315. doi: <https://doi.org/10.1016/j.virol.2006.11.027>
- Steven, S., Yen Ting, L., Chonggang, X., Ethan, R.-S., Nick, H., & Ruian, K. (2020). High Contagiousness and Rapid Spread of Severe Acute Respiratory Syndrome Coronavirus 2. *Emerging Infectious Disease Journal*, *26*(7), 1470-1477. doi: 10.3201/eid2607.200282

- Stewart, R. C. (2010). Protein histidine kinases: assembly of active sites and their regulation in signaling pathways. *Current Opinion in Microbiology*, 13(2), 133-141. doi: 10.1016/j.mib.2009.12.013
- Stohlman, S. A., Fleming, J. O., Patton, C. D., & Lai, M. M. (1983). Synthesis and subcellular localization of the murine coronavirus nucleocapsid protein. *Virology*, 130(2), 527-532.
- Sturman, L. S., Holmes, K., & Behnke, J. (1980). Isolation of coronavirus envelope glycoproteins and interaction with the viral nucleocapsid. *Journal of Virology*, 33(1), 449-462.
- Subissi, L., Posthuma, C. C., Collet, A., Zevenhoven-Dobbe, J. C., Gorbalenya, A. E., Decroly, E., . . . Imbert, I. (2014). One severe acute respiratory syndrome coronavirus protein complex integrates processive RNA polymerase and exonuclease activities. *Proceedings of the National Academy of Sciences of the United States of America (PNAS)*, 111(37), E3900-3909. doi: 10.1073/pnas.1323705111
- Sui, J., Li, W., Murakami, A., Tamin, A., Matthews, L. J., Wong, S. K., . . . Marasco, W. A. (2004). Potent neutralization of severe acute respiratory syndrome (SARS) coronavirus by a human mAb to S1 protein that blocks receptor association. *Proceedings of the National Academy of Sciences of the United States of America*, 101(8), 2536-2541. doi: 10.1073/pnas.0307140101
- Sui, J., Li, W., Roberts, A., Matthews, L. J., Murakami, A., Vogel, L., . . . Marasco, W. A. (2005). Evaluation of human monoclonal antibody 80R for immunoprophylaxis of severe acute respiratory syndrome by an animal study, epitope mapping, and analysis of spike variants. *Journal of Virology*, 79(10), 5900-5906. doi: 10.1128/jvi.79.10.5900-5906.2005
- Sun, Y., Kobe, B., & Qi, J. (2020). Targeting multiple epitopes on the spike protein: a new hope for COVID-19 antibody therapy. *Signal Transduction and Targeted Therapy*, 5(1), 208. doi: 10.1038/s41392-020-00320-6
- Surjit, M., Kumar, R., Mishra, R. N., Reddy, M. K., Chow, V. T., & Lal, S. K. (2005). The severe acute respiratory syndrome coronavirus nucleocapsid protein is phosphorylated and localizes in the cytoplasm by 14-3-3-mediated translocation. *J Virol*, 79(17), 11476-11486. doi: 10.1128/jvi.79.17.11476-11486.2005
- Surjit, M., Liu, B., Chow, V. T., & Lal, S. K. (2006). The nucleocapsid protein of severe acute respiratory syndrome-coronavirus inhibits the activity of cyclin-cyclin-dependent kinase complex and blocks S phase progression in mammalian cells. *Journal of Biological Chemistry*, 281(16), 10669-10681.
- Surjit, M., Liu, B., Jameel, S., Chow, V. T., & Lal, S. K. (2004). The SARS coronavirus nucleocapsid protein induces actin reorganization and apoptosis in COS-1 cells in the absence of growth factors. *Biochemical Journal*, 383(1), 13-18.

- Szelazek, B., Kabala, W., Kus, K., Zdzalik, M., Twarda-Clapa, A., Golik, P., . . . Dubin, G. (2017). Structural Characterization of Human Coronavirus NL63 N Protein. *Journal of Virology*, 91(11), e02503-02516. doi: 10.1128/JVI.02503-16
- Szybalski, W. (1992). Use of the HPRT gene and the HAT selection technique in DNA-mediated transformation of mammalian cells: first steps toward developing hybridoma techniques and gene therapy. *Bioessays*, 14(7), 495-500. doi: 10.1002/bies.950140712
- Tahara, S. M., Dietlin, T. A., Bergmann, C. C., Nelson, G. W., Kyuwa, S., Anthony, R. P., & Stohlman, S. A. (1994). Coronavirus translational regulation: leader affects mRNA efficiency. *Virology*, 202(2), 621-630.
- Tai, W., Zhao, G., Sun, S., Guo, Y., Wang, Y., Tao, X., . . . Zhou, Y. (2016). A recombinant receptor-binding domain of MERS-CoV in trimeric form protects human dipeptidyl peptidase 4 (hDPP4) transgenic mice from MERS-CoV infection. *Virology*, 499, 375-382. doi: 10.1016/j.virol.2016.10.005
- Tan, J. H., Ludeman, J. P., Wedderburn, J., Canals, M., Hall, P., Butler, S. J., . . . Payne, R. J. (2013). Tyrosine sulfation of chemokine receptor CCR2 enhances interactions with both monomeric and dimeric forms of the chemokine monocyte chemoattractant protein-1 (MCP-1). *Journal of Biological Chemistry*, 288(14), 10024-10034.
- Tang, J., Zhang, N., Tao, X., Zhao, G., Guo, Y., Tseng, C.-T. K., . . . Zhou, Y. (2015). Optimization of antigen dose for a receptor-binding domain-based subunit vaccine against MERS coronavirus. *Human Vaccines & Immunotherapeutics*, 11(5), 1244-1250. doi: 10.1080/21645515.2015.1021527
- Tang, X.-C., Agnihothram, S. S., Jiao, Y., Stanhope, J., Graham, R. L., Peterson, E. C., . . . Marasco, W. A. (2014). Identification of human neutralizing antibodies against MERS-CoV and their role in virus adaptive evolution. *Proceedings of the National Academy of Sciences*, 111(19), E2018-E2026. doi: 10.1073/pnas.1402074111
- te Velthuis, A. J., van den Worm, S. H., & Snijder, E. J. (2012). The SARS-coronavirus nsp7+nsp8 complex is a unique multimeric RNA polymerase capable of both de novo initiation and primer extension. *Nucleic Acids Research*, 40(4), 1737-1747. doi: 10.1093/nar/gkr893
- te Velthuis, A. J. W. (2014). Common and unique features of viral RNA-dependent polymerases. *Cellular and Molecular Life Sciences*, 71(22), 4403-4420. doi: 10.1007/s00018-014-1695-z
- ter Meulen, J., Bakker, A. B. H., van den Brink, E. N., Weverling, G. J., Martina, B. E. E., Haagmans, B. L., . . . Osterhaus, A. D. M. E. (2004). Human monoclonal antibody as prophylaxis for SARS coronavirus infection in ferrets. *The Lancet*, 363(9427), 2139-2141. doi: https://doi.org/10.1016/S0140-6736(04)16506-9

- Thelwall, M. (2020). Coronavirus research before 2020 is more relevant than ever, especially when interpreted for COVID-19 *arXiv preprint arXiv:2006.03901* (pp. 1-15).
- Thiel, V., Ivanov, K. A., Putics, A., Hertzog, T., Schelle, B., Bayer, S., . . . Doerr, H. W. (2003). Mechanisms and enzymes involved in SARS coronavirus genome expression. *Journal of General Virology*, *84*(9), 2305-2315.
- Thompson, C. M., Aucoin, M. G., & Kamen, A. A. (2016). Production of virus-like particles for vaccination *Baculovirus and Insect Cell Expression Protocols* (Vol. 1350, pp. 299-315): Springer.
- Tian, X., Li, C., Huang, A., Xia, S., Lu, S., Shi, Z., . . . Ying, T. (2020). Potent binding of 2019 novel coronavirus spike protein by a SARS coronavirus-specific human monoclonal antibody. *Emerging Microbes & Infections*, *9*(1), 382-385. doi: 10.1080/22221751.2020.1729069
- Tijms, M. A., van der Meer, Y., & Snijder, E. J. (2002). Nuclear localization of non-structural protein 1 and nucleocapsid protein of equine arteritis virus. *J Gen Virol*, *83*(Pt 4), 795-800. doi: 10.1099/0022-1317-83-4-795
- Tilocca, B., Soggiu, A., Sanguinetti, M., Musella, V., Britti, D., Bonizzi, L., . . . Roncada, P. (2020). Comparative computational analysis of SARS-CoV-2 nucleocapsid protein epitopes in taxonomically related coronaviruses. *Microbes and Infection*, *22*(4), 188-194. doi: <https://doi.org/10.1016/j.micinf.2020.04.002>
- Timani, K. A., Liao, Q., Ye, L., Zeng, Y., Liu, J., Zheng, Y., . . . Zhu, Y. (2005). Nuclear/nucleolar localization properties of C-terminal nucleocapsid protein of SARS coronavirus. *Virus Research*, *114*(1-2), 23-34. doi: 10.1016/j.virusres.2005.05.007
- Timani, K. A., Ye, L., Ye, L., Zhu, Y., Wu, Z., & Gong, Z. (2004). Cloning, sequencing, expression, and purification of SARS-associated coronavirus nucleocapsid protein for serodiagnosis of SARS. *Journal of Clinical Virology*, *30*(4), 309-312.
- Tomar, S., Johnston, M. L., St John, S. E., Osswald, H. L., Nyalapatla, P. R., Paul, L. N., . . . Mesecar, A. D. (2015). Ligand-induced Dimerization of Middle East Respiratory Syndrome (MERS) Coronavirus nsp5 Protease (3CLpro): IMPLICATIONS FOR nsp5 REGULATION AND THE DEVELOPMENT OF ANTIVIRALS. *The Journal of Biological Chemistry*, *290*(32), 19403-19422. doi: 10.1074/jbc.M115.651463
- Traggiai, E., Becker, S., Subbarao, K., Kolesnikova, L., Uematsu, Y., Gismondo, M. R., . . . Lanzavecchia, A. (2004). An efficient method to make human monoclonal antibodies from memory B cells: potent neutralization of SARS coronavirus. *Nature Medicine*, *10*(8), 871-875. doi: 10.1038/nm1080
- Trier, N., Hansen, P., & Houen, G. (2019). Peptides, Antibodies, Peptide Antibodies and More. *International Journal of Molecular Sciences*, *20*(24), 6289. doi: 10.3390/ijms20246289

- Tripathi, N. K., & Shrivastava, A. (2019). Recent Developments in Bioprocessing of Recombinant Proteins: Expression Hosts and Process Development. *Frontiers in Bioengineering and Biotechnology*, 7(420). doi: 10.3389/fbioe.2019.00420
- Trowitzsch, S., Bieniossek, C., Nie, Y., Garzoni, F., & Berger, I. (2010). New baculovirus expression tools for recombinant protein complex production. *Journal of Structural Biology*, 172(1), 45-54.
- Tseng, Y.-T., Wang, S.-M., Huang, K.-J., Lee, A. I. R., Chiang, C.-C., & Wang, C.-T. (2010). Self-assembly of severe acute respiratory syndrome coronavirus membrane protein. *The Journal of Biological Chemistry*, 285(17), 12862-12872. doi: 10.1074/jbc.M109.030270
- Tyrrell, D., & Bynoe, M. (1965). Cultivation of a novel type of common-cold virus in organ cultures. *British Medical Journal*, 1(5448), 1467.
- Tyrrell, D. A., & Bynoe, M. L. (1966). Cultivation of viruses from a high proportion of patients with colds. *The Lancet*, 1(7428), 76-77. doi: 10.1016/s0140-6736(66)92364-6
- Ujike, M., & Taguchi, F. (2015). Incorporation of spike and membrane glycoproteins into coronavirus virions. *Viruses*, 7(4), 1700-1725.
- Uma, M., Rao, P. P., Nagalekshmi, K., & Hegde, N. R. (2016). Expression and purification of polioviral proteins in *E. coli*, and production of antisera as reagents for immunological assays. *Protein Expression and Purification*, 128, 115-122. doi: 10.1016/j.pep.2016.08.014
- Unal, E. S., Zhao, R., Qiu, A., & Goldman, I. D. (2008). N-linked glycosylation and its impact on the electrophoretic mobility and function of the human proton-coupled folate transporter (HsPCFT). *Biochimica et Biophysica Acta*, 1778(6), 1407-1414. doi: 10.1016/j.bbamem.2008.03.009
- van Boheemen, S., de Graaf, M., Lauber, C., Bestebroer, T. M., Raj, V. S., Zaki, A. M., . . . Fouchier, R. A. (2012). Genomic characterization of a newly discovered coronavirus associated with acute respiratory distress syndrome in humans. *MBio*, 3(6), e00473-00412. doi: 10.1128/mBio.00473-12
- van der Hoek, L., Pyrc, K., Jebbink, M. F., Vermeulen-Oost, W., Berkhout, R. J., Wolthers, K. C., . . . Berkhout, B. (2004). Identification of a new human coronavirus. *Nat Med*, 10(4), 368-373. doi: 10.1038/nm1024
- van der Mijl, J. C., Labots, M., Piersma, S. R., Pham, T. V., Knol, J. C., Broxterman, H. J., . . . Jiménez, C. R. (2015). Evaluation of different phospho-tyrosine antibodies for label-free phosphoproteomics. *Journal of Proteomics*, 127(Pt B), 259-263. doi: 10.1016/j.jprot.2015.04.006.
- Van Doremalen, N., Bushmaker, T., & Munster, V. (2013). Stability of Middle East respiratory syndrome coronavirus (MERS-CoV) under different environmental conditions. *Eurosurveillance*, 18(38), 20590.

- Van Griensven, J., Edwards, T., de Lamballerie, X., Semple, M. G., Gallian, P., Baize, S., . . . Antierens, A. (2016). Evaluation of convalescent plasma for Ebola virus disease in Guinea. *New England Journal of Medicine*, *374*(1), 33-42.
- Van Regenmortel, M. H. (2009). What is a B-cell epitope? *Methods in Molecular Biology (Clifton, N.J.)*, *524*, 3-20. doi: 10.1007/978-1-59745-450-6_1
- van Zutphen, L. F., Baumans, V., Beynen, A. C., & Restani, P. (1996). *Principles of laboratory animal science* (1st ed.): Elsevier.
- Veiga, A. B. G. d., Martins, L. G., Riediger, I., Mazetto, A., Debur, M. d. C., & Gregianini, T. S. More than just a common cold: Endemic coronaviruses OC43, HKU1, NL63, and 229E associated with severe acute respiratory infection and fatality cases among healthy adults. *Journal of Medical Virology*, *93*(2), 1002-1007. doi: 10.1002/jmv.26362
- Venkatesan, G., Balamurugan, V., Gandhale, P., Singh, R., & Bhanuprakash, V. (2010). Viral zoonosis: a comprehensive review. *Journal of Advanced Veterinary and Animal Research*, *5*(2), 77-92.
- Vennema, H., Godeke, G. J., Rossen, J. W., Voorhout, W. F., Horzinek, M. C., Opstelten, D. J., & Rottier, P. J. (1996). Nucleocapsid-independent assembly of coronavirus-like particles by co-expression of viral envelope protein genes. *The EMBO Journal*, *15*(8), 2020-2028.
- Verheije, M. H., Hagemeijer, M. C., Ulasli, M., Reggiori, F., Rottier, P. J., Masters, P. S., & de Haan, C. A. (2010). The coronavirus nucleocapsid protein is dynamically associated with the replication-transcription complexes. *Journal of Virology*, *84*(21), 11575-11579. doi: 10.1128/JVI.00569-10
- Verma, S., Lopez, L. A., Bednar, V., & Hogue, B. G. (2007). Importance of the Penultimate Positive Charge in Mouse Hepatitis Coronavirus A59 Membrane Protein. *Journal of Virology*, *81*(10), 5339-5348. doi: 10.1128/jvi.02427-06
- Vigerust, D. (2011). Protein glycosylation in infectious disease pathobiology and treatment. *Central European Journal of Biology*, *6*(5), 802. doi: 10.2478/s11535-011-0050-8
- Vigerust, D. J., & Shepherd, V. L. (2007). Virus glycosylation: role in virulence and immune interactions. *Trends in Microbiology*, *15*(5), 211-218. doi: 10.1016/j.tim.2007.03.003
- Vijgen, L., Keyaerts, E., Moës, E., Thoelen, I., Wollants, E., Lemey, P., . . . Van Ranst, M. (2005). Complete genomic sequence of human coronavirus OC43: molecular clock analysis suggests a relatively recent zoonotic coronavirus transmission event. *Journal of Virology*, *79*(3), 1595-1604.
- Vlasova, A. N., Zhang, X., Hasoksuz, M., Nagesha, H. S., Haynes, L. M., Fang, Y., . . . Saif, L. J. (2007). Two-way antigenic cross-reactivity between severe acute respiratory syndrome coronavirus (SARS-CoV) and group 1 animal CoVs is mediated through an antigenic site in

- the N-terminal region of the SARS-CoV nucleoprotein. *Journal of Virology*, 81(24), 13365-13377. doi: 10.1128/jvi.01169-07
- Volkman, L. E., & LE, V. (1977). Autographa californica nuclear polyhedrosis virus: comparative infectivity of the occluded, alkali-liberated, and nonoccluded forms. *Journal of Invertebrate Pathology*, 30(1), 102-103. doi: 10.1016/0022-2011(77)90045-3.
- Volkman, L. E., Summers, M. D., & Hsieh, C. H. (1976). Occluded and nonoccluded nuclear polyhedrosis virus grown in *Trichoplusia ni*: comparative neutralization comparative infectivity, and in vitro growth studies. *Journal of Virology*, 19(3), 820-832.
- Voß, D., Pfefferle, S., Drosten, C., Stevermann, L., Traggiai, E., Lanzavecchia, A., & Becker, S. (2009). Studies on membrane topology, N-glycosylation and functionality of SARS-CoV membrane protein. *Virology Journal*, 6(1), 79. doi: 10.1186/1743-422X-6-79
- Voysey, M., Clemens, S. A. C., Madhi, S. A., Weckx, L. Y., Folegatti, P. M., Aley, P. K., . . . Zuidewind, P. (2021). Safety and efficacy of the ChAdOx1 nCoV-19 vaccine (AZD1222) against SARS-CoV-2: an interim analysis of four randomised controlled trials in Brazil, South Africa, and the UK. *The Lancet*, 397(10269), 99-111. doi: 10.1016/S0140-6736(20)32661-1
- Wampler, J. (1996). Tutorial on peptide and protein structure *Athens: University of Georgia*.
- Wang, C., Li, W., Drabek, D., Okba, N. M. A., van Haperen, R., Osterhaus, A. D. M. E., . . . Bosch, B.-J. (2020). A human monoclonal antibody blocking SARS-CoV-2 infection. *Nature Communications*, 11(1), 2251. doi: 10.1038/s41467-020-16256-y
- Wang, J.-h. (2002). Protein recognition by cell surface receptors: Physiological receptors versus virus interactions. *Trends in Biochemical Sciences*, 27(3), 122-126. doi: 10.1016/S0968-0004(01)02038-2
- Wang, N., Shi, X., Jiang, L., Zhang, S., Wang, D., Tong, P., . . . Wang, X. (2013). Structure of MERS-CoV spike receptor-binding domain complexed with human receptor DPP4. *Cell Research*, 23(8), 986-993. doi: 10.1038/cr.2013.92
- Wang, R., & Brattain, M. G. (2007). The maximal size of protein to diffuse through the nuclear pore is larger than 60kDa. *FEBS Letters*, 581(17), 3164-3170. doi: 10.1016/j.febslet.2007.05.082
- Wang, Y., Li, X., Liu, W., Gan, M., Zhang, L., Wang, J., . . . Zhao, J. (2020). Discovery of a subgenotype of human coronavirus NL63 associated with severe lower respiratory tract infection in China, 2018. *Emerging Microbes & Infections*, 9(1), 246-255. doi: 10.1080/22221751.2020.1717999
- Wang, Y., Shi, H., Rigolet, P., Wu, N., Zhu, L., Xi, X.-G., . . . Wang, T. (2010). Nsp1 proteins of group I and SARS coronaviruses share structural and functional similarities. *Infection, Genetics and Evolution*, 10(7), 919-924.

- Warne, T., Chirnside, J., & Schertler, G. F. X. (2003). Expression and purification of truncated, non-glycosylated turkey beta-adrenergic receptors for crystallization. *Biochimica et Biophysica Acta (BBA) - Biomembranes*, 1610(1), 133-140. doi: [https://doi.org/10.1016/S0005-2736\(02\)00716-2](https://doi.org/10.1016/S0005-2736(02)00716-2)
- Watanabe, R., Sawicki, S. G., & Taguchi, F. (2007). Heparan sulfate is a binding molecule but not a receptor for CEACAM1-independent infection of murine coronavirus. *Virology*, 366(1), 16-22.
- Wathelet, M. G., Orr, M., Frieman, M. B., & Baric, R. S. (2007). Severe Acute Respiratory Syndrome Coronavirus Evades Antiviral Signaling: Role of nsp1 and Rational Design of an Attenuated Strain. *Journal of Virology*, 81(21), 11620-11633. doi: 10.1128/jvi.00702-07
- Webb, S., Morris, C., & Sprent, J. (1990). Extrathymic tolerance of mature T cells: Clonal elimination as a consequence of immunity. *Cell*, 63(6), 1249-1256. doi: 10.1016/0092-8674(90)90420-J
- Wei, X., Li, X., & Cui, J. (2020). Evolutionary perspectives on novel coronaviruses identified in pneumonia cases in China. *National Science Review*, 7(2), 239-242. doi: 10.1093/nsr/nwaa009
- Weill, C., Autelitano, F., Guenet, C., Heitz, F., Goeldner, M., & Ilien, B. (1997). Pharmacological and structural integrity of muscarinic M2 acetylcholine receptors produced in Sf9 insect cells. *European Journal of Pharmacology*, 333(2), 269-278. doi: [https://doi.org/10.1016/S0014-2999\(97\)01139-4](https://doi.org/10.1016/S0014-2999(97)01139-4)
- Weiss, S. R., & Navas-Martin, S. (2005). Coronavirus Pathogenesis and the Emerging Pathogen Severe Acute Respiratory Syndrome Coronavirus. *Microbiology and Molecular Biology Reviews*, 69(4), 635-664. doi: 10.1128/mmb.69.4.635-664.2005
- Weston, C. R., & Davis, R. J. (2007). The JNK signal transduction pathway. *Current Opinion in Cell Biology*, 19(2), 142-149. doi: 10.1016/j.ceb.2007.02.001
- White, T. C., Yi, Z., & Hogue, B. G. (2007). Identification of mouse hepatitis coronavirus A59 nucleocapsid protein phosphorylation sites. *Virus Research*, 126(1-2), 139-148.
- Widge, A. T., Roupael, N. G., Jackson, L. A., Anderson, E. J., Roberts, P. C., Makhene, M., . . . Beigel, J. H. (2020). Durability of Responses after SARS-CoV-2 mRNA-1273 Vaccination. *New England Journal of Medicine*, 384(1), 80-82. doi: 10.1056/NEJMc2032195
- Widjaja, I., Wang, C., van Haperen, R., Gutiérrez-Álvarez, J., van Dieren, B., Okba, N. M. A., . . . Bosch, B.-J. (2019). Towards a solution to MERS: protective human monoclonal antibodies targeting different domains and functions of the MERS-coronavirus spike glycoprotein. *Emerging Microbes & Infections*, 8(1), 516-530. doi: 10.1080/22221751.2019.1597644
- Wiersinga, W. J., Rhodes, A., Cheng, A. C., Peacock, S. J., & Prescott, H. C. (2020). Pathophysiology, transmission, diagnosis, and treatment of coronavirus disease 2019 (COVID-19): a review. *JAMA*, 324(8), 782-793.

- Womble, D. D. (2000). GCG: The Wisconsin Package of Sequence Analysis Programs *Bioinformatics methods and protocols* (Vol. 132, pp. 3-22): Springer.
- Wong, G., Liu, W., Liu, Y., Zhou, B., Bi, Y., & Gao, George F. (2015). MERS, SARS, and Ebola: The Role of Super-Spreaders in Infectious Disease. *Cell Host Microbe*, *18*(4), 398-401. doi: 10.1016/j.chom.2015.09.013
- Woo, P. C. Y., Lau, S. K. P., Chu, C.-m., Chan, K.-h., Tsoi, H.-w., Huang, Y., . . . Yuen, K.-y. (2005). Characterization and Complete Genome Sequence of a Novel Coronavirus, Coronavirus HKU1, from Patients with Pneumonia. *Journal of Virology*, *79*(2), 884-895. doi: 10.1128/jvi.79.2.884-895.2005
- Wrapp, D., Wang, N., Corbett, K. S., Goldsmith, J. A., Hsieh, C.-L., Abiona, O., . . . McLellan, J. S. (2020). Cryo-EM structure of the 2019-nCoV spike in the prefusion conformation. *Science*, *367*(6483), 1260-1263. doi: 10.1126/science.abb2507
- Wright, P. E., & Dyson, H. J. (2015). Intrinsically disordered proteins in cellular signalling and regulation. *Nature Reviews Molecular Cell Biology*, *16*(1), 18-29. doi: 10.1038/nrm3920
- Wu, A., Peng, Y., Huang, B., Ding, X., Wang, X., Niu, P., . . . Jiang, T. (2020). Genome Composition and Divergence of the Novel Coronavirus (2019-nCoV) Originating in China. *Cell Host & Microbe*, *27*(3), 325-328. doi: https://doi.org/10.1016/j.chom.2020.02.001
- Wu, C.-H., Chen, P.-J., & Yeh, S.-H. (2014). Nucleocapsid phosphorylation and RNA helicase DDX1 recruitment enables coronavirus transition from discontinuous to continuous transcription. *Cell Host & Microbe*, *16*(4), 462-472.
- Wu, C.-H., Yeh, S.-H., Tsay, Y.-G., Shieh, Y.-H., Kao, C.-L., Chen, Y.-S., . . . Chen, P.-J. (2009). Glycogen synthase kinase-3 regulates the phosphorylation of severe acute respiratory syndrome coronavirus nucleocapsid protein and viral replication. *Journal of Biological Chemistry*, *284*(8), 5229-5239.
- Wu, H.-S., Hsieh, Y.-C., Su, I.-J., Lin, T.-H., Chiu, S.-C., Hsu, Y.-F., . . . Hsiao, P.-W. (2004). Early detection of antibodies against various structural proteins of the SARS-associated coronavirus in SARS patients. *Journal of Biomedical Science*, *11*(1), 117-126.
- Wulan, W. N., Heydet, D., Walker, E. J., Gahan, M. E., & Ghildyal, R. (2015). Nucleocytoplasmic transport of nucleocapsid proteins of enveloped RNA viruses. *Frontiers in Microbiology*, *6*(553). doi: 10.3389/fmicb.2015.00553
- Wurm, T., Chen, H., Hodgson, T., Britton, P., Brooks, G., & Hiscox, J. A. (2001). Localization to the nucleolus is a common feature of coronavirus nucleoproteins, and the protein may disrupt host cell division. *J Virol*, *75*(19), 9345-9356. doi: 10.1128/jvi.75.19.9345-9356.2001
- Wyllie, A., Kerr, J. R., & Currie, A. (1980). Cell death: the significance of apoptosis. *International Review of Cytology*, *68*, 251-306. doi: https://doi.org/10.1016/S0074-7696(08)62312-8

- Xu, J., Jia, W., Wang, P., Zhang, S., Shi, X., Wang, X., & Zhang, L. (2019). Antibodies and vaccines against Middle East respiratory syndrome coronavirus. *Emerging Microbes & Infections*, 8(1), 841-856. doi: 10.1080/22221751.2019.1624482
- Xu, R., Shi, M., Li, J., Song, P., & Li, N. (2020). Construction of SARS-CoV-2 Virus-Like Particles by Mammalian Expression System. *Frontiers in Bioengineering and Biotechnology*, 8, 862. doi: 10.3389/fbioe.2020.00862
- Yamada, Y. K., Yabe, M., Ohtsuki, T., & Taguchi, F. (2000). Unique N-linked glycosylation of murine coronavirus MHV-2 membrane protein at the conserved O-linked glycosylation site. *Virus Research*, 66(2), 149-154. doi: [https://doi.org/10.1016/S0168-1702\(99\)00134-3](https://doi.org/10.1016/S0168-1702(99)00134-3)
- Yamaoka, Y., Matsuyama, S., Fukushi, S., Matsunaga, S., Matsushima, Y., Kuroyama, H., . . . Ryo, A. (2016). Development of Monoclonal Antibody and Diagnostic Test for Middle East Respiratory Syndrome Coronavirus Using Cell-Free Synthesized Nucleocapsid Antigen. *Frontiers in Microbiology*, 7(509). doi: 10.3389/fmicb.2016.00509
- Yan, H., Xiao, G., Zhang, J., Hu, Y., Yuan, F., Cole, D. K., . . . Gao, G. F. (2004). SARS coronavirus induces apoptosis in Vero E6 cells. *Journal of Medical Virology*, 73(3), 323-331.
- Yang, C., Zhang, C., Dittman, J. D., & Whitham, S. A. (2009). Differential requirement of ribosomal protein S6 by plant RNA viruses with different translation initiation strategies. *Virology*, 390(2), 163-173. doi: 10.1016/j.virol.2009.05.018
- Yang, W., Chen, W., Huang, J., Jin, L., Zhou, Y., Chen, J., . . . Liu, G. (2019). Generation, identification, and functional analysis of monoclonal antibodies against porcine epidemic diarrhea virus nucleocapsid. *Applied Microbiology and Biotechnology*, 103(9), 3705-3714. doi: 10.1007/s00253-019-09702-5
- Yang, Y.-S., Wang, C.-C., Chen, B.-H., Hou, Y.-H., Hung, K.-S., & Mao, Y.-C. (2015). Tyrosine sulfation as a protein post-translational modification. *Molecules*, 20(2), 2138-2164.
- Yang, Z.-y., Werner, H. C., Kong, W.-p., Leung, K., Traggiai, E., Lanzavecchia, A., & Nabel, G. J. (2005). Evasion of antibody neutralization in emerging severe acute respiratory syndrome coronaviruses. *Proceedings of the National Academy of Sciences of the United States of America*, 102(3), 797-801. doi: 10.1073/pnas.0409065102
- Ye, Z.-W., Yuan, S., Yuen, K.-S., Fung, S.-Y., Chan, C.-P., & Jin, D.-Y. (2020). Zoonotic origins of human coronaviruses. *International Journal of Biological Sciences*, 16(10), 1686-1697. doi: 10.7150/ijbs.45472
- Yeager, C. L., Ashmun, R. A., Williams, R. K., Cardellicchio, C. B., Shapiro, L. H., Look, A. T., & Holmes, K. V. (1992). Human aminopeptidase N is a receptor for human coronavirus 229E. *Nature*, 357(6377), 420-422.

- Yeoh, S., & Bayliss, R. (2018). New tools for evaluating protein tyrosine sulfation and carbohydrate sulfation. *The Biochemical Journal*, 475(19), 3035-3037. doi: 10.1042/BCJ20180480
- Yin, Y., & Wunderink, R. G. (2018). MERS, SARS and other coronaviruses as causes of pneumonia. *Respirology*, 23(2), 130-137. doi: 10.1111/resp.13196
- Ying, T., Du, L., Ju, T. W., Prabakaran, P., Lau, C. C., Lu, L., . . . Dimitrov, D. S. (2014). Exceptionally potent neutralization of Middle East respiratory syndrome coronavirus by human monoclonal antibodies. *Journal of Virology*, 88(14), 7796-7805. doi: 10.1128/jvi.00912-14
- Yoo, D., Wootton, S. K., Li, G., Song, C., & Rowland, R. R. (2003). Colocalization and interaction of the porcine arterivirus nucleocapsid protein with the small nucleolar RNA-associated protein fibrillarin. *J Virol*, 77(22), 12173-12183. doi: 10.1128/jvi.77.22.12173-12183.2003
- Yoshimoto, F. K. (2020). The Proteins of Severe Acute Respiratory Syndrome Coronavirus-2 (SARS CoV-2 or n-COV19), the Cause of COVID-19. *The Protein Journal*, 39(3), 198-216. doi: 10.1007/s10930-020-09901-4
- You, J.-H., Reed, M. L., & Hiscox, J. A. (2007). Trafficking motifs in the SARS-coronavirus nucleocapsid protein. *Biochemical and Biophysical Research Communications*, 358(4), 1015-1020.
- You, J., Dove, B. K., Enjuanes, L., DeDiego, M. L., Alvarez, E., Howell, G., . . . Hiscox, J. A. (2005). Subcellular localization of the severe acute respiratory syndrome coronavirus nucleocapsid protein. *Journal of General Virology*, 86(12), 3303-3310. doi: <https://doi.org/10.1099/vir.0.81076-0>
- Zakhartchouk, A. N., Viswanathan, S., Mahony, J. B., Gauldie, J., & Babiuk, L. A. (2005). Severe acute respiratory syndrome coronavirus nucleocapsid protein expressed by an adenovirus vector is phosphorylated and immunogenic in mice. *Journal of General Virology*, 86(Pt 1), 211-215. doi: 10.1099/vir.0.80530-0
- Zaki, A. M., van Boheemen, S., Bestebroer, T. M., Osterhaus, A. D., & Fouchier, R. A. (2012). Isolation of a novel coronavirus from a man with pneumonia in Saudi Arabia. *New England Journal of Medicine*, 367(19), 1814-1820. doi: 10.1056/NEJMoa1211721
- Zaroff, S., & Tan, G. (2019). Hybridoma technology: the preferred method for monoclonal antibody generation for in vivo applications. *Biotechniques*, 67(3), 90-92. doi: 10.2144/btn-2019-0054
- Zeng, Z.-Q., Chen, D.-H., Tan, W.-P., Qiu, S.-Y., Xu, D., Liang, H.-X., . . . Zhou, R. (2018). Epidemiology and clinical characteristics of human coronaviruses OC43, 229E, NL63, and HKU1: a study of hospitalized children with acute respiratory tract infection in Guangzhou, China. *European Journal of Clinical Microbiology & Infectious Diseases*, 37(2), 363-369. doi: 10.1007/s10096-017-3144-z

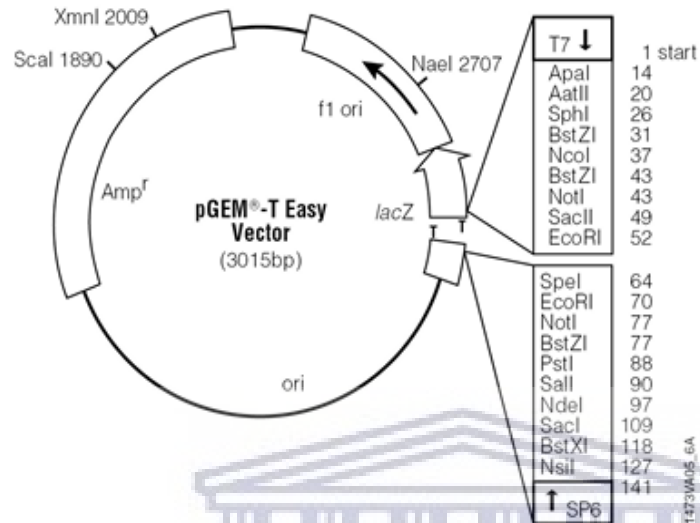
- Zhang, J.-Z., Ng, M. H., Xia, N. S., Lau, S. H., Che, X. Y., Chau, T. N., . . . Im, S. W. K. (2001). Conformational antigenic determinants generated by interactions between a bacterially expressed recombinant peptide of the hepatitis E virus structural protein. *Journal of Medical Virology*, 64(2), 125-132. doi: 10.1002/jmv.1027
- Zhang, M.-Y., Choudhry, V., Xiao, X., & Dimitrov, D. S. (2005). Human monoclonal antibodies to the S glycoprotein and related proteins as potential therapeutics for SARS. *Current Opinion in Molecular Therapeutics*, 7(2), 151-156.
- Zhang, N., Channappanavar, R., Ma, C., Wang, L., Tang, J., Garron, T., . . . Du, L. (2016). Identification of an ideal adjuvant for receptor-binding domain-based subunit vaccines against Middle East respiratory syndrome coronavirus. *Cellular & Molecular Immunology*, 13(2), 180-190. doi: 10.1038/cmi.2015.03
- Zhang, Y., Chen, X., Gueydan, C., & Han, J. (2018). Plasma membrane changes during programmed cell deaths. *Cell Research*, 28(1), 9-21. doi: 10.1038/cr.2017.133
- Zhao, G.-p. (2007). SARS molecular epidemiology: a Chinese fairy tale of controlling an emerging zoonotic disease in the genomics era. *Philosophical Transactions of the Royal Society B: Biological Sciences*, 362(1482), 1063-1081. doi: 10.1098/rstb.2007.2034
- Zhao, G., Shi, S.-Q., Yang, Y., & Peng, J.-P. (2006). M and N proteins of SARS coronavirus induce apoptosis in HPF cells. *Cell Biology and Toxicology*, 22(5), 313-322.
- Zhao, J., & Perlman, S. (2010). T cell responses are required for protection from clinical disease and for virus clearance in severe acute respiratory syndrome coronavirus-infected mice. *Journal of Virology*, 84(18), 9318-9325. doi: 10.1128/JVI.01049-10
- Zhao, X., Li, G., & Liang, S. (2013). Several affinity tags commonly used in chromatographic purification. *Journal of Analytical Methods in Chemistry*, 2013(581093). doi: <https://doi.org/10.1155/2013/581093>
- Zheng, C., Brownlie, R., Babiuk, L. A., & van Drunen Littel-van den Hurk, S. (2005). Characterization of the Nuclear Localization and Nuclear Export Signals of Bovine Herpesvirus 1 VP22. *Journal of Virology*, 79(18), 11864-11872. doi: 10.1128/jvi.79.18.11864-11872.2005
- Zheng, J. (2020). SARS-CoV-2: an Emerging Coronavirus that Causes a Global Threat. *International Journal of Biological Sciences*, 16(10), 1678-1685. doi: 10.7150/ijbs.45053
- Zhou, B., Liu, J., Wang, Q., Liu, X., Li, X., Li, P., . . . Cao, C. (2008). The nucleocapsid protein of severe acute respiratory syndrome coronavirus inhibits cell cytokinesis and proliferation by interacting with translation elongation factor 1 α . *Journal of Virology*, 82(14), 6962-6971.
- Zhou, G., & Zhao, Q. (2020). Perspectives on therapeutic neutralizing antibodies against the Novel Coronavirus SARS-CoV-2. *International Journal of Biological Sciences*, 16(10), 1718-1723. doi: 10.7150/ijbs.45123

- Zhou, J., & Rossi, J. (2017). Aptamers as targeted therapeutics: current potential and challenges. *Nature Reviews Drug Discovery*, 16(3), 181-202.
- Zhou, M., & Collisson, E. W. (2000). The amino and carboxyl domains of the infectious bronchitis virus nucleocapsid protein interact with 3' genomic RNA. *Virus Research*, 67(1), 31-39. doi: 10.1016/s0168-1702(00)00126-x
- Zhou, P., Li, Z., Xie, L., An, D., Fan, Y., Wang, X., . . . Li, Q. Research progress and challenges to coronavirus vaccine development. *Journal of Medical Virology*, 93, 741– 754. doi: 10.1002/jmv.26517
- Zhou, W., Wang, W., Wang, H., Lu, R., & Tan, W. (2013). First infection by all four non-severe acute respiratory syndrome human coronaviruses takes place during childhood. *BMC Infectious Diseases*, 13(1), 433. doi: 10.1186/1471-2334-13-433
- Zhou, Y., Vedantham, P., Lu, K., Agudelo, J., Carrion, R., Nunneley, J. W., . . . Simmons, G. (2015). Protease inhibitors targeting coronavirus and filovirus entry. *Antiviral Research*, 116, 76-84. doi: <https://doi.org/10.1016/j.antiviral.2015.01.011>
- Zhu, N., Zhang, D., Wang, W., Li, X., Yang, B., Song, J., . . . Tan, W. (2020). A Novel Coronavirus from Patients with Pneumonia in China, 2019. *New England Journal of Medicine*, 382(8), 727-733. doi: 10.1056/NEJMoa2001017
- Zhu, Z., Chakraborti, S., He, Y., Roberts, A., Sheahan, T., Xiao, X., . . . Dimitrov, D. S. (2007). Potent cross-reactive neutralization of SARS coronavirus isolates by human monoclonal antibodies. *Proceedings of the National Academy of Sciences*, 104(29), 12123-12128. doi: 10.1073/pnas.0701000104
- Zhu, Z., Lian, X., Su, X., Wu, W., Marraro, G. A., & Zeng, Y. (2020). From SARS and MERS to COVID-19: a brief summary and comparison of severe acute respiratory infections caused by three highly pathogenic human coronaviruses. *Respiratory Research*, 21(1), 224. doi: 10.1186/s12931-020-01479-w
- Zhu, Z., Prabakaran, P., Chen, W., Broder, C. C., Gong, R., & Dimitrov, D. S. (2013). Human monoclonal antibodies as candidate therapeutics against emerging viruses and HIV-1. *Virologica Sinica*, 28(2), 71-80.
- Ziebuhr, J., Snijder, E. J., & Gorbalenya, A. E. (2000). Virus-encoded proteinases and proteolytic processing in the Nidovirales. *Journal of General Virology*, 81(4), 853-879.
- Zinkernagel, R. M. (1996). Immunology Taught by Viruses. *Science*, 271(5246), 173-178. doi: 10.1126/science.271.5246.173
- Zinkernagel, R. M. (2000). Localization dose and time of antigens determine immune reactivity. *Seminars in Immunology*, 12(3), 163-171. doi: <https://doi.org/10.1006/smim.2000.0253>

- Zinkernagel, R. M., Ehl, S., Aichele, P., Oehen, S., Kündig, T., & Hengartner, H. (1997). Antigen localisation regulates immune responses in a dose- and time-dependent fashion: a geographical view of immune reactivity. *Immunological Reviews*, 156, 199-209. doi: 10.1111/j.1600-065x.1997.tb00969.x
- Zitzmann, J., Sprick, G., Weidner, T., Schreiber, C., & Czermak, P. (2017). Process optimization for recombinant protein expression in insect cells *New Insights into Cell Culture Technology* (pp. 43-98).
- Zlateva, K. T., Coenjaerts, F. E., Crusio, K. M., Lammens, C., Leus, F., Viveen, M., . . . Gorbalenya, A. E. (2013). No novel coronaviruses identified in a large collection of human nasopharyngeal specimens using family-wide CODEHOP-based primers. *Archives of Virology*, 158(1), 251-255.
- Zumla, A., Hui, D. S., & Perlman, S. (2015). Middle East Respiratory Syndrome. *Lancet (London, England)*, 386(9997), 995-1007. doi: 10.1016/s0140-6736(15)60454-8
- Zúñiga, S., Cruz, J. L., Sola, I., Mateos-Gómez, P. A., Palacio, L., & Enjuanes, L. (2010). Coronavirus nucleocapsid protein facilitates template switching and is required for efficient transcription. *Journal of Virology*, 84(4), 2169-2175.
- Züst, R., Cervantes-Barragan, L., Habjan, M., Maier, R., Neuman, B. W., Ziebuhr, J., . . . Thiel, V. (2011). Ribose 2'-O-methylation provides a molecular signature for the distinction of self and non-self mRNA dependent on the RNA sensor Mda5. *Nature immunology*, 12(2), 137-143. doi: 10.1038/ni.1979
- Züst, R., Miller, T. B., Goebel, S. J., Thiel, V., & Masters, P. S. (2008). Genetic Interactions between an Essential 3' cis-Acting RNA Pseudoknot, Replicase Gene Products, and the Extreme 3' End of the Mouse Coronavirus Genome. *Journal of Virology*, 82(3), 1214-1228. doi: 10.1128/jvi.01690-07
- Zuwała, K., Golda, A., Kabala, W., Burmistrz, M., Zdzalik, M., Nowak, P., . . . Pyrc, K. (2015). The Nucleocapsid Protein of Human Coronavirus NL63. *PLOS ONE*, 10(2), e0117833. doi: 10.1371/journal.pone.0117833

Appendix 1. Plasmid vectors used in the study

pGEM shuttle vector



Vector map for pGEM available at <https://www.promega.com/-/media/files/resources/protocols/technical-manuals/0/pgem-t-and-pgem-t-easy-vector-systems-protocol.pdf>

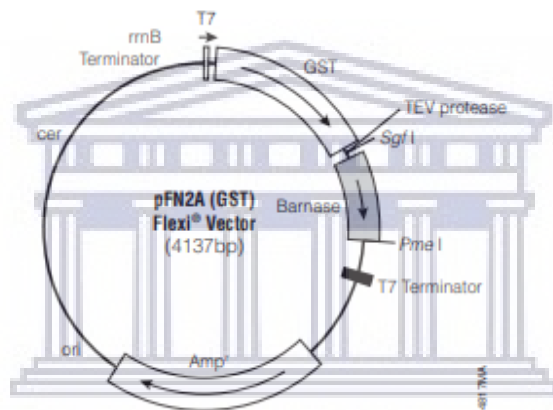
UNIVERSITY of the
WESTERN CAPE

pFN2a (pFlexi) bacterial expression vector

pFN2A (GST) Flexi® Vector Features and Circle Map

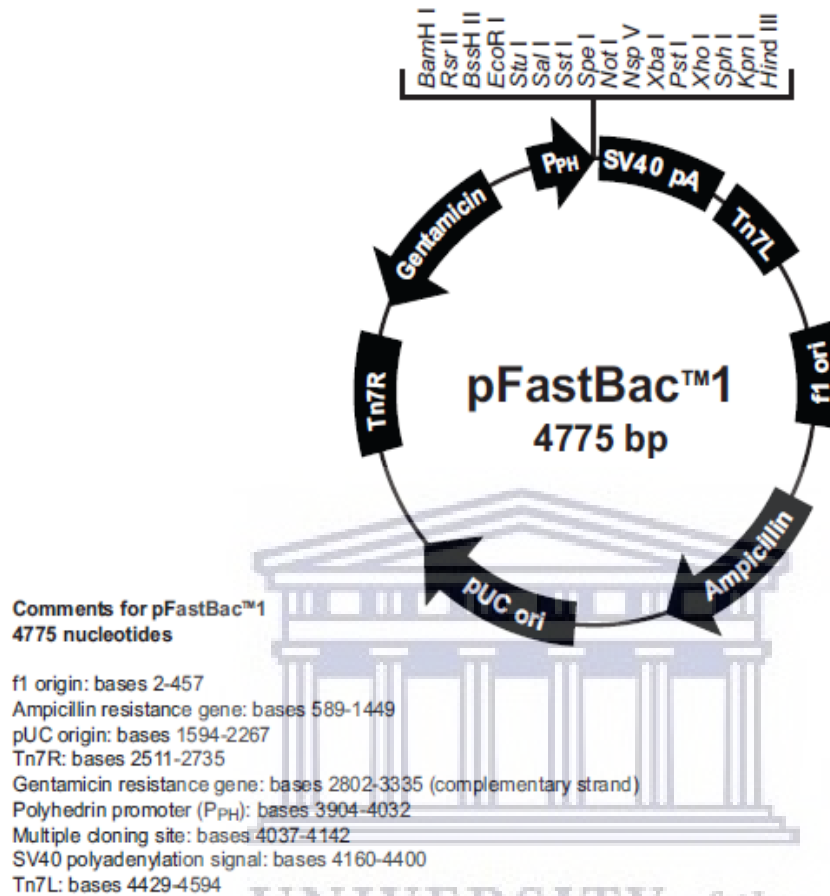
The following features are present in the vector based on nucleotide sequence.

T7 RNA polymerase promoter (-17 to +3)	21-40
GST coding region	70-723
TEV protease site	742-762
SgfI site	760-767
barnase coding region	791-1126
PmeI site	1128-1135
T7 terminator	1255-1302
β -lactamase (Amp ^r) coding region	1636-2496
ColE1-derived plasmid origin of replication	2651-2687
cer site (site for <i>E. coli</i> XerCD recombinase)	3358-3643
rrnB transcription terminator	3694-4095



Vector map for pFN2A available at <https://www.promega.com/-/media/files/resources/protocols/product-information-sheets/a/pfn2a-gst-flexi-vector-protocol.pdf?la=en>

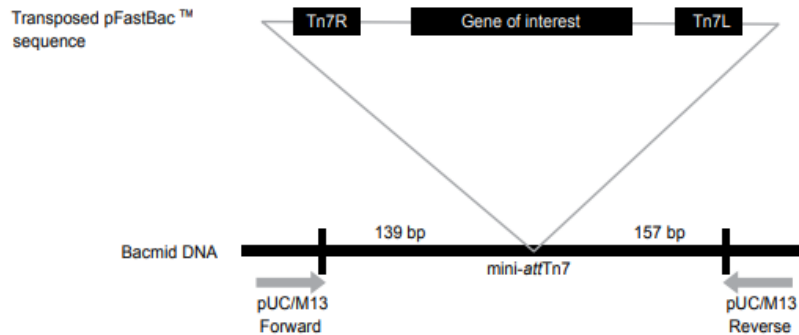
pFastbac1 transposable insect vector



Vector map for pFastbac1 available at http://tools.thermofisher.com/content/sfs/manuals/bactobac_man.pdf

Recombinant bacmid insect expression vector

Recombinant bacmid DNA is greater than 135 kb in size. As restriction analysis is difficult to perform with DNA of this size, use PCR analysis to verify the presence of your gene of interest in the recombinant bacmid. Use the pUC/M13 Forward and Reverse primers that hybridize to sites flanking the mini-*att*Tn7 site within the *lacZ*-complementation region to facilitate PCR analysis.



Guidelines and instructions are provided in this section to perform PCR using the pUC/M13 Forward and Reverse primers.

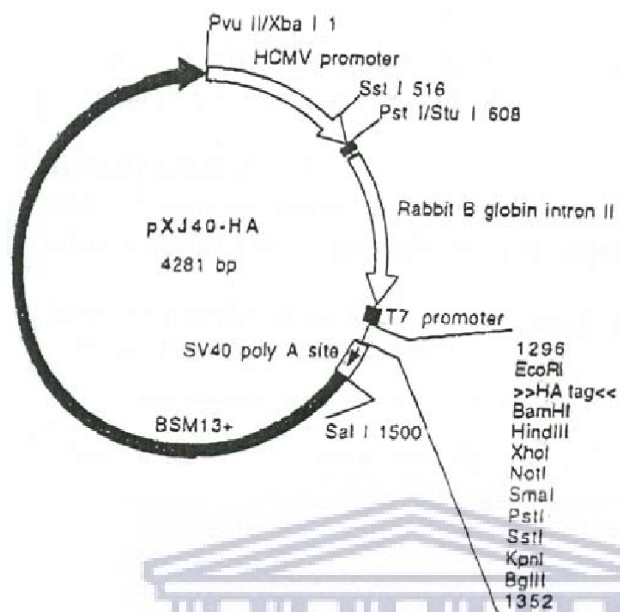
Vector map for recombinant Bacmid available at https://www.thermofisher.com/document-connect/document-connect.html?url=https%3A%2F%2Fassets.thermofisher.com%2FTFS-Assets%2FLSG%2Fmanuals%2FMAN0000414_BactoBacExpressionSystem_UG.pdf&title=VXNlciBHdWlkZTogQmFjLXRvLUJhYyBCYWN1bG92aXJ1cyBFeHByZXNzaW9uIFN5c3RlbQ==

or

<http://wolfson.huji.ac.il/expression/bac.pdf>

UNIVERSITY of the
WESTERN CAPE

pXJ40 mammalian expression vector



Vector map for pXJ40-FLAG and pXJ40-HA mammalian expression plasmids (Manisha et al., 2020).



Appendix 2. Media, buffers, and stains

Luria-Bertani broth

Tryptone powder	10g/L
Yeast extract powder	5g/L
Sodium chloride	10g/L

Luria-Bertani (LB) agar

Tryptone powder	10g/L
Yeast extract powder	5g/L
Sodium chloride	10g/L
Bacteriological agar	15g/L

SOC media

Tryptone powder	20g/L
Yeast extract powder	5g/L
Sodium chloride	0.5g/L

Potassium chloride (250mM) 10ml/L

pH to 7.0 with concentrated sodium hydroxide (NaOH)

Dilute in distilled water up to final volume

Autoclave to sterilise (SOB media)

Add (to make SOC):

Magnesium chloride (2M)* 5mL/L

Glucose (1M)* 20mL/L

*Both magnesium chloride and glucose are made up in distilled water (w/v) to the desired concentrations and sterilised by autoclaving separately before being added to SOC media.

Sf9 cell culture media

Graces supplemented insect media
+ 10% FBS
+ 1% Antibiotic-Penicillin/Streptomycin

Sf9 plaquing media

10mL Fetal Bovine Serum (FBS)
+ 50mL 2X Grace's insect medium
= 60mL (1)
25mL 4% agarose
+ 25mL distilled water
= 50mL (2)

50mL of (1)
+ 50mL of (2)
**= 100mL complete
plaquing medium**

COS7 full growth media

Dulbecco's Modified Eagle Media (DMEM) (41966029, Gibco)

+ FBS

+ 1% Antibiotic-Penicillin/Streptomycin (15140122, ThermoFisher Scientific)

Sp2/hybridoma full growth media

RPMI-1640 (A1049101, Gibco)

+ 10% FBS (Gibco, ThermoFisher Scientific)

+ 1% Antibiotic/Antimycotic solution (PenStrep/Amphotericin B – A5955, Sigma)

+ 1X Glutamax (35050061, ThermoFisher Scientific)

Alternatively:

EX-CELL media (H4281, Merck)

+ 10% FBS (Gibco, ThermoFisher Scientific)

+ 1% Antibiotic/Antimycotic solution (PenStrep/Amphotericin B – A5955, Sigma)

+ 1X Glutamax (35050061, ThermoFisher Scientific)

+ 0.25mM Sodium Pyruvate (11360070, ThermoFisher Scientific)

HAT media (post-fusion hybridomas)

RPMI-1640 (A1049101, Gibco)

+ 10% FBS (Gibco-ThermoFisher Scientific)

+ 1% Antibiotic/Antimycotic solution (PenStrep/Amphotericin B – A5955, Sigma)

+ 1X Glutamax (35050061, ThermoFisher Scientific)

+ 1X HAT supplement (21060017, Gibco-ThermoFisher Scientific)

+ 10 - 50µM β-Mercaptoethanol (21985023, ThermoFisher Scientific)

HT media (post-HAT hybridomas)

RPMI-1640 (A1049101, Gibco)

+ 10% Fetal Bovine Serum (Gibco-ThermoFisher scientific)

+ 1% Antibiotic/Antimycotic solution (PenStrep/Amphotericin B – A5955, Sigma)

+ 1X Glutamax (35050061, ThermoFisher Scientific)

+ 1X HT supplement (11067030, Gibco-ThermoFisher Scientific)

+ 10 - 50µM β-Mercaptoethanol (21985023, ThermoFisher Scientific)

E.coli lysis buffer

Tris (pH 8.0) (648314, Millipore-Merck)	50mM
Sodium chloride (S7653, Sigma-Aldrich)	150mM
Lysozyme (L6876, Sigma-Aldrich)	0.4mg/mL – add lysozyme just before use

RIPA lysis buffer:

Tris-HCl (pH 7.5) (77-86-1, Roche-Merck)	25mM
Sodium chloride	150mM
EDTA (E5134, Sigma-Aldrich)	1mM
Sodium deoxycholate (302-95-4, Merck)	0.5%
Triton-X (T8787, Sigma-Aldrich)	1%
Sodium Dodecyl Sulphate (SDS) (L3771, Merck)	0.1%
Diluted in distilled water up to final volume	
PMSF (10837091001, Roche-Merck)	1mM – add PMSF just before use

Alternative Sf9 lysis buffer

Tris-HCl (pH7.5)	62.5mM
SDS	2%

SDS-PAGE running buffer

10X, 1L:

Tris base	30.2g [25mM]
Glycine (G8898, Sigma-Aldrich)	144g [192mM]
SDS	10g [0.1%]

Diluted in distilled water up to final volume

Stored at room temperature

Dilute to 1X before use

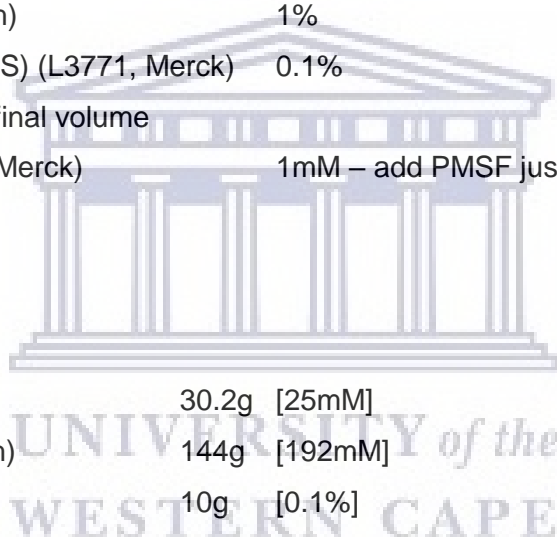
Western blot transfer buffer

10X:

Tris base	25mM
Glycine	192mM
SDS	0.1%

Diluted in distilled water up to final volume

Stored at room temperature



1X:

10X transfer buffer	10%
Methanol (106009, Supelco-Merck)	20 – 40%

Diluted in distilled water up to final volume
Stored at -20°C

ELISA blocking buffer

2% – 5% Human/Bovine Serum Albumin (w/v or v/v)
Diluted in 1X phosphate-buffered saline (PBS)

ELISA/western blot wash buffer

10X PBS	10%
10% Tween 20 (P9416, Sigma-Aldrich)	0.1%

Diluted in distilled water to final volume

10X TBE

Tris base	108g/L
Boric acid (B7901, Sigma-Aldrich)	55g/L
EDTA	9.3g/L

Diluted in distilled water to final volume, stir to dissolve using a magnetic stirrer (it will take 30 – 60 minutes)

Autoclave to sterilise

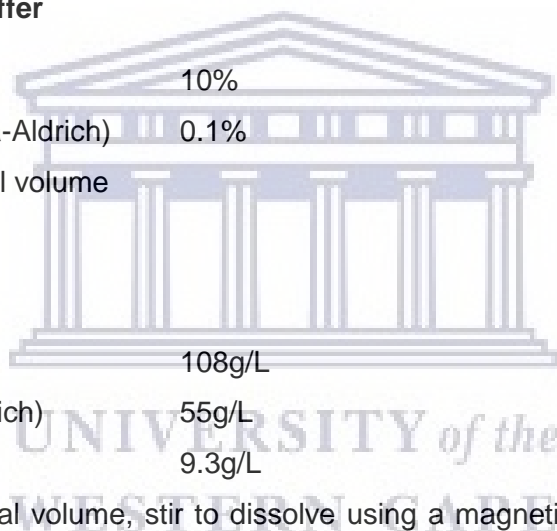
Diluted to 1X before use

10X TAE

Tris base	48.4g/L
Glacial acetic acid (100063, Supelco-Merck)	11.4mL/L
EDTA	3.72g/L

Diluted in distilled water to final volume

Diluted to 1X before use



MTT (Thiazolyl Blue Tetrazolium Bromide) stain

MTT powder (M5655, Sigma) 5mg/mL
Diluted in distilled water
0.22 μ M filter-sterilised
Store at -20°C

Ponceau stain

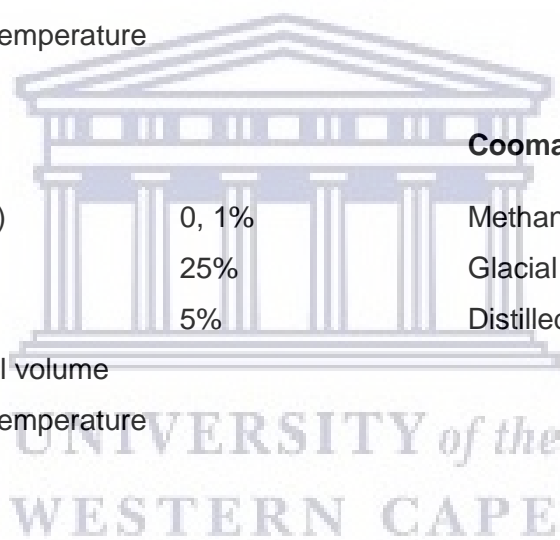
Ponceau S powder (w/v) (P3504, Sigma-Aldrich) 0.1%
Glacial acetic acid 5%
Diluted in distilled water to final volume
Stored in clear bottle at room temperature

Coomassie stain

Brilliant Blue G (27815, Sigma) 0, 1%
Methanol 25%
Glacial acetic acid 5%
Diluted in distilled water to final volume
Stored in clear bottle at room temperature

Coomassie destain

Methanol 30%
Glacial acetic acid 10%
Distilled water 60%



Appendix 3. List of reagents

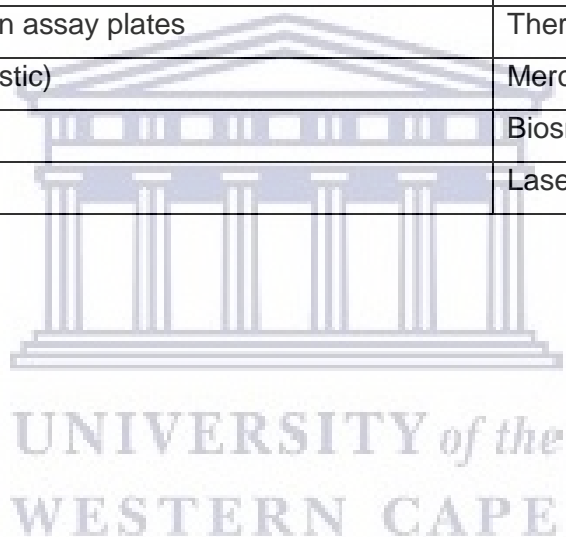
List of reagents		
Product	Supplier	Catalogue number
1X ProTEV buffer	Promega	V602A
2X Grace's Media (supplemented)	ThermoFisher Scientific	11667037
6X blue/orange loading dye	Promega	G1881
Acetone	Supelco - Merck	100014
Agar, bacteriological	Merck	A5306-250G
Agarose	SeaKem®	50004
Agarose, 4%	Gibco	18300012
Ampicillin, sodium salt	Calbiochem	CAS 69-52-3 171254
Antibiotic/Antimycotic solution (PenStrep/Amphotericin B)	Sigma	A5955
Anti-NL63 N mouse monoclonal	Immunologia y Genetica Aplicada Sa (Eurofins INGENASA)	M.30.HCo.I2D4
BamH1	Promega	R6021
BSA (acetylated)	Promega	R3961
Buffer D	Promega	R004A
Buffer H	Promega	R008A
Calf Intestinal Alkaline Phosphatase (CIAP)	Promega	M1821
Cellfectin II	Gibco	10362100
Complete Freund's adjuvant	Sigma	F5881
DAPI	ThermoFisher Scientific	62248
D-Glucose	Merck	G8270
DH10BAC <i>E.coli</i> competent cells	Gibco	10361012
DH5α <i>E.coli</i> competent cells	Invitrogen	18258012
DMEM	Gibco	41966029
DNA ligase buffer (10X)	Promega	C126A
DNA marker (100bp, 1KB)	Promega	G2101, G5711

dNTPs	Promega	U1511
DTT	Promega	P117B
EcoR1	Promega	R6011
EDTA	Sigma-Aldrich	E5134
Ethanol (99.99%)	Supelco - Merck	100983
Ethidium Bromide	Promega	H5041
EX CELL media	Merck	H4281
Fetal Bovine Serum (FBS)	Gibco	10500064, 10082147
Gentamicin	Gibco	15750060
Glutamax	Thermofisher Scientific	35050061
Goat anti-mouse IgG-HRP	Santa Cruz Biotechnology (SCBT)	sc-2005
Goat anti-rabbit IgG-HRP	SCBT	sc-2004
Gotaq flexi buffer 1ml	Promega	M891A
GoTaq Flexi DNA Polymerase	Promega	M8291
Grace's Media (1x supplemented)	Gibco	11605045
Grace's media unsupplemented	Gibco	11595030
HAT supplement	ThermoFisher Scientific	21060017
Hind3(III)	Promega	R6041
HT supplement	ThermoFisher Scientific	11067030
Incomplete Freund's adjuvant	Sigma	F5506 – 10ML
IPTG	Promega	V395D
JM109 <i>E.coli</i> competent cells	Promega	L2005
Kanamycin	Merck	10106801001
KRX <i>E.coli</i> competent cells	Promega	L3002
Lipofectamine 2000	Thermofisher Scientific	11668019
L-Rhamnose	Merck	83650
Lysozyme	Sigma-Aldrich	L6876
MagneGST protein purification system	Promega	V8600
Magnesium Chloride	Sigma-Aldrich	814733
MgCl ₂ (25mM)	Promega	A3511

MTT	Sigma	M5655
Not1	Promega	R6431
Nuclease-free water	Promega	P1195
Nucleobond PC100 DNA purification kit	Machery-Nagel	740573.100
Nucleobond XtraMidi DNA purification kit	Machery-Nagel	740410.50
OptiMEM	Gibco	31985062
PBS (1X)	Gibco	10010023
Penicillin/Streptomycin	ThermoFisher Scientific	15140122
peqGOLD cycle-pure kit	VWR Life Science	13-6293-01
pFastbac1 (pFB1) vector	Gibco	10360014
pFN2A (GST) Flexi® Vector	Promega	C8461
pGEM-T easy vector	Promega	A362A
Pierce BCA Protein Assay Kit	Merck	23225
Polyethylene Glycol (PEG)	Supelco - Merck	02393
Potassium Chloride	Supelco - Merck	104936
ProTEV plus	Promega	V610A
ProTEV protease enzyme	Promega	V6101
PureYield Plasmid Miniprep System	Promega	A1223
PVDF membrane	ThermoFisher Scientific	88518
Qubit dsDNA BR Assay Kit	ThermoFisher Scientific	Q32850
Qubit Protein Assay Kit	ThermoFisher Scientific	Q33211
Rabbit Anti-Mouse IgG Antibody, HRP conjugate	Merck	AP160P
RPMI-1640	Gibco	A1049101
SDS Gel preparation kit	Merck	08091
Sodium Chloride	Sigma-Aldrich	S7653
Sodium deoxy cholate	Merck	302-95-4
Sodium Hydroxide (NaOH)	Supelco - Merck	106462
Sodium Pyruvate	ThermoFisher Scientific	11360070
Sulfuric acid H ₂ SO ₄	Supelco - Merck	100731
T4 DNA ligase	Promega	M1801

Tetracycline	Gibco	A39246
Tetramethylbenzidine (TMB) Microwell substrate	Sera care-KPL	5120-0053(50-76-11)
TMB membrane substrate	Sera care-KPL	5420-0025(50-77-00)
Tris (pH 8.0)	Millipore - Merck	648314
Tryptone powder	Millipore	T9410-1KG
Tween-20	Sigma-Aldrich	P1379-100ML
Wizard Plus SV Miniprep System	Promega	A1330
Wizard SV Gel and PCR Clean-Up System	Promega	A9281
Xgal	Promega	V3941
Xho1	Promega	R6161
Yeast extract powder	Millipore	113885
β -Mercaptoethanol	ThermoFisher Scientific	21985023
Tris base	Roche - Merck	77-86-1
Sodium deoxy cholate	Merck	302-95-4
Triton-X	Sigma-Aldrich	T8787
Sodium Dodecyl sulphate	Merck	L3771
PMSF	Roche-Merck	10837091001
Glycine	Sigma-Aldrich	G8898
Methanol	Supelco - Merck	106009
Boric acid	Sigma-Aldrich	B7901
Glacial acetic acid	Supelco - Merck	100063
Ponceau S powder	Sigma-Aldrich	P3504
Brilliant Blue G	Sigma-Aldrich	27815

List of consumable materials	
Product	Supplier
Microcentrifuge tubes (0,2mL; 0,5mL; 1,5mL; 2mL)	ExtraGene, USA
Pipette tips (10uL; 0,2mL; 1mL)	Lasec, South Africa
24-well Falcon® Clear Flat Bottom TC-treated Multiwell Cell Culture Plate	Corning, USA
6-well CELLSTAR® cell culture plates	Greiner bio-one
Cell culture flasks (T25, T75, T125)	Biosmart, South Africa
Cell scrapers	Biosmart, South Africa
Conical tubes (15ml, 50mL)	Biosmart, South Africa
Disposable syringes (20mL, 10mL, 5mL)	Biosmart, South Africa
Greiner 96-well flat bottom plates	Merck
Nunc Maxisorp 96-well protein assay plates	ThermoFisher Scientific
BRAND® Pasteur pipette (plastic)	Merck
Petri dishes (60mm, 100mm)	Biosmart, South Africa
Syringe filters (0.22µM)	Lasec, South Africa



Appendix 4. Primer sequences

Gene-specific HCoV-NL63 N full-length gene primers

Primer	Nucleotide sequence
<i>N-FLAG forward</i>	GCT GGA TCC ATG GCT AAT GTA AAT TGG GCC
<i>N-FLAG reverse</i>	CCG CTC GAG TTA ATG CAA AAC CTC GTT GAC
<i>N-3'HA forward</i>	GCT GGA TCC ATG GCT AAT GTA AAT TGG GCC
<i>N-3'HA reverse</i>	CCG CTC GAG AAT AAC ATG CAA AAC CTC GTT GAC

Gene-specific HCoV-NL63 N internal gene primers (sequencing)

Primer	Nucleotide sequence
<i>N-int forward</i>	CTC GTT GGA AGC GTG TTC CTA
<i>N-int reverse</i>	GCT ACA AGC ATT TTG TAG GTG

Gene-specific HCoV-NL63 M full-length gene primers

Primer	Nucleotide sequence
<i>M forward</i>	GCG AAT TCA ATG TCT AAT AGT AGT GTG CCT C
<i>M reverse</i>	GCT CTA GAT TAC ATT AAA TGA AGC AAT TCT C

Gene-specific HCoV-NL63 M internal gene primers

Primer	Nucleotide sequence
<i>Bac M forward</i>	GAC TTT GGC GCC GTG TTA AA
<i>Bac M reverse</i>	GGA CGT AGA ATG CCC AAC CA



UNIVERSITY *of the*
WESTERN CAPE